Norwegian University of Life Sciences
Faculty of Chemistry, Biotechnology and Food Science

Philosophiae Doctor (PhD)
Thesis 2021:58

Studies of molecular determinants of virulence in *Aliivibrio salmonicida* and *Vibrio anguillarum*

Studier av molekylære determinanter for virulens i *Aliivibrio salmonicida* og *Vibrio anguillarum*

Anna Skåne

Studies of molecular determinants of virulence in *Aliivibrio salmonicida* and *Vibrio anguillarum*

Studier av molekylære determinanter for virulens i *Aliivibrio salmonicida* og *Vibrio anguillarum*

Philosophiae Doctor (PhD) Thesis

Anna Skåne

Norwegian University of Life Sciences
Faculty of Chemistry, Biotechnology and Food Science

Ås, 2021

Thesis number 2021:58
ISSN 1894-6402
ISBN 978-82-575-1830-1

Acknowledgements

The work leading up to this thesis was carried out at the Protein Engineering and Proteomics group (PEP) at the Faculty of Chemistry, Biotechnology and Food Science at the Norwegian University of Life Sciences during the period of 2016 to 2021. The work was funded by the Norwegian Research Council grant 249865.

First and foremost, I would like to express my gratitude to supervisor Gustav Vaaje-Kolstad and co-supervisors Fatemeh Askarian, Geir Mathiesen and Henning Sørum. Gustav, thank you for giving me the opportunity to work on this project. It's been five years of ups and downs, and I am grateful for your enthusiasm and help in so many ways. Fatemeh, thank you for guiding me in the right direction when things were "very very wrong" 😊. Although you are extremely busy, you have always found the time to help, and often far beyond what is expected. Geir, thank you for your constant support and genuine interest in my progress from start to end. I am also grateful that you gave me the opportunity to teach microbiology. Henning, I value your contribution, especially to the salmon challenges, and our discussions helped me see the bigger picture.

I want to thank my present and former colleagues at PEP and KBM for contributing to making it an enjoyable and including place to work. A great appreciation to all co-authors, and everyone that helped in one way or another.

To my family and friends, I know I have been very hard to reach for longer periods of time. Thank you for your understanding and support. Anita, I am sincerely grateful for your many road trips and visits. Mathilde, the past years would not have been the same without our friendship. Beate, thank you for all the motivational and supportive conversations that helped me get through the final year.

A special thanks to "Mor", who made sure I took the time to eat and sleep while writing the most part of this thesis.

Heiabakkane, May 2021

Table of contents

1 Abbreviations

AA10	Auxiliary activities family 10
AI	Autoinducer
C3	Complement component 3
CDS	Coding sequence
CWV	Cold-water vibriosis
DIP	2,2′-dipyridyl
Fur	Ferric uptake regulator
GH18	Glycoside hydrolases 18
GlcNAc	*N*-acetyl-D-glucosamine
$(GlcNAc)_2$	Chitobiose
H_2O_2	Hydrogen peroxide
In vitro	“Within the glass”
In vivo	“Within the living”
IS	Insertion sequence
i.p.	Intraperitoneal
LB	Luria Bertani broth
LPMO	Lytic polysaccharide monooxygenase
LPS	Lipopolysaccharide
ORF	Open reading frame
OMVs	Outer membrane vesicles
ROS	Reactive oxygen species
QS	Quorum sensing

2 List of papers

Paper I

Anna Skåne*, Giusi Minniti*, Jennifer S.M. Loose, Sophanit Mekasha, Bastien Bissaro, Geir Mathiesen, Magnus Ø. Arntzen and Gustav Vaaje-Kolstad

The fish pathogen *Aliivibrio salmonicida* LFI1238 can degrade and metabolize chitin despite major gene loss in the chitinolytic pathway.

*Equal contribution

Paper II

Anna Skåne, Per Kristian Edvardsen, Gabriele Cordara, Jennifer S.M. Loose, Kira D. Leitl, Ute Krengel, Henning Sørum, Fatemeh Askarian* and Gustav Vaaje-Kolstad*

Chitinolytic enzymes confer pathogenicity of *Aliivibrio salmonicida* LFI1238 in the invasive phase of cold-water vibriosis (CWV)

*Equal contribution

Paper III

Anna Skåne, Jennifer S.M. Loose, Gustav Vaaje-Kolstad* and Fatemeh Askarian*

Comparative proteomic profiling reveals specific adaption of *Vibrio anguillarum* to oxidative stress, iron deprivation and humoral components of innate immunity.

*Equal contribution

3 Abstract

The arsenal of virulence factors possessed by a bacterium can determine its ability to infect the host and cause disease. Chitinases and chitin-active lytic polysaccharide monooxygenases (LPMOs) have been indicated to play an important role not only in chitin degradation- but also virulence. The genome of *Aliivibrio salmonicida*, the causative agent of a cold-water vibriosis (CWV) in farmed salmonids, has gone through a substantial gene decay, possibly adapting the bacteria to its pathogenic lifestyle. One of the most affected pathways is the chitinolytic pathway, which is responsible for obtaining nutrients from chitin. Intrestingly, two LPMO and one chitinase encoding genes remain intact. A major part of this PhD project was therefore aimed at investigating whether the chitinase (*As*Chi18A) and LPMOs (*As*LPMO10A and *As*LPMO10B) of *Al. salmonicida* in fact could depolymerize chitin and determine if these enzymes play a role in the pathogenic properties of the bacterium.

In the first study, *Al. salmonicida* was found to be able to utilize chitin as nutrient source, a finding supported by biochemical evidence showing chitin depolymerizing activities for both LPMOs and the chitinase. Investigation of gene deletion variants showed that all three enzymes were required for optimal chitin degradation by the bacterium, although the chitinase was playing the most important role. Interestingly, the chitinase displayed approximately 50-fold lower chitin degrading activity compared to chitinases that were obtained from other well know chitin degrading bacteria, which might indicate the putative adaption of the bacterium to other substrates. Finally, proteomic analysis of chitin catabolism by *Al. salmonicida* showed that *As*LPMO10A was abundantly expressed under all examined conditions including presence of glucose, whereas *As*LPMO10B and the chitinase were mostly detected during growth on chitin.

The second study investigated the potential roles of *As*LPMO10A and *As*LPMO10B as virulence factors. In vivo challenge experiments showed that the two LPMOs promoted the virulence properties of the bacterium during the invasive phase of CWV. Intriguinly, exposure of the single and double LPMO-deletion variants to Atlantic salmon serum showed alternation of *A. salmonicida* proteome response compared to the wild type. This further indicates the use of alternative mechanisms for adaption by the bacterium to the host-mimicking conditions upon deletion of the LPMOs.

The final study of the thesis was performed on another bacterium causing vibriosis, namely *Vibrio anguillarum*. Using comparative label-free quantitative proteomics,

the response of the bacterium was analyzed after exposure to several virosis-associated stress conditions like iron-deprivation, hydrogen peroxide (oxidative stress) and innate immune components (Atlantic salmon serum). Most notably, all stress conditions resulted in significant modulation of metabolic pathways and particular virulence determinants.

Taken together, the findings of this thesis provide novel insight into the ecology and virulence properties of chitinolytic enzymes in *Al. salmonicida* and the global proteomic adaptions of *V. anguillarum* to several vibriosis associated stressors.

4 Norsk sammendrag

Arsenalet av virulensfaktorer tilgjengelig for en bakterie spiller en viktig rolle for evnen den har til å infisere verten og forårsake sykdom. Kitinaser og kitin-aktive lytisk polysakkarid monooksygenaser (LPMOer) er indikert til å spille en viktig rolle i nedbryting av kitin, men også som virulensfaktorer. Genomet til *Aliivibrio salmonicida*, som forårsaker kaldtvannsvibriose (CWV) hos oppdrettslaks, har gjennomgått et betydelig genforfall. Genforfallet er muligens en tilpasning av bakterien til dens patogene livsstil. En rekke av de ødelagte genene er ansvarlig for å skaffe næringstoffer fra kitin, hvilket kan tyde på at bakterien har mistet evnen til å nyttegjøre seg av kitin som næringskilde. Til tross for dette, er to LPMO-kodende gener og et kitinase-kodene gen intakte. Det kan ergo tenkes at disse enzymene kan ha andre roller enn nedbrytning av kitin. En stor del av dette PhD-prosjektet ble derfor rettet mot å undersøke om kitinasen (*As*Chi18A) og LPMOene (*As*LPMO10A og *As*LPMO10B) til *Al. salmonicida* kunne depolymerisere kitin, og om disse enzymene kunne spille en rolle for de patogene egenskapene til bakterien.

Den første studien avslørte at *Al. salmonicida* kan bruke kitin som næringskilde. Funnet ble støttet av biokjemiske bevis som viste at både kitinasen og LPMOene har depolymeriserene aktiviteter. Bruk av genedelesjonsvarianter viste at alle tre enzymene var nødvendige for optimal kitin-nedbrytning, og at kitinasen spilte den viktigste rollen. Videre hadde kitinasen 50 ganger lavere kitin-nedbrytende aktivitet sammenlignet med kitinaser fra velkjente kitin-nedbrytende bakterier, noe som kunne indikere en tilpasning til andre substrater. Ved bruk av proteomisk analyse av *Al. salmonicida*, ble *As*LPMO10A funnet rikelig uttrykt i alle testede forhold (også under vekst på glukose), mens *As*LPMO10B og kitinasen omtrent bare ble påvist under vekst på kitin.

Den andre studien undersøkte *As*LPMO10A og *As*LPMO10B som potensielle virulensfaktorer. Smitteforsøk med Atlantisk laks viste at LPMOene fremmet virulens hos *Al. salmonicida*, og at dette var knyttet til det invasive stadiet av CWV. Videre viste eksponering av de ulike delesjonsvarientene for lakseserum, forskjellig proteomisk respons sammenlignet med villtypen, noe som indikerer bruk av alternative mekanismer for tilpasning til vertsbetingelser i fravær av LPMOene.

Den siste studien ble utført på *Vibrio anguillarum*, en annen bakterie som forårsaker vibriose. Ved bruk av komparativ proteomikk ble bakteriens respons analysert etter eksponering for miljømessige stressforhold som jernmangel,

hydogenperoksid (oksidativt stress) og serum fra Atlantisk laks. Alle stressforhold førte til signifikant modulering av metabolisme og spesifikke virulensfaktorer.

Funnene i dette prosjektet gir ny innsikt i økologien og virulensegenskapene knyttet til *Al. salmonicida's* kitinolytiske enzymer, og gir ny innsikt i *V. anguillarum's* globale proteomiske tilpasning til uilke vibriose-assosierte stressfaktorer.

5 Introduction

Vibrionaceae is a large family of bacteria widely distributed in the environment, of which many are opportunistic pathogens associated with diseases in both humans and vertebrates. The taxonomy of Vibrionaceae have been subject to multiple changes over the years, and currently consists of 11 genera (*Vibrio, Photobacterium*, *Aliivibrio, Salinvibrio, Enterovibrio, Grimontia, Candidatus Photodesmus, Allomonas, Catenococcus, Echinimonas* and *Photococcus*) (1). In humans, opportunistic pathogens within the Vibrionaceae family (*e.g*. *Vibrio cholerae*, *Vibrio vulnificus*, *Vibrio parahaemolyticus*) are commonly associated with consumption of contaminated water or seafood (2). They may cause gastrointestinal infections, septicemia, skin and soft tissue infections (2). In fish and aquatic animals, examples of pathogens within this family includes *Aliivibrio* (*Vibrio*) *salmonicida, Vibrio (Listonella) anguillarum, Vibrio vulnificus, Vibrio ordalii, Vibrio harveyi, Vibrio alginolyticus, Aliivibrio wodanis* and *Photobacterium damselae* subsp. *damselae* (3, 4). The work leading up to this thesis was carried out on *Al salmonicida* and *V. anguillarum,* causative agents of vibriosis in aquaculture.

The introduction of this thesis will elucidate the importance of chitin in the environmental ecology of Vibrionaceae, virulence determinants associated with these bacterial species and chitinolytic enzymes as multifunctional proteins.

5.1 *Aliivibrio salmonicida*

Allivibrio salmonicida is a gram negative, facultative anaerobic, motile, curved rod with multiple polar flagella (Figure 1)(5). This bacterium was previously known as *Vibrio salmonicida* (5) before reclassification to the *Aliivibrio* genus (6). *Al. salmonicida* grows at 1-22 °C and 0-4 % NaCl, but the optimal salinity is 1.5 % with an optimal growth temperature at 15 °C on solid media and 10 °C in liquid media (7). Colonies are small, round, raised and translucent.

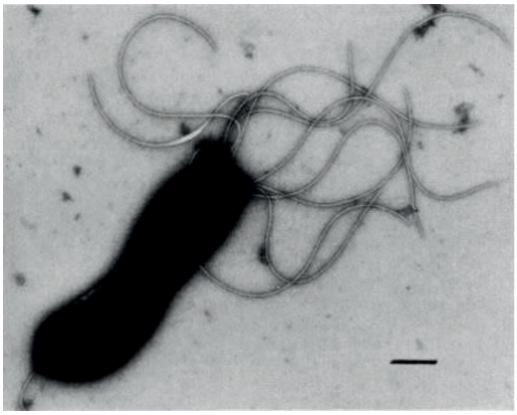

Figure 1. Scanning electron microscopy of *Aliivibrio salmonicida*. Adapted from Egidius et al (5).

Genome sequencing of strain LFI1238 by Hjerde et al., revealed several genomic features of this bacterium. Like most Vibrionaceae, its genome is composed of two chromosomes. The largest chromosome (I) harbors essential genes, while the smaller chromosome (II) harbors accessory genes (8). A highly interesting feature of the *Al. salmonicida* genome is the number of inactive genes and abundance of insertion sequence elements (IS elements). In total, 291 IS elements are responsible for the inactivation of at least 156 coding sequences (CDSs). IS elements are short, self-replicating DNA sequences that are capable of spreading across the genome, and the high abundance of IS elements in *Al. salmonicida* LFI1238 is proposed to reflect an ability to adapt to the environment (8, 9). The genome sequencing also demonstrated the presence of four plasmids. Eleven different plasmid profiles have been identified for *Al. salmonicida* across 342 clinical isolates (10). None of these plasmids have been reported to be associated with virulence.

History and epidemiology of cold-Water vibriosis

Cold-water vibriosis (CWV) is a disease mainly affecting salmonids (*Salmo salar* L. and *Oncorhynchus mykiss*) and to a lesser extent gadidae (*Gadus morhua* L.). CWV is characterized by high mortality and extensive hemorrhages, and has been named “hemorrhagic syndrome” and “Hitra disease” (11). The first recorded cases of CWV occurred in 1977 Hammerfest, and late autumn and winter 1979/1980 around the islands Hitra and Frøya in Norway (11). In the following years, CWV persisted around the coast of Norway and spread to the Bergen and Stavanger region in 1983 (12). From the late 1980s the etiological agent was also isolated from diseased cod (*Gadus morhua*) (13, 14).

CWV was regarded as the most severe threat to Norwegian aquaculture, leading to high mortalities, economic losses, and extensive consumption of antibiotics, which peaked in 1987 with 200 outbreaks (15). Treatment with antibiotics was a major concern. By the time symptoms appeared it was often too late for efficient treatment, and isolated strains of the etiological agent, *Al. salmonicida* from various locations showed resistance to a variety of antibiotics (16).

Development of a vaccine consisting of a bacterin made from formalin-killed *Al. salmonicida,* and later an oil-adjuvanted furunculosis/CWV vaccine has kept the disease under control (17-19). A rise in the number of CWV infections in Atlantic salmon was reported in 2011-2013, but according to the Norwegian fish health report 2015, altered conditions related to vaccination contributed to this situation (15).

CWV is endemic along the whole Norwegian cost line. However, cases have also been recorded in Scotland, Faroe islands, Iceland, United States and Canada (20, 21). Outbreaks of CWV mainly occur when the water temperature is low (<10 °C), from late autumn to early spring. The route of transmission is between fish within the same farm and between neighboring farm locations. *Al .salmonicida* can survive for more than 1 year in a suspended state (22), and the abundance of the bacterium in the water surrounding fish farms fluctuates with seasonal variation (23, 24).

The intact salmon skin has been demonstrated to be the portal of entry of *Al. salmonicida* (25). Multiple studies describe the presence of *Al. salmonicida* in the blood of experimentally challenged Atlantic salmon. Bjelland et al. showed the presence of the bacterium in the blood of Atlantic salmon 2 hours after immersion challenge, and proposed rapid development of septicemia (26). Later, Kashulin and Sørum showed that only 3 minutes exposure of *Al. salmonicida* was enough to recover high numbers of the pathogen from the blood of infected fish (25).

Symptoms and pathology

Clinical signs of CWV include extensive internal hemorrhaging around organs, abdominal wall, and posterior gastro-intestinal tract (5, 12, 27). External hemorrhages around the abdomen may be present (Figure 2). *Al. salmonicida* is usually found in high numbers in blood and hematopoietic tissues, and there is often evidence of anemia internally. Moribund fish may display loss of appetite, fatigue, and changes in swimming pattern (12).

Figure 2. External signs of Cold-water vibriosis. CWV can be observed by the external hemorrhaging (red spots) indicated on the skin between the pectoral and ventral fins. Photo: Anna Skåne.

Once the bacterium enters the bloodstream (25), *Al. salmonicida* will actively proliferate in blood upon passing a latent stage (25, 26, 28). In Atlantic salmon, the most severe cell damage of affected fish is found in areas with a rich blood supply. The first cellular damage appears in leukocytes and the endothelial cells of the capillaries (29). The histopathological changes observed in infected fish has been shown to correspond to the bacterial burden, and to be related to the host immune response towards the pathogen (29-31). In vitro and in vivo studies have demonstrated that *Al. salmonicida* is actively and rapidly phagocytosed (31, 32), and histochemical studies of stored tissues from the first known outbreaks of CWV have showed that positive antigen reactions are pronounced within the phagocytic cells of the spleen and kidney (30).

5.2 *Vibrio anguillarum* and vibriosis

Description of species

Vibrio anguillarum is a gram negative, motile, curved rod with one single polar flagellum (Figure 3). Over the years, *V. anguillarum* has been subject to changes in classification. Based on genetic variation in the 5S rRNA region, two new genera were established (*Listonella* and *Shewanella* (33)), excluding *V. anguillarum* from the Vibrionaceae family, until later reclassification to the *Vibrio* genus (34).

V. anguillarum can grow between 15 and 38.5 °C, with optimum temperature 25 °C and presence of 1-2 % NaCl (35). The growth rate of *V. anguillarum* is known to increase with temperature (36). Colonies are round, raised, shiny and cream-colored (37).

Figure 3. Immunogold electron microscopy *of Vibrio anguillarum* NB10. Adapted from (38).

So far, 23 serotypes of *V. anguillarum* have been described, of which majorly serotypes O1 and O2, and to a limited extent O3, are associated with vibriosis in fish. The other *V. anguillarum* serotypes are in general nonpathogenic and isolated from seawater, plankton and sediments. The bacterium contains two chromosomes which have been sequenced in several strains of serotypes O1, O2 and O3 (39-41). The first complete genome sequence of *V. anguillarum* strain 775 revealed various genomic features including the virulence plasmid pJM1, 10 genomic islands (GIs) and several potential virulence factors (39). Plasmid profiling of *V. anguillarum* showed that serotype O1 strains associated with disease in fish, in general harbor a pJM1 or pJM1-like plasmid (42-44). In contrast, it has been

suggested that the presence or absence of the pJM1 plasmid is not an essential factor for *V. anguillarum* to cause disease in fish larvae (45).

History, epidemiology and clinical signs

In 1909 Bergman proposed the name *Vibrio anguillarum* for the causing agent of "red pest" in eels (*Anguilla anguilla* L.) (46). Prior to this, Canestrini reported *Bacterium anguillarum* as the causing agent of an epidemic disease affecting the same species dating back to the 1880s (47), and Bergman proposed that is was the same etiological agent. By 1970s *V. anguillarum* was found to be the causing agent of vibriosis in several marine organisms including eels (48), rainbow trout (49), flounder (50), turbot (51) and Pacific salmonids (52). Today it is known that *V. anguillarum* causes vibriosis in more than 50 species of fish, and occasionally causes disease in mollusks and crustaceans (53, 54).

Typical external clinical signs of vibriosis include weight loss, lethargy, hemorrhages or red spots on the ventral and lateral areas of the fish, as well as swollen and dark skin lesions. The eyes may also be affected, resulting in ulceration and exophthalmia (54). Based on these clinical signs, vibriosis is also known as salt-water furunculosis (55), boil disease (56) and ulcer disease (57). Internally, the bacterium is found in high concentrations in the blood and hematopoietic tissues. Several vaccines have been developed, including heat- or formalin killed *V. anguillarum*, whole cell bacterin and live-attenuated vaccines (58-62).

Factors contributing to outbreaks of vibriosis includes water quality and pollution, population density and temperature, and outbreaks of vibriosis caused by *V. anguillarum* only occurs at water temperature above 15 °C (37). Multiple environmental factors (e.g. anaerobiosis and darkness (63), presence of divalent cations such as Ca^{2+} and Mg^{2+} (64)) have been shown to enhance survival and pathogenicity in *V. anguillarum*. Notably, copper is an initiating factor of vibriosis in eels (48), and exposure of Chinook salmon and rainbow trout to copper increase their susceptibility to infection by *V. anguillarum* (65).

The infection route of *V. anguillarum* is commonly through the fish skin, but also by oral ingestion of the pathogen through contaminated water or food (66-69). Although the portal of entry has been a subject of discussion within the literature, it is evident that chemotaxis and interactions of *V. anguillarum* towards mucosal surfaces is important (70, 71). Particularly, colonization of the fish skin is critical to cause disease (66, 72), and the gut represents a site of adhesion, colonization and proliferation using the intestinal mucus as a nutrient source (73).

Although *V. anguillarum* mostly is related to fish disease, a recent human death has been reported. In 2017, a 65-year-old woman died from septic shock and multi-organ failure after being admitted to the hospital emergency department in Maine with skin- and tissue infection. *V. anguillarum* was identified in blood cultures obtained after admission, serving the first known case of this bacteria associated with human disease. However, due to the patient's history and various co-morbidities is was not possible to conclude weather *V. anguillarum* was the sole cause of her decline (74).

5.3 Vibrionaceae and chitin- associated interactions

Although several Vibrionaceae members can cause disease in humans, fish and invertebrates, they do not rely on their hosts for survival and are natural inhabitants of marine and brackish waters. These bacteria also occur as free-living inhabitants in the water, sediments or in symbiotic relations, and most species are nonpathogenic. This chapter will elucidate the mechanisms of how some members of Vibrionaceae persist and spread in the environment and emphasize associations between marine bacteria and chitin, one of the most abundant biopolymers in nature.

Chitin as nutrient source

Chitin is a linear polysaccharide that consists of *N*-acetyl-D-glucosamine (GlcNAc) units linked by β-1,4 glycosidic bonds. When synthesized, the chitin chains associate and form stable fiber structures with crystalline properties. Chitin exists in three allomorphs based on the organization of the chitin chains in the fibers: α-chitin (anti-parallel) β-chitin (parallel) and γ-chitin (mixture of parallel and anti-parallel) (75). Chitin is a dominant constituent of rigid structures such as the exoskeleton of crustaceans and insects, and the cell wall of fungi and some algae (76-79). Some reports also indicate that chitin is found in the scales and gut of fish (80, 81), but this is still controversial. Despite the chemical resistance, insolubility and robustness of chitin, microorganisms have developed efficient enzymatic machineries for its degradation (82, 83).

Chitin is the dominant marine polysaccharide as it is used for many functional purposes by a large variety of marine organisms. The ability of chitin degradation is characteristic for several marine bacteria and is a trait that can give advantages for survival and proliferation in the marine environment (83, 84). The chitin degradation pathway is conserved within the Vibrionaceae (85, 86). In the presence of chitin, chitinolytic enzymes are secreted by the bacterium for the purpose of depolymerizing the insoluble chitin chains to soluble small chitooligosaccharides that can be taken up and catabolized by the bacterium. The secreted chitinolytic enzymes are mainly represented by chitinases of family 18 glycoside hydrolases (GH18) and lytic polysaccharide monooxygenases (LPMOs) of family 10 auxiliary activities (AA10), as classified by the carbohydrate active enzyme database (CAZy; (87)). The hydrolytic GH18 chitinases have diverse modes of action and can depolymerize the chitin chains processively from either the reducing or non-reducing end of the chitin chains (also called exo-activity or exo-processivity), or attack the chitin polymer at random sites in the chain (endo-activity) (88). The LPMOs are copper-dependent redox-enzymes that bind directly to the crystalline parts of the chitin, which are not accessible to the chitinases, and cleave chitin chains by an oxidative mechanism using O_2 or H_2O_2 as a co-substrate

(89-91). The nicks in the chitin chains caused by the endo-chitinases and LPMOs represent new binding sites for the exo-chitinases and the complementarity of these enzymes result in an overall synergic reaction (92). The main degradation products resulting from the chitin degradation are *N*-acetyl-D-glucosamine (GlcNAc) and chitobiose ($(GlcNAc)_2$), and to a lesser extent, native and oxidized chitooligosaccharides ($(GlcNAc)_{3-6}$), the latter (aldonic acids; GlcNAcA) arising from LPMO activity. The chitin depolymerization machinery is illustrated in Figure 4.

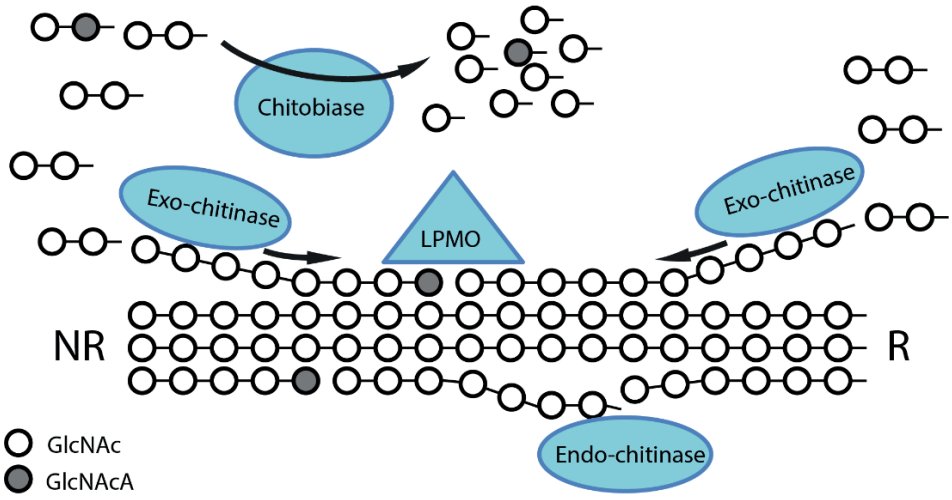

Figure 4. Enzymatic chitin depolymerization. The schematic illustration shows chitin chains (white circles, GlcNAc, connected by lines) being hydrolyzed either by endo-chitinases or exo-chitinases that can have directional specificities, processing chitin chains either from the reducing (R) or non-reducing (NR) ends. The LPMO binds to the ordered, crystalline region of the chitin and introduces chain breaks by an oxidative reaction, yielding an oxidized *N*-acetylglucosamine moiety (*N*-acetylglucosaminic acid; GlcNAcA, grey circles) at the former reducing end. A chitobiase (also called β-*N*-acetylhexosaminidase) cleaves the dimeric sugars resulting from chitinase hydrolysis to monomers (usually an event that takes place in the periplasm). The figure is modified from (88).

The products resulting from an extracellular chitinolytic activity are transported into the periplasm by unspecific porins (93, 94) or by specific chitobiase and chitooligosaccharides ($(GlcNAc)_{2-6}$) transport proteins, named chitoporins (95, 96). In the periplasm, family GH20 *N*-acetylhexosaminidases (also called chitobiases) or *N,N*-diacetylchitobiose phosphorylases hydrolyze the imported chitooligosaccharides to monomeric sugars (97). Phosphotransferase systems are usually responsible for transport of GlcNAc or deacetylated GlcN across the inner membrane, whereas $(GlcNAc)_2$ may in some instances be transported by an ABC

transporter (86). Once present in the cytosol, GlcNAc, GlcN or GlcNAc1P are further processed by enzymes of the amino-sugar catabolic pathway. The reaction products from the LPMO reactions, i.e. chitooligosaccharide aldonic acids are also most likely processed by the mechanisms described above, but this is yet to be demonstrated experimentally.

While several opportunistic pathogens are efficient chitin degraders (*e. g. V cholerae (98), V. anguillarum* (99)*, V. harveyi* (100)), *Al. salmonicida* is proposed incapable of degrading chitin. Firstly, several genes associated with the chitinolytic machinery (*e.g.* several chitinases, a chitoporin and a protein important for regulating expression of the chitin degradative loci) contain mutations or insertions of mobile genetic elements (8). Secondly, neither Hjerde et al or Egidius et al observed chitin degradation by the bacterium, albeit the latter study reported that GlcNAc was utilized (5, 8).

Regulation of chitin catabolism

Utilizing chitin as a nutrient source requires several steps and involves various proteins with different functions (as described above). Consequently, the expression of these genes is under tight regulation. A central mechanism for this regulation in Vibrionaceae involves a two-component chitin catabolic sensor/kinase, namely a periplasmic binding protein (also called CBP) specific for (GlcNAc)n and a histidine sensor kinase (ChiS) (101). The proposed mechanisms of this regulation is that upon the absence of environmental signal, the periplasmic binding protein is bound to ChiS, while in presence of chitooligosaccharides the periplasmic binding protein dissociates from ChiS, in turn activating this sensor kinase, finally resulting in expression of several genes involved in catabolism of chitin (98, 101). In *V. cholerae* activation of ChiS has also been shown to promote horizontal gene transfer, type 6 secretion system (T6SS) dependent interbacterial killing (102) and pathogenesis (103).

The role of chitin in environmental persistence

Biofilm formation and attachment to chitinous surfaces is an important part of the aquatic lifestyle of several Vibrionaceae, and a diverse range of surfaces are available for attachment. Most studied are the associations of *V. cholerae* with chitinous plankton (*e. g.* Zooplankton and phytoplankton, Figure 5), in both marine and freshwater environments (104). Attached to zooplankton, *V. cholerae* can survive longer in seawater than that in its free-living planktonic state, as they are protected from the external environment (105, 106). Furthermore, zooplankton serving as a reservoir of *V. cholerae* are eaten by larger crustaceans (*e. g.* shrimp), which then in turn, contributes to transmission from the marine environment to the food-chain causing food-borne human disease (107). A role for chitin attachment

in environmental persistence has also been implicated in *V. vulnificus*, where C- and E-genotype strains have different ecologies. The E-genotype which is associated with an advantage of inhabitation of oysters is significantly more efficient and capable of binding chitin compared to the C-genotypes that are more successful in infecting the human host (108).

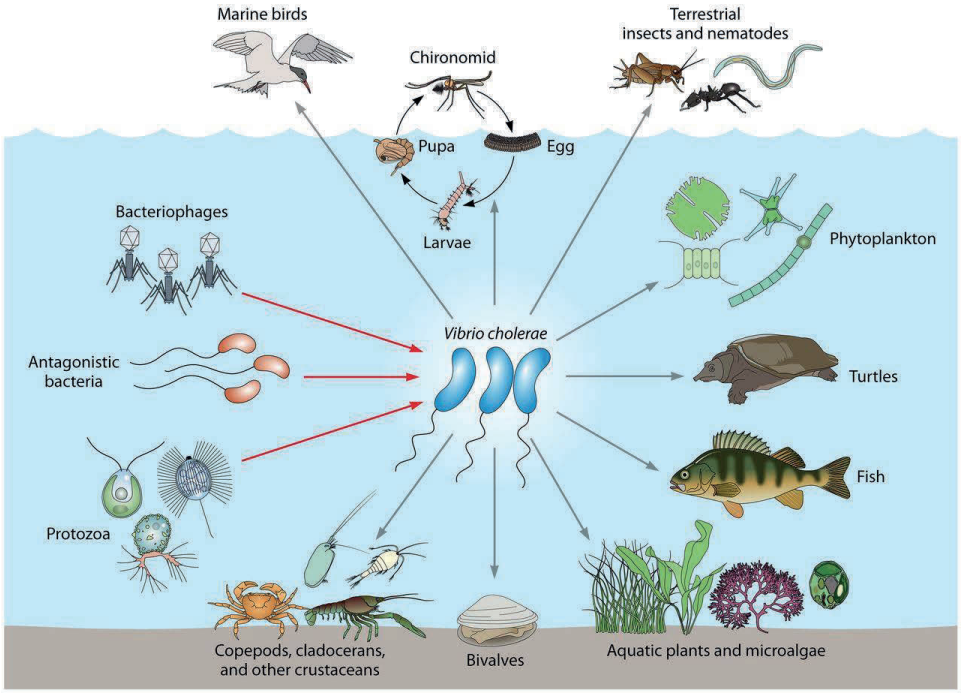

Figure 5: *Vibrio cholerae* interactions in its natural environment. Grey arrows indicate reservoirs such as the mentioned crustaceans and phytoplankton, while red arrow indicate antagonistic relationships. Figure adapted from (109).

Chitin- induced chemotaxis

Chemotaxis towards chitin-related sugars have been reported in several species. Firstly, chemotaxis is related to acquiring nutrients. For example, the chemotaxis of *Vibrio furnissii* toward chitin oligosaccharides is increased up to 3-fold for starved cells. It has been proposed that the bacterium secretes a chitinase, which upon contact- and depolymerization of chitin in the environment produces a chemotaxis gradient of $(GlcNAc)_n$ that attract the bacteria (110, 111). Furthermore, the transition of *Aliivibrio fischeri* from the planktonic lifestyle to symbiotic colonization of the squid host requires multiple regulatory changes. In this context, it has been demonstrated that colonization of the light organ requires *N*-acetylated sugars as a chemotaxis signal for *Al. fischeri* (112). Once inside the light organ, the HTH-type luminescence regulator (LitR) induces luminescence (113).

Chitin- induced competence

In addition to being a relevant nutrient source in the marine environment, chitin also induces natural competence and transformation in several species. Natural competence is a process of horizontal gene transfer that allows bacteria to take up free DNA from the environment and incorporate the foreign DNA into their own genome, thereby becoming naturally transformed. Chitin-induced competence was first reported in *V. cholerae* (114), but later also identified in other species of the Vibrionaceae family, namely *V. vulnificus* (115), *Al. fischeri* (116) and *V. parahaemolyticus* (117). In *V. cholerae*, the most prominent experimentally demonstrated examples of chitin-induced transformation is the spread of an un-mobilizable cholera toxin prophage between strains (118), and serogroup conversion of an O1 strain by O37 genomic DNA (119). Chitin-induced competence is associated with a regulator TfoS that senses chitin degradation products and activates competence in *V. cholerae*, by sequentially upregulating TfoR and TfoX (120). Similarly, TfoX is essential for competence in *V. parahaemolyticus* (117) and *Al. fischeri* (116). The latter study also showed that TfoX homologs are present in all sequenced Vibrionaceae. Furthermore, it has been proposed that there is a link between ChiS and TfoS activation (121).

5.4 Virulence determinants of the Vibrionaceae

The ability of a bacterium to infect its host and cause disease majorly depends on the expression, regulation and synthesis of a variety of specific proteins and molecules. These determinants of virulence, called virulence factors, may contribute to several parts of pathogenesis like attachment, colonization, immune evasion, immune suppression, and nutrient acquisition. In this chapter virulence determinants in Vibrionaceae are described with main focus on the *Vibrio* and *Aliivibrio* genera elucidating the importance of motility, quorum sensing, iron acquisition, toxins, outer membrane vesicles and especially chitinolytic enzymes.

Flagellar motility and chemotaxis

Motility is associated with chemotactic movement, the ability of bacteria to swim towards attractants or environmental stimuli, and plays a vital role for Vibrionaceae in the aquatic environment and in virulence (122). Flagella are helical propellers protruding from the surface of bacteria. These organelles facilitate movement through rotary motors embedded in the cell membrane (123, 124). The flagellation pattern (*e. g.* number and arrangement) varies within the Vibrionaceae family and includes single or multiple polar flagella, peritrichous flagella and even mixed flagellation (125). Transcription of flagella-related genes is tightly regulated by several regulatory proteins and transcription factors (126, 127). Tight regulation is important as motility is highly cost-effective and essential for adaption to changing environment or transition to the host. For example, *V. parahaemolyticus* possess a dual flagellar system that is differentially expressed depending on the surrounding environment (128, 129).

Several in vitro and in vivo studies have demonstrated the importance of motility in pathogenesis. For example, non-motile strains of *V. cholerae* show reduced colonization of mouse intestine compared to motile strains (130, 131), whereas the flagellum deficient FlgE deletion mutant of *V. vulnificus* show reduced virulence in mice, and also decreased adherence to cell lines in vitro (132). The Flagellin A (FlaA) or Motility protein A (MotA) of *V. anguillarum* were essential for virulence in rainbow trout in immersion challenge experiments, but not when intraperitoneal injection (i.p injection) was used (38). In contrast, MotA and FlaA deletion mutants of *Al. salmonicida* resulted in reduced virulence in immersion challenge of Atlantic salmon, but deletion of FlaA also reduced virulence after i. p injection (133). Thus, the authors suggested that the flagella of *Al. salmonicida* may be involved in parts of pathogenesis not related to motility.

Chemotactic motility towards components in the mucosal surfaces covering skin and guts is important for *V. anguillarum*. The pathogen can utilize intestinal and

skin mucus as nutrient source (134, 135), and a chemotactic response is observed when the bacteria is exposed to mucus in vitro (70).

Quorum sensing

Quorum sensing (QS) is a bacterial cell-to-cell communication system controlling gene expression in a population-dependent manner. Small chemical molecules called autoinducers (AIs) are produced, secreted and recognized by surrounding bacteria influencing a wide range of processes, including virulence.

One of the most studied QS systems is that in *Al. fischeri*, a marine bacterium that induces bioluminescence in a cell-population-dependent manner in association with its symbiotic host, the Hawaiian bobtail squid (*Euprymna scolopes*)) (136). Three QS systems are described for *Al. fischeri*, specifically LuxI-LuxR, AinS-AinR and LuxS-LuxPQ. In some detail, homoserine lactone autoinducer (AHL) N-3-oxo-HSL (termed AI-1) is synthesized by LuxI (137). At high cell density, AI-1 interacts with a transcription factor LuxR, resulting in expression of bioluminescence genes, *luxICDABE* (138, 139). AinS synthesize AHL autoinducer N-octanoyl-L-homoserine (C8-HSL) which interacts with hybrid sensor kinase AinR (140). LuxS produces furanosyl diester (AI-2), that binds LuxP to form a LuxP-AI-2 complex, which is sensed by LuxO, a hybrid sensor kinase LuxQ (141).

QS systems and regulators have multiple associations with virulence. LuxO of *V. cholerae* affects biofilm formation and protease production (142), and QS dependent biofilm in *V. cholerae* are important for colonization (143). *V. alginolyticus* LuxS is involved in regulation of flagellar biosynthesis, protease production, extracellular polysaccharide production and biofilm development (144), while LuxO and SmcR have been shown to regulate cytotoxicity (145). Particularly, members of the highly conserved TetR family are master regulators of QS. This family include HapR in *V. cholerae* (146), SmcR in *V. vulnificus* (147), LitR in *Al. fischeri* and *Al. salmonicida* (148), OpaR in *V. parahaemolyticus* (149) and VanT in *V. anguillarum* (150), of which many are associated with virulence.

Several QS systems are encoded in the genome of *Al. salmonicida,* including LuxS-LuxPQ, LuxI-LuxR, and AinS-AinR and the lux operon (8). Despite the presence of the lux operon, *Al. salmonicida* is a cryptic bioluminescent bacterium (151). Nevertheless, a LuxA deletion strain of *Al. salmonicida* showed reduced and delayed mortality in vivo, indicating a role of the Lux operon in virulence (152). Moreover, Atlantic salmon challenged with an *Al. salmonicida* LitR deletion mutant showed reduced mortality compared to groups exposed to the wild-type. In vitro, deletion of the LitR encoding gene resulted in several phenotypical changes such as increased adhesion, aggregation, and ability to form a biofilm (148). LuxI has

also been shown to regulate the expression of a high number of genes, of which many are associated with motility and biofilm formation (153).

V. anguillarum, harbors the QS systems VanI-VanR (154), VanM-VanN (155), and VanP-Q (156), but no direct link with virulence has been shown. However, the QS regulated VanT is involved in regulation of biofilm formation and protease production (150). Furthermore, QS is an important part of the stress response. The sigma factor and stress response regulator RpoS (157), which is linked to QS, regulates expression of the master regulator VanT (158).

Iron acquisition

A major property of the marine and host environment is the limited availability of iron, an essential micronutrient for all living organisms and important cofactor in several cellular processes. Bacteria have developed a variety of iron acquisition strategies that are important for survival and persistence within the host (159, 160).

Several bacteria and members of the Vibrioneceae synthesize siderophores, small molecules that bind ferric iron with high affinity. Synthesis of siderophore molecules (*e. g.* vibriobactin in *V. cholerae*) is mediated by proteins encoded by gene clusters (*e. g. vibABCDEFH*). Specific receptors recognize the siderophore-ferric complexes in the outer membrane (*e.g.* ViuA for vibriobactin), which are further transported into periplasm via the TonB systems (Figure 6). Ligand-specific periplasmic binding proteins- and inner membrane permeases further transport siderophore complexes into the cytoplasm where the iron molecules are released from the siderophores (Figure 6).

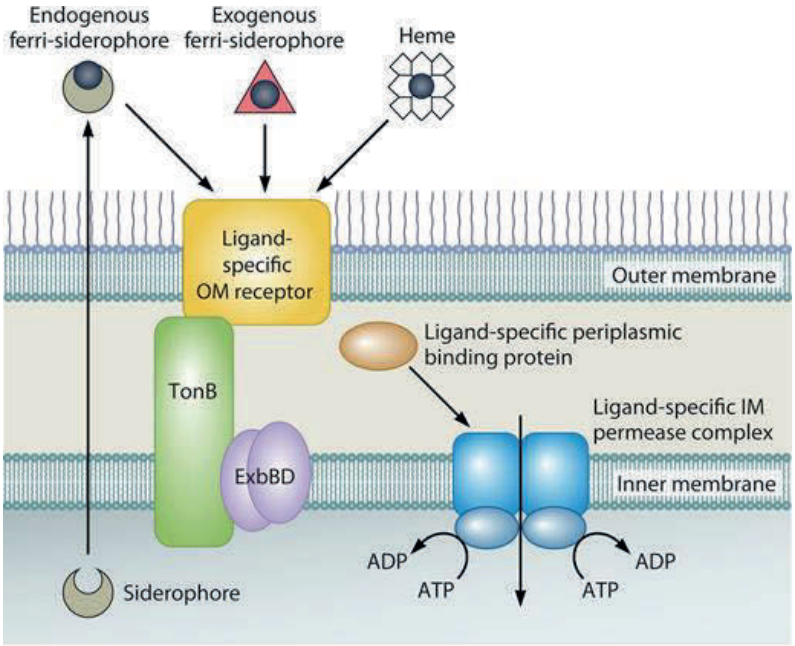

Figure 6. Siderophore uptake and transport. Siderophores are produced inside the cytosol and transported extracellularly where it binds ferric iron. The endogenous siderophore-ferric iron complex is recognized by ligand specific receptors. Other receptors that recognize exogenous ferric-siderophores may be present. Transport into the periplasmic space is dependent on TonB systems. The figure is adapted from (161).

The siderophore biosynthesis gene clusters and corresponding receptors are widely distributed within Vibrionaceae. Most species have at least one siderophore system, but the number of different receptors encoded typically exceeds that of the biosynthetic clusters (162). For example, the receptors IrgA, VctA, FhuA, PeuA and DesA, are found in many species within the Vibrionaceae, despite the corresponding siderophores not being synthesized (162). The ability to aquire iron from multiple siderophores could be an advantage in the environment and in host colonization. A recent study with *V. cholerae* showed enhanced growth in the presence of other siderophore producing species in simulated marine, low-iron environments and within a murine host model (163).

Depending on the serotype and strain, *V. anguillarum* can synthesise three siderophores: anguibactin, vancherobactin and piscibactin. The major part of serotype O1 strains harbors the pJM1 plasmid that contains genes encoding anguibactin synthesis and thus produce anguibactin. Vanchrobactin is produced by strains lacking the pJM1 plasmid, while some strains belonging to serotypes O1, O2 and O3 harbor genes for production of both vanchrobactin and piscibactin (164). The role of each siderophore in virulence of *V. anguillarum* is not completely

understood, but evidence exists for anguibactin and piscibactin being important for the pathogenicity of the bacterium (164-166). Firstly, the pJM1 plasmid harboring anguibactin synthesis genes and regulators (*AngABCEB/GMTHRNUD*) is highly associated with virulence (165, 166). The Ferric-anguibactin siderophore complex is recognized by the receptor FatA, and AngR has been demonstrated to be important for regulation of anguibactin production and virulence (167). Secondly, the production of the siderophore piscibactin by *V. anguillarum* is a relatively recent discovery (164). Piscibactin is the main siderophore produced by closely related *V. ordalii* (168), and the piscibactin genes (*irp*) in *V. anguillarum* and *V. ordalii* are located in a High-Pathogenicity Island (*irp-HPI*) which is found among many species of the Vibrionaceae family (162). Piscibactin contributes to the virulence of *V. anguillarum* more than that of vanchrobactin in turbot (164), and it is preferentially produced at low temperatures (169).

Siderophore production is also known for *Al. salmonicida,* which synthesizes significant amounts of the siderophore bisucaberin at low temperatures (170). The genes encoding synthesis of bisucaberin are highly upregulated under iron limiting conditions and production of the siderophore is strongly regulated by the ferric uptake regulator Fur (171).

In addition to siderophore related stategies, bacteria can acquire iron from heme and hemoglobin. Free heme is captured by outer membrane transporters (*e. g. V. cholerae* HutA (172) and *V. anguillarum* HuvA (173)), and transported inside the cell through an energy-dependent process facilitated by TonB1 and TonB2 complexes. In *V. anguillaurm* both heme uptake and siderophore uptake is dependent on TonB systems. TonB2, but not TonB1, functions in the transport of anguibactin and enterobactin, while both TonB proteins can operate in the transport of ferrichrome and heme. Deleting the gene encoding TonB2 synthesis in *V. anguillarum* resulted in a significant reduction in virulence (174). The author of the latter study concluded that a functional TonB2 system is essential for ferric-anguibactin transport and thus also virulence.

Other iron transport systems reported in Vibrionaceae and several gram negative pathogens are sequestration of iron from transferrin, uptake of Fe(II) ions via the Feo system (*feoABC*), secretion of extracellular Fe(III)-reductases or uptake of Fe(III) through the Fbp system (*fbpABC*$_1$ and *fbpABC*$_2$) (175, 176), although the role of these mechanisms in virulence is not clear.

Endo- and exotoxins

Bacterial toxins are virulence factors that may induce damage to host cells or modulate host immune components. Toxins are majorly classified into two groups; exotoxins secreted by the bacterium, or endotoxins that are a part of the bacterial cell such as the lipopolysaccharide antigen (LPS) of gram negative bacteria (Figure 7).

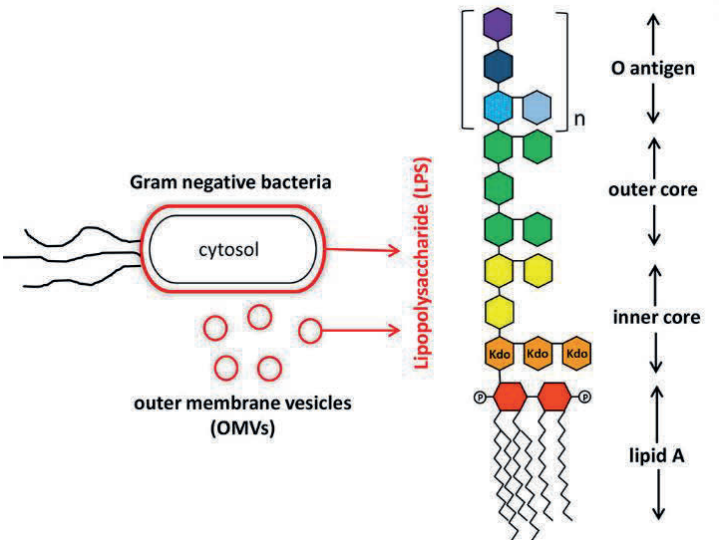

Figure 7. Structure of the lipopolysaccharide (LPS). The LPS structure consists of a core lipid part, and a polysaccharide component (O-antigen). Illustration adapted from (177)

The LPS O-antigen structure of *V. anguillarum* was shown to be important for serum resistance in a study performed by Boesen et al, (178). In the latter study, high molecular weight O-antigen side chains were indicated to prevent the activated complement from damaging the bacterium. The importance of LPS in virulence has also been studied by disabling parts of the O-antigen assembly apparatus through the deletion of genes encoding O-antigen ligases. These enzymes participate in the synthesis of LPS by facilitating the binding of O-antigen to the core oligosaccharide-lipid A complex. A study where the duplicated gene *Waal*, that encodes a putative O-antigen ligase, was deleted in *Al. salmonicida*, the deletion strain, resulted in a significant reduction of virulence in vivo (179).

In contrast to the endotoxin, the exotoxins include a broad range of proteins with different mode of action (*e.g.* hemolysins, proteases, collagenases, phospholipases, cytotoxins).

Hemolysins are important virulence factors, especially in pathogenic Vibrionaceae (180-182). These molecules may cause damage to host erythrocytes, neutrophils and polymorphonuclear cells. The major types of hemolysins found in

Vibrionaceae are TDH (thermostable direct hemolysin) family, HlyA (E1 Tor hemolysin) family, TLH (thermolabile hemolysin) family and the δ-VPH (thermostable hemolysin) family (182). Examples from these families have for instance been studied in *V. parahaemolyticus* (183), *Photobacterium damselae subsp. damselae* (former *Vibrio damsela*) (184, 185), *V. cholerae* (186), and *V. vulnificus* (187). Several hemolysins have been identified in *V. anguillarum* (Vah1-5), in addition to a repeat-in-toxin (*rtx*) operon that contributes to hemolytic activity (188, 189). The general trend observed for the functional properties of the hemolysins, is that deletion strains are less virulent (184, 188-191), and that the recombinant enzymes show cytotoxic activity towards cell lines, especially in damage of erythrocytes (187, 192-194),

Proteolytic enzymes hydrolyze peptide bonds and have various physiological roles. Enzymes with proteolytic activity secreted from pathogenic Vibrionaceae are mainly metalloproteases or serine proteases that either have direct roles in virulence by digesting host proteins or indirect by processing other virulence factors (195). For example, the *V. cholerae* hemagglutinin/protease activates the major virulence factor, cholera enterotoxin (CT) by nicking off the subunit associated with its inactive form (196), while the metalloprotease Vvp of *V. vulnificus* is associated with hemorrhagic septicemia and vascular permeability in rats (197, 198), utilization of heme (199) and colonization of mucosal surfaces in eels (200). *V. anguillarum* secretes a zinc metalloprotease (EmpA) that contributes to virulence in several species of fish (*e.g.* rainbow trout (201), Atlantic salmon (202) and turbot (203)). EmpA is expressed when growing on salmon gastrointestinal (GI) mucus (202, 204), and is suggested to play a role in the colonization and growth within the host intestine (202), swarming motility and hemolytic activity (203).

Although the genome of *Al. salmonicida* harbors several putative hemolysins and proteases, no toxin activity has been described, and expression of hemolysin genes are indicated downregulated after entering the host (28).

Outer membrane vesicles

Membrane vesicles (OMVs) are spherical structures secreted from the surface of many gram negative bacteria (Figure 8). Several bacterial components are found in these structures, including periplasmic and outer membrane proteins, LPS, DNA, RNA, cytoplasmic proteins, toxins and chaperones (Figure 8). Typically, OMVs are carrying both cytosolic and periplasmic contents, encased in the outer membrane embedded with LPS and outer membrane proteins (205). Pathogens often produce more OMVs compared to non-pathogenic bacteria, and secretion has been associated with host-pathogen interactions, biofilm formation, toxin delivery and bacterial survival (206). Since these vesicles can induce an

immunogenic response, they have been investigated and studied for use in vaccines (207).

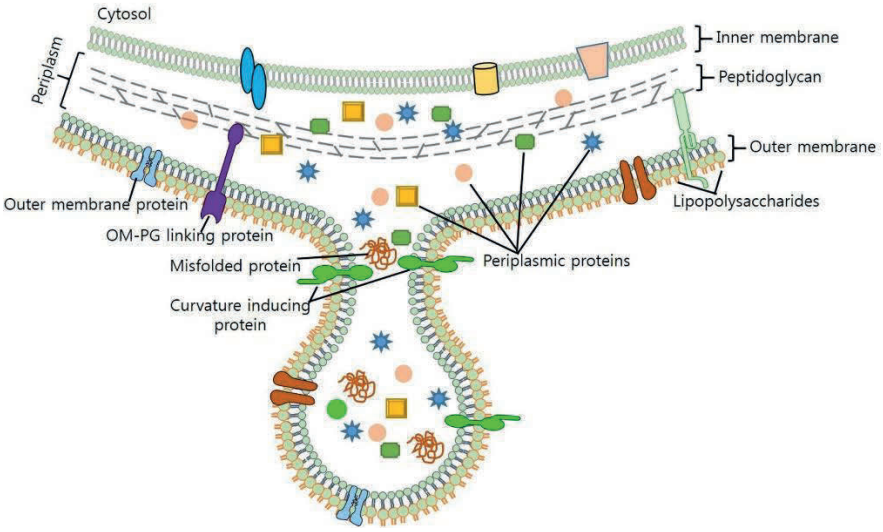

Figure 8: OMV production in gram negative bacteria. Figure depicts the composition of OMV, cargo selection and loading as part of OMVs. Adapted from (208)

Al. salmonicida was observed to produce small membrane blebs emerging from the outer membrane adhering to intra- and intercellular material (29). These blebs may be OMVs later observed by atomic force microscopy (26). Little is known about the importance of these in virulence of *Al. salmonicida*. Closely related *Al. fischeri* has been demonstrated to produce OMVs that trigger host development favoring the symbiosis between *Al. fischeri* and its squid host (209).

V. anguillarum is shown to produce OMVs presenting enzyme activities including metalloprotease, hemolysin and phospholipase. The OMVs stimulated the production of inflammatory cytokines such as TNF-α, IL-1β and IL-6 in a Japanese flounder model (*Paralichthys olivaceus*) (210).

Resistance to oxidative stress

Resistance to oxidative stress resulting from exposure to reactive oxygen species (ROS) is an important determinant of virulence. ROS include superoxide anion, hydrogen peroxide (H_2O_2), hydroxyl radicals, hypochlorous acid and chloramines (211). ROS can be encountered in the host environment as an early response of host innate immunity. Excess amount of ROS can be produced by phagocyte NADPH-oxidase in response to pathogen recognition (212). ROS can damage DNA, proteins, and lipids, and to repair oxidized proteins, bacteria utilize several enzymes (*e. g*. thioredoxin, glutaredoxin and methionine sulfoxide reductase) (213). Bacteria have developed defense systems to manage oxidative stress by

producing enzymes that detoxify the ROS (*e.g.* catalase, peroxiredoxin and superoxide dismutase). For example, catalase detoxify H_2O_2 by converting H_2O_2 to oxygen and water (214). Peroxiredoxins degrade peroxides such as H_2O_2 and alkyl hydroperoxides, but are also involved in detoxification of reactive nitrogen species (215, 216). Another mechanism of managing ROS is to indirectly inhibit the activity of the NADPH-oxidases. For example, in *V. parahaemolyticus,* an effector called VopL limits the host ROS production, by inhibiting assembly of the NADPH oxidase at the cell membrane (217). Some pathogenic bacteria even exploit ROS to their advantage. *E.g. V. vulnificus* RtxA1 modulates a GTPase that play an important role in the activation of host NADPH-oxidase. By modulating this GTPase, the pathogen induce ROS generation within the intestine of mice, thereby causing cell death to the host intestinal epithelial cells (218). In many bacteria, including Vibrionaceae, the response to oxidative stress is controlled by a transcriptional activator OxyR (LysR family of transcriptional regulators) (219, 220).

The inhibition of leukocyte respiratory burst has been reported as a major evasion mechanism of *V. anguillarum* in sea bass (221). It is also suggested that *V. anguillarum* is able to inhibit production of superoxide anions by trout macrophages in vitro (222). No extensive studies exist on the general response of *V. anguillarum* to oxidative stress caused by H_2O_2, whereas *Al. salmonicida* upregulates gene expression of catalase, peroxidase, glutaredoxin and thioredoxins in presence of H_2O_2 (223).

Chitinolytic enzymes

The hypothesis suggesting that chitinolytic enzymes can be virulence factors has existed for decades due to the regular identification of such proteins or encoding genes as up-regulated in pathogenesis-related “omics” studies. Despite these many indications, these enzymes have not received much attention in the context of virulence, possibly since they are primarily related to chitin depolymerization for nutritional purposes. Nevertheless, many studies exist that provide evidence linking chitinases and LPMOs (formerly known as chitin binding proteins “CBPs”) to pathogenesis. Due to the emphasis on chitinolytic enzymes as virulence factors in this PhD thesis, the following text will not be limited to the Vibrionaceae.

Chitinases as virulence factors

As previously stated, chitinases are hydrolytic enzymes that cleave the β-1,4 glycosidic bond of chitin chains. Since many heterogenous carbohydrate structures contain β-1,4 connected GlcNAc moieties, or monosaccharides similar to GlcNAc, it is not unexpected that chitinases may have evolved to accept substrates other than chitin. Indeed, some examples exist of such chitinases and many are related to virulence. For example, Frederiksen et al. showed that a

variety of bacterial chitinases, including enzymes from the pathogens *Listeria monocytogenes* and *Salmonella enterica* serovar Typhimurium, could bind and hydrolyze LacNac (Galβ1-4GlcNAc) and LacdiNAc (GalNAcβ1-4GlcNAc), carbohydrate motifs found in mammals (224). In the context of virulence, the gene encoding the *S. enterica* chitinase has been observed upregulated during infection of macrophage and epithelial cells (225, 226), further indicating a role of th enzyme in virulence. The two *L. monocytogenes* chitinases (ChiA and ChiB) are also coupled to virulence, as they are both regulated by the virulence regulator PrfA (227). The function of the *L. monocytogenes* ChiA chitinase has also been indicated to suppress host innate immunity in an in vivo study showing that ChiA was needed to maintain bacterial replication in the host (228). Interestingly, expression of the *L. monocytogenes* chitinases is also regulated by chitin (227) and both enzymes are chitinolytic (229), indicating a possible dual functionality of these proteins. The chitinase ChiA2 of *V. cholerae* has been shown to de-glycosylate mucins and to be important for the survival and pathogenesis of the bacterium in the host intestine (230). The authors of the latter study suggested a nutritional role for this chitinase, as it would provide the bacterium with soluble carbohydrates. ChiA2 is also indicated to be important for chitin degradation and catabolism for *V. cholerae* (86), indicating a possible dual functionality also for this enzyme. Another chitinase that has been linked to virulence is ChiA from *Legionella pneumophila*. This enzyme is required for the persistence of the bacterium in the lungs of mice (231), and a recent study showed that it can hydrolyze mucin by a novel metal-dependent mechanism (232).

There are also several “omics”-type studies linking chitinases to virulence by circumstantial evidence. For example, the gene encoding the *Enterococcus faecalis* chitinase *Ef*Chi18A (EF0361) is upregulated upon exposure of the bacterium to blood or urine (233, 234), the *Pseudomonas aeruginosa* PA14 chitinase ChiC (PA2300) has been observed up-regulated in modified artificial-sputum medium that mimics the lung sputum environment of cystic fibrosis individuals (235), and the secreted proteome of winter ulcer bacterium *Moritella viscosa* which is cytotoxic to cell lines in vitro, has been observed to contain chitinases (236).

LPMOs as virulence factors

LPMOs represent a recently discovered enzyme family, as the activity was first identified in 2010 (89). Prior to 2010 LPMOs were called chitin or cellulose binding proteins (CBPs) as one of their prominent properties was the ability to bind to these insoluble polysaccharides. The function of the CBPs was unclear as these proteins were thought to be non-catalytic, but nevertheless secreted along with other glycoside hydrolases by bacteria and fungi feeding on carbohydrate containing

substrates (237, 238). Since their discovery, the majority of the studies on LPMOs have been related to carbohydrate degradation and biomass conversion (reviewed in (239, 240)), and little attention has been given their potential roles in virulence, despite the existence of evidence for the latter.

The most important pre-LPMO studies of virulence related LPMOs/CBPs describe the properties of the *V. cholerae* colonization factor GbpA. This LPMO/CBP was originally shown to bind GlcNAc and was therefore given the name GlcNAc binding protein A (GbpA) (241, 242). Deletion of the GbpA encoding gene from the *V. cholerae* genome rendered the bacterium unable to colonize the host gut, indicating importance for host colonization and giving it the additional name "colonization factor" (242, 243). Combining the fact that the protein was found to bind mucins and that the *V. cholerae* GbpA deletion variant showed reduced ability to bind to mucin-containing epithelial cell surfaces, suggested that the role of GbpA was to enable binding and colonization of the bacterium to host mucosal surfaces.

In parallel to the work on GbpA, several studies reported up-regulation of CBPs/LPMOs/GbpA orthologs, further coupling the function of these proteins to virulence. For example, the *E. faecalis* LPMO (*Ef*CBM33) encoding gene, was similarly to the chitinase of this bacterium, upregulated when the bacterium was exposed to human blood or urine (233, 234). The *Yersinia enterocolitica* LPMO, ChiY, was proposed to be a potential virulence factor based on its secretion by the type II secretion system (244), whereas the *Serratia marcescens* LPMO CBP21 was related to virulence based on its ability to mediate adhesion between bacteria and human colonic epithelial cells (245). Importantly, an in vivo experiment attempting to determine the roles of the chitinolytic enzymes of *L. monocytogenes* showed that the LPMO/ LPMO2467 deletion variant (and also the chitinase deletion mutants), were defective for growth in spleen and liver in mice (246).

Data relating LPMO activity to virulence was very recently reported in a study elucidating the function of the *P. aeruginosa* LPMO, CbpD (247). CbpD was shown to promote the survival of the bacterium in human blood, a function that was dependent on the LPMO being catalytically active. Lack of CbpD hindered *P. aeruginosa* in establishing a lethal systemic infection in mice. The function of the protein was related to attenuation of the terminal part of the complement system. This function of CbpD was markedly different from what has been proposed for GbpA, indicating that LPMOs may be utilized differently depending on the pathogenic strategy of the bacterium. The role of CbpD in virulence had earlier been indicated by studies showing its induction by human respiratory mucus (248) and its high abundance in the secretome of cystic fibrosis associated *P. aeruginosa* strain (249).

Finally, it should be noted that not many studies of LPMOs from fish pathogens exist. However, *Aeromonas salmonicida* has been subjected to a comprehensive secretome analysis (virulent vs. non-virulent) and this study identified all chitinases and the LPMO as potential virulence factors (250).

6 Outline and aims of the thesis

Determining how virulence factors are orchestrated to enable pathogenic bacteria to bypass host defenses is important for understanding the underlying biology of pathogenesis and to provide new clues and targets for combating infections. Two vibriosis causing bacteria were investigated in this project, *Aliivibrio salmonicida* and *Vibrio anguillarum*. There was conflicting reports in the literature about the ability of *Al. salmonicida* to catabolize chitin and the disruption of many genes in the chitin utilization pathway could indicate that the chitinolytic enzyme genes remaining intact in the genome of the bacterium could have other roles, for example in virulence. On the other hand, *V. anguillarum* is an efficient chitin degrading bacteria, but few comparative studies on its proteome under different conditions have been reported. Thus, the aim of the current study was to investigate the molecular determinants of virulence in *Al. salmonicida* and *V. anguillarum* using a multidisciplinary approach. The following topics were specifically addressed:

Paper I: Is the putative chitinolytic machinery of *Al. salmonicida* able to depolymerize chitin? Does chitin provide nutrition for the bacterium?

A variety of complementary experimental methods was used to address these questions, including cultivation assays, production of recombinant enzymes, biochemical assays, label-free quantitative protemics and In-frame gene deletions of the bacteria.

Paper II: Are the chitinolytic enzymes of *Al. salmonicida* part of the bacteriums pathogenicity?

To test this hypothesis the pathogenicity of *Al. salmonicida* and LPMO deletion variants was investigated in an immersion challenge experiment were the development of CWV in Atlantic salmon smolts was monitored.

Paper III: How does *V. anguillarum* respond to host-mimicking stress factors? Will iron deprevation, oxidative stress or presence of host components result in altered proteome?

By exposing the bacterium to a variety of host mimicking stress factors such as iron deprivation, oxidative stress (hydrogen peroxide) and Atlantic salmon serum, comparative label-free quantitative proteomics was used to determine the proteomic responses of *V. anguillarum*.

7 Summary of papers

Paper I: The fish pathogen *Aliivibrio salmonicida* LFI1238 can degrade and metabolize chitin despite major gene loss in the chitinolytic pathway

Aliivibrio salmonicida LFI1238 is thought to be incapable of utilizing chitin as a nutrient source since approximately half of the genes representing the chitinolytic pathway are disrupted by insertion sequences. In this paper, the chitinolytic potential of *Al. salmonicida* was thoroughly portrayed by a combination of biochemical characterization of the chitinolytic enzymes, gene deletion and cultivation experiments, gene expression analysis and proteomics. Cultivation assays showed that *Al. salmonicida* LFI128 can utilize GlcNAc, $(GlcNAc)_2$ and β-chitin as sole carbon sources, and that all three enzymes were needed for this ability. However, the chitinase was found more important than the LPMOs. Biochemical characterization of the recombinant enzymes showed that *As*Chi18A has low chitinolytic activity compared to chitinases from well-known efficient chitin degrading bacteria. The activity of *As*Chi18A was also lower than *As*LPMO10A and *As*LPMO10B, but synergy was observed when combining the chitinase with LPMOs. Finally, label-free proteomics identified expression of *As*Chi18A, *As*LPMO10A and *As*LPMO10B, in which *As*LMP10A was generally found among the most abundant proteins. The proteomics data further revealed proteins with a putative role in uptake, transport or downstream processing of chitin degradation products, and peptides produced from chitinase pseudogenes.

In conclusion, our results show that *Al. salmonicida* LFI1238 can utilize chitin as a nutrient source and that the GH18 chitinase and the two LPMOs are needed for this ability.

Paper II: Chitinolytic enzymes confer pathogenicity of *Aliivibrio salmonicida* LFI1238 in the invasive phase of cold-water vibriosis (CWV)

Aliivibrio salmonicida is the causative agent of cold-water vibriosis (CWV), and virulence-associated factors that are essential for the full spectrum of *Al. salmonicida* pathogenicity are largely unknown. Chitinases and chitin-active lytic polysaccharide monooxygenases (LPMOs) have been indicated to play roles in both chitin degradation and virulence in a variety of pathogenic bacteria. The *Al. salmonicida* LFI1238 genome harbours genes encoding two LPMOs family AA10 (*AsLPMO10A, AsLPMO10B*) and one chitinase GH18 (*AsChi18A*). All three enzymes can depolymerize chitin and are important for the ability of the bacterium to utilize chitin as a nutrient source. However, the low chitinolytic activity of the chitinase, and constitutive expression of *As*LPMO10A indicated additional roles. In this paper the role of chitinolytic enzymes on the pathogenesis of *Al. salmonicida* LFI238 in Atlantic salmon (*Salmo salar* L.) was investigated. In vivo challenge experiments using deletion mutants of two LPMOs encoding genes *AsLPMO10A* and *AsLPMO10B*, showed that these enzymes were not critical for the host entry or viability of *Al. salmonicida* in the blood of infected fish in early stages of the disease development. However, the bacterial burden in blood and organs was significantly lowered in the invasive phase of CWV after a period of latency (incubation period), especially for fish infected with the *As*LPMO10B deletion strain. In vitro proteomic profiling of deletion mutants compared to wild type in presence and absence of salmon serum resulted in a significantly altered proteome, with a higher number of proteins affected upon exposure to serum. Finally, we were able to solve the three dimensional structure of the *As*LPMO10B catalytic AA10 domain, which revelaed high structural similarity to entomopathogenic LPMOs.

In conclusion, the study found contribution of the LPMOs in the pathogenicity of *Al. salmonicida* in the invasive phase of CWV in Atlantic salmon.

Paper III: Comparative proteomic profiling reveals specific adaptation of *Vibrio anguillarum* to oxidative stress, iron deprivation and humoral components of innate immunity

The gram negative bacterium *Vibrio (Listonella) anguillarum* is the causative agent of vibriosis, a disease associated with severe hemorrhagic septicemia in various marine and brackish water cultured and wild fish, as well as in marine invertebrates. *V. anguillarum* has developed several key strategies to adapt to and to respond to host-associated stresses, resulting in resistance against antimicrobial immune responses. This study aimed to obtain molecular insights into the proteome response of *V. anguillarum* upon exposure to conditions that mimics vibriosis-related stress such as oxidative stress, complement components, and iron deprivation. We also studied how the translation of virulence factors may be governed by growth phase and nutrient availability. Allthough all tested conditions showed proteomic alterations and adaptation, only nine proteins were commonly significantly regulated in all treatments. Exposure to Atlantic salmon serum and iron deprivation resulted in up-regulation of proteins related to iron acquisition and virulence. In general, exposure to vibriosis-associated stresses resulted in modulation of multiple metabolic pathways, indicating the importance of regulating metabolite levels, and the struggle of the bacterium to obtain physiological adaptation.

In conclusion, our data show that *V. anguillarum* adjusts its proteome response differentially according to the environmental stresses and that only a few proteins are commonly regulated across all conditions.

8 Results and discussion

8.1 *Aliivibrio salmonicida* can degrade and utilize chitin

Chitin is important in the ecology of marine bacteria and for several members of the Vibrionaceae family. Prior to our studies, the available literature suggested that *Al. salmonicida* was incapable of utilizing chitin, and there were conflicting results regarding the ability of the bacterium to grow on GlcNAc. As already noted, *Al. salmonicida* is present in the sediments surrounding fish farms, and the microbe can survive for longer periods in suspended state or attached to particles (22, 24). Based on this, it was of interest to investigate the potential of *Al. salmonicida* in utilization of chitin.

Cultivation assays using defined minimal media for *Al. salmonicida* (Asmm) showed that *Al. salmonicida* strain LFI1238 could utilize GlcNAc, $(GlcNAc)_2$ and β-chitin as sole carbon sources (**Paper I**). Our results are in contrast with other studies showing the inability of *Al. salmonicida* to utilize GlcNAc and chitin as nutrient source (8). Employment of different experimental approaches may explain different experimental outcome. Firstly, the growth experiments in paper I were done in liquid Asmm, while other studies used Asmm agar plates containing GlcNAc (8). The same experimental approach was initially attempted in our studies, but solid Asmm did not result in growth of the bacterium even with glucose as carbon source. Thus, it is unlikely to observe growth of the bacterium on solid Asmm supplemented with GlcNAc, possibly explaining the negative results obtained by other studies (8). Furthermore, when planning growth experiments using chitin, the choice of chitin type can influence the experimental outcome. The first step in complete solubilization and depolymerization of chitin is the process of cleaving the polymer into water-soluble oligomers (88), thus for bacteria that grow slowly it is beneficial to use a chitin variant that is easily accessible. The β-chitin used in **paper I** has lower recalcitrance (i.e. easier to degrade by chitinases) compared to α-chitin used in the other study (8), and this can further explain the different conclusions made in the respective studies.

*As*Chi18A plays a central role in chitin degradation

Our results demonstrated that the chitinase and both LPMOs are important for the complete degradation of chitin, however, the individual roles of these enzymes are not straightforward to determine. Deletion of *As*Chi18A reduced the ability of *Al. salmonicida* to degrade β-chitin to a larger extent compared to what was observed for the LPMO deletion strains (**paper I).** This indicates that expression of the

chitinase is the most important factor in the ability of *Al. salmonicida* to depolymerize chitin. In this perspective, it has been suggested that the presence of a ChiA gene in the genomes of Vibrionaceae is a good indicator for chitin metabolism (86).

An important observation made when characterizing the *Al .salmonicida* chitinolytic system was the low efficiency of *Al. salmonicida* in utilizing chitin compared to other Vibrionaceae or well-known efficient chitin degrading bacteria such as *Serratia marcescens* and *Cellvibrio japonicus* (88, 251). Biochemical assays using recombinant *As*Chi18A yielded 50-fold less $(GlcNAc)_2$ compared to *Sm*Chi18A, -B, -C and *Cj*Chi18D (**paper I**). This could be related to the number of chitinases expressed by these bacteria and the predicted pseudogenes of *Al. salmonicida*. It can also be due to low enzymatic activity of *As*Chi18A. The low enzymatic activity indicates that chitin might not be the only plausible substrate for *As*Chi18A. As previously stated, both *L. monocytogenes* and *V. cholerae* harbor chitinolytic activity, but the chitinases are demonstrated to possess activity towards multiple substrates.

Neither of the *V. cholerae* chitinases have been enzymatically characterized with regards to chitin. In addition, the domain arrangements of *As*Chi18A and *Vc*ChiA2 are different compared to each other. Thus, it is not easy to predict whether *As*Chi18A possess a similar dual role to that of *Vc*Chi2. It is however clear that the chitinase genes are an important part of the evolutionary process and adaption of Vibrionaceae (86). The chitinase encoding genes are affected by horizontal gene transfer and duplication (85). This can lead to determinal mutations within the sequences, possibly followed by reduced or loss of ability to degrade chitin, such as predicted for *Al salmonicida* (8). For example, a recent comparative study of marine *Vibrio rotiferianus* and *V. harveyi* showed that while the examined chitinases only differed in 15 amino acids, the enzymatic activity, degradation products, the oligomeric structures and the responses towards environmental conditions (*e. g.* temperature and pH) were different (252).

Both chitinases in *L. monocytogenes* have enzymatic activity towards crystalline chitin on a level comparable to one of the chitinases from *S. marcescens* (*Sm*ChiC) (229). This suggests that *As*Chi18A is less efficient than the *L. monocytogenes* chitinases in degrading chitin. Homology modelling of *As*Chi18A revealed a structure with a shallow binding cleft and arrangement of active site residues that is similar to non-processive endo-chitinases (**paper I**). Interestingly, a recent study characterizing the two *L. monocytogenes* chitinases *Lm*ChiA and *Lm*ChiB showed that the catalytic domain of *Lm*ChiA has a shallow open binding cleft. Furthermore, *Lm*ChiA has sequence similarity with non- processive endo chitinase *Sm*ChiC

(63.21 %) (253). In addition, *Lm*ChiA has an acidic pH optimum (pH 6), which is suggested playing a role in associations with macrophages that contain acidic vacuolar compartments (253, 254). With this in mind, it is tempting to speculate why *As*Chi18A has the unusual property of a double pH optimum (**paper I),** and weather this is related to utilization of the chitinase in various environments**.** Furthermore, incubation of *As*Chi18A with mucus from Atlantic salmon skin revealed an unidentifiable product. Thus, it is tempting to speculate whether *As*Chi18A have enzymaic activity towards mucins such as been shown for *V. cholerae* and *L. pneumophila* (230, 232).

*As*LPMO10A appear to be constitutively expressed

The cultivation assays showed that deletion of the chitinase had larger impact on the ability of the bacterium to grow on chitin compared to the LPMO deletions. However, deletion of the single LPMOs resulted in reduced growth similar to deletion of both LPMOs. This contrasted the biochemical assays using recombinant enzymes that showed that *As*LPMO10A yields twice as much soluble oxidized products compared to *As*LPMO10B (**paper I**). Interstingly, the proteomic analysis of the wild type strain indicated that *As*LMPO10A seems to be constitutively expressed and the expression is independent on the presence of chitin or chitooligosaccharides in the growth medium. The proteomic analysis in **paper II** further strengthened this hypothesis when identified peptides of *As*LMPO10A in samples obtained during growth in LB with or without the presence of serum in both wild type and the *As*LPMO10B deletion strain. This was intriguing, because the virulence related LPMO of *V. cholerae*, GbpA, is ubiquitous expressed in both clinical and environmental strains (255). As previously noted, GbpA of *V. cholerae* has a vital role in attachment to zooplankton and in colonization of human intestinal cells. It has been suggested that the latter role evolved from a primary function in the environment (242). Furthermore, the presence of *V. cholerae* GbpA is regulated by a novel cell-density mechanism, which is proposed to enhance the transition between the host and the aquatic environment (256). Similarly, expression of the GbpA homolog in *V. vulnificus*, is growth-phase dependent and decreases in the stationary phase. The regulation is proposed to play a role in detachment from oyster associated biofilms in the transition to the colonization of the host (257, 258). Moreover, the *V. vulnificus* GbpA binds to mucins and deletion of this gene resulted in lowered mortality of mice compared to wild type (257). Finally, the proteomic analysis in **paper I** and **II** were both analysed in exponential growth, and the gene expression analysis did not detect expression of *AsLPMO10A* in the stationary phase of samples obtained during growth in glucose or chitin. Although speculative, this indicates that the expression appear constitutive in the exponential phase, but this might not be the case for higher cell-

densities. Indeed Khider et al, showed a 10-fold down-regulation of this gene at high cell density compared to low cell density (259).

Expression of pseudogenes

In paper I, peptides from one of the Chitinase A fragments (here called *As*Chi18Bp) were identified in the proteomic analysis, along with peptides from two other pseudogenes (here called *As*Chi19p and *As*Chi18C). Interestingly, *As*Chi18Bp was one out of few proteins only identified in samples obtained grown on chitin but not on glucose. Identification of these pseudogenes as transcribed and translated, leads to several questions. Is the expression of these simply an ancestral revenant, triggered by presence of chitin? Are the translated proteins functional? The cultivation assays clearly show that if these are still functional, a putative contribution in chitin utilization is minimal, since the triple deletion variant is essentially unable to grow on insoluble chitin (**paper I**). The current consensus for explaining the function of gene loss is related to the lack of expression of these genes. However, some studies show transcription and expression of pseudogenes, *e.g*. Feng et al. (260) and Kuo & Osman (261). The latter study by Kuo & Osman, indicates that recently formed pseudogenes may still have intact upstream regulatory regions that may allow transcription and subsequent translation. For *Al. salmonicida* LFI1238 the evolutionary transpositional history of the IS-elements has been investigated, and it is proposed that some of these elements may still be actively transposing. One of the microevolutionary lines is indicated to end adjacent to the VSAL_I1414 gene encoding *As*Chi18Cp. Compared to the other pseudogene chitinases, *As*Chi18Cp is the only one located next to a Vsa2 element where all three ORFs are intact (**paper I**). However, further transposition is suggested to be unlikely (9).

Notably, **in paper II**, the Δ*As*LPMO10B and ΔAB strains up-regulated expression of three transposases. Two of these (encoded by VSAL_I0039 and VSAL_I0029) belongs the Rpn/YhgA-like nuclease family. In *Escherichia coli,* members of this family increases RecA-independent recombination and contributes to horizontal gene transfer (262). The Vsa2 related transposase resulted in 16 different proteins IDs in the proteomics data, and is correspondingly encoded by multiple genes. One of these genes (VSAL_I1417) is part of the Vsa2 element truncating *As*Chi18Cp. In the Vsa2 elements disrupting *As*Chi19p and *As*Chi18C the corresponding gene is predicted to be pseudogenes. The expression of the mentioned transposases may reflect the adaptational ability of *Al. salmonicida*, but it is not clear if this has anything to do with expression of the disrupted chitinases, or what the result of the expression is.

As for the question if transcription and translation of *As*Chi18Bp is influenced by the presence of chitin in the environment, the answer is not straight-forward. Firstly, our study revealed transcription of the *As*Chi18Bp pseudogene during growth in various carbon sources, but only in the exponential phase (paper I), and as stated for the proteomic analysis it was unique to the samples obtained from growth on chitin (only evaluated in the exponential phase). Furthermore, all four pseudogenes were identified in a study evaluating the global transcriptomic response of *Al salmonicida* upon exposure to H_2O_2 (223), albeit no significant changes in the transcription of these genes were obtained. On the other hand, a comparative study on the transcriptomic profile of a LuxI deletion mutant (ΔLuxI) of *Al. salmonicida* LFI1238, revealed significant upregulation of *As*Chi18Bp in ΔLuxI compared to wild type Moreover, the fold change was remarkably higher (8.6) at high cell density compared to low cell density (3.87) (153). Notably, the same study showed high impact of LuxI deletion on the transcription of *As*LPMO10A at high cell density, with almost 40-fold upregulation (153). In light of these studies it may seem that even though these chitinases are disrupted, their regulators are still functional. If there is a biological function of these pseudogenes and their regulation is still not clear.

Regulation of chitin metabolism

Since we revealed the ability of *Al. salmonicida* to degrade and metabolize chitin, it opens a question of whether this trait is regulated in similar manners to that of closely related species. Interestingly, the proteomic analysis in paper I did not identify key regulatory proteins such as ChiS and Tfox. As previously stated, these regulatory proteins are important for regulation of chitin catabolism and competence in other bacterial species in the Vibrionaceae (86, 263, 264). Of note, ChiS is an integral membrane protein, which are generally under-represented in proteomics due to challenges in solubilizing these proteins (265, 266). Thus, we cannot completely exclude the possibility that this protein is present in the membrane of *Al. salmonicida*. Nevertheless, the gene encoding the periplasmic chitin-binding protein, which activates ChiS (263), is disrupted in the *Al. salmonicida* genome (8). In contrast to the chitinase pseudogenes, we did not include the periplasmic binding protein in the analysis. Nevertheless, proteins implicated to have a role in downstream processing, especially those related to amino sugar metabolisms were majorly identified at similar abundance in presence of chitin and glucose, suggesting that other regulatory mechanisms could have developed over time.

8.2 The role of *Al. salmonicida* chitinolytic enzymes in pathogenicity

The findings in **paper I** showed that the chitinolytic enzymes of *Al. salmonicida* are able to bind to chitin, are enzymatically active on chitin, and that the bacterium can utilize this substrate as nutrient source. The low activity of the enzymes and slow growth rate of the bacterium on chitin, however, indicated that additional roles might be possible for these proteins. Thus, to gain insight into the potential roles of the chitinolytic enzymes in virulence, the gene deletion strains obtained in **paper I** were used for in vivo challenge experiments in **paper II** using Atlantic salmon parr/smolts.

*As*LPMOs are important in the invasive phase of CWV

The in vivo challenge experiments showed that neither of the LPMOs were critical for the pathogen to cross the outer barrier. Wild type and mutants were recovered from infected salmon after 10 minutes of exposure to *Al. salmonicida* containing seawater with no significant difference in colony forming units (CFU) pr mL of blood (**paper II**). It must be noted that the high concentration of bacteria in the challenge bath may have concealed a putative role of these enzymes in crossing the outer barrier, and a lower infection dose and higher sample size could have been beneficial, if this was the only hypothesis to be adressed.

After a period of latency (incubation period), deletion of *As*LPMO10A and *As*LPMO10B resulted in decreased bacterial burden in the Atlantic salmon host compared to wild type, especially for *As*LPMO10B. Both mutant strains (and the double deletion strain ΔAB) were attenuated in the spleen and liver of infected fish eight days post immersion challenge (**paper II**). However, only deletion of *As*LPMO10B resulted in decreased bacterial burden in blood (**paper II**).

The reduced bacterial burden in the mutant strains compared to wild type could have different explanations. More experiments are needed to investigate the exact mechanism, but some hypotheses can be made based on existing knowledge of LPMO functions in virulence. For example, the reduced bacterial burden observed for the LPMO deletion variants could be related to LPMO-mediated attenuation of the terminal complement pathway since *P. aeruginosa* LPMO, so called, CbpD was attributed to such a function (247). Several pathogens, including marine bacteria, have developed strategies to evade the first line of defense. For example, the gram negative fish pathogen *Aeromonas hydrophila* inhibits the complement pathways by degrading complement component C3 in grass carp (267). Although the work by Chen et al showed that a metalloprotease was present in large amounts and that this was the central molecule responsible for C3 cleavage, it is

noteworthy that the crude extracellular protease extract that efficiently cleaved purified C3 and C3 in grass carp serum, contained an LPMO (267). Moreover, the complement system is play important role in orchestration of opsonization and phagocytosis. Head kidney and spleen are known to be important for clearing *Al. salmonicida* (30-32). Although speculative, decreased ability to phagocytose *Al. salmonicida* deletion mutants fits with the observation that the bacterial cells are fewer in one of the immune-related organs such as spleen. It must be noted that phagocytic mononuclear cells are also present in the liver sinusoids of many teleost fish (268-270), although it is not clear if this can explain the reduced bacterial burden of Δ*As*LPMO10B and ΔAB in the liver. Decreased bacterial burden in liver and spleen was also observed for in *L. monocytogenes* (246) and *P. aeruginosa* (247)(REF) upon deletion of LPMO genes during systemic infection. Notably, Chaudhuri et al, injected mice with deletion mutants of LmChiA, *Lm*ChiB and LMO2467, where *Lm*ChiA resulted in the most severe reduction of colonization, especially in the spleen. The *Lm*ChiA was later found to modulate host immunity by inhibiting increased expression of the host nitric oxide synthase (228). Thus, it is not unlikely that the reduced bacterial burden of *e.g As*LPMO10B in blood can be explained by some of these examples.

The results of Chaudhuri et al, 2010 and Chaudhuri et al, 2013 raises the question about the role of *As*Chi18A in pathogenicity by *Al. salmonicida*. A putative role of *As*Chi18A in pathogenicity was not thoroughly portrayed such as for the LPMO strains. The reason for not investigating the chitinase was majorly due to experimental limitations such as bacterial cultivation. Intriguingly, according to the CAZy database, the *Al. salmonicida* strain VS224 isolated from Atlantic salmon (10), contains two family AA10 LPMOs in its genome with 100 % identity to *As*LPMO10A and *As*LPMO10B, but no chitinase. This indicates that the LPMOs may be conserved between *Al. salmonicida* strains, and that if *As*Chi18A has a role in virulence it could be strain specific. Of note, the chitinase and LPMOs of *Al. salmonicida* are encoded on different chromosomes. The *As*Chi18A (and chitinase pseudogenes) are located on chromosome I, while the LPMO encoding genes are located on chromosome II.

The effect of LPMO deletion on the proteome

*As*LPMO10A was found among the most abundant proteins in the proteomic data of **paper I,** and both LPMOs showed the same growth deficiency on chitin. It is notable that the *As*LPMO10B deletion strain resulted in the most significant altered phenotype in vivo. When *Al. salmonicida* wild type and deletion variants were exposed to Atlantic salmon serum, the LPMO deletion strains showed significant alterations in their proteome. Firstly, in the absence of serum, the *As*LPMO10A deletion strain differentially regulated 61 proteins compared to 27 and 32 in

ΔLPMO10B and ΔAB, respectively. Most of the regulated proteins in the ΔAB strains were observed upregulated (**paper II**). In the presence of serum, the overall changes in protein abundance (number of significantly regulated proteins) was higher for the ∆B and ∆AB strains. The latter resulted in significant regulation of 94 proteins, almost three times higher than what was shown in the absence of serum. A substantial change in the proteomic profile of the *P. aeruginosa cbpD* deletion strain upon exposure to human serum, has also been reported, indicating the important role of CbpD in the pathogenicity of *P. aeruginosa* (247). The differential response in the deletion variants may reflect different roles of these proteins. While *As*LPMO10A was shown expressed independent on growth media (**paper I** and **paper II**), *As*LPMO10B was mostly identified in presence of chitin and at lower levels (**paper I**), possibly indicating different functions.

Given the multiple roles of *V. cholerae* and *V. vulnificus* GpbA that are associated with chitin degradation, attachment to abiotic surfaces, interactions with mucins and lowered mortality in mice models, it is tempting to speculate that the proteome changes of *As*LPMO10A reflects similar roles related to both the environment and the host. In light of this, GbpA of *V. cholerae* has been characterized and shown to have a modular structure that facilitates binding to different host surfaces (271). It is proposed that once inside the host intestine, GbpA binds to mucin via its N-terminal domain, while domain 2 and 3 bind to the *V. cholerae* surface, which in turn leads to microcolony formation. Moreover, the full-length of *As*LPMO10A has 61% sequence identity to *V. cholerae* GbpA and shows the same multi-modular architecture indicating the possibility of functionally similar roles. Assuming that the *As*LPMO10B on the other hand is more important for the viability of *Al. salmonicida* in the blood of the host, this may be reflected in the increased number of differentially regulated proteins compared to the wild type strain in the presence of serum. A possibility that the two LPMOs have overlapping roles or interact with each other can neither be excluded. However, deletion of *As*LPMO10B did not significantly altered the translation of *As*LPMO10A (**paper II**).

Given the substantially altered proteomes of LPMO deletion strains compared to wild type, the use of multiple deletions within the same strain should be carefully addressed when planning such studies. Evaluation of deletion mutants is limited to predicting the consequence of loss of function. The phenotype of altering two genes can differ from the sum of the individual effect, a phenomenon that is called epistasis (272), which makes it challenging to determine the cumulative effect resulting from the double deletion.

The structure of *As*LPMO10B

The crystallographic analysis of the *As*LPMO10B catalytic domain (**paper II**), revealed a structure very similar to that of viral fusolin. The viral fusolins are released from entomopoxviruses and form so-called “spindels” that are highly associated with virulence of these viruses in insects (273). The exact mechanism of how the viral fusolins enhance virulence is largely unknown, but they are associated with disruption of the peritrophic matrix in the midgut (274, 275). The peritrophoc matrix consitiute of glycoproteins, chitin and proteins in matrix covering the midgut epithelium, serving as a physical barrier (276). Allthough these viral spindels are important for virulence and the LPMO domain of *As*LPMO10B is very similar, it does not necessarily mean that the mechanisms of these two enzymes are the same, but it demonstrates the variety of functions of these enzymes and their “emerging” role as virulence factors.

8.3 Comparative proteomic profiling of *V. anguillarum*

The complete repertoire of virulence factors determines the ability of a bacterial pathogen to establish infection and cause disease. Furthermore, the utilization of this repertoire must be adapted to the various host defense strategies and different circumstances. Considering this, the third paper describes the response of *V. anguillarum* to several conditions mimicking those that the pathogen may encounter within a fish host.

Oxidative stress

Comparative proteomic profiling of *V. anguillarum* in presence and absence of H_2O_2, revealed several interesting regulatory changes. Firstly, the concentration of H_2O_2 greatly affected the global proteomic response as the number of differentially regulated proteins increased with increasing concentration of this oxidant. This was somewhat expected as the applied concentrations were within a broad range, the highest concentration being lethal for many bacteria (277). Nevertheless, the proteomic analysis may indicate enzymes necessary for *V. anguillarum* in resisting ROS, and the lowest concentration (1 µM) is particularly interesting due to the low number of regulated proteins, which indicate specific response. The lowest concentration is the most representable of the possible administration of oxidative stress as a host killing defense, especially during phagocytosis where oxidant concentrations are reported in this concentration range (211).

The three most upregulated proteins (Dihydrolipoamide dehydrogenase, Neutrophil activating protein A and Peroxiredoxin) are related to cell redox homeostasis and oxidative stress. Peroxiredoxins exert peroxidase activity towards H_2O_2 and protect cells from oxidative stress (278), whereas dihydrolipoamide dehydrogenase belongs to the class-I pyridine nucleotide-disulfide oxidoreductase family are known to be sensitive to H_2O_2 (279). It is also worth noting that the data revealed a superoxide dismutase (SOD) (VAA_03368) that is highly expressed at equal levels under all conditions. Superoxide is a ROS that is substantially more toxic than H_2O_2. The activity of SOD on superdioxides yields H_2O_2. Nevertheless, SODs are important for virulence in several pathogens including *V. alginolyticus* (280), *Vibrio shiloi* (281) and *V. vulnificus* (282).

A highly interesting finding is the mentioned regulation of Neutrophil activating protein A (NapA), which was also upregulated in higher concentrations. NapA, is a member of the DNA-binding protein from starved cells (Dps). Deletion of Dps in *V. cholerae* reduced the ability of *V. cholerae* to colonize adult mice intestine and impaired the resistance of the bacterium to hydroperoxides and environmental

stressors (283). Similar results are observed for *Salmonella enterica* (284) and *H. pylori* (285), suggesting that NapA may have a role in *V. anguillarum* in adapting to oxidative stress.

Iron acquisition

The proteomic data obtained in **paper III** suggested that iron acquisition strategies such as expression of the HuvA receptor may be part of the *V. anguillarum* general stress response. However, some findings indicate that *V. anguillarum* adapts these strategies according to different environmental circumstances. Firstly, siderophore-related mechanisms appear to be more requisite upon presence of salmon serum compared to iron depletion. Considering that *V. anguillarum* causes hemorrhagic septicemia this could be a trait important for viability in the blood of the fish.

Two siderophore related proteins, VabB and FhuA, were found upregulated under iron deprivation, suggesting that these are related to general environmental changes of iron levels. FhuA is one of the described siderophores that possibly enables *V. anguillarum* to “steal” iron from siderophores produced by other organisms. VabB on the other hand is related to synthesis of vanchrobactin, which as previously stated is not synthesized in strains harboring the pJM1 plasmid (like *V. anguillarum* NB10 used in this study). Considering this, *V. anguillarum* has been demonstrated to adapt the expression of virulence factors responding to environmental signals such as iron levels and temperature. Interestingly, *V. anguillarum* strain RV22 (serotype O2), lacking the pJM1 plasmid, was shown to upregulate genes encoding the siderophore system vanchrobactin and downregulate those of piscibactin at 25 °C after exposure to 50 µM DIP. Moreover, it has been suggested that Vanchrobactin is more critical for the general environmental behaviour and not necessarily as important within the host.

Finally, a siderophore interacting protein (SIP- protein) is highly interesting, since this protein was only significantly upregulated in the presence of serum with a log2 fold change of ~4. This could be related to the upregulation of anguibactin related proteins. However, little is known about the role of SIP in iron acquisition of *V. anguillarum* (286).

An important difference in the iron deprivation conditions and the serum conditions is that the putative availability of free iron is higher in the Atlantic salmon serum conditions (putative presence of free iron in the medium). Interestingly, Fur was only significantly up-regulated in presence of serum (and only marginally with log2 fold change 0.6). Fur is a negative regulator of iron uptake, and at low intracellular Fe^{2+} levels it inhibits transcription of several genes (including, but not limited to iron

acquisition) by binding to the promotor (287). The proteomics data identified several up-regulated proteins related to iron acquisition after incubation with serum (*e.g* FatA, AngB, AngH). The up-regulation of Fur could indicate that the sampling was performed at a time when *V. anguillarum* had acquired sufficient intracellular iron levels. It must be noted that Fur controls a variety of genes, and that regulation of iron acquisition is not limited to this protein (286, 288).

The importance of metabolic adaptation

One of the findings that stood out in the third study of this thesis, **paper III**, was the modulation of bacterial metabolism as an important mechanism in adapting to environmental changes. Interestingly, supplementation of H_2O_2, the iron chelator DIP or salmon serum to the minimal media, resulted in down-regulation of proteins related to metabolic pathways. This indicates that the response of *V. anguillarum* to oxidative stress, iron-depletion and immune components is not limited to specific proteins indicated to overcome the specific stressor (*e. g*. peroxidases and iron-acquisition related proteins), but also involves the modulation of metabolism-associated pathways. This can be connected to the dynamic relationship between the bacterium and the host as the pathogen must adapt to the hostile environment created by the host defenses (289). Firstly, the bacterium does not face only one "nutritional status" within the host throughout infection (290, 291), and the available nutritional sources can be limited or varied depending on the localization within the host (*e.g*. intestine, blood, macrophages) and the status of the host, which in turn may be affected by the presence of pathogen and bacteria-derived secondary metabolites (292).

Putative virulence determinants

The proteomics data of **paper III** reveal some regulated proteins annotated "uncharacterized" that are especially interesting.Two of these will be discussed here, a maltoporin (VAA_02891) that was found differentially regulated, in serum (Log2 fold change -2.503) and under iron deprivation (Log2 fold change 1.478), and a predicted transcriptional regulator MarR (multiple antibiotic resistance regulator (VAA_01403)) that was upregulated in presence of serum (Log2 fold change 2.468).

MarR family transcriptional regulators are ubiquitous in bacteria and archaea (293). The ability of bacteria to regulate gene expression in response to changes in intracellular metabolites or to environmental cues, is important, and the MarR family transcription factors regulate various cellular processes, including stress response and virulence (293, 294). Members of this family play important roles in the virulence properties of several pathogens. For example, the DNA binding

domain of *V. cholerae* AphA transcriptional regulator is structurally similar to those of MarR (295), and is important in activating expression of virulence related genes (296), whereas a *V. vulnificus* MarR type transcriptional regulator named PecS is involved in processes necessary for managing oxidative stress (297, 298). It is not unlikely that this uncharacterized protein in *V. anguillarum* play a similar role in modulating expression of genes important for septicemia, but it could also have other functions.

VAA_02891 is annotated as “maltoporin” in taxonomic identifier 55601 (NCBI). Maltoporins (LamB family proteins) are abundant in gram negative bacteria and are first and foremost associated with the diffusion of carbohydrates (maltodextrins) across the outer membrane (299). Based on this, it is not surprising that this protein was down-regulated in the stationary growth phase, since several proteins related to metabolism of various carbohydrates were downregulated. Incubation with serum and DIP resulted in differential regulation of this protein (down-regulated in serum and up-regulated in DIP). Interestingly, injecting Zebrafish with LamB protein, resulted in reduced susceptibility towards vibriosis (300). The same study revealed that the antigenic epitopes of LamB in *Vibrio* species (including *V. anguillarum*) are highly conserved and propose this protein as a versatile vaccine candidate. *V. anguillarum* maltoporin has been identified as downregulated at higher salinities (3.5 %), and Kao et al, suggested that higher osmolarity inhibits carbohydrate transport (301). Finally, deletion of a LamB protein in *Aeromonas veronii*, an opportunistic pathogen responsible for septicemia and ulcers in freshwater fish, has been shown to reduce the lethality of this bacterium in Zebrafish and mice (302). Deletion of LamB in *A. veronii* affected motility, biofilm formation and adhesion of *Epithelioma papulosum cyprini* cells in vitro (302). The finding that *V. anguillarum* down-regulates maltoporin in presence of serum can be related to the general changes in composition of the growth media, and/or altered preferation of carbon source. Up-regulation under iron deprivation is not easy to hypothesize, but it could be related to increasing the membrane permeability to ions (303). In presence of maltodextrins, the ion translocation ability of maltoporins are blocked (304). In the end, the differential regulation of *V. anguillarum* maltoporin is an excellent example of *V. anguillarum* altering its metabolism under different circumstances such as encountered over the course of vibriosis.

The LPMO of *V. anguillarum*

A discussion around a putative role of the *V. anguillarum* LPMO cannot be overlooked since this bacterium, similar to *Al. salmonicida* and most other members of the Vibrionaceae, have one or more LPMOs encoded in their genomes. The genome of *V. anguillarum* encodes five chitinases and one LPMO,

and the bacterium is reported to degrade chitin (99, 305). The LPMO is more similar to *As*LPMO10B (100% query cover and 68.37% identity) than it is to *As*LPMO10A (34 % query cover and 28.87 % identity). It is tempting to speculate whether the LPMO of *V. anguillarum* and *As*LPMO10B could be expressed in similar manner, since we did not identify *Va*LPMO in either of the M9 conditions in **paper III**. Gene expression analysis showed transcription of the gene, but the translational level may be too low to be identified in the proteomic analysis. Moreover, the implications that copper may increase susceptibility to infection by *V. anguillarum* is interesting in this perspective as LPMOs are copper dependent enzymes. It must also be noted that the secretome of *V. anguillarum* was not analysed in this study, which possibly could have contained the *Va*LPMO. Interestingly, the gene expression of *VaLPMO* has, in another study, been shown to increase ~19-fold in the presence of 10% salmon serum (247), possibly indicating a role in virulence.

9 Conclusion and future perspectives

9.1 Conclusion

Determining how virulence factors are orchestrated is important for understanding the underlying biology of pathogenesis and to provide new clues and targets for combating infections. The work presented in this thesis reveal several aspects of host-pathogen interactions and the dynamic interactions between pathogens, the environment and their hosts.

Paper I revealed that *Al. salmonicida* LFI1238 can utilize chitin as a nutrient source and that the GH18 chitinase and the two LPMOs are needed for this ability. Biochemical characterization of the enzymes showed that the activity was significantly lower than that of well-studies chitinolytic anzymes in chitin degrading bacteria. Proteomic analysis revealed that *As*LPMO10A was highly abundant in the proteome during growth on chitin and glucose, while expression of the chitinase and LPMO10B was influenced by chitin in the growth media.

In paper II, the LPMOs of *Al. salmonicida* were found important for its pathogenicity in Atlantic salmon. Deletion of *As*LPMO10A and *As*LPMO10B resulted in reduced bacterial burden within the host compared to wild type. The reduced bacterial burden appeared to be related to serum resistance, especially for *As*LPMO10B. The study also revealed significant alterations in the proteome of gene deletion strains and showed that the 3D structure of the *As*LPMO10B AA10 domain is structurally similar to entomopathogenic LPMOs . The combined findings of paper I and II also gives strong support to the notion that bacteria can use LPMOs and chitinases for multiple purposes.

In paper III, the proteome response of *V. anguillarum* upon exposure to vibriosis-related conditions such as oxidative stress, salmon serum immune components, and iron deprivation, revealed that environmental stressors induce differential responses in *V. anguillarum*. Most importantly, iron acquisition mechanisms were regulated differentialy upon presence of serum components and the iron chelator (DIP). Modulation of metabolism was found as a response to several stress-conditions.

9.2 Future perspectives

The present thesis provides new findings related to the molecular determinants of virulence in *Al. salmonicida* and *V. anguillarum*. Paper II represent the first study on LPMOs as virulence determinants of fish pathogens. Since LPMOs (and chitinases) are present in the genome of several pathogens, studies investigating the multifunctional role of these proteins represent a great opportunity to discover new targets for *e.g.* vaccines or anti-virulence therapy. Some studies also report chitin as an immunostimulant (306), protecting the host from opportunistic pathogens (307, 308), or even chitin binding proteins from *e.g.* kuruma shrimp to help in the clearance of *V. anguillarum* (309). Together all these finding represent emerging and interesting perspectives of host-pathgen interactions related to chitin and chitin-related proteins.

Future work investigating the mechanisms around the role of the *Al. salmonicida* LPMOs would be of great interest, since this could add to the current knowledge and even identify new mechanisms of for example immune modulation. Relevant experiments could investigate interactions of the bacterium or recombinant enzymes with host cell lines, macrophages, complement components and mucins in vitro. The host immune response could also be investigate further, however, consideration should be made in the use of experimental animals. Since our studies indicate that immune components of Atlantic salmon blood could be important, an i.p injection, followed by early sampling of head kidney, spleen and liver, and at the same time sampling blood to assess the expression of *As*LPMOs could give insigtht into the dynamics between the pathogen and is host.

The findings that *Al.salmonicida* can degrade and catabolize chitin opens up new question around the natural reservoir of this bacterium and the role of chitin-associated interactions. Could its association with chitin stimulate DNA uptake and virulence like for *V. cholerae*? Further, a study investigating the expression of pseudogenes and their regulation would be of great interest for determining their putative functional roles in *Al. salmonicida* biology. This is especially interesting because the *Al. salmonicida* VS224 strain was found not to have an intact chitinase in its genome, but several chitinase pseudogenes. This could indicate the the VS224 strain is unable to utilize chitin, but since the LPMOs are intact it suggests that chitin-associated interactions are important in this strain as well, or that the LPMOs solely are virulence factors. A comprehensive study on the transcription and translation of pseudogenes in these *Al. salmonicida* strains was beyond the scope of this study.

The ability *of V. anguillarum* to modulate metabolism as a response to stress is an interesting characteristic that could be of interest to investigate further, as it could reveal new targets for battling infections. Moreover a study looking into the LPMO of *V. anguillarum* seems appropriate given the recent knowledge about LPMOs as virulence factors and also because of the more experimental tools available for this organism compared to *Al. salmonicida* (*e.g.* the zebrafish model system is available for *V. anguillarum*, but not the psychrophilic *Al. salmonicida*). For example, it could be of interest to perform a challenge comparing a *V. anguillarum* LPMO deletion mutant with the wild type strain. Zebrafish have been used to visualize infection by Green fluorescent protein- labelling of the bacteria (69), and this would provide an excellent tool to monitor and investigate the role of this protein in pathogenicity. Finally, since several *V. anguillarum* strains have been sequenced, it would be interesting to perform a comparative genomic study looking into the LPMOs in the genome of this species.

10 References

1. Schoch CL, Ciufo S, Domrachev M, Hotton CL, Kannan S, Khovanskaya R, Leipe D, McVeigh R, O'Neill K, Robbertse B, Sharma S, Soussov V, Sullivan JP, Sun L, Turner S, Karsch-Mizrachi I. 2020. NCBI Taxonomy: a comprehensive update on curation, resources and tools. Database (Oxford) 2020.
2. Baker-Austin C, Oliver JD, Alam M, Ali A, Waldor MK, Qadri F, Martinez-Urtaza J. 2018. *Vibrio spp*. infections. Na Rev Dis Primers 4:1-19.
3. Austin B, Austin DA. 2012. Vibrionaceae Representatives, p 357-411, Bacterial Fish Pathogens: Disease of Farmed and Wild Fish doi:10.1007/978-94-007-4884-2_11. Springer Netherlands, Dordrecht.
4. Rivas AJ, Lemos ML, Osorio CR. 2013. *Photobacterium damselae* subsp. *damselae*, a bacterium pathogenic for marine animals and humans. Front Microbiol 4:283-283.
5. Egidius E, Wiik R, Andersen K, Hoff KA, Hjeltnes B. 1986. *Vibrio salmonicida Sp*-Nov, a New Fish Pathogen. Int J Syst Bacteriol 36:518-520.
6. Urbanczyk H, Ast JC, Higgins MJ, Carson J, Dunlap PV. 2007. Reclassification of *Vibrio fischeri, Vibrio logei, Vibrio salmonicida* and *Vibrio wodanis* as *Aliivibrio fischeri* gen. nov., comb. nov., *Aliivibrio logei* comb. nov., *Aliivibrio salmonicida* comb. nov. and *Aliivibrio wodanis* comb. nov. Int J of Syst Evol Microbiol 57:2823-2829.
7. Colquhoun DJ. 2002. *Vibrio salmonicida*, the causative agent of cold-water vibriosis: factors relating to pathogenesis and vaccine protection. The Norwegian School of Veterinary Medicine, Oslo.
8. Hjerde E, Lorentzen MS, Holden MT, Seeger K, Paulsen S, Bason N, Churcher C, Harris D, Norbertczak H, Quail MA, Sanders S, Thurston S, Parkhill J, Willassen NP, Thomson NR. 2008. The genome sequence of the fish pathogen *Aliivibrio salmonicida* strain LFI1238 shows extensive evidence of gene decay. BMC Genomics 9:616.
9. Kashulin A, Sørum H, Hjerde E, Willassen NP. 2015. IS elements in *Aliivibrio salmonicida* LFI1238: Occurrence, variability and impact on adaptability. Gene 554:40-49.
10. Sørum H, Poppe TT, Olsvik O. 1988. Plasmids in *Vibrio salmonicida* isolated from salmonids with hemorrhagic syndrome (Hitra disease). J Clin Microbiol 26:1679-83.
11. Egidius E, Andersen K, Clausen E, Raa J. 1981. Cold-water vibriosis or 'Hitra disease' in Norwegian salmonid farming. J Fish Dis 4:353-354.
12. Poppe TT, Håstein T, Salte R. 1985. "Hitra Disease" (Haemorrhagic Syndrome) in Norwegian Salmon Farming: Present Status, Fish Shellfish Pathol.

13. Schrøder MB, Espelid S, Jørgensen TØ. 1992. Two serotype of *Vibrio salmonicida* isolated from diseased cod (*Gadus morhua* L.); virulence, immunological studies and advanced experiments. Fish Shellfish Immunol 2.
14. Sørum H, Hvaal AB, Heum M, Daae FL, Wiik R. 1990. Plasmid profiling of *Vibrio salmonicida* for epidemiological studies of cold-water vibriosis in Atlantic salmon (*Salmo salar*) and cod (Gadus morhua). Appl Environ Microbiol 56.
15. Hjeltnes B WC, Bang jensen B, Haukaas A (red). 2016. The Fish Health Report 2015. The Norwegian Veterinary Institute,
16. Hjeltnes B, Andersen K, Egidius E. 1987. Multiple antibiotic resistance in *Vibrio salmonicida*. Bull Eur Assoc Fish Pathol 7.
17. Lillehaug A, Sørum RH, Ramstad A. 1990. Cross-protection after immunization of Atlantic salmon, *Salmo salar* L., against different strains of *Vibrio salmonicida*. J Fish Dis 13:519-523.
18. Hjeltnes B, Andersen K, Ellingsen H-M. 1989. Vaccination against *Vibrio salmonicida* The effect of different routes of administration and of revaccination. Aquaculture 83:1-6.
19. Eggset G, Mikkelsen H, Killie J-EA. 1997. Immunocompetence and duration of immunity against *Vibrio salmonicida* and *Aeromonas salmonicida* after vaccination of Atlantic salmon (*Salmo salar* L.) at low and high temperatures. Fish Shellfish Immunol 7:247-260.
20. Bruno D, Hastings TS, Ellis A, Wootten R. 1985. Outbreak of a cold water vibriosis in Atlantic salmon in Scotland. Bull Eur Assoc Fish Pathol 5:62-63.
21. Sørum H, Myhr E, Zwicker BM, Lillehaug A. 1993. Comparison by plasmid profiling of *Vibrio salmonicida* strains isolated from diseased fish from different North European and Canadian areas of the Atlantic Ocean. Can J Fish Aquat Sci 50.
22. Hoff KA. 1989. Survival of *Vibrio anguillarum* and *Vibrio salmonicida* at different salinities. Appl Environ Microbiol 55:1775-86.
23. Enger Ø, Husevåg B, Goksøyr J. 1991. Seasonal variation in presence of *Vibrio salmonicida* and total bacterial counts in Norwegian fish-farm water. Can J Microbiol 37:618-623.
24. Enger O, Husevag B, Goksoyr J. 1989. Presence of the fish pathogen *Vibrio salmonicida* in fish farm sediments. Appl Environ Microbiol 55:2815-8.
25. Kashulin A, Sørum H. 2014. A novel in vivo model for rapid evaluation of *Aliivibrio salmonicida* infectivity in Atlantic salmon. Aquaculture 420–421:112-118.
26. Bjelland AM, Johansen R, Brudal E, Hansen H, Winther-Larsen HC, Sørum H. 2012. Vibrio salmonicida pathogenesis analyzed by experimental challenge of Atlantic salmon (Salmo salar). Microbial Pathogenesis 52:77-84.
27. Holm KO, Strom E, Stensvag K, Raa J, Jorgensen T. 1985. Characteristics of a V*ibrio sp*. Associated with the "Hitra Disease" of Atlantic Salmon in Norwegian Fish Farms. Fish Pathology 20:125-129.

28. Bjelland A, Fauske AK, Nguyen A, Orlien I, Østgaard I, Sørum H. 2013. Expression of *Vibrio salmonicida* virulence genes and immune response parameters in experimentally challenged Atlantic salmon (*Salmo salar* L.). Front Microbiol 4.
29. Totland GK, Nylund A, Holm KO. 1988. An ultrastructural study of morphological changes in Atlantic salmon, *Salmo salar* L., during the development of cold water vibriosis. J Fish Dis 11:1-13.
30. Evensen Ø, Espelid S, Håstein T. 1991. Immunohistochemical identification of *Vibrio salmonicida* in stored tissues of Atlantic salmon *Salmo salar* from the first known outbreak of cold-water vibriosis ('Hitra disease'). Dis Aquat Org 10:185-189.
31. Brattgjerd S, Evensen O. 1996. A sequential light microscopic and ultrastructural study on the uptake and handling of *Vibrio salmonicida* in phagocytes of the head kidney in experimentally infected Atlantic salmon (*Salmo salar* L.). Vet Pathol 33:55-65.
32. Espelid S, Jørgensen TØ. 1992. Antigen processing of *Vibrio salmonicida* by fish (*Salmo salar* L.) macrophages in vitro. Fish Shellfish Immunol 2:131-141.
33. MacDonell MT, Colwell RR. 1985. Phylogeny of the Vibrionaceae, and Recommendation for Two New Genera, *Listonella* and *Shewanella*. Syst Appl Microbiol 6:171-182.
34. Dikow RB. 2011. Systematic relationships within the Vibrionaceae (Bacteria: *Gammaproteobacteria*): steps toward a phylogenetic taxonomy. Cladistics 27:9-28.
35. Guérin-Faublée V, Rosso L, Vigneulle M, Flandrois J-P. 1995. The effect of incubation temperature and sodium chloride concentration on the growth kinetics of *Vibrio anguillarum* and *Vibrio anguillarum*-related organisms. J App Bacteriol 78:621-629.
36. Groberg Jr. WJ, Rohovec JS, Fryer JL. 1983. The effects of water temperature on infection and antibody formation induced by *Vibrio anguillarum* in juvenile Coho salmon (*Oncorhynchus kisutch*). J World Maric Soc 14:240-248.
37. Austin B, Austin D. 2007. Bacterial Fish Pathogens: Diseases of Farmed and Wild Fish doi:10.1007/978-1-4020-6069-4.
38. Milton DL, O'Toole R, Horstedt P, Wolf-Watz H. 1996. Flagellin A is essential for the virulence of *Vibrio anguillarum*. J Bacteriol 178:1310-1319.
39. Naka H, Dias GM, Thompson CC, Dubay C, Thompson FL, Crosa JH. 2011. Complete genome sequence of the marine fish pathogen *Vibrio anguillarum* harboring the pJM1 virulence plasmid and genomic comparison with other virulent strains of V. anguillarum and V. ordalii. Infect Immun 79:2889-900.
40. Li G, Mo Z, Li J, Xiao P, Hao B. 2013. Complete Genome Sequence of *Vibrio anguillarum* M3, a Serotype O1 Strain Isolated from Japanese Flounder in China. Genome Announcements 1:e00769-13.
41. Busschaert P, Frans I, Crauwels S, Zhu B, Willems K, Bossier P, Michiels C, Verstrepen K, Lievens B, Rediers H. 2015. Comparative genome sequencing to assess the genetic diversity and virulence attributes of 15 *Vibrio anguillarum* isolates. J Fish Dis 38:795-807.

42. Larsen JL, Olsen JE. 1991. Occurrence of plasmids in Danish isolates of *Vibrio anguillarum* serovars O1 and O2 and association of plasmids with phenotypic characteristics. Appl Environ Microbiol 57:2158-2163.
43. Pedersen K, Larsen JL. 1995. Evidence for the existence of distinct populations of *Vibrio anguillarum* serogroup O1 based on plasmid contents and ribotypes. Appl Environ Microbiol 61:2292-2296.
44. Skov MN, Pedersen K, Larsen JL. 1995. Comparison of Pulsed-Field Gel Electrophoresis, Ribotyping, and Plasmid Profiling for Typing of *Vibrio anguillarum* Serovar O1. Appl Environ Microbiol 61:1540-5.
45. Castillo D, Alvise PD, Xu R, Zhang F, Middelboe M, Gram L. 2017. Comparative Genome Analyses of *Vibrio anguillarum* Strains Reveal a Link with Pathogenicity Traits. mSystems 2:e00001-17.
46. Bergman AM. 1909. Die rote Beulenkrankheit des Aals. : Mit 2 Tafeln, Stuttgart.
47. Canestrini G. 1893. La malattia dominante delle anguille. Atti Ist Veneto Sci Lett Arti Cl Sci Mat Nat 7:809-814.
48. Rødsæther MC, Olafsen J, Raa J, Myhre K, Steen JB. 1977. Copper as an initiating factor of vibriosis (*Vibrio anguillarum*) in eel (*Anguilla anguilla*). J Fish Biol 10:17-21.
49. Holt G. 1970. Vibriosis (*Vibrio Anguillarum*) as an Epizootic Disease in Rainbow Trout (*Salmo Gairdneri*). Acta Vet Scand 11:600-603.
50. Levin MA, Wolke RE, Cabelli VJ. 1972. *Vibrio anguillarum* as a cause of disease in winter flounder (*Pseudopleuronectes americanus*). Can J Microbiol 18:1585-1592.
51. Horne MT, Richards RH, Roberts RJ, Smith PC. 1977. Peracute vibriosis in juvenile turbot *Scophthalmus maximus*. J Fish Biol 11:355-361.
52. Evelyn TPT. 1971. First Records of Vibriosis in Pacific Salmon Cultured in Canada, and Taxonomic Status of the Responsible Bacterium, *Vibrio anguillarum*. Journal of the Fisheries Research Board of Canada 28:517-525.
53. Hickey ME, Lee J-L. 2018. A comprehensive review of *Vibrio (Listonella) anguillarum*: ecology, pathology and prevention. Rev Aquac 10:585-610.
54. Frans I, Michiels CW, Bossier P, Willems KA, Lievens B, Rediers H. 2011. *Vibrio anguillarum* as a fish pathogen: virulence factors, diagnosis and prevention. J Fish Dis 34:643-661.
55. Rucker RR. Status of fish diseases and relation to production, p 98-101. *In* (ed),
56. Kubota S. 1963. Studies on the diseases of marine-culture fishes-I. General description and preliminary discussion of fish diseases at Mie Prefecture. J Fac Fish, Pref Univ Mie 6:107-124.
57. Bagge J, Bagge O. 1956. *Vibrio anguillarum* som arsag til ulcussygdom hos torsk (*Gardus callarias*, Linne). Nordisk Veterinarmedicin 8:481-492.
58. Norqvist A, Hagström A, Wolf-Watz H. 1989. Protection of rainbow trout against vibriosis and furunculosis by the use of attenuated strains of *Vibrio anguillarum*. Appl Environ Microbiol 55:1400-1405.
59. Johnson KA, Flynn JK, Amend DF. 1982. Duration of immunity in salmonids vaccinated by direct immersion with *Yersinia ruckeri* and *Vibrio anguillarum* bacterins. J Fish Dis 5:207-213.

60. Panagiotis A, Dimitrios K, Elizabeth MC. 2006. Efficacy of a *Listonella anguillarum* (syn. *Vibrio anguillarum*) vaccine for juvenile sea bass *Dicentrarchus labrax*. Dis Aquat Org 71:19-24.
61. Corripio-Miyar Y, Mazorra de Quero C, Treasurer JW, Ford L, Smith PD, Secombes CJ. 2007. Vaccination experiments in the gadoid haddock, *Melanogrammus aeglefinus* L., against the bacterial pathogen *Vibrio anguillarum*. Vet Immunol Immunopathol 118:147-153.
62. Mikkelsen H, Lund V, Martinsen L-C, Gravningen K, Schrøder MB. 2007. Variability among *Vibrio anguillarum* O2 isolates from Atlantic cod (*Gadus morhua* L.): Characterisation and vaccination studies. Aquaculture 266:16-25.
63. Eguchi M, Fujiwara E, Miyamoto N. 2000. Survival of *Vibrio anguillarum* in freshwater environments: adaptation or debilitation? Journal of Infection and Chemotherapy 6:126-129.
64. Miyamoto N, Eguchi M. 1997. Response to low osmotic stress in a fish pathogen, *Vibrio anguillarum*. FEMS Microbiol Ecol 22:225-231.
65. Baker RJ, Knittel MD, Fryer JL. 1983. Susceptibility of Chinook salmon, *Oncorhynchus tshawytscha* (Walbaum), and rainbow trout, *Salmo gairdneri* Richardson, to infection with *Vibrio anguillarum* following sublethal copper exposure. J Fish Dis 6:267-275.
66. Weber B, Chen C, Milton DL. 2010. Colonization of fish skin is vital for *Vibrio anguillarum* to cause disease. Environ Microbiol Rep 2:133-139.
67. Svendsen YS, Bøgwald J. 1997. Influence of artificial wound and non-intact mucus layer on mortality of Atlantic salmon *(Salmo salar* L.) following a bath challenge with *Vibrio anguillarum* and *Aeromonas salmonicida*. Fish Shellfish Immunol 7:317-325.
68. Grisez L, Sorgeloos P, Ollevier F. 1996. Mode of infection and spread of *Vibrio anguillarum* in turbot *Scophthalmus maximus* larvae after oral challenge through live feed. Dis Aquat Org 26:181-187.
69. O'Toole R, Von Hofsten J, Rosqvist R, Olsson P-E, Wolf-Watz H. 2004. Visualisation of zebrafish infection by GFP-labelled *Vibrio anguillarum*. Microb Pathog 37:41-46.
70. O'Toole R, Lundberg S, Fredriksson SA, Jansson A, Nilsson B, Wolf-Watz H. 1999. The chemotactic response of *Vibrio anguillarum* to fish intestinal mucus is mediated by a combination of multiple mucus components. J Bacteriol 181:4308-17.
71. Bordas MA, Balebona MC, Rodriguez-Maroto JM, Borrego JJ, Morinigo MA. 1998. Chemotaxis of pathogenic Vibrio strains towards mucus surfaces of gilt-head sea bream (*Sparus aurata* L.). Appl Environ Microbiol 64:1573-1575.
72. Bordas MA, Balebona MC, Zorrilla I, Borrego JJ, Moriñigo MA. 1996. Kinetics of adhesion of selected fish-pathogenic Vibrio strains of skin mucus of gilt-head sea bream (*Sparus aurata* L.). Appl Environ Microbiol 62:3650-4.
73. Olsson J, Jöborn A, Westerdahl A, Blomberg L, Kjelleberg S, Conway P. 1998. Survival, persistence and proliferation of *Vibrio anguillarum* in juvenile turbot, *Scophthalmus maximus* (L.), intestine and faeces. J Fish Dis 21:1-9.

74. Sinatra JA, Colby K. 2018. Notes from the Field: Fatal *Vibrio anguillarum* Infection in an Immunocompromised Patient - Maine, 2017. MMWR Morb Mortal Wkly Rep 67:962-963.
75. Rudall KM, Kenchington W. 1973. The Chitin System. Biological Reviews 48:597-633.
76. Wang Y, Chang Y, Yu L, Zhang C, Xu X, Xue Y, Li Z, Xue C. 2013. Crystalline structure and thermal property characterization of chitin from Antarctic krill (*Euphausia superba*). Carbohydrate Polymers 92:90-97.
77. Raabe D, Romano P, Sachs C, Fabritius H, Al-Sawalmih A, Yi SB, Servos G, Hartwig HG. 2006. Microstructure and crystallographic texture of the chitin–protein network in the biological composite material of the exoskeleton of the lobster *Homarus americanus*. Materials Science and Engineering: A 421:143-153.
78. Acosta N, Jiménez C, Borau V, Heras A. 1993. Extraction and characterization of chitin from crustaceans. Biomass and Bioenergy 5:145-153.
79. Bacon JS, Davidson ED, Jones D, Taylor IF. 1966. The location of chitin in the yeast cell wall. Biochem J 101:36C-38C.
80. Tang WJ, Fernandez J, Sohn JJ, Amemiya CT. 2015. Chitin is endogenously produced in vertebrates. Curr Biol 25:897-900.
81. Wagner G, Lo J, Laine R, Almeder M. 1993. Chitin in the epidermal cuticle of a vertebrate (*Paralipophrys trigloides*, Blenniidae, Teleostei). Cell Mol Life Sci 49:317-319.
82. Gooday GW. 1990. The ecology of chitin degradation. Adv Microb Ecol 11:387-430.
83. Keyhani NO, Roseman S. 1999. Physiological aspects of chitin catabolism in marine bacteria. Biochim Biophys Acta 1473:108-22.
84. Erken M, Lutz C, McDougald D. 2015. Interactions of Vibrio spp. with zooplankton. Microbiol Spectr 3.
85. Lin H, Yu M, Wang X, Zhang XH. 2018. Comparative genomic analysis reveals the evolution and environmental adaptation strategies of vibrios. BMC Genomics 19:135.
86. Hunt DE, Gevers D, Vahora NM, Polz MF. 2008. Conservation of the chitin utilization pathway in the Vibrionaceae. Appl Environ Microbiol 74.
87. Lombard V, Golaconda Ramulu H, Drula E, Coutinho PM, Henrissat B. 2014. The carbohydrate-active enzymes database (CAZy) in 2013. Nucleic Acids Res 42:D490-5.
88. Vaaje-Kolstad G, Horn SJ, Sørlie M, Eijsink VG. 2013. The chitinolytic machinery of *Serratia marcescens*--a model system for enzymatic degradation of recalcitrant polysaccharides. Febs j 280:3028-49.
89. Vaaje-Kolstad G, Westereng B, Horn SJ, Liu Z, Zhai H, Sørlie M, Eijsink VGH. 2010. An Oxidative Enzyme Boosting the Enzymatic Conversion of Recalcitrant Polysaccharides. Science 330:219-222.
90. Bissaro B, Røhr ÅK, Müller G, Chylenski P, Skaugen M, Forsberg Z, Horn SJ, Vaaje-Kolstad G, Eijsink VGH. 2017. Oxidative cleavage of polysaccharides by monocopper enzymes depends on H2O2. Nat Chem Biol 13:1123-1128.

91. Quinlan RJ, Sweeney MD, Lo Leggio L, Otten H, Poulsen J-CN, Johansen KS, Krogh KBRM, Jørgensen CI, Tovborg M, Anthonsen A, Tryfona T, Walter CP, Dupree P, Xu F, Davies GJ, Walton PH. 2011. Insights into the oxidative degradation of cellulose by a copper metalloenzyme that exploits biomass components. PNAS 108:15079-15084.
92. Nakagawa YS, Kudo M, Loose JS, Ishikawa T, Totani K, Eijsink VG, Vaaje-Kolstad G. 2015. A small lytic polysaccharide monooxygenase from *Streptomyces griseus* targeting alpha- and beta-chitin. Febs j 282:1065-79.
93. Uchiyama T, Kaneko R, Yamaguchi J, Inoue A, Yanagida T, Nikaidou N, Regue M, Watanabe T. 2003. Uptake of N,N'-diacetylchitobiose [(GlcNAc)2] via the phosphotransferase system is essential for chitinase production by *Serratia marcescens* 2170. J Bacteriol 185:1776-82.
94. Eisenbeis S, Lohmiller S, Valdebenito M, Leicht S, Braun V. 2008. NagA-dependent uptake of N-acetyl-glucosamine and N-acetyl-chitin oligosaccharides across the outer membrane of *Caulobacter crescentus*. J Bacteriol 190:5230-8.
95. Keyhani NO, Li XB, Roseman S. 2000. Chitin catabolism in the marine bacterium Vibrio furnissii - Identification and molecular cloning of a chitoporin. Journal of Biological Chemistry 275:33068-33076.
96. Suginta W, Chumjan W, Mahendran KR, Schulte A, Winterhalter M. 2013. Chitoporin from *Vibrio harveyi,* a channel with exceptional sugar specificity. J Biol Chem 288:11038-11046.
97. Park JK, Keyhani NO, Roseman S. 2000. Chitin catabolism in the marine bacterium *Vibrio furnissii* - Identification, molecular cloning, and characterization of a N-N '-diacetylchitobiose phosphorylase. J Biol Chem 275:33077-33083.
98. Meibom KL, Li XB, Nielsen AT, Wu CY, Roseman S, Schoolnik GK. 2004. The *Vibrio cholerae* chitin utilization program. Proc Natl Acad Sci USA 101.
99. Takiguchi Y, Shimahara K. 1988. N,N-Diacetylchitobiose production from chitin by *Vibrio anguillarum* strain E-383a. Lett Appl Microbiol 6:129-131.
100. Svitil AL, Chadhain S, Moore JA, Kirchman DL. 1997. Chitin Degradation Proteins Produced by the Marine Bacterium Vibrio harveyi Growing on Different Forms of Chitin. Applied and Environmental Microbiology 63:408-413.
101. Li X, Roseman S. 2004. The chitinolytic cascade in *Vibrios* is regulated by chitin oligosaccharides and a two-component chitin catabolic sensor/kinase. Proc Natl Acad Sci USA 101.
102. Chourashi R, Das S, Dhar D, Okamoto K, Mukhopadhyay AK, Chatterjee NS. 2018. Chitin-induced T6SS in *Vibrio cholera*e is dependent on ChiS activation. Microbiology 164:751-763.
103. Chourashi R, Mondal M, Sinha R, Debnath A, Das S, Koley H, Chatterjee NS. 2016. Role of a sensor histidine kinase ChiS of *Vibrio cholerae* in pathogenesis. Int J Med Microbiol 306:657-665.
104. Lutz C, Erken M, Noorian P, Sun S, McDougald D. 2013. Environmental reservoirs and mechanisms of persistence of *Vibrio cholerae*. Front Microbiol 4.

105. Huq A, Small EB, West PA, Huq MI, Rahman R, Colwell RR. 1983. Ecological relationships between *Vibrio cholerae* and planktonic crustacean copepods. Appl Environ Microbiol 45:275-283.
106. Pruzzo C, Vezzulli L, Colwell RR. 2008. Global impact of V*ibrio cholerae* interactions with chitin. Environ Microbiol 10:1400-1410.
107. Sultana M, Nahar S, Naser MN, Nair GB, Watanabe H, Ohnishi M, Yamamoto S, Endtz H, Cravioto A, Sack RB, Hasan NA, Sadique A, Huq A, Colwell RR, Alam M. 2012. Role of Shrimp Chitin in the Ecology of Toxigenic *Vibrio cholerae* and Cholera Transmission. Front Microbiol 2.
108. Williams TC, Ayrapetyan M, Oliver JD. 2014. Implications of chitin attachment for the environmental persistence and clinical nature of the human pathogen *Vibrio vulnificus*. Appl Environ Microbiol 80:1580-1587.
109. Sakib SN, Reddi G, Almagro-Moreno S. 2018. Environmental Role of Pathogenic Traits in *Vibrio cholerae*. J Bacteriol 200:e00795-17.
110. Bassler BL, Gibbons PJ, Yu C, Roseman S. 1991. Chitin utilization by marine bacteria. Chemotaxis to chitin oligosaccharides by *Vibrio furnissii*. J Biol Chem 266:24268-75.
111. Bassler B, Gibbons P, Roseman S. 1989. Chemotaxis to chitin oligosaccharides by *Vibrio furnissii*, a chitinivorous marine bacterium. Biochem Biophys Res Commun 161:1172-1176.
112. Mandel MJ, Schaefer AL, Brennan CA, Heath-Heckman EAC, DeLoney-Marino CR, McFall-Ngai MJ, Ruby EG. 2012. Squid-Derived Chitin Oligosaccharides Are a Chemotactic Signal during Colonization by *Vibrio fischeri*. Appl Environ Microbiol 78:4620-4626.
113. Fidopiastis PM, Miyamoto CM, Jobling MG, Meighen EA, Ruby EG. 2002. LitR, a new transcriptional activator in *Vibrio fischeri*, regulates luminescence and symbiotic light organ colonization. Mol Microbiol 45:131-143.
114. Meibom KL, Blokesch M, Dolganov NA, Wu C-Y, Schoolnik GK. 2005. Chitin Induces Natural Competence in *Vibrio cholerae*. Science 310:1824-1827.
115. Gulig PA, Tucker MS, Thiaville PC, Joseph JL, Brown RN. 2009. USER Friendly Cloning Coupled with Chitin-Based Natural Transformation Enables Rapid Mutagenesis of *Vibrio vulnificus*. Appl Environ Microbiol 75:4936-4949.
116. Pollack-Berti A, Wollenberg MS, Ruby EG. 2010. Natural transformation of *Vibrio fischeri* requires tfoX and tfoY. Environ Microbiol 12:2302-2311.
117. Debnath A, Mizuno T, Miyoshi S-i. 2020. Regulation of Chitin-Dependent Growth and Natural Competence in *Vibrio parahaemolyticus*. Microorganisms 8:1303.
118. Udden SMN, Zahid MSH, Biswas K, Ahmad QS, Cravioto A, Nair GB, Mekalanos JJ, Faruque SM. 2008. Acquisition of classical CTX prophage from *Vibrio cholerae* O141 by El Tor strains aided by lytic phages and chitin-induced competence. PNAS 105:11951-11956.
119. Blokesch M, Schoolnik GK. 2007. Serogroup Conversion of *Vibrio cholerae* in Aquatic Reservoirs. PLoS Path 3:e81.
120. Dalia AB, Lazinski DW, Camilli A. 2014. Identification of a Membrane-Bound Transcriptional Regulator That Links Chitin and Natural Competence in *Vibrio cholerae*. mBio 5:e01028-13.

121. Yamamoto S, Mitobe J, Ishikawa T, Wai SN, Ohnishi M, Watanabe H, Izumiya H. 2014. Regulation of natural competence by the orphan two-component system sensor kinase ChiS involves a non-canonical transmembrane regulator in *Vibrio cholerae*. Mol Microbiol 91:326-347.
122. Khan F, Tabassum N, Anand R, Kim Y-M. 2020. Motility of *Vibrio spp.*: regulation and controlling strategies. Appl Microbiol Biotechnol 104:8187-8208.
123. Minamino T, Imada K, Namba K. 2008. Molecular motors of the bacterial flagella. Curr Opin Struct Biol 18:693-701.
124. Asai Y, Kawagishi I, Sockett RE, Homma M. 1999. Hybrid Motor with H+- and Na+-Driven Components Can Rotate *Vibrio* Polar Flagella by Using Sodium Ions. J Bacteriol 181:6332-6338.
125. Echazarreta MA, Klose KE. 2019. Vibrio Flagellar Synthesis. Front Cell Infect Microbiol 9.
126. Syed KA, Beyhan S, Correa N, Queen J, Liu J, Peng F, Satchell KJF, Yildiz F, Klose KE. 2009. The *Vibrio cholerae* flagellar regulatory hierarchy controls expression of virulence factors. J Bacteriol 191:6555-6570.
127. Klose KE, Mekalanos JJ. 1998. Differential Regulation of Multiple Flagellins in *Vibrio cholerae*. J Bacteriol 180:303-316.
128. Atsumi T, Maekawa Y, Yamada T, Kawagishi I, Imae Y, Homma M. 1996. Effect of viscosity on swimming by the lateral and polar flagella of *Vibrio alginolyticus*. J Bacteriol 178:5024-6.
129. McCarter LL. 2004. Dual Flagellar Systems Enable Motility under Different Circumstances. Microb Physiol 7:18-29.
130. Guentzel MN, Berry LJ. 1975. Motility as a virulence factor for *Vibrio cholerae*. Infect Immun 11:890-897.
131. Richardson K. 1991. Roles of motility and flagellar structure in pathogenicity of *Vibrio cholerae*: analysis of motility mutants in three animal models. Infect Immun 59:2727-2736.
132. Lee J-H, Rho JB, Park K-J, Kim CB, Han Y-S, Choi SH, Lee K-H, Park S-J. 2004. Role of flagellum and motility in pathogenesis of *Vibrio vulnificus*. Infect Immun 72:4905-4910.
133. Nørstebø SF, Paulshus E, Bjelland AM, Sørum H. 2017. A unique role of flagellar function in *Aliivibrio salmonicida* pathogenicity not related to bacterial motility in aquatic environments. Microb Pathog 109:263-273.
134. Larsen MH, Larsen JL, Olsen JE. 2001. Chemotaxis of *Vibrio anguillarum* to fish mucus: role of the origin of the fish mucus, the fish species and the serogroup of the pathogen. FEMS Microbiol Ecol 38:77-80.
135. Garcia T, Otto K, Kjelleberg S, Nelson DR. 1997. Growth of *Vibrio anguillarum* in Salmon Intestinal Mucus. Appl Environ Microbiol 63:1034-1039.
136. Nealson KH, Platt T, Hastings JW. 1970. Cellular control of the synthesis and activity of the bacterial luminescent system. J Bacteriol 104:313-322.
137. Eberhard A, Burlingame AL, Eberhard C, Kenyon GL, Nealson KH, Oppenheimer NJ. 1981. Structural identification of autoinducer of *Photobacterium fischeri* luciferase. Biochemistry 20:2444-9.
138. Kuo A, Blough NV, Dunlap PV. 1994. Multiple N-acyl-L-homoserine lactone autoinducers of luminescence in the marine symbiotic bacterium *Vibrio fischeri*. J Bacteriol 176:7558-65.

139. Hanzelka BL, Greenberg EP. 1995. Evidence that the N-terminal region of the *Vibrio fischeri* LuxR protein constitutes an autoinducer-binding domain. J Bacteriol 177:815-817.
140. Gilson L, Kuo A, Dunlap PV. 1995. AinS and a new family of autoinducer synthesis proteins. J Bacteriol 177:6946-6951.
141. Miyamoto CM, Lin YH, Meighen EA. 2000. Control of bioluminescence in *Vibrio fischeri* by the LuxO signal response regulator. Mol Microbiol 36:594-607.
142. Vance RE, Zhu J, Mekalanos JJ. 2003. A Constitutively Active Variant of the Quorum-Sensing Regulator LuxO Affects Protease Production and Biofilm Formation in *Vibrio cholerae*. Infect Immun 71:2571-2576.
143. Zhu J, Mekalanos JJ. 2003. Quorum sensing-dependent biofilms enhance colonization in *Vibrio cholerae*. Dev Cell 5:647-56.
144. Ye J, Ma Y, Liu Q, Zhao DL, Wang QY, Zhang YX. 2008. Regulation of *Vibrio alginolyticus v*irulence by the LuxS quorum-sensing system. J Fish Dis 31:161-169.
145. Shao C-P, Lo H-R, Lin J-H, Hor L-I. 2011. Regulation of cytotoxicity by quorum-sensing signaling in *Vibrio vulnificu*s is mediated by SmcR, a repressor of hlyU. J Bacteriol 193:2557-2565.
146. Jobling MG, Holmes RK. 1997. Characterization of hapR, a positive regulator of the *Vibrio cholerae* HA/protease gene hap, and its identification as a functional homologue of the *Vibrio harveyi* luxR gene. Mol Microbiol 26:1023-1034.
147. Lee DH, Jeong HS, Jeong HG, Kim KM, Kim H, Choi SH. 2008. A Consensus Sequence for Binding of SmcR, a *Vibrio vulnificu*s LuxR Homologue, and Genome-wide Identification of the SmcR Regulon. J Biol Chem 283:23610-23618.
148. Bjelland AM, Sørum H, Tegegne DA, Winther-Larsen HC, Willassen NP, Hansen H. 2012. LitR of *Vibrio salmonicida* Is a Salinity-Sensitive Quorum-Sensing Regulator of Phenotypes Involved in Host Interactions and Virulence. Infect Immun 80:1681-1689.
149. Kernell Burke A, Guthrie LTC, Modise T, Cormier G, Jensen RV, McCarter LL, Stevens AM. 2015. OpaR Controls a Network of Downstream Transcription Factors in *Vibrio parahaemolyticus* BB22OP. PLoS One 10:e0121863.
150. Croxatto A, Chalker VJ, Lauritz J, Jass J, Hardman A, Williams P, Cámara M, Milton DL. 2002. VanT, a Homologue of *Vibrio harveyi* LuxR, Regulates Serine, Metalloprotease, Pigment, and Biofilm Production in *Vibrio anguillarum*. J Bacteriol 184:1617-1629.
151. Fidopiastis PM, Sørum H, Ruby EG. 1999. Cryptic luminescence in the cold-water fish pathogen *Vibrio salmonicida*. Arch Microbiol 171:205-9.
152. Nelson EJ, Tunsjø HS, Fidopiastis PM, Sørum H, Ruby EG. 2007. A Novel *lux* Operon in the Cryptically Bioluminescent Fish Pathogen *Vibrio salmonicida* Is Associated with Virulence. Appl Environ Microbiol 73:1825-1833.
153. Khider M, Hansen H, Hjerde E, Johansen JA, Willassen NP. 2019. Exploring the transcriptome of *luxI*− and *ΔainS* mutants and the impact of N-3-oxo-hexanoyl-L- and N-3-hydroxy-decanoyl-L-homoserine lactones on biofilm formation in *Aliivibrio salmonicida*. PeerJ 7:e6845.

154. Milton DL, Hardman A, Camara M, Chhabra SR, Bycroft BW, Stewart GS, Williams P. 1997. Quorum sensing in *Vibrio anguillarum*: characterization of the vanI/vanR locus and identification of the autoinducer N-(3-oxodecanoyl)-L-homoserine lactone. J Bacteriol 179:3004-3012.
155. Milton DL, Chalker VJ, Kirke D, Hardman A, Cámara M, Williams P. 2001. The LuxM homologue VanM from *Vibrio anguillarum* directs the synthesis of N-(3-hydroxyhexanoyl)homoserine lactone and N-hexanoylhomoserine lactone. J Bacteriol 183:3537-47.
156. Croxatto A, Pride J, Hardman A, Williams P, Cámara M, Milton DL. 2004. A distinctive dual-channel quorum-sensing system operates in *Vibrio anguillarum*. Mol Microbiol 52:1677-89.
157. Ma L, Chen J, Liu R, Zhang XH, Jiang YA. 2009. Mutation of rpoS gene decreased resistance to environmental stresses, synthesis of extracellular products and virulence of *Vibrio anguillarum*. FEMS Microbiol Ecol 70:130-6.
158. Weber B, Croxatto A, Chen C, Milton DL. 2008. RpoS induces expression of the *Vibrio anguillarum* quorum-sensing regulator VanT. Microbiology 154:767-780.
159. Skaar EP. 2010. The Battle for Iron between Bacterial Pathogens and Their Vertebrate Hosts. PLoS Path 6:e1000949.
160. Sheldon JR, Laakso HA, Heinrichs DE. 2016. Iron Acquisition Strategies of Bacterial Pathogens. Microbiol Spectr 4.
161. Payne SM, Mey AR, Wyckoff EE. 2015. *Vibrio* Iron Transport: Evolutionary Adaptation to Life in Multiple Environments. Microbiol Mol Biol Rev 80:69-90.
162. Thode SK, Rojek E, Kozlowski M, Ahmad R, Haugen P. 2018. Distribution of siderophore gene systems on a Vibrionaceae phylogeny: Database searches, phylogenetic analyses and evolutionary perspectives. PLoS One 13:e0191860.
163. Byun H, Jung IJ, Chen J, Larios Valencia J, Zhu J. 2020. Siderophore piracy enhances *Vibrio cholerae* environmental survival and pathogenesis. Microbiology (Reading, Engl) 166:1038-1046.
164. Balado M, Lages MA, Fuentes-Monteverde JC, Martínez-Matamoros D, Rodríguez J, Jiménez C, Lemos ML. 2018. The Siderophore Piscibactin Is a Relevant Virulence Factor for *Vibrio anguillarum* Favored at Low Temperatures. Front Microbiol 9:1766.
165. Crosa JH. 1980. A plasmid associated with virulence in the marine fish pathogen *Vibrio anguillarum* specifies an iron-sequestering system. Nature 284:566-568.
166. Wolf MK, Crosa JH. 1986. Evidence for the Role of a Siderophore in Promoting *Vibrio anguillarum* Infections. Microbiology 132:2949-2952.
167. Wertheimer AM, Verweij W, Chen Q, Crosa LM, Nagasawa M, Tolmasky ME, Actis LA, Crosa JH. 1999. Characterization of the *angR* Gene of *Vibrio anguillarum*: Essential Role in Virulence. Infect Immun 67:6496-6509.
168. Ruiz P, Balado M, Fuentes-Monteverde JC, Toranzo AE, Rodríguez J, Jiménez C, Avendaño-Herrera R, Lemos ML. 2019. The Fish Pathogen *Vibrio ordalii* Under Iron Deprivation Produces the Siderophore Piscibactin. Microorganisms 7:313.

169. Lages MA, Balado M, Lemos ML. 2019. The Expression of Virulence Factors in *Vibrio anguillarum* Is Dually Regulated by Iron Levels and Temperature. Front Microbiol 10:2335-2335.
170. Winkelmann G, Schmid DG, Nicholson G, Jung G, Colquhoun DJ. 2002. Bisucaberin – A dihydroxamate siderophore isolated from *Vibrio salmonicida*, an important pathogen of farmed Atlantic salmon (*Salmo salar*). BioMetals 15:153-160.
171. Thode SK, Kahlke T, Robertsen EM, Hansen H, Haugen P. 2015. The immediate global responses of *Aliivibrio salmonicida* to iron limitations. BMC Microbiol 15:9.
172. Henderson DP, Payne SM. 1994. Characterization of the *Vibrio cholerae* outer membrane heme transport protein HutA: sequence of the gene, regulation of expression, and homology to the family of TonB-dependent proteins. J Bacteriol 176:3269-3277.
173. Mazoy R, Osorio CR, Toranzo AE, Lemos ML. 2003. Isolation of mutants of *Vibrio anguillarum* defective in haeme utilisation and cloning of *huvA*, a gene coding for an outer membrane protein involved in the use of haeme as iron source. Arch Microbiol 179:329-38.
174. Stork M, Di Lorenzo M, Mourino S, Osorio CR, Lemos ML, Crosa JH. 2004. Two tonB systems function in iron transport in *Vibrio anguillarum,* but only one is essential for virulence. Infect Immun 72.
175. Richard KL, Kelley BR, Johnson JG. 2019. Heme Uptake and Utilization by Gram-Negative Bacterial Pathogens. Front Cell Infect Microbiol 9:81-81.
176. Wyckoff EE, Mey AR, Leimbach A, Fisher CF, Payne SM. 2006. Characterization of Ferric and Ferrous Iron Transport Systems in *Vibrio cholerae*. J Bacteriol 188:6515-6523.
177. Lin T-L, Shu C-C, Chen Y-M, Lu J-J, Wu T-S, Lai W-F, Tzeng C-M, Lai H-C, Lu C-C. 2020. Like Cures Like: Pharmacological Activity of Anti-Inflammatory Lipopolysaccharides From Gut Microbiome. Frontiers in Pharmacol 11.
178. Boesen HT, Pedersen K, Larsen JL, Koch C, Ellis AE. 1999. *Vibrio anguillarum* resistance to rainbow trout (*Oncorhynchus mykiss*) serum: role of O-antigen structure of lipopolysaccharide. Infect Immun 67:294-301.
179. Norstebo SF, Lotherington L, Landsverk M, Bjelland AM, Sorum H. 2018. *Aliivibrio salmonicida* requires O-antigen for virulence in Atlantic salmon (*Salmo salar L.*). Microb Pathog 124:322-331.
180. Shinoda S. 1999. Protein toxins produced by pathogenic *vibrios*. J Nat Toxins 8:259-269.
181. Iida T, Honda T. 1997. Hemolysins Produced by *Vibrios*. J Toxicol Toxin Re 16:215-227.
182. Zhang XH, Austin B. 2005. Haemolysins in *Vibrio* species. J Appl Microbiol 98.
183. Ceccarelli D, Hasan N, Huq A, Colwell R. 2013. Distribution and dynamics of epidemic and pandemic *Vibrio parahaemolyticus* virulence factors. Front Cell Infect Microbiol 3.

184. Rivas AJ, Balado M, Lemos ML, Osorio CR. 2011. The *Photobacterium damselae* subsp. *damselae* hemolysins damselysin and HlyA are encoded within a new virulence plasmid. Infect Immun 79:4617-4627.
185. Osorio CR, Vences A, Matanza XM, Terceti MS. 2018. *Photobacterium damselae* subsp. *damselae*, a Generalist Pathogen with Unique Virulence Factors and High Genetic Diversity. J Bacteriol 200:e00002-18.
186. Cinar HN, Kothary M, Datta AR, Tall BD, Sprando R, Bilecen K, Yildiz F, McCardell B. 2010. *Vibrio cholerae* Hemolysin Is Required for Lethality, Developmental Delay, and Intestinal Vacuolation in *Caenorhabditis elegans*. PLoS One 5:e11558.
187. Yamanaka H, Satoh T, Katsu T, Shinoda S. 1987. Mechanism of Haemolysis by *Vibrio vulnificus* Haemolysin. Microbiology 133:2859-2864.
188. Li L, Rock JL, Nelson DR. 2008. Identification and Characterization of a Repeat-in-Toxin Gene Cluster in *Vibrio anguillarum*. Infect Immun 76:2620-2632.
189. Rodkhum C, Hirono I, Crosa JH, Aoki T. 2005. Four novel hemolysin genes of *Vibrio anguillarum* and their virulence to rainbow trout. Microb Pathog 39.
190. Lee JH, Kim MW, Kim BS, Kim SM, Lee BC, Kim TS, Choi SH. 2007. Identification and characterization of the *Vibrio vulnificus rtxA* essential for cytotoxicity in vitro and virulence in mice. J Microbiol 45:146-52.
191. Olivier V, Haines GK, Tan Y, Satchell KJF. 2007. Hemolysin and the Multifunctional Autoprocessing RTX Toxin Are Virulence Factors during Intestinal Infection of Mice with *Vibrio cholerae* El Tor O1 Strains. Infect Immun 75:5035-5042.
192. Ikigai H, Akatsuka A, Tsujiyama H, Nakae T, Shimamura T. 1996. Mechanism of membrane damage by El Tor hemolysin of *Vibrio cholerae* O1. Infect Immun 64:2968-2973.
193. Kothary MH, Lowman H, McCardell BA, Tall BD. 2003. Purification and Characterization of Enterotoxigenic El Tor-Like Hemolysin Produced by *Vibrio fluvialis*. Infect Immun 71:3213-3220.
194. Han J-H, Lee J-H, Choi Y-H, Park J-H, Choi T-J, Kong I-S. 2002. Purification, characterization and molecular cloning of *Vibrio fluvialis* hemolysin. Biochim Biophys Acta Proteins Proteom 1599:106-114.
195. Miyoshi S-I. 2013. Extracellular proteolytic enzymes produced by human pathogenic *vibrio* species. Front Microbiol 4.
196. Booth BA, Boesman-Finkelstein M, Finkelstein RA. 1984. *Vibrio cholerae* hemagglutinin/protease nicks cholera enterotoxin. Infect Immun 45:558-560.
197. Miyoshi S-i, Nakazawa H, Kawata K, Tomochika K-i, Tobe K, Shinoda S. 1998. Characterization of the Hemorrhagic Reaction Caused by *Vibrio vulnificus* Metalloprotease, a Member of the Thermolysin Family. Infect Immun 66:4851-4855.
198. Miyoshi S-i, Sugiyama K, Suzuki Y, Furuta H, Miyoshi N, Shinoda S. 1987. Enhancement of vascular permeability due to histamine-releasing effect of *Vibrio vulnificus* protease in rat skin. FEMS Microbiol Lett 40:95-98.
199. Nishina Y, Miyoshi S, Nagase A, Shinoda S. 1992. Significant role of an exocellular protease in utilization of heme by *Vibrio vulnificus*. Infect Immun 60:2128-2132.

200. Valiente E, Lee C-T, Hor L-I, Fouz B, Amaro C. 2008. Role of the metalloprotease Vvp and the virulence plasmid pR99 of *Vibrio vulnificus* serovar E in surface colonization and fish virulence. Environ Microbiol 10:328-338.
201. Norqvist A, Norrman B, Wolf-Watz H. 1990. Identification and characterization of a zinc metalloprotease associated with invasion by the fish pathogen *Vibrio anguillarum*. Infect Immun 58:3731-6.
202. Denkin SM, Nelson DR. 2004. Regulation of *Vibrio anguillarum* empA Metalloprotease Expression and Its Role in Virulence. Appl Environ Microbiol 70:4193-4204.
203. Han Y, Mo Z, Xiao P, Hao B, Li J, Yang G. 2011. Characterization of EmpA protease in *Vibrio anguillarum* M3. J Ocean Univ China 10:379-384.
204. Denkin SM, Nelson DR. 1999. Induction of Protease Activity in *Vibrio anguillarum* by Gastrointestinal Mucus. Appl Environ Microbiol 65:3555-3560.
205. Bitto NJ, Kaparakis-Liaskos M. 2017. The Therapeutic Benefit of Bacterial Membrane Vesicles. Int J Mol Sci 18:1287.
206. Tandberg JI, Lagos LX, Langlete P, Berger E, Rishovd A-L, Roos N, Varkey D, Paulsen IT, Winther-Larsen HC. 2016. Comparative Analysis of Membrane Vesicles from Three *Piscirickettsia salmonis* Isolates Reveals Differences in Vesicle Characteristics. PLoS One 11:e0165099-e0165099.
207. Caruana JC, Walper SA. 2020. Bacterial Membrane Vesicles and Their Applications as Vaccines and in Biotechnology, p 219-251. *In* Kaparakis-Liaskos M, Kufer TA (ed), Bacterial Membrane Vesicles: Biogenesis, Functions and Applications doi:10.1007/978-3-030-36331-4_10. Springer International Publishing, Cham.
208. Jan AT. 2017. Outer Membrane Vesicles (OMVs) of Gram-negative Bacteria: A Perspective Update. Front Microbiol 8.
209. Aschtgen M-S, Wetzel K, Goldman W, McFall-Ngai M, Ruby E. 2016. *Vibrio fischeri*-derived outer membrane vesicles trigger host development. Cell microbiol 18:488-499.
210. Hong G-E, Kim D-G, Park E-M, Nam B-H, Kim Y-O, Kong I-S. 2009. Identification of *Vibrio anguillarum* Outer Membrane Vesicles Related to Immunostimulation in the Japanese Flounder, *Paralichthys olivaceus*. Biosci Biotechnol Biochem 73:437-439.
211. Hodgkinson JW, Grayfer L, Belosevic M. 2015. Biology of Bony Fish Macrophages. Biology 4:881-906.
212. Panday A, Sahoo MK, Osorio D, Batra S. 2015. NADPH oxidases: an overview from structure to innate immunity-associated pathologies. Cell Mol Immunol 12:5-23.
213. Ezraty B, Gennaris A, Barras F, Collet J-F. 2017. Oxidative stress, protein damage and repair in bacteria. Nat Rev Microbiol 15:385-396.
214. Barnes AC, Bowden TJ, Horne MT, Ellis AE. 1999. Peroxide-inducible catalase in *Aeromonas salmonicida* subsp. *salmonicida* protects against exogenous hydrogen peroxide and killing by activated rainbow trout, *Oncorhynchus mykiss* L., macrophages. Microb Pathog 26:149-58.

215. Ahn J, Jang KK, Jo I, Nurhasni H, Lim JG, Yoo J-W, Choi SH, Ha N-C. 2018. Crystal structure of peroxiredoxin 3 from *Vibrio vulnificus* and its implications for scavenging peroxides and nitric oxide. IUCrJ 5:82-92.
216. Rhee SG. 2016. Overview on Peroxiredoxin. Mol Cells 39:1-5.
217. de Souza Santos M, Salomon D, Orth K. 2017. T3SS effector VopL inhibits the host ROS response, promoting the intracellular survival of *Vibrio parahaemolyticus*. PLoS Path 13:e1006438.
218. Chung K-J, Cho E-J, Kim MK, Kim YR, Kim S-H, Yang H-Y, Chung K-C, Lee SE, Rhee JH, Choy HE, Lee T-H. 2010. RtxA1-Induced Expression of the Small GTPase Rac2 Plays a Key Role in the Pathogenicity of *Vibrio vulnificus*. J Infect Dis 201:97-105.
219. Wang H, Chen S, Zhang J, Rothenbacher FP, Jiang T, Kan B, Zhong Z, Zhu J. 2013. Catalases Promote Resistance of Oxidative Stress in *Vibrio cholerae*. PLoS One 7:e53383.
220. Bang Y-J, Lee Z-W, Kim D, Jo I, Ha N-C, Choi SH. 2016. OxyR2 Functions as a Three-state Redox Switch to Tightly Regulate Production of Prx2, a Peroxiredoxin of *Vibrio vulnificus*. J Biol Chem 291:16038-16047.
221. Sepulcre MP, Sarropoulou E, Kotoulas G, Meseguer J, Mulero V. 2007. *Vibrio anguillarum* evades the immune response of the bony fish sea bass (*Dicentrarchus labrax* L.) through the inhibition of leukocyte respiratory burst and down-regulation of apoptotic caspases. Mol Immunol 44:3751-3757.
222. Boesen HT, Larsen MH, Larsen JL, Ellis AE. 2001. In vitro interactions between rainbow trout (*Oncorhynchus mykiss*) macrophages and *Vibrio anguillarum* serogroup O2a. Fish Shellfish Immunol 11:415-431.
223. Pedersen HL, Hjerde E, Paulsen SM, Hansen H, Olsen L, Thode SK, Santos MT, Paulssen RH, Willassen NP, Haugen P. 2010. Global responses of *Aliivibrio salmonicida* to hydrogen peroxide as revealed by microarray analysis. Mar Genomics 3:193-200.
224. Frederiksen RF, Yoshimura Y, Storgaard BG, Paspaliari DK, Petersen BO, Chen K, Larsen T, Duus JØ, Ingmer H, Bovin NV. 2015. A Diverse Range of Bacterial and Eukaryotic Chitinases Hydrolyzes the LacNAc (Galβ1–4GlcNAc) and LacdiNAc (GalNAcβ1–4GlcNAc) Motifs Found on Vertebrate and Insect Cells. J Biol Chem 290:5354-5366.
225. Eriksson S, Lucchini S, Thompson A, Rhen M, Hinton JC. 2003. Unravelling the biology of macrophage infection by gene expression profiling of intracellular *Salmonella enterica*. Mol Microbiol 47:103-18.
226. Hautefort I, Thompson A, Eriksson-Ygberg S, Parker ML, Lucchini S, Danino V, Bongaerts RJ, Ahmad N, Rhen M, Hinton JC. 2008. During infection of epithelial cells *Salmonella enterica* serovar *Typhimurium* undergoes a time-dependent transcriptional adaptation that results in simultaneous expression of three type 3 secretion systems. Cell Microbiol 10:958-84.
227. Larsen MH, Leisner JJ, Ingmer H. 2010. The chitinolytic activity of *Listeria monocytogenes* EGD is regulated by carbohydrates but also by the virulence regulator PrfA. Appl Environ Microbiol 76:6470-6.
228. Chaudhuri S, Gantner BN, Ye RD, Cianciotto NP, Freitag NE. 2013. The *Listeria monocytogenes* ChiA Chitinase Enhances Virulence through Suppression of Host Innate Immunity. mBio 4:e00617-12.

229. Paspaliari DK, Loose JS, Larsen MH, Vaaje-Kolstad G. 2015. *Listeria monocytogenes* has a functional chitinolytic system and an active lytic polysaccharide monooxygenase. Febs j 282:921-936.
230. Mondal M, Nag D, Koley H, Saha DR, Chatterjee NS. 2014. The *Vibrio cholerae* extracellular chitinase ChiA2 is important for survival and pathogenesis in the host intestine. PLoS One 9:e103119.
231. DebRoy S, Dao J, Söderberg M, Rossier O, Cianciotto NP. 2006. *Legionella pneumophila* type II secretome reveals unique exoproteins and a chitinase that promotes bacterial persistence in the lung. PNAS 103:19146-19151.
232. Rehman S, Grigoryeva LS, Richardson KH, Corsini P, White RC, Shaw R, Portlock TJ, Dorgan B, Zanjani ZS, Fornili A, Cianciotto NP, Garnett JA. 2020. Structure and functional analysis of the *Legionella pneumophila* chitinase ChiA reveals a novel mechanism of metal-dependent mucin degradation. PLoS Path 16:e1008342.
233. Vebø HC, Snipen L, Nes IF, Brede DA. 2009. The transcriptome of the nosocomial pathogen *Enterococcus faecalis* V583 reveals adaptive responses to growth in blood. PLoS One 4:e7660.
234. Vebø HC, Solheim M, Snipen L, Nes IF, Brede DA. 2010. Comparative genomic analysis of pathogenic and probiotic *Enterococcus faecalis* isolates, and their transcriptional responses to growth in human urine. PLoS One 5:e12489.
235. Fung C, Naughton S, Turnbull L, Tingpej P, Rose B, Arthur J, Hu H, Harmer C, Harbour C, Hassett DJ, Whitchurch CB, Manos J. 2010. Gene expression of *Pseudomonas aeruginosa* in a mucin-containing synthetic growth medium mimicking cystic fibrosis lung sputum. J Med Microbiol 59:1089-1100.
236. Tunsjø HS, Paulsen SM, Berg K, Sørum H, L'Abée-Lund TM. 2009. The winter ulcer bacterium *Moritella viscosa* demonstrates adhesion and cytotoxicity in a fish cell model. Microb Pathog 47:134-42.
237. Suzuki K, Suzuki M, Taiyoji M, Nikaidou N, Watanabe T. 1998. Chitin binding protein (CBP21) in the culture supernatant of *Serratia marcescens* 2170. Biosci Biotechnol Biochem 62:128-135.
238. Schrempf H. 2001. Recognition and degradation of chitin by streptomycetes. Antonie Van Leeuwenhoek 79:285-9.
239. Johansen KS. 2016. Lytic Polysaccharide Monooxygenases: The Microbial Power Tool for Lignocellulose Degradation. Trends Plant Sci 21:926-936.
240. Corrêa TL, dos Santos LV, Pereira GA. 2016. AA9 and AA10: from enigmatic to essential enzymes. Appl Microbiol Biotechnol 100:9-16.
241. Sasmal D, Guhathakurta B, Ghosh AN, Pal CR, Datta A. 1992. N-acetyl-D-glucosamine-specific lectin purified from Vibrio cholerae 01. FEMS Microbiol Lett 77:217-24.
242. Kirn TJ, Jude BA, Taylor RK. 2005. A colonization factor links *Vibrio cholerae* environmental survival and human infection. Nature 438:863-6.
243. Bhowmick R, Ghosal A, Das B, Koley H, Saha DR, Ganguly S, Nandy RK, Bhadra RK, Chatterjee NS. 2008. Intestinal adherence of *Vibrio cholerae* involves a coordinated interaction between colonization factor GbpA and mucin. Infect Immun 76:4968-4977.

244. Shutinoski B, Schmidt MA, Heusipp G. 2010. Transcriptional regulation of the Yts1 type II secretion system of *Yersinia enterocolitica* and identification of secretion substrates. Mol Microbiol 75:676-91.
245. Kawada M, Chen C-C, Arihiro A, Nagatani K, Watanabe T, Mizoguchi E. 2008. Chitinase 3-like-1 enhances bacterial adhesion to colonic epithelial cells through the interaction with bacterial chitin-binding protein. Lab Invest 88:883-895.
246. Chaudhuri S, Bruno JC, Alonzo F, 3rd, Xayarath B, Cianciotto NP, Freitag NE. 2010. Contribution of chitinases to *Listeria monocytogenes* pathogenesis. Appl Environ Microbiol 76:7302-7305.
247. Askarian F, Uchiyama S, Masson H, Sørensen HV, Golten O, Bunæs AC, Mekasha S, Røhr ÅK, Kommedal E, Ludviksen JA, Arntzen MØ, Schmidt B, Zurich RH, van Sorge NM, Eijsink VGH, Krengel U, Mollnes TE, Lewis NE, Nizet V, Vaaje-Kolstad G. 2021. The lytic polysaccharide monooxygenase CbpD promotes *Pseudomonas aeruginosa* virulence in systemic infection. Nat Commun 12:1230.
248. Cattoir V, Narasimhan G, Skurnik D, Aschard H, Roux D, Ramphal R, Jyot J, Lory S. 2013. Transcriptional response of mucoid *Pseudomonas aeruginosa* to human respiratory mucus. mBio 3:e00410-12.
249. Scott NE, Hare NJ, White MY, Manos J, Cordwell SJ. 2013. Secretome of transmissible *Pseudomonas aeruginosa* AES-1R grown in a cystic fibrosis lung-like environment. J Proteome Res 12:5357-69.
250. Vanden Bergh P, Heller M, Braga-Lagache S, Frey J. 2013. The Aeromonas salmonicida subsp. salmonicida exoproteome: global analysis, moonlighting proteins and putative antigens for vaccination against furunculosis. Proteome Sci 11:44.
251. Gardner JG. 2016. Polysaccharide degradation systems of the saprophytic bacterium *Cellvibrio japonicus*. World J Microbiol Biotechnol 32:121.
252. He X, Yu M, Wu Y, Ran L, Liu W, Zhang X-H. 2020. Two Highly Similar Chitinases from Marine *Vibrio* Species have Different Enzymatic Properties. Marine Drugs 18:139.
253. Churklam W, Aunpad R. 2020. Enzymatic characterization and structure-function relationship of two chitinases, LmChiA and LmChiB, from *Listeria monocytogenes*. Heliyon 6:e04252.
254. Chatterjee SS, Hossain H, Otten S, Kuenne C, Kuchmina K, Machata S, Domann E, Chakraborty T, Hain T. 2006. Intracellular Gene Expression Profile of *Listeria monocytogenes*. Infect Immun 74:1323.
255. Stauder M, Huq A, Pezzati E, Grim CJ, Ramoino P, Pane L, Colwell RR, Pruzzo C, Vezzulli L. 2012. Role of GbpA protein, an important virulence-related colonization factor, for *Vibrio cholerae*'s survival in the aquatic environment. Environ Microbiol Rep 4:439-45.
256. Jude BA, Martinez RM, Skorupski K, Taylor RK. 2009. Levels of the secreted *Vibrio cholerae* attachment factor GbpA are modulated by quorum-sensing-induced proteolysis. J Bacteriol 191:6911-7.
257. Jang KK, Gil SY, Lim JG, Choi SH. 2016. Regulatory Characteristics of *Vibrio vulnificus* gbpA Gene Encoding a Mucin-binding Protein Essential for Pathogenesis. J Biol Chem 291:5774-5787.

258. Kim SM, Park JH, Lee HS, Kim WB, Ryu JM, Han HJ, Choi SH. 2013. LuxR Homologue SmcR Is Essential for *Vibrio vulnificus* Pathogenesis and Biofilm Detachment, and Its Expression is Induced by Host Cells. Infect Immun 81:3721-3730.
259. Khider M, Hjerde E, Hansen H, Willassen NP. 2019. Differential expression profiling of DeltalitR and DeltarpoQ mutants reveals insight into QS regulation of motility, adhesion and biofilm formation in Aliivibrio salmonicida. BMC Genomics 20:220.
260. Feng Y, Chien KY, Chen HL, Chiu CH. 2012. Pseudogene recoding revealed from proteomic analysis of *salmonella* serovars. J Proteome Res 11:1715-9.
261. Kuo C-H, Ochman H. 2010. The Extinction Dynamics of Bacterial Pseudogenes. PLoS Genet 6:e1001050.
262. Kingston AW, Ponkratz C, Raleigh EA. 2017. Rpn (YhgA-Like) Proteins of *Escherichia coli* K-12 and Their Contribution to RecA-Independent Horizontal Transfer. J Bacteriol 199:e00787-16.
263. Klancher CA, Yamamoto S, Dalia TN, Dalia AB. 2020. ChiS is a noncanonical DNA-binding hybrid sensor kinase that directly regulates the chitin utilization program in *Vibrio cholerae*. Proc Natl Acad Sci U S A 117:20180-20189.
264. Metzger LC, Matthey N, Stoudmann C, Collas EJ, Blokesch M. 2019. Ecological implications of gene regulation by TfoX and TfoY among diverse Vibrio species. Environ Microbiol 21:2231-2247.
265. Vuckovic D, Dagley LF, Purcell AW, Emili A. 2013. Membrane proteomics by high performance liquid chromatography–tandem mass spectrometry: Analytical approaches and challenges. Proteomics 13:404-423.
266. Vit O, Petrak J. 2017. Integral membrane proteins in proteomics. How to break open the black box? J Proteom 153:8-20.
267. Chen D-D, Li J-H, Yao Y-Y, Zhang Y-A. 2019. *Aeromonas hydrophila* suppresses complement pathways via degradation of complement C3 in bony fish by metalloprotease. Fish Shellfish Immunol 94:739-745.
268. Hampton JA, Klaunig JE, Goldblatt PJ. 1987. Resident sinusoidal macrophages in the liver of the brown bullhead (*Ictalurus nebulosus*): An ultrastructural, functional and cytochemical study. Anat 219:338-346.
269. Rocha E, Monteiro RA, Pereira CA. 1994. The liver of the brown trout, *Salmo trutta fari*o: a light and electron microscope study. J Anat 185 (Pt 2):241-249.
270. Agius C, Roberts RJ. 2003. Melano-macrophage centres and their role in fish pathology. J Fish Dis 26:499-509.
271. Wong E, Vaaje-Kolstad G, Ghosh A, Hurtado-Guerrero R, Konarev PV, Ibrahim AFM, Svergun DI, Eijsink VGH, Chatterjee NS, van Aalten DMF. 2012. The *Vibrio cholerae* colonization factor GbpA possesses a modular structure that governs binding to different host surfaces. PLoS Path 8:e1002373-e1002373.
272. Phillips PC. 2008. Epistasis — the essential role of gene interactions in the structure and evolution of genetic systems. Nat Rev Genet 9:855-867.

273. Chiu E, Hijnen M, Bunker RD, Boudes M, Rajendran C, Aizel K, Oliéric V, Schulze-Briese C, Mitsuhashi W, Young V. 2015. Structural basis for the enhancement of virulence by viral spindles and their in vivo crystallization. PNAS 112:3973-3978.
274. Mitsuhashi W, Kawakita H, Murakami R, Takemoto Y, Saiki T, Miyamoto K, Wada S. 2007. Spindles of an entomopoxvirus facilitate its infection of the host insect by disrupting the peritrophic membrane. J Virol 81:4235-4243.
275. Mitsuhashi W, Shimura S, Miyamoto K, Sugimoto TN. 2019. Spatial distribution of orally administered viral fusolin protein in the insect midgut and possible synergism between fusolin and digestive proteases to disrupt the midgut peritrophic matrix. Arch Virol 164:17-25.
276. Lehane MJ. 1997. Peritrophic matrix structure and function. Annu Rev Entomol 42:525-50.
277. Thomas EL, Milligan TW, Joyner RE, Jefferson MM. 1994. Antibacterial activity of hydrogen peroxide and the lactoperoxidase-hydrogen peroxide-thiocyanate system against oral *streptococci*. Infect Immun 62:529-535.
278. Heo S, Kim S, Kang D. 2020. The Role of Hydrogen Peroxide and Peroxiredoxins throughout the Cell Cycle. Antioxidants (Basel) 9.
279. Yan LJ, Sumien N, Thangthaeng N, Forster MJ. 2013. Reversible inactivation of dihydrolipoamide dehydrogenase by mitochondrial hydrogen peroxide. Free Radic Res 47:123-33.
280. Chen Y, Wu F, Pang H, Tang J, Cai S, Jian J. 2019. Superoxide dismutase B (sodB), an important virulence factor of *Vibrio alginolyticus*, contributes to antioxidative stress and its potential application for live attenuated vaccine. Fish Shellfish Immunol 89:354-360.
281. Banin E, Vassilakos D, Orr E, Martinez RJ, Rosenberg E. 2003. Superoxide Dismutase Is a Virulence Factor Produced by the Coral Bleaching Pathogen *Vibrio shiloi*. Curr Microbiol 46:0418-0422.
282. Kang IH, Kim JS, Lee JK. 2007. The virulence of *Vibrio vulnificus* is affected by the cellular level of superoxide dismutase activity. J Microbiol Biotechnol 17:1399-402.
283. Xia X, Larios-Valencia J, Liu Z, Xiang F, Kan B, Wang H, Zhu J. 2017. OxyR-activated expression of Dps is important for *Vibrio cholerae* oxidative stress resistance and pathogenesis. PLoS One 12:e0171201.
284. Pacello F, Ceci P, Ammendola S, Pasquali P, Chiancone E, Battistoni A. 2008. Periplasmic Cu,Zn superoxide dismutase and cytoplasmic Dps concur in protecting *Salmonella enterica* serovar Typhimurium from extracellular reactive oxygen species. Biochim Biophys Acta 1780:226-32.
285. Satin B, Del Giudice G, Della Bianca V, Dusi S, Laudanna C, Tonello F, Kelleher D, Rappuoli R, Montecucco C, Rossi F. 2000. The Neutrophil-Activating Protein (Hp-Nap) of *Helicobacter pylori* Is a Protective Antigen and a Major Virulence Factor. J Exp Med 191:1467-1476.
286. Li Y, Ma Q. 2017. Iron Acquisition Strategies of *Vibrio anguillarum*. Front Cell Infect Microbiol 7 342.
287. Hassan H, Troxell B. 2013. Transcriptional regulation by Ferric Uptake Regulator (Fur) in pathogenic bacteria. Front Cell Infect Microbiol 3.

288. Chen Q, Crosa JH. 1996. Antisense RNA, Fur, Iron, and the Regulation of Iron Transport Genes in *Vibrio anguillarum*. J Biol Chem 271:18885-18891.
289. Passalacqua KD, Charbonneau M-E, O'Riordan MXD. 2016. Bacterial Metabolism Shapes the Host-Pathogen Interface. Microbiol Spectr 4:10.1128/microbiolspec.VMBF-0027-2015.
290. Rohmer L, Hocquet D, Miller SI. 2011. Are pathogenic bacteria just looking for food? Metabolism and microbial pathogenesis. Trends Microbiol 19:341-8.
291. Eisenreich W, Dandekar T, Heesemann J, Goebel W. 2010. Carbon metabolism of intracellular bacterial pathogens and possible links to virulence. Nat Rev Microbiol 8:401-412.
292. Olive AJ, Sassetti CM. 2016. Metabolic crosstalk between host and pathogen: sensing, adapting and competing. Nat Rev Microbiol 14:221-34.
293. Deochand DK, Grove A. 2017. MarR family transcription factors: dynamic variations on a common scaffold. Crit Rev Biochem Mol Biol 52:595-613.
294. Ellison DW, Miller VL. 2006. Regulation of virulence by members of the MarR/SlyA family. Curr Opin Microbiol 9:153-159.
295. De Silva RS, Kovacikova G, Lin W, Taylor RK, Skorupski K, Kull FJ. 2005. Crystal Structure of the Virulence Gene Activator AphA from *Vibrio cholerae* Reveals It Is a Novel Member of the Winged Helix Transcription Factor Superfamily*. J Biol Chem 280:13779-13783.
296. Kovacikova G, Lin W, Skorupski K. 2004. *Vibrio cholerae* AphA uses a novel mechanism for virulence gene activation that involves interaction with the LysR-type regulator AphB at the tcpPH promoter. Mol Microbiol 53:129-142.
297. Bhattacharyya N, Lemon T, Grove A. 2015. Characterization of a PecS Family Transcriptional Regulator in *Vibrio vulnificus*. The FASEB Journal 29:880.2.
298. Bhattacharyya N, Lemon TL, Grove A. 2019. A role for *Vibrio vulnificus* PecS during hypoxia. Sci Rep 9:2797.
299. Schirmer T, Keller TA, Wang YF, Rosenbusch JP. 1995. Structural basis for sugar translocation through maltoporin channels at 3.1 A resolution. Science 267:512-4.
300. Lun J, Xia C, Yuan C, Zhang Y, Zhong M, Huang T, Hu Z. 2014. The outer membrane protein, LamB (maltoporin), is a versatile vaccine candidate among the *Vibrio* species. Vaccine 32:809-15.
301. Kao D-Y, Cheng Y-C, Kuo T-Y, Lin S-B, Lin C-C, Chow L-P, Chen W-J. 2009. Salt-responsive outer membrane proteins of *Vibrio anguillarum* serotype O1 as revealed by comparative proteome analysis. J App Microbiol 106:2079-2085.
302. Yang B, Zhang D, Wu T, Zhang Z, Raza SHA, Schreurs N, Zhang L, Yang G, Wang C, Qian A, Kang Y, Shan X. 2019. Maltoporin (LamB protein) contributes to the virulence and adhesion of *Aeromonas veronii* TH0426. J Fish Dis 42:379-389.
303. Qiu N, Misra R. 2019. Overcoming Iron Deficiency of an *Escherichia coli tonB* Mutant by Increasing Outer Membrane Permeability. J Bacteriol 201:e00340-19.

304. Kullman L, Winterhalter M, Bezrukov SM. 2002. Transport of Maltodextrins through Maltoporin: A Single-Channel Study. Biophys J 82:803-812.
305. Osawa R, Koga T. 1995. An investigation of aquatic bacteria capable of utilizing chitin as the sole source of nutrients. Lett Appl Microbiol 21:288-291.
306. Esteban MA, Mulero V, Cuesta A, Ortuño J, Meseguer J. 2000. Effects of injecting chitin particles on the innate immune response of gilthead seabream (*Sparus aurata* L.). Fish Shellfish Immunol 10:543-554.
307. Villoria Recio M, Lee B-H, Lillebæk EMS, Kallipolitis BH, Gahan CGM, Ingmer H, Larsen MH. 2020. Chitin Attenuates Expression of Listeria monocytogenes Virulence Genes in vitro. Frontiers in Microbiology 11.
308. Wang S-H, Chen J-C. 2005. The protective effect of chitin and chitosan against *Vibrio alginolyticus* in white shrimp Litopenaeus vannamei. Fish Shellfish Immunol 19:191-204.
309. Xu S, Jing M, Kong D-M, Wang Y-R, Zhou Q, Liu W-Y, Jiao F, Li Y-J, Xie S-Y. 2021. Chitin binding protein from the kuruma shrimp *Marsupenaeus japonicus* facilitates the clearance of *Vibrio anguillarum*. Dev Comp Immunol 117:103981.

11 Scientific papers I-III

Paper I

The fish pathogen *Aliivibrio salmonicida* LFI1238 can degrade and metabolize chitin despite major gene loss in the chitinolytic pathway

Anna Skåne[1], Giusi Minniti[1], Jennifer S.M. Loose, Sophanit Mekasha, Bastien Bissaro, Geir Mathiesen, Magnus Ø. Arntzen and Gustav Vaaje-Kolstad*

Faculty of Chemistry, Biotechnology and Food Science, Norwegian University of Life Sciences (NMBU), Ås, Norway

The fish pathogen *Aliivibrio salmonicida* LFI1238 can degrade and metabolize chitin despite major gene loss in the chitinolytic pathway

Anna Skåne[1], Giusi Minniti[1], Jennifer S.M. Loose, Sophanit Mekasha, Bastien Bissaro, Geir Mathiesen, Magnus Ø. Arntzen and Gustav Vaaje-Kolstad*

Faculty of Chemistry, Biotechnology and Food Science, Norwegian University of Life Sciences (NMBU), Ås, Norway

[1]These authors contributed equally to the work
*Corresponding author. Email; gustav.vaaje-kolstad@nmbu.no

ABSTRACT

The fish pathogen *Aliivibrio (Vibrio) salmonicida* LFI1238 is thought to be incapable of utilizing chitin as a nutrient source since approximately half of the genes representing the chitinolytic pathway are disrupted by insertion sequences. In the present study, we combined a broad set of analytical methods to investigate this hypothesis. Cultivation studies revealed that *Al. salmonicida* grew efficiently on *N*-acetylglucosamine (GlcNAc) and chitobiose ($(GlcNAc)_2$), the primary soluble products resulting from enzymatic chitin hydrolysis. The bacterium was also able to grow on chitin particles, albeit at a lower rate compared to the soluble substrates. The genome of the bacterium contains five disrupted chitinase genes (pseudogenes) and three intact genes encoding a glycoside hydrolase family 18 (GH18) chitinase and two auxiliary activity family 10 (AA10) lytic polysaccharide monooxygenases (LPMOs). Biochemical characterization showed that the chitinase and LPMOs were able to depolymerize both α- and β-chitin to $(GlcNAc)_2$ and oxidized chitooligosaccharides, respectively. Notably, the chitinase displayed up to 50-fold lower activity compared to other well-studied chitinases. Deletion of the genes encoding the intact chitinolytic enzymes showed that the chitinase was important for growth on β-chitin, whereas the LPMO gene-deletion variants only showed minor growth defects on this substrate. Finally, proteomic analysis of *Al. salmonicida* LFI1238 growth on β-chitin showed expression of all three chitinolytic enzymes, and intriguingly also three of the disrupted chitinases. In conclusion, our results show that *Al. salmonicida* LFI1238 can utilize chitin as a nutrient source and that the GH18 chitinase and the two LPMOs are needed for this ability.

Dataset is available for download through the following link:

http://arken.nmbu.no/~gustko/Paper_I/Supplemental%20Dataset%201.xlsx

INTRODUCTION

Chitin is one of the most abundant biopolymers in nature and is a primary component of rigid structures such as the exoskeleton of insects and crustaceans, and the cell wall of fungi and some algae (1-4). Some reports also indicate that chitin is found in the scales and gut of fish (5, 6). This linear polysaccharide consists of *N*-acetyl-D-glucosamine (GlcNAc) units linked by β-1,4 glycosidic bonds that associates with other chitin chains to form insoluble chitin fibers. Despite the recalcitrance of chitin, the polymer is readily degraded and metabolized by chitinolytic microorganisms in the environment (7, 8).

Most bacteria solubilize and depolymerize chitin by secreting chitinolytic enzymes. Such enzymes include chitinases from family 18 and 19 of the glycoside hydrolases (GH18 and -19) and lytic polysaccharide monooxygenases (LPMOs) from family 10 of the auxiliary activities (AA10), according to classification by the carbohydrate active enzyme database (CAZy; http://www.cazy.org/) (9). Whereas chitinases cleave chitin chains by a hydrolytic mechanism (10, 11), LPMOs perform chitin depolymerization by an oxidative reaction (12-14). The latter enzymes usually target the crystalline parts of chitin fibers that are inaccessible for the chitinases. When combined, chitinases and LPMOs act synergistically, providing efficient depolymerization of this recalcitrant carbohydrate (12, 15-17). The products of enzymatic chitin degradation are mainly GlcNAc and $(GlcNAc)_2$, but also native and oxidized chitooligosaccharides, the latter (aldonic acids) arising from LPMO activity.

The chitin degradation pathway is conserved in the *Vibrionaceae* (18, 19). Here, GlcNAc and $(GlcNAc)_2$ are transported into the periplasm by unspecific porins (20, 21) or by dedicated transport proteins for chitooligosaccharides ($(GlcNAc)_{2-6}$), named chitoporins (22, 23). Once transported to the periplasm, $(GlcNAc)_{2-6}$ may be hydrolyzed to GlcNAc by family GH20 *N*-acetylhexosaminidases or *N,N*-diacetylchitobiose phosphorylases (24). Transport of GlcNAc or deacetylated GlcN across the inner membrane can occur through phosphotransferase systems, while $(GlcNAc)_2$ may be transported through the action of an ABC transporter (18). Once located in the cytosol GlcNAc, GlcNAc1P or GlcN enter the amino-sugar metabolism. It should be noted that the fate of chitooligosaccharide aldonic acid is not known.

Chitin degradation can be achieved by several marine bacteria, and can give advantages for survival and proliferation in the marine environment (8, 25). Some pathogens have chitin central in their lifecycle, the most prominent example being the human pathogen *Vibrio cholerae* that uses chitin-containing zoo-plankton as transfer vectors and nutrition (26, 27). The ability of the Gram-negative marine bacterium *Aliivibrio salmonicida* (previously *Vibrio salmonicida*), to utilize chitin or GlcNAc as a nutrient source is controversial. This pathogenic bacterium, which is the causative agent of cold water vibriosis in salmonids, was identified as a new vibrio-like bacteria in 1986 (28). Upon discovery and initial characterization of the pathogen (strain HI 7751), Egidius et al. did not observe degradation of chitin by the bacterium when growing on agar plates containing purified chitin. On the other hand, the monomeric building block of chitin, GlcNAc, was readily consumed by the bacterium. When the genome of the bacterium was sequenced two decades

later (strain LFI1238), it was shown that insertion sequence (IS) elements caused disruption of almost 10% of the protein encoding genes (29, 30). Especially effected was the chitin utilization pathway where seven genes, including three chitinases and a chitoporin, were either disrupted or truncated (29). In addition, the gene encoding the periplasmic chitin-binding protein (VSAL_I2576, also called CBP) was disrupted by a frameshift. The CBP ortholog in *V. cholerae* (VC_0620) has been shown to activate the two-component chitin catabolic sensor/kinase ChiS that regulates chitin utilization (31, 32). The gene encoding the ChiS ortholog in *Al. salmonicida* is intact (29), along with the Tfox encoding gene which protein product also is involved in regulation of enzymes related to chitin degradation in the *Vibrionaceae* (33, 34). Of the putative secreted chitinolytic enzymes, only one chitinase and two lytic polysaccharide monooxygenases remained intact in the *Al. salmonicida* genome. It was suggested that such extensive gene disruption could indicate inactivation of this pathway and indeed, the authors could not observe neither degradation of insoluble chitin nor utilization of GlcNAc as a nutrient source (29).

In order to obtain a deeper understanding of the roles of the *Al. salmonicida* chitinolytic enzymes, we have analyzed the chitin degradation potential of *Al. salmonicida* LFI1238 by biochemical characterization of the secreted chitinolytic enzymes, gene deletion and cultivation experiments, gene expression analysis and proteomics.

RESULTS

Al. salmonicida can utilize both GlcNAc and $(GlcNAc)_2$ as nutrient sources

To assess the ability of *Al. salmonicida* LFI1238 (abbreviated *"Al. salmonicida"* to avoid confusion with *Aeromonas salmonicida*) to grow on GlcNAc and $(GlcNAc)_2$, the wild type strain was cultivated in minimal medium supplemented with 0.2% glucose (11.1 mM; control experiment), 0.2 % GlcNAc (9.0 mM), or 0.2 % $(GlcNAc)_2$ (4.7 mM) over a period of 92 hours. The cultivation experiments showed that *Al. salmonicida* can utilize both GlcNAc and $(GlcNAc)_2$ as sole carbon sources (Fig. 1). Growth rates were compared by calculating the specific rate constants (μ) and generation time across the exponential phase (Table S1), showing little difference between the three carbon sources. In order to correlate GlcNAc and $(GlcNAc)_2$ consumption with the bacterial growth, the concentration of these sugars in the culture supernatant were determined at different time points during growth (Fig. 1E, F). The data show decreasing concentrations of GlcNAc during growth and complete depletion within 40 hours (Fig. 1E). In comparison, $(GlcNAc)_2$ is utilized at a slower speed, becoming depleted after 80 hours (Fig. 1F).

Sequence analysis and homology modelling.

Since *Al. salmonicida* was able to utilize both GlcNAc and $(GlcNAc)_2$, the major products of enzymatic chitin degradation, it was of interest to analyze the chitinolytic potential of the bacterial genome, investigating the details of both intact genes and pseudogenes. A previous study had already identified the presence of three putatively secreted chitinolytic enzymes (29). Annotation of putative CAZy domains of these three enzymes using the dbCAN server (35) showed that the chitinase sequence, here named *As*Chi18A, (that contains 881 amino acids, which

is unusually large for a chitinase) contains predicted CBM5 and CBM73 chitin binding domains and a C-terminal GH18 domain, the latter modest in size (only 324 amino acids; Fig. 2A). The protein sequence also shows long regions that were not annotated. Attempts to functionally annotate these regions with other sequence analysis servers such as InterPro, Pfam and SMART were inconclusive. The relatively small size of the GH18 catalytic domain indicates an enzyme stripped of most sub-domains that often are in place to form a substrate binding cleft. Indeed, homology modelling using Swiss-Model (36) revealed a model structure with a shallow substrate binding cleft, reminiscent of a non-processive *endo*-chitinase, which is clearly observed when compared to the processive *exo*-chitinase *Sm*Chi18A from *Serratia marcescens* that has a deep substrate binding cleft and the shallow-clefted, non-processive chitinase ChiNCTU2 from *Bacillus cereus* ((37); Fig. 2B). *As*Chi18A also shows an arrangement of active site residues that is similar to that of the latter enzyme (Fig. S1).

Annotation of the LPMO sequences showed that both proteins contained an N-terminal catalytic AA10 domain and a C-terminal CBM73 or CBM5 chitin-binding domain in *As*LPMO10A and –B, respectively (Fig. 2A). Like the chitinase, both LPMOs displayed regions in the sequence that were not possible to annotate using standard bioinformatics tools. Pair-wise sequence alignment of the two LPMOs revealed only a 20% identity between the catalytic domains. Blast search and modelling by homology of the individual catalytic domains showed that the catalytic module of *As*LPMO10A was similar to CBP21 from *S. marcescens* (49.5% identity, Fig. 2 C*;* (38, 39)) and to the catalytic AA10 domain of GbpA, a *Vibrio cholerae* colonization factor ((40); 65.6% identity). The similarity of full-length *As*LPMO10A to *V. cholera* GbpA (61% sequence identity) and their similar multi-modular architecture (both have a N-terminal AA10 LPMO domain, followed by a "GbpA2" domain, an un-annotated domain and a C-terminal CBM73 domain) indicate the possibility of functionally similar roles. The catalytic AA10 domain of *As*LPMO10B is, as already noted, very unlike *As*LPMO10A. From sequence database searches, orthologs were identified in a large variety of species from the *Vibrionaceae* family, and also in other marine bacteria like *Shewanella* and *Pseudoalteromonas*. None of these related enzymes have hitherto been biochemically characterized. When searching for similar sequences in the PDB database, the most similar structure to the *As*LPMO10B catalytic domain belongs to the viral proteins called "spindolins" (43.5% identity, but the alignment contains many insertions/ deletions). There exist no activity data for spindolins, but it is assumed that they are active towards chitin (41). It is therefore not straightforward to assign an activity to *As*LPMO10B based on sequence analysis. In order to analyze the putative structural difference between the LPMO domains, homology models were made using the Swiss-Model homology modelling software (36). When compared to CBP21, one of the best characterized family AA10 LPMOs, both *Al. salmonicida* LPMOs show several differences that may influence both substrate binding and catalysis (Fig. 2C): *As*LPMO10A is relatively similar to CBP21 but displays some differences that may be of functional relevance: amino acids W62, R119, K195 in *As*LPMO10A correspond to amino acids Y54, T111 and N185 in CBP21 that all have been shown to have influence on substrate binding and the functional stability of the enzyme (42, 43). *As*LPMO10B shows an active site environment similar to CBP21 but has an extension of the putative binding surface that positions a putatively

solvent exposed Trp (W46) further away from the active site histidines than for Y54 in CBP21 and W62 in *As*LPMO10A. Whether these differences are important for the substrate binding properties of the enzymes is not straightforward to interpret based on the data presented in this study, since both *Al. salmonicida* proteins have CBMs that very likely contribute to chitin binding.

Analysis of pseudogenes related to chitin catabolism

In addition to the intact genes encoding the chitinase, *As*Chi18A and LPMOs, *As*LPMO10A and -B, the genome of *Al. salmonicida* LFI12338 harbors multiple pseudogenes encoding truncated or fragmented enzymes related to chitin catabolism that are assumed to be non-functional (ORF identifiers VSAL_I2352, VSAL_I0763, VSAL_I0902, VSAL_I1108, VSAL_I1414 and VSAL_I1942). Interestingly, transcription of *Al. salmonicida* pseudogenes (including chitinase-related pseudogenes) has been observed (44-46). In addition, *Al. salmonicida* is motile despite two flagellar synthesis genes (*fliF*/VSAL_I2308 and (*flaG*/VSAL_I12316) being disrupted by premature stop codons (29). Thus, we performed a deeper analysis of the *Al. salmonicida* pseudogenes related to the chitinolytic machinery to investigate their putative functionality. The analysis revealed that VSAL_I2352 (predicted chitoporin) contains a frameshift after codon 266, which most likely will result in a non-functional protein if expressed. On the other hand, VSAL_I0763 (chitinase fragment), VSAL_I0902 (truncated chitinase), VSAL_I1108 (truncated chitodextrinase), VSAL_I1414 (disrupted chitinase) and VSAL_I1942 (disrupted chitinase) are rather truncated or disrupted by the type Vsa_2 insertion sequence (IS) elements (Fig. 3A), resulting in coding sequences (CDSs) of varying lengths that may give functional protein if expressed (Fig. 3B). Annotation of putative CAZy domains predicted that VSAL_I0902 (truncated chitinase fragment), VSAL_I1108 (truncated chitodextrinase) and VSAL_I1942 (disrupted chitinase) contain regions encoding GH18 domains, while VSAL_I1414 (disrupted chitinase) was predicted to contain a region encoding a GH19 domain (Fig. 3B). No functional domain was predicted for VSAL_I0763 (sequence containing 609 nucleotides truncated by upstream IS element and subsequent recombinations). It is believed that VSAL_I0902 and VSAL_I0763 are fragments belonging to one single chitinase (29).

In conclusion, four truncated chitinase genes contain regions encoding GH-domains which may give functional protein if translated.

***As*Chi18A and *As*LPMO10A and -B binds chitin**

In order to determine the biochemical properties of putatively chitinolytic enzymes (the pseudogene encoded chitinases were not expressed and characterized), *As*Chi18A and *As*LPMO10A and -B were cloned, expressed and purified (Fig. S2). The presence of putative chitin binding modules on all three chitinolytic enzymes prompted investigation of the substrate binding properties of the proteins. Using purified protein, α-chitin and β-chitin were used as substrates in particle sedimentation assays (Fig. 4). All proteins showed binding to the substrate particles and *As*LPMO10B seems to bind slightly weaker to the substrates used compared to *As*LPMO10A.

_As_Chi18A displays low chitinolytic activity

Since all three enzymes bound to chitin, the catalytic properties of the purified chitinase and two LPMOs were analyzed. Using β-chitin as substrate, the activity and operational stability of *As*Chi18A was followed over several hours at temperatures ranging from 10-60 °C. The progress curves observed for *As*Chi18A indicate an optimal operational stability, i.e. the highest temperature for which enzyme activity remains stable over time, at approximately 30 °C (Fig. 5A). Similar to other GH18 chitinases, the dominant product of chitin hydrolysis by *As*Chi18A was $(GlcNAc)_2$ with small amounts of GlcNAc (< 5%).

In order to compare *As*Chi18A activity with other well-characterized chitinases, the chitin degradation potential of the enzyme was compared with the four GH18 chitinases of *S. marcescens* (*Sm*Chi18A, -B, -C and -D) (47-49) and, *Cj*Chi18D, which is the most potent chitinase of *Cellvibrio japonicus* (50). Activities were monitored at pH 6.0 (Fig. 5C), which is the pH where the *S. marcescens* and *C. japonicus* chitinases have their optima (47, 51, 52), and at pH 7.5 (Fig. 5D), which is a typical pH of sea water and the near pH-optimum of *As*Chi18A. Strikingly, *Sm*Chi18A, -B, -C and *Cj*Chi18D yielded more than 50-fold more $(GlcNAc)_2$ than *As*Chi18A after 24 h incubation at pH 6. At pH 7.5, the differences in yields were lower (in the range of 25-40-fold larger yields, except for *Sm*Chi18D), most likely reflecting the difference in pH optima. It should be noted that the presence of NaCl in concentrations similar to sea water (~0.6 M) only marginally influenced *As*Chi18A activity (Fig. S3).

_As_LPMO10A and -B are active towards chitin

Both *Al. salmonicida* LPMOs were able to oxidize α- and β-chitin, yielding aldonic acid chitooligosaccharide products with degree of polymerization ranging from 3 to 8 (Fig. S4). Such product profiles are commonly observed for family AA10 LPMOs that target chitin (12, 14, 53). The two enzymes displayed slightly different operational stabilities when probed at temperatures ranging from 10 to 60 °C (Fig. 6). *As*LPMO10A showed an operational stability similar to that of *As*Chi18A, being approximately 30 °C (Fig. 6A, B). In contrast, *As*LPMO10B showed an operational stability lower than 30 °C (Fig. 6C, D). Comparison of the LPMO activities showed that *As*LPMO10A seems generally more active than *As*LPMO10B, the former enzyme yielding approximately twice as much soluble oxidized products than the latter (Fig. 6B, D).

Combination of the chitinase and LPMOs shows enzyme synergies

For the putative chitinolytic system of *Al. salmonicida* the situation was different than any other chitinolytic system studied since the chitin degradation potential of the chitinase was substantially lower than that of the LPMOs (Fig. 5C, D and Fig. 6). Usually, the chitinase of a chitinolytic system is substantially more efficient in substrate solubilization than the LPMO. Nevertheless, synergies were observed when combining the *As*Chi18A with *As*LPMO10B giving an almost double yield than the sum of products calculated by adding the sum of their individual yields, for both α- and β-chitin (Fig. 7). *As*LPMO10A, on the other hand, showed a weaker synergy when combined with *As*Chi18A.

_As_Chi18A is important for growth of _Al. salmonicida_ on chitin

Since the *Al. salmonicida* chitinase and LPMOs were able to depolymerize both α- and β-chitin to soluble sugars that are metabolizable for the bacterium (GlcNAc and $(GlcNAc)_2$), the ability of the bacterium to utilize chitin particles as a carbon source was assessed. For this experiment, β-chitin was used for its higher purity and lower recalcitrance compared to α-chitin. To unravel the roles of *As*Chi18A and *As*LPMO10A and -B in chitin degradation, *Al. salmonicida* gene deletion strains were included in the cultivation experiments. The two single LPMO deletion strains showed a moderate decrease of the growth rate compared to the wild type, displaying a 30% increase in generation time (Fig. 8A and Table 1). In contrast to the biochemical assays that showed stronger synergy between recombinant *As*Chi18A and *As*LPMO10B compared to *As*LPMO10A, the cultivation assays showed that deletion of the single LPMOs resulted in the same growth reduction as deletion of both LPMOs. Deletion of the *AsChi18A* gene decreased growth to a larger extent than observed for the LPMO mutant strains (Fig. 8A), indicating that *As*Chi18A is more important than the LPMOs for the ability of *Al. salmonicida* to utilize chitin as a carbon source. The triple deletion mutant (ΔAΔBΔChi) was least able to utilize chitin as a source of nutrients, which also was clear from an agar-plate chitin solubilization assay where only a marginal disappearance of chitin was observed (Fig. S5). Growth of ΔAΔBΔChi and wild type on LB25 medium was on the other hand similar (Fig. S6), indicating that the gene deletions only influenced chitin utilization and not metabolism in general.

It should be noted that the wild type bacteria incubated in the minimal medium (Asmm) without added chitin obtained growth to OD 0.37±0.05 after 7 days incubation (Fig. 8 panel A and Table 1) due to the presence essential amino acids and traces of the LB25 pre-culture medium. Furthermore, it can also be observed that all bacterial strains incubated in the defined media supplemented with chitin increased ~0.1 in OD within the first 24 hours. This is most likely caused by the presence of chitin monomers, dimers, oligosaccharides or other nutrients in the chitin substrate that could be utilized by the bacteria without the need of the chitinase or LPMOs.

To evaluate whether growth of the bacterium correlated with chitinolytic activity, the culture supernatant of wild type growing on β-chitin was sampled once a day in the period of highest growth (days 5-8) and analyzed for hydrolytic activity towards the soluble chitooligosaccharide, chitopentaose. Indeed, the chitin hydrolytic potential of the culture supernatant increased from day 5 to day 8 (Fig. 8B), indicating secretion of one or more chitinases (only dimeric and trimeric products were observed; large concentrations of GlcNAc would indicate the presence of a secreted *N*-acetylhexosaminidase).

Gene expression analysis by PCR amplification of cDNA

Encouraged by the biochemically functional chitinolytic machinery of *Al. salmonicida* and the ability of the bacterium to metabolize chitin degradation products and chitin particles, it was of interest to couple these traits to transcription of genes representing the enzymes in the chitinolytic machinery. The pseudogene encoding parts of a family GH18 chitinase (*VSAL_I0902*; *As*Chi18B_p) was also included in the analysis. RNA was isolated from *Al. salmonicida* LFI1238 grown on glucose, GlcNAc, $(GlcNAc)_2$ and β-chitin (same cultures as shown in Fig. 1 and 8),

from both exponential and stationary phase. Gene expression was assessed qualitatively by agarose gel chromatography (Table 2). The gene expression was assessed as positive if the target gene was amplified in two out of three biological replicates and at the same time no amplification was observed in PCR samples obtained in the control reactions having no reverse transcriptase during cDNA synthesis (examples shown in Fig. S7). The resulting data indicated that *AsChi18A*, *AsLPMO10B* and, surprisingly, the chitinase pseudogene, *AsChi18B*$_p$, were expressed in the exponential phase during growth on all carbon sources. Similarly, expression of *AsChi18A* and *AsLPMO10A* were detected in the stationary phase, however not in all conditions. Expression of *AsLPMO10B* was only detected in the exponential phase during growth on GlcNAc.

Proteomic analysis of expressed carbohydrate active enzymes (CAZymes)
To obtain a more complete understanding of chitin degradation by *Al. salmonicida* during growth, label free quantitative proteomics was used to identify and quantify proteins secreted by the bacterium when growing on this insoluble polysaccharide. Guided by the gene expression analysis (Table 2), cultures were grown to exponential phase on 1% β-chitin before harvesting and separation into supernatant and cell pellet fractions for analysis of both secreted and intracellular proteins. For analysis of bacteria and proteins binding to chitin, chitin from the growing culture was collected and boiled directly in sample buffer. These samples are referred to as “chitin-bound” samples and are enriched in proteins with high affinity for chitin. In total, 1179 proteins were identified (Supplementary data file 1), from which 20 were annotated as CAZymes, including glycoside hydrolases, transferase activities, lipid biosynthesis, glycogen metabolism, peptidoglycan (murein) and carbohydrate metabolic processes (Fig. 9, Table S2). In more detail, both LPMOs (*As*LPMO10A and *As*LPMO10B) and *As*Chi18A were identified, albeit not in all samples and at variable intensities. *As*LPMO10A was present at highest abundance amongst the CAZymes, especially in the chitin-bound samples. The protein was identified in all three biological replicates in all sampled conditions except in the bacterial pellet obtained from growth on glucose, where the protein only was identified in one biological replicate (Fig. 9).

*As*Chi18A and *As*LPMO10B were only detected in the culture supernatant in one or two of the biological replicates obtained from growth on glucose, and in two out of three replicates of the chitin-bound samples. *As*Chi18A was only identified in the chitin-bound sample and the culture supernatant of the glucose grown samples. However, the chitinase was found at noticeable higher intensity in the chitin-bound samples compared to the supernatant samples obtained from cultivation on glucose.

Importantly, a GH20 β-*N*-acetylhexosaminidase (Uniprot ID: B6EGV7) was identified amongst the CAZymes. All samples showed a relatively similar abundance of this GH20. This enzyme, also called Chitobiase, is vital for hydrolyzing $(GlcNAc)_2$ into two GlcNAc units, but also has the ability to depolymerize longer chitooligosaccharides (even aldonic acid chitooligosaccharides resulting from LPMO activity) (53). Sequence analysis revealed 58% identity between the *Al. salmonicida* GH20 identified (~100% sequence coverage) and the biochemically characterized β-*N*-acetylhexosaminidase *Vh*NAG1 from *Vibrio harvey* 650 (54). The amino acids

involved in catalysis and substrate binding are conserved (Fig. S8) indicating a function of the *Al. salmonicida* GH20 in chitin catabolism. It should be noted that *N,N*-diacetylchitobiose phosphorylases also can perform a role similar to β-*N*-acetylhexosaminidases. Interestingly, a family 3 glycosyl hydrolase (GH3), annotated as beta-hexosaminidase was also identified. GH3s have a broad range of substrate specificities, which mostly involves peptidoglycan recycling pathways. However, the marine bacteria *Pseudoalteromonas piscicida*, *Vibrio furnissi* and *Thermotoga maritima* encode GH3s that are believed to participate in intracellular chitin metabolism (55-57). The *As*GH3 enzyme was detected at similar levels in both glucose and chitin cultures, indicating that it is not dependent on chitin degradation. Also, the amino acid sequence of *As*GH3 was similar to the NagZ enzymes of this GH family (e.g. 67% sequence identity to NagZ of *V. cholerae*), which removes β-*N*-acetylglucosamine from ends of peptidoglycan fragments (58). 4-alpha-glucanotransferase (GH77) and membrane-bound lytic murein transglycosylase (GH23) were only detected when the bacterium was grown on glucose. A putative glycosyl transferase family 2 (GT2) was only detected in the chitin substrate fraction. GTs are generally involved in biosynthesis by transferring sugar moieties from activated donor molecules to specific acceptor molecules, forming glycosidic bonds.

Analysis of the chitin catabolic pathway in *Al. salmonicida*

To assess the chitin catabolic pathway used by the bacterium, the proteomics data were scrutinized with the aim of identifying expressed proteins with a putative role in uptake, transport or downstream processing of chitin degradation products. An illustration of relevant findings and the suggested pathway is shown in Fig. 10. Guided by the biochemical assays and cultivation experiments, secreted *As*Chi18A, *As*LPMO10A and *As*LPMO10B are indicated to hydrolyze and cleave chitin into smaller oligosaccharides. It must be noted that *As*Chi18Bp, *As*Chi19Ap and *As*Chi18Cp are illustrated in context with *As*Chi18A based on conserved domains, rather than evidence of participating in extracellular hydrolysis of chitin. Interestingly, the chitinase pseudogene, *As*Chi18Bp, is one of few proteins exclusively identified in chitin samples. The GH20 β-*N*-acetylhexosaminidase, which shows a ~3 fold increase in abundance during growth on chitin compared to glucose ($p=0.0082$, paired two-tailed t-test; Fig. S9), is indicated to hydrolyze $(GlcNAc)_2$ into GlcNAc in the periplasmic space.

Utilization of extracellular sugars requires uptake and transportation across both the outer and inner membranes. With the lack of a functional chitoporin, other proteins relevant for outer membrane transport were investigated. Of proteins related to transport through the outer membrane, 14 proteins were identified, including outer membrane assembly factors and outer membrane proteins of the OmpA family, OmpU, TolC. These proteins are not generally known for sugar transport but cannot be excluded. For transport of sugars across the inner membrane, the most relevant transporters identified were 9 proteins assigned to the phosphoenolpyruvate-dependent sugar phosphotransferase system and two *N*-acetylglucosamine and glucose permeases (NagE). The latter transporters are likely contributing to translocation of GlcNAc across the inner membrane and showed increased abundance in chitin samples compared to glucose (Fig. 10). Two PTS component IIA and two Lactose/Cellobiose specific IIB subunits where

identified, of which the lactose/cellobiose specific subunits likely contribute to sugar transportation across the inner membrane, were found upregulated during growth on chitin compared to glucose. Furthermore, out of 9 ABC transporter proteins identified, the four components not related to iron or amino acid transport were assessed. The ABC transport protein, “ATP binding component” (B6EMA3) shows increased abundance in the chitin-bound samples, whereas “ATP-binding protein” (B6ESL1) was only identified during growth on chitin. However, it is uncertain whether these proteins are involved in transport of GlcNAc/$(GlcNAc)_2$. It should be noted that no ABC transporter proteins specific for $(GlcNAc)_2$, or GlcNAc specific subunits could be identified, although these are common in transport of such sugars (59-61).

In terms of downstream processing of GlcNAc, the monosaccharide is most likely converted into GlcNAc6P by the permease NagE or *N*-acetylglucosamine kinase NagK (Fig. 10). N-acetylglucosamine deacetylase is encoded by the genome of *Al. salmonicida*, albeit was not identified in this experiment. Deacetylation of GlcNAc6P would result in GlcN-6P, a product further processed into Fru-6P by glucosamine-6-phosphate deaminase, an enzyme which was found at higher abundance in the chitin pellet samples compared to glucose (Fig. 10). Alternatively, GlcN-6P can be processed (in three steps) by Phosphoglucosamine mutase (EC 5.4.2.10), the bifunctional protein GlmU (*N*-acetylglucosamine-1-phosphate uridyltransferase (EC 2.3.1.157) and UDP-*N*-acetylglucosamine pyrophosphorylase (EC 2.7.7.23) into UDP-GlcNAc, a sugar that can be processed to other UDP sugars or utilized in pathways such as lipopolysaccharide biosynthesis or peptidoglycan synthesis. These enzymes were found in all conditions analyzed (Fig. 10).

DISCUSSION

Knowing whether *Al. salmonicida* is able to utilize chitin as a source of carbon (and nitrogen) is important for understanding the ecology of the bacterium and its implications for pathogenicity. The literature contains conflicting information about this topic, but in the present study, we clearly demonstrate that *Al. salmonicida* is capable of degrading chitin to soluble chitooligosaccharides and to utilize these as a nutrient source. This capability is dependent on the single chitinase in the *Al. salmonicida* genome, despite the low in vitro activity of chitinase, and the ability of the LPMOs to degrade chitin. In the absence of *As*Chi18A, only products from LPMOs activity will be available to the bacterium. These products are oxidized chitooligosaccharides with a high degree of polymerization, that most likely cannot be taken up by the bacterium due to the absence of a specific outer membrane transporter (chitoporin). The fact that minor growth of the bacterium still is achieved in the absence of the chitinase is most likely due to the presence of a GH20 *N*-acetylhexosaminidase in the culture supernatant, that can depolymerize LPMO-generated chitooligosaccharides to GlcNAc, which can be taken up and catabolized by the bacterium. Another explanation may be that the chitooligosaccharides are cleaved by secreted pseudo-chitinases, proteins indeed observed by the proteomics data. In support for the latter hypothesis, minor growth on β-chitin and indications of degradation of colloidal chitin was observed for the

Al. salmonicida ΔAΔBΔChi variant (Figs 8 and S5, respectively). Notably, the importance of a single chitinase for growth on chitin is not unique to *Al. salmonicida* LFI1238. In *C. japonicus, Cj*Chi18D is essential for the degradation of α-chitin despite the expression of three additional chitinases and two LPMOs (50). Similarly, a systematic genetic dissection of chitin degradation and uptake in *Vibrio cholerae* found the chitinase ChiA2 critical for growth on chitin, but not sufficient alone (62).

Both *As. salmonicida* LPMOs are required for obtaining maximum growth on chitin, an observation that is different than for the efficient chitin degrader *C. japonicus* where deletion of the chitin-active LPMO only resulted in delayed growth, but did not affect growth rate (50). This may be explained by the 50-fold lower activity of *As*Chi18A compared to *Cj*Chi18D of *C. japonicus*. In the latter organism, the contribution of the LPMOs in chitin solubilization is most likely minor compared to *Al. salmonicida*, for which the rate of depolymerization is almost equal for the LPMOs and the chitinase. *As*LPMO10A and -B are distinctly different in domain organization and sequence and the former enzyme is more active towards β-chitin than the latter. This may be related to the chitin binding properties of the enzymes as *As*LPMO10A binds better to both α- and β-chitin than *As*LPMO10B (Fig. 4). Alternatively, the difference in activity can be related to the ability of the components in the reaction mixture to generate reactive oxygen species such as hydrogen peroxide, e.g. by the oxidase activity of LPMOs as shown in several studies (63-65). In such a scenario, the discovery that LPMOs can use H_2O_2 as a co-substrate, and that the concentration of H_2O_2 in solution may be rate limiting for LPMO reactions (13, 66, 67), may account for activity differences between LPMOs when no external H_2O_2 is added to the enzyme reaction (only reductant).

The contribution of the LPMOs for chitin utilization by *Al. salmonicida* is most likely related to the synergy obtained when combining the LPMOs with the chitinase. Such synergy can be explained by the ability of *As*LPMO10s to cleave chitin chains that are inaccessible to *As*Chi18A (i.e. in the crystalline regions of the substrate). The newly formed chitin chain ends formed by LPMO activity, represent new points of attachment for the chitinases, thereby increasing substrate accessibility. Indeed, several studies have demonstrated this phenomenon (16, 68-70), including a study on the virulence-related LPMO from *Listeria monocytogenes* (71).

A surprising observed was made when combining both LPMOs and the chitinase in a chitin degradation reaction (Fig. 7, panels B&D). Here, no synergy was observed for β-chitin degradation and a lower than theoretical yield was obtained for α-chitin. This was unexpected since the bacterial cultivation assay indicated a cooperative relationship between the LPMOs as the reduced growth observed for two single LPMO deletion strains were similar to that observed for the double LPMO mutant strain (*As*ΔLPMO10A-ΔLPMO10B). The explanation for the lack of synergy is not straightforward, but it may be that a total concentration of 2 □M LPMO is too much for these reactions, giving rise to less bound enzyme to the substrate and thereby production of harmful reactive oxygen species (ROS) by the non-bound LPMO molecules. It is well established that LPMOs not bound to the substrate are more prone to autooxidation (13, 43, 72). Another explanation could be that a non-optimal enzyme stoichiometry could create competition for substrate binding sites. Indeed, Both LPMOs were expressed during growth on β-chitin,

although *As*LPMO10A was detected in substantially higher abundance. As a matter of fact, *As*LPMO10A was the protein showing the highest abundance among the detected CAZymes, also when the bacterium was cultivated on glucose. This could imply that this LPMO has additional functions (this is discussed in more detail below). All three chitinolytic enzymes were observed in highest abundance in the samples obtained from the chitin particles, indicating high affinity of the enzymes towards chitin, a trait corroborated by the substrate binding experiments.

The proteomic analysis identified peptides from three pseudogenes. Interestingly, *As*Chi18Bp was only identified during growth on chitin, in contrast to the gene expression analysis where it was detected during growth in all carbon sources. This suggests a regulatory mechanism of translation influenced by the presence of chitin particles and that the relevant transcription factor regulating this gene still is functional. It is not uncommon that bacterial pseudogenes are expressed (73, 74) and Kuo & Ochman have hypothesized that this may be related to the regulatory region of the pseudogenes still remaining intact (74). It must be noted that translation of a pseudogene does not necessarily equal a functional protein. Indeed, our data showing a large growth impairment upon *AsChi18A* deletion suggest that translation of pseudogenes is insufficient for chitin degradation, although, as previously noted, a minor growth also can be observed for the triple knock out strain. Pseudogenes have long been considered to only represent dysfunctional outcomes of genome evolution, and the multitude of pseudogenes in *Al. salmonicida* LFI1238 possibly reflects its adaption to a pathogenic lifestyle. On the other hand, there is increasing evidence indicating that pseudogenes can have functional biological roles, and recent studies have shown that pseudogenes potentially regulate expression of protein-coding genes (reviewed in (75, 76)).

An intriguing observation of chitin catabolism by *Al. salmonicida* is the absence of key regulatory proteins such as ChiS and Tfox in the proteomics data. These regulatory proteins are important for chitin catabolism in other bacterial species in the *Vibrionacea* (18, 31, 33, 34). There is no doubt that *Al. salmonicida* is capable of chitin catabolism, thus the bacterium may have evolved an alternative mechanism for regulating the chitin utilization loci. In support of this hypothesis, the gene encoding the periplasmic chitin binding protein, which activates ChiS when bound to $(GlcNAc)_2$ (31), is disrupted in the *Al. salmonicida* genome (29).

Although the *Al. salmonicida* chitinolytic system clearly is active and functional, there are some observations that may indicate other or additional functions of the chitinolytic enzymes. Firstly, the activity of the chitinase is substantially lower that what would be expected for an enzyme dedicated to chitin hydrolysis. Secondly, the dominantly expressed LPMO (*As*LPMO10A) is not essential for chitin degradation and is also abundantly expressed when the bacterium is cultivated on glucose. These observations could be associated with the adaption of a pathogenic lifestyle where the need for chitin as a nutrient source has been reduced, but could also indicate other or additional functions, as for example roles in virulence. The notion of chitinases having additional functions has been shown in several studies, for example cleavage of mucin glycans by the *V. cholerae* chitinase Chi2A (77) and hydrolysis of LacdiNAc (GalNAcβ1-4GlcNAc) and LacNAc (Galβ1-4GlcNAc) by the *L. monocytogenes* and *Salmonella typhimurium*

chitinases (78). Such substrates were not evaluated by activity assays with *As*Chi18A. Moreover, incubation of *As*Chi18A with mucus collected from Atlantic salmon skin revealed an unidentifiable product (different from the negative control), but determination of its identity was unsuccessful.

Compared to other virulence related chitinases, *As*Chi18A has a similar size, but different modular architechture. For example, ChiA2 from *V. cholerae*, which has been shown to improve survival of the bacterium in the host intestine, also contains around 800 amino acids, but the GH18 domain is close to the N-terminus and a CBM44 and a CBM5 chitin-binding domain are present on the C-terminal side. As already noted, ChiA2 has been shown to cleave intestinal mucin (releasing GlcNAc), but has a deep substrate binding cleft and resembles an *exo*-chitinase (85% sequence identity to the structurally resolved *exo*-chitinase of *Vibrio harveyi*; (79)). An unusual property of *As*Chi18A is its double pH optimum, shown by enzyme activity being approximately equal at pH 4 and 7 (Fig. 5B). Chitinases usually display a single pH optimum, but double pH optima are not uncommon for hydrolytic enzymes, e.g. like phytase from *Aspergillus niger* (80) and β-galactosidase from *Lactobacillus acidophilus* (81). It is possible that this property is associated with the chitinase being utilized in environments that vary in pH. If the *Al. salmonicida* chitinase has evolved an additional role than chitin degradation, the same question applies for the LPMOs. Both LPMOs are active towards chitin, but it is not certain that this is the intended substrate of these enzymes. For instance, GbpA, an LPMO from *V. cholera*, has activity towards chitin (53), but its main function seems to be related to bacterial colonization of transfer vectors (e.g. zoo-plankton), the host epithelium (e.g. human intestine) or both (82, 83). The LPMO of *L. monocytogenes* is also active towards chitin (71), but the gene encoding this enzyme is not expressed when the bacterium grows on chitin (on the other hand, the *L. monocytogenes* chitinase-encoding genes are expressed when the bacterium is grown on chitin (71, 84)). The LPMO of the human opportunistic pathogen *Pseudomonas aeruginosa*, CbpD, was recently shown to be a chitin-active virulence factor that attenuates the terminal complement cascade of the host (85). In the present study, both LPMOs were expressed in the presence of chitin, but also in the glucose control condition, indicating that regulation is not controlled by chitin or soluble chitooligosaccharides. Thus, chitin may represent a potential substrate for these LPMOs, but possibly not the (only) biologically relevant substrate.

On the other hand, some LPMOs are designed to only disrupt and disentangle chitin fibers, rather than to contribute to their degradation in a metabolic context, namely the viral family AA10 LPMOs (also called spindolins) (41). These LPMOs are harbored by insect-targeting entomopox- and baculoviruses, and have been shown to disrupt the chitin containing peritrophic matrix that lines the midgut of insect larvae (86). The main function proposed for the viral LPMOs is to destroy the midgut lining in order to allow the virus particles to access the epithelial cells that are located underneath. Since the scales and gut of fish are indicated to contain chitin (5, 6), it is tempting to speculate that the role of the fish pathogen LPMOs is similar to that of viral LPMOs, namely to disrupt this putatively protective chitin layer in order to provide an entry point to the bacteria for infection.

In conclusion, the present study shows that *Al. salmonicida* LFI1238 can degrade and catabolize chitin as a sole carbon source, despite possessing a chitinolytic pathway assumed to be incomplete. Our findings imply that the bacterium can utilize chitin to proliferate in the marine environment, although possibly not as efficient as other characterized chitinolytic marine bacteria. Nevertheless, it is likely that this ability can be of relevance for the spread of this pathogen in the ocean. Finally, our discovery that pseudogenes are actively transcribed and translated indicates that such genes cannot be disregarded as being functionally important.

METHODS AND MATERIALS

Bacterial strains and culturing conditions

Al. salmonicida strain LFI1238 originally isolated from the head kidney of diseased farmed cod (*Gadhus morhua; (29)*) and mutant strains (see below) were routinely cultivated at 12 °C in liquid Luria Broth (LB) supplemented with 2.5% sodium chloride (LB25; 10 g/L tryptone, 5 g/L yeast extract, 12.5 g/L NaCl) or solid LB25 supplemented with 15 g/L agar powder (LA25), and if applicable 2% (w/v) colloidal chitin made from α-chitin (gift from Silje Lorentzen). Growth analysis was performed at 12 °C in *Al. salmonicida* specific minimal media (Asmm: 100 mM KH_2PO_4, 15 mM $NH_4(SO_4)_2$, 3.9 µM $FeSO_4{\times}7H_2O$, 2.5 % NaCl, 0.81 mM $MgSO_4{\times}7H_2O$, 2 mM valine, 0.5 mM isoleucine, 0.5 mM cysteine, 0.5 mM methionine and 40 mM glutamate). Prior to inoculation of Asmm media, strains were grown up to 48 hours in 10-15 mL LB25 at 200 rpm. 1 mL bacteria were harvested by centrifugation at 6000 × *g* for 1 minute, followed by immediate resuspension of the pellet in 1 mL Asmm. The cell suspension was transferred to the final cultures by a 1:50 dilution in media supplemented with 0.2% glucose, 0.2% N-acetyl-D-glucosamine, 0.2 % diacetyl-chitobiose (Megazyme, Bray, County Wicklow, USA) or 1 % β-chitin from squid pen purchased from France Chitine (Batch 20140101, Orange, France). Culture volumes ranged from 5-50 mL. Final cultures were incubated at 12 °C with shaking at 175 rpm. Growth was measured by optical density (OD_{600}) using Ultrospec® 10 Cell Density Meter (Biochrom). The baseline was set by using sterile Asmm media with or without 1% β-chitin. OD_{600} measurements of the β-chitin cultures was performed by allowing the cultures to settle for 30 seconds before collecting 1 mL for measurement.

Generation of gene deletion strains

LFI1238 derivative in-frame deletion mutants *ΔAsChi18A, ΔAsLPMO10A, ΔAsLPMO10B, ΔAsLPMO10A-ΔLPMO10B and ΔLPMO10A-ΔLPMO10B-ΔChi18A* (also referred to as DADBDChi) were constructed by allelic exchange as described by others (87, 88). For clarification, Table 3 lists the target genes, their associated protein name, predicted carbohydrate-active enzyme family (CAZyme family) and corresponding CAZyme annotated name applied throughout this study.

Primers were ordered from eurofins Genomics (Ebersberg, Germany), and designed with restriction sites and regions complementary to the pDM4 cloning vector to allow for in-fusion cloning. Table 4 lists primers used for construction of the deletion alleles. For construction of ΔAsChi18A, the flanking regions upstream and downstream of the *AsChi18A* gene were amplified using primer pairs

GH18_YF/GH18_IR and GH18_IF/GH18_YR, respectively. The two PCR fragments were fused by overlapping extension PCR where complementarity in the 5′ regions of the primers resulted in linkage of the *AsChi18A* -flanking regions. Δ*AsLPMO10A* and Δ*AsLPMO10B* was constructed in the same manner as described for *ΔAsChi18A* using the listed primers (Table 4).

The final PCR products were inserted into the suicide vector pDM4 by In-Fusion ® HD cloning (Takara Bio USA, Inc). In short, pDM4 linearized with SpeI and XhoI was gently mixed with 5× In-Fusion HD Enzyme premix, purified PCR fragment (purified using Nucleospin® Gel and PCR Clean-up, MACHEREY-NAGEL GmbH & Co. KG), and H_2O to acquired final volume. Ratio of insert and linearized vector was determined using the online tool "In-Fusion molar ratio calculator" (Takara Bio USA, Inc). The reaction mix was incubated at 50 °C for 15 min. Following incubation, the reaction mix was placed on ice for 20 min and transformed into *E. coli* S17-1 λpir by standard transformation techniques.

Conjugation was performed as described by others (87-90). In brief, pelleted cells from 1 mL *E.coli* S17-1 donor cells (OD_{600} 0.60-0.80) and 1 mL *Al. salmonicida* LFI1238 recipient cells (OD_{600} 1.00-1.40) were washed in LB, mixed and transferred to LA1 as a spot. The spot plate was incubated 6 hours in room temperature and ~17 hours at 12 °C. The next day, the cell spot was collected and resuspended in 2 mL LB25, grown for 24 hours with shaking and spread onto LA25 containing chloramphenicol (2 µL/mL). Potential transconjugates were re-streaked on LA25 2CAM, incubated for 3-5 days and tested for integration of the pDM4 construct by colony PCR using a combination of primers annealing within and outside the integrated plasmid (Table S3). Next, confirmed transconjugates were grown in LB25 to OD_{600} 0.4 and spread onto LA25 containing 5% sucrose. Colonies appearing within 5 days were tested for excision of the integrated plasmid by sequentially patching single colonies onto LA25 plates containing 2CAM or 5% sucrose. Mutants showing loss of resistance to CAM and presence of gene-deletion product (colony PCR using primer pairs *AsΔChi18A*_For/ *AsΔChi18A*_Rev), was confirmed by GATC Biotech Sanger sequencing (Eurofins genomics, Germany).

Mutant strains containing multiple gene deletions were generated in a step-wise manner. Specifically, LFI1238ΔAsLPMO10A were recipient cells for pDM4-ΔAsLPMO10B. Similarly, the resulting ΔAsLPMO10A/ΔLPMO10B strain were recipient cells for pDM4-ΔAsChi18A, thus generating the triple mutant strain ΔLPMO10A/ΔLPMO10B/ΔChi18A. All strains and vectors are listed in Table 5.

Cloning, expression and purification

Codon-optimized genes encoding the following *As*LPMO10A (residues 1-491, UniProt ID; B6EQB6), *As*LPMO10B (residues 1-395, UniProt ID; B6EQJ6) and *As*Chi18A (residues 1-846, UniProt ID; B6EH15) from *Al. salmonicida* (LFI1238) were purchased from GenScript (Piscataway, NJ, USA). Gene-specific primers (Table 6), with sequence overhangs corresponding to the pre-linearized pNIC-CH expression vector (AddGene, Cambridge, Massachusetts, USA) were used to amplify the genes in order to insert them into the vector by a ligation independent cloning method (91). All the cloned genes contained their native signal peptides. Sequence-verified plasmids were transformed into ArcticExpress (DE3) competent

cells (Agilent Technologies, California, USA) for protein expression. Cells harboring the plasmids were inoculated and grown in Terrific Broth (TB) medium supplemented with 50 µg/mL of kanamycin (50 mg/mL stock). Cells producing the full-length *As*LPMO10s were cultivated in flask-media at 37 °C until OD = 0.700, cooled down for 30 min at 4 °C, induced with 0.5 mM IPTG and incubated for 44 hours at 10 °C with shaking at 200 rpm. Cells producing *As*Chi18A were grown in a Harbinger LEX bioreactor system (Epiphyte Three Inc, Toronto, Canada) using the same procedure described above, although the cell were cultured for a shorter time period (12 hours) and air was pumped into the culture by spargers. Successively, cells were harvested using centrifugation and the periplasmic extracts were generated by osmotic shock (92). The periplasmic fractions, containing the mature proteins (signal peptide-free), were sterilized by filtration (0.2 µm) before purification (see below).

*As*LMO10A and *As*LPMO10B were purified by anion exchange chromatography using a 5 mL HiTrap DEAE FF column (GE Healthcare) followed by hydrophobic interaction chromatography (HIC) using a 5 mL HiTrap Phenyl FF (HS) column (GE Healthcare). For the ion exchange procedure, proteins in the periplasmic extract were applied on the column using a binding buffer containing 50 mM Bis-Tris-HCl pH 6.0. After all non-bound proteins had passed through the column, bound proteins were eluted by applying a linear gradient (0 to 100 % in 20 column volumes with a flow rate of 1 mL/min), using an elution buffer containing Bis-Tris-HCl pH 6.0 and 500 mM NaCl. Fractions were collected and analyzed for the presence of LPMO using SDS-PAGE. Fractions containing LPMO were pooled and adjusted to 1M $(NH_4)_2SO_4$ and applied on the HIC column using a binding buffer consisting of 50 mM Tris-HCl pH 7.5 and 1 M $(NH_4)_2SO_4$. Following elution of unbound proteins, bound proteins were eluted by applying a linear gradient (0 to 100% over 20 column volumes with a flow rate of 1.5 mL/min), using an elution buffer containing 50 mM Tris-HCl pH 7.5. In addition, *As*LPMO10B was further purified by size exclusion chromatography using a HiLoad 16/60 Superdex 75 column operated at 1 mL/min and with a running buffer containing 1X PBS, pH 7.4.

*As*Chi18A was purified by immobilized metal affinity chromatography using a HisTrap FF 5 mL column (GE Healthcare). The periplasmic extract containing *As*Chi18A was applied on the column using a binding buffer consisting of 20 mM Tris-HCl pH 8.0 and 5 mM imidazole, using a flow rate of 3 mL/min. Bound proteins were eluted from the column by applying a linear gradient (0 to 100 % over 20 column volumes with a flow rate of 3 mL/min) with an elution buffer containing 20 mM Tris-HCl pH 8.0 and 500 mM imidazole. Fractions containing the pure protein, identified by SDS-PAGE, were pooled and concentrated using Amicon Ultra centrifugal filters (Millipore, Cork, Ireland).

Protein purity was analyzed by SDS-PAGE. Concentrations of the pure proteins were determined by measuring A_{280} and using the theoretical molar extinction coefficients of the respective enzyme (calculated using the ExPASy ProtParam tool) to estimate the concentration in mg/mL. Before use, *As*LPMO10A and *As*LPMO10B were saturated with Cu(II) by incubation with excess of $CuSO_4$ in a molar ratio of 1:3 for 30 minutes at room temperature. The excess Cu(II) was

eliminated by passing the protein through a PD MidiTrap G-25 desalting column (GE Healthcare) equilibrated with 50 mM Tris-HCl pH 8.0 and 150 mM NaCl.

Preparation of substrates

The substrates used in the assays were either squid pen β-chitin (France Chitin, Orange, France), shrimp shell α-chitin purchased from Chitinor As (Avaldsnes, Norway) and skin mucus of *Salmo salar*. Skin mucus was collected from freshly killed farmed Atlantic salmon purchased from the Solbergstrand Marine Research Facility (Drøbak, Norway). The mucus was gently scraped off the skin of the fish using a spatula and stored in plastic sample tubes at -20°C until use.

Enzyme activity assays

For activity assays, chitin was suspended in 20 mM Tris-HCl pH 7.5, in 2 mL Eppendorf tubes to yield a final concentration of 10 mg/mL. All reactions were incubated at 30 °C and stirred in an Eppendorf Comfort Thermomixer at 700 rpm. For LPMO reactions, the final enzyme concentrations were 1 µM and reactions were started by the addition of 1 mM of ascorbic acid (this activates the LPMOs). Similar reaction conditions were used for *As*Chi18A, although the final enzyme concentration used was 0.5 µM and ascorbic acid was not added in the reactions. At regular intervals, samples were taken from the reactions and the soluble fractions were separated from the insoluble substrate particles using a 96-well filter plate (Millipore) operated with a vacuum manifold. Subsequently, the soluble fraction of *As*LPMO10s-catalyzed reactions were incubated with 1.5 µM of a chitobiase from *S. marcescens* (also known as *Sm*CHB or *Sm*GH20A) at 37 °C overnight in order to convert LPMO products (oxidized chitooligosaccharides of various degree of polymerization) to *N*-acetylglucosamine (GlcNAc) and chitobionic acid (GlcNAcGlcNAc1A) as previously described in (53, 93), followed by a sample dilution with 50 mM H_2SO_4 in a ratio of 1:1 prior quantification by HPLC (see below). The soluble fractions of *As*Chi18A reactions, were diluted with H_2SO_4 after the filtration step, which stopped the enzymatic reaction, before quantification of $(GlcNAc)_2$ by HPLC (see below). Additionally, in order to collect samples for product profiling by matrix-assisted laser desorption/ionization time of flight mass spectrometry (MALDI-TOF MS, see below) of the two *As*LPMO10s-catalyzed reactions, 5 µL of the soluble fraction was sampled after filtration and kept at -20 °C prior to analysis.

Analysis and quantification of native and oxidized chitooligosaccharides, $(GlcNAc)_2$ and GlcNAc

Qualitative analysis of the native and oxidized products of the *As*LPMO10A and -B soluble fractions were performed by MALDI-TOF MS using a method developed by G. Vaaje-Kolstad et al. (12). For this analysis, 1 µL of sample was mixed with 2 µL 2,5-dihydroxybenzoic acid (9 $g.L^{-1}$, prepared in 150:350 H_2O/Acetonitrile), applied to a MTP 384 target plate in ground steel TF (Bruker Daltonics) and dried under a stream of warm air. The samples were analyzed with an Ultraflex MALDI-TOF/TOF instrument (Bruker Daltonics GmbH, Bremen, Germany) equipped with a Nitrogen 337 nm laser beam, using Bruker FlexAnalysis software. Quantitative analysis of all soluble products formed by the chitinolytic enzymes or GlcNAc or $(GlcNAc)_2$ in culture supernatants was performed by ion exclusion chromatography

using a Dionex Ultimate 3000 UHPLC system (Dionex Corp., Sunnyvale, CA, USA), equipped with a Rezex RFQ-Fast acid H^+ (8%) 7.8% x 100 mm column (Phenomenex, Torrance, CA). The column was pre-heated to 85 °C and was operated by running 5 mM H_2SO_4 as a mobile phase at a flow rate of 1 mL/min. The products were separated isocratically and detected by UV absorption at 194 nm. The amount of GlcNAc and $(GlcNAc)_2$ were quantified using standard curves. Pure GlcNAc and $(GlcNAc)_2$ were obtained from Sigma and Megazyme, respectively. In order to quantify chitobionic acid (GlcNAcGlcNAc1A), a standard was produced in-house by treating chitobiose (Megazyme, Bray, Irleand) with a chitooligosaccharide oxidase (ChitO) from *Fusarium graminearum* , which yields 100% conversion of chitobiose to chitobionic acid, a method previously described by J. S. M. Loose et al. (53). Standards were regularly analysed in each run.

Analysis of chitinase activity in culture supernatants

To analyze presence of chitinolytic activity in the supernatant of *Al. salmonicida* when growing on β-chitin, 1 mL sample of wild type bacterial culture was harvested at time points during growth on chitin. The sample was centrifugated and the supernatant filter sterilized using 0.22µm sterile Ultra-free centrifugal filters. 500 µL filter sterilized supernatant was concentrated to 100 µL using Amicon ultra centrifugal filter units with 3 000 Da cut-off (Merck Millipore, Cork Ireland) and washed three times in 10 mM Tris pH 7.5, 0.2 M NaCl (Tris-HCl NaCl). The concentrated supernatant containing secreted enzymes were stored in Tris-HCl at 4 °C until use. The presence of chitinolytic activity was assessed by mixing 100 µM chitopentaose with 15 µL enzyme cocktail in 20 mM Tris pH 7.5 0.2 M NaCl and incubated at 30 °C. The generated products were analyzed and quantified by ion exclusion chromatography as described above.

Protein binding assays

The binding capacity of *As*LPMO10s and *AsChi*18A on α-chitin and β-chitin was tested, suspending 10 mg/mL of substrate in 20 mM Tris-HCl pH 7.5 to a total volume of 350 µL in 2 mL Eppendorf tubes. Reactions were started by the addition of *As*LPMO10A or –B (0.75 µM final concentration) or *AsChi*18A (0.50 µM), which were incubated in 2 mL Eppendorf tubes, at 30 °C and stirred in an Eppendorf Comfort Thermomixer at 700 rpm. Samples were taken (100 µL) after 2 hours and immediately filtrated using a 96-well filter plate (Millipore) operated with a vacuum manifold to obtain the unbound protein fraction. In order to assess the percentage of bound proteins to the substrate, control samples with only enzyme and buffer were performed, representing the maximum quantity of protein present in the samples (100%). The protein concentration in each sample was determined using the Bradford assays (Bio-Rad, Munich, Germany).

RNA isolation and gene expression analysis

To analyze expression of specific genes as previously done by e.g. T. M. Wagner et al. (94), samples were taken at mid exponential phase (OD = 0.6-0.7) and early stationary phase (OD = 1.0-1.3).1 mL sample of each culture was directly transferred to 2 mL RNAprotect cell reagent (Qiagen, Hilden, Germany). The samples were vortexed 5 sec, incubated 5 min at room temperature and subsequently harvested by centrifugation at 4000 × *g*, for 10 min at 4 °C. The supernatant was carefully decanted, and the cell pellet stored at -20 °C until cell

lysis and RNA isolation. RNA isolation was performed using Qiagen RNeasy Mini Kit (Qiagen, Hilden, Germany) using the Quick-Start protocol. In order to disrupt the bacterial cell wall before isolation, the pellet was lysed using 200 µL Tris-EDTA pH 8.0 supplemented with 1 mg/mL lysozyme, vortexed for 10 sec and subsequently incubated at room temperature for 45 min. 700 µL buffer RLT (kit buffer, Qiagen) supplemented with 10 µL/mL β-mercaptoethanol was added to the sample and mixed vigorously before proceeding with the protocol. The quantity of isolated RNA was determined using NanoDrop.

Residual genomic DNA (gDNA) was removed using The Heat&Run gDNA removal kit (ArcticZymes®, Tromsø, Norway). 8 µL of the RNA samples was transferred to a RNase free Eppendorf tube on ice. For each 10 µL reaction, 1 µL of 10× reaction buffer and 1 µL Heat-labile-dsDNase was added. The suspension was gently mixed and incubated at 37 °C for 10 min. To inactive the enzyme, samples were immediately transferred to 58 °C for 5 min. The RNA concentration was measured using the nanodrop before proceeding to copy DNA (cDNA) synthesis.

cDNA synthesis was performed using iScript™ Reverse Transcription Supermix (Bio-Rad, Hercules, CA, USA). For each sample, 100 ng RNA, 4 µL 5× iScript™ Reverse transcription Supermix and RNase free water to a total volume of 20 µL was assembled in PCR reaction tubes. All samples were additionally prepared with iScript™ no reverse transcriptase control supermix to account for residual gDNA in downstream analysis. The cDNA synthesis of the samples were performed by using a SimpliAmp™ Thermal Cycler (Thermo Fischer Scientific, USA) with the following steps: priming at 25 °C for 5 min, reverse transcription at 46 °C for 20 min, and inactivation of the reverse transcriptase at 95 °C for 1 min. The synthesized cDNA was stored at -20 °C until analysis.

The cDNA samples were screened for presence of *AsChi18A, AsLPMO10A, AsLPMO10B* and *VSAL_I0902*/*AsChi18Bp* by PCR amplification using Red Taq DNA polymerase 2× Master mix (VWR, Oslo, Norway) according to the manufacturers protocol. The PCR reaction was carried out using 30 cycles, annealing temperature 58 °C (*AsChi18A, AsLPMO10A, AsLPMO10B*) or 56 °C (*VSAL_I0902*/*AsChi18Bp*) and 30 sec extension. To evaluate gDNA presence, samples prepared with no reverse transcriptase during cDNA synthesis (referred to as -RT control) was applied as template for primer pairs *AsLPMO10A* and VSAL_I0902.

PCR products were visualized by agarose gel electrophoresis of the total 20 µL PCR reaction in 1.3 % agarose 1xTAE electrophoresis buffer (Thermo scientific, Vilnius, Lithuania). The agarose was supplemented with peqGreen DNA/RNA dye (peqlab brand, VWR, Oslo, Norway) for visualization. After gel visualization, the gene expression was assessed as positive if the target gene was amplified in two out of three biological replicates and at the same time no amplification was observed in PCR samples prepared with the -RT controls. A complete list of primers used for amplification of target genes is shown in Table S4.

Sample preparation and proteomic analysis

Biological triplicates of *Al. salmonicida* LFI1238 was incubated in 50 mL Asmm supplemented with 1 % β-chitin. At mid-exponential phase, cultures were harvested and fractioned into supernatant and pellet by centrifugation at 4 000 × *g* for 10 min at 4°C. β-chitin aliquots from the culture flasks were transferred to 2 mL Safe-Lock Eppendorf tubes (Eppendorf, Hamburg, Germany) and boiled directly for 5 min in 30 µL NuPAGE LDS sample buffer and NuPAGE sample reducing agent (Invitrogen™, CA, USA). Filter sterilized supernatant was concentrated using Vivaspin® 20 centrifugal concentrators (Vivaproducts, Littleton, MA, USA) by centrifugation at 4 000 rpm and 4 °C until it reached 1 mL concentrate. The bacterial pellet was lysed in 2 mL 1× BugBuster™ protein extraction reagent (Novagen), incubated by slow shaking for 20 min, followed by centrifugation and protein precipitation. Proteins were precipitated by adding trichloroacetic acid (TCA) to 10 % and incubation over-night at 4 °C. The precipitated proteins were harvested by centrifugation at 16 000 × *g* and 4°C for 15 min and washed twice in ice-cold 90 % acetone/0.01 M HCl. All final samples were boiled in 30 µL NuPAGE LDS sample buffer and sample reducing agent for 5 min and loaded on Mini-PROTEAN® TGX Stain- Free™ Gels (Bio-Rad laboratories, Hercules, CA, USA). Electrophoresis was performed at 300 V for 3 min using the BIO-RAD Mini-PROTEAN® Tetra System. Gels were stained with Coomassie Brilliant Blue R250 and 1×1 mm cube gel pieces were excised and transferred to 2 mL LoBind tubes containing 200 µL H_2O. Sequentially, the gel pieces were washed 15 min in 200 µl H_2O and decolored by incubating 2×15 min in 200 µL 50% acetonitrile, 25mM ammonium bicarbonate (AmBic). Next, reduction was performed by incubating the gel pieces in dithiothreitol (10 mM DTT/100mM AmBic) for 30 minutes at 56 °C and alkylation was done with iodo-acetamide (55 mM IAA/100mM AmBic) for 30 minutes at room temperature. After removal of the IAA solution, the gel pieces were dehydrated using 200µL 100% acetonitrile and digested using 30-45 µL of 10 ng/µL trypsin solution overnight at 37 °C. The next day, digestion was stopped by addition of 40 µL 1% trifluoroacetic acid (TFA). Peptides were extruded from the gel pieces by 15 minutes sonication and desalted using C18 ZipTips (Merch Millipore, Darmstadt, Germany), according to manufacturer's instructions.

Peptides were essentially analyzed as previously described (95). In brief, peptides were loaded onto a nanoHPLC-MS/MS system (Dionex Ultimate 3000 UHPLC; Thermo Scientific) coupled to a Q-Exactive hybrid quadrupole orbitrap mass spectrometer (Thermo Scientific). Peptides were separated using an analytical column (Acclaim PepMap RSLC C18, 2 µm, 100 Å, 75 µm i.d. ´ 50 cm, nanoViper) with a 90-minutes gradient from 3.2 to 44 % [v/v] acetonitrile in 0.1% [v/v] formic acid) at flow rate 300 nL/min. The Q-Exactive mass spectrometer was operated in data-dependent mode acquiring one full scan (400-1500 m/z) at R=70000 followed by (up to) 10 dependent MS/MS scans at R=35000. The raw data were analyzed using MaxQuant version 1.6.3.3 and proteins were identified and quantified using the MaxLFQ algorithm (96). The data were searched against the UniProt *Al. salmonicida* proteome (UP000001730; 3513 sequences) supplemented with common contaminants such as human keratin and bovine serum albumin. In addition, reversed sequences of all protein entries were concatenated to the database to allow for estimation of false discovery rates. The tolerance levels used for matching to the database were 4.5 ppm for MS and 20 ppm for MS/MS.

Trypsin/P was used as digestion enzyme and 2 missed cleavages were allowed. Carbamidomethylation of cysteine was set as fixed modification and protein N-terminal acetylation, oxidation of methionines and deamidation of asparagines and glutamines were allowed as variable modifications. All identifications were filtered in order to achieve a protein false discovery rate (FDR) of 1%. Perseus version 1.6.2.3 (97) were used for data analysis, and the quantitative values were log2-transformed, and grouped according to carbon source and condition (substrate/supernatant/pellet). Proteins were only considered detected if they were present in at least two replicates in at least one condition. All identified proteins were annotated with putative carbohydrate-active functions as predicted by dbCAN2 (98), biological functions (GO and Pfam) downloaded from UniProt, and for subcellular location using SignalP5.0 (99).

Pseudogenes

Pseudogenes are gene sequences that have been mutated or disrupted into an inactive form over the course of evolution and is commonly thought of as "junk DNA". The genome of *Al. salmonicida* LFI1238 contains a significant number of IS elements, and several genes are truncated and annotated as such pseudogenes. Since pseudogenes in general are believed to be non-functional, putative products of these are commonly not included in proteome databases. Consequently, a proteomic analysis towards the annotated proteome of *Al. salmonicida* LFI1238 will not detect products of these genes. To include these in our analysis, a few required steps were taken. Firstly, pseudogenes of three chitinases, a chitoporin and a chitodextrinase were selected as genes of interests based on the publication by Hjerde et al (29). Next, the truncated nucleotide sequence of a pseudogene was retrieved by searching the complete genome sequence annotation of *Al. salmonicida LFI1238* chromosome I (FM178379.1) for the specific gene locus. The gene locus of each selected pseudogene is shown in Table 7. The nucleotide sequences were translated to putative protein sequences using the translate tool at ExPASy Bioinformatics Resource Portal (100). The translate tool identifies potential start and stop codons of the query sequence by assessing reading frames 1-3 of forward and reverse DNA strand. Manually, putative peptides larger or equal to 6 amino acids were selected as supplement for the proteomic analysis. Pseudogene products of which unique peptides were identified was assigned a putative CAZy annotation using dbCAN2.

Data availability

The mass spectrometry proteomics data have been deposited to the ProteomeXchange Consortium via the PRIDE (101) partner repository with the dataset identifier PXD021397.

ACKNOWLEDGEMENTS

This work was funded by grant 249865 (GV-K, AS, MØA and JSML) from the Norwegian Research Council and by a PhD fellowships from the Norwegian University of Life Sciences, Faculty of Chemistry Biotechnology and Food Science to GiM. BB has received the support of the EU in the framework of the Marie-Curie FP7 COFUND People Programme, through the award of an AgreenSkills fellowship (under grant agreement n° 267196). The authors would like to thank Simen Foyn Nørstebø (Faculty of Veterinary Medicine, Department of Food Safety and Infection Biology, Norwegian university of life sciences) for providing bacterial

strains for deletion mutagenesis and for valuable advice regarding the protocol and Anne Cathrine Bunæs for assistance in purification of proteins.

AUTHOR CONTRIBUTIONS

AS: Planned experiments, performed experiments, analyzed data, wrote the paper. JSML: planned experiments, wrote the paper. GiM: Planned experiments, performed experiments, analyzed data, wrote the paper. JSML: planned experiments, wrote the paper. SM: performed experiments, analyzed data, wrote the paper. BB: performed experiments, analyzed data, wrote the paper. MØA: performed experiments, analyzed data, wrote the paper. GeM: planned experiments, wrote the paper. GV-K: conceptualized the study, planned experiments, analyzed data, wrote the paper, supervised the study.

CONFLICTS OF INTEREST

The authors declare no conflict of interest.

REFERENCES

1. Wang Y, Chang Y, Yu L, Zhang C, Xu X, Xue Y, Li Z, Xue C. 2013. Crystalline structure and thermal property characterization of chitin from Antarctic krill (*Euphausia superba*). Carbohyd Polym 92:90-97.
2. Raabe D, Romano P, Sachs C, Fabritius H, Al-Sawalmih A, Yi SB, Servos G, Hartwig HG. 2006. Microstructure and crystallographic texture of the chitin–protein network in the biological composite material of the exoskeleton of the lobster *Homarus americanus*. Mat Sci Eng A 421:143-153.
3. Acosta N, Jiménez C, Borau V, Heras A. 1993. Extraction and characterization of chitin from crustaceans. Biomass Bioenerg 5:145-153.
4. Bacon JS, Davidson ED, Jones D, Taylor IF. 1966. The location of chitin in the yeast cell wall. Biochem J 101:36C-38C.
5. Tang WJ, Fernandez J, Sohn JJ, Amemiya CT. 2015. Chitin is endogenously produced in vertebrates. Curr Biol 25:897-900.
6. Wagner G, Lo J, Laine R, Almeder M. 1993. Chitin in the epidermal cuticle of a vertebrate (*Paralipophrys trigloides,* Blenniidae, Teleostei). Cell Mol Life Sci 49:317-319.
7. Gooday GW. 1990. The ecology of chitin degradation. Adv Microb Ecol 11:387-430.
8. Keyhani NO, Roseman S. 1999. Physiological aspects of chitin catabolism in marine bacteria. Biochim Biophys Acta 1473:108-22.
9. Lombard V, Golaconda Ramulu H, Drula E, Coutinho PM, Henrissat B. 2014. The carbohydrate-active enzymes database (CAZy) in 2013. Nucleic Acids Res 42:D490-5.
10. Brameld KA, Shrader WD, Imperiali B, Goddard WA. 1998. Substrate assistance in the mechanism of family 18 chitinases: Theoretical studies of potential intermediates and inhibitors. J Mol Biol 280:913-923.
11. Terwisscha van Scheltinga AC, Armand S, Kalk KH, Isogai A, Henrissat B, Dijkstra BW. 1995. Stereochemistry of chitin hydrolysis by a plant chitinase/lysozyme and X-ray structure of a complex with allosamidin: evidence for substrate assisted catalysis. Biochemistry 34:15619-15623.
12. Vaaje-Kolstad G, Westereng B, Horn SJ, Liu Z, Zhai H, Sørlie M, Eijsink VGH. 2010. An oxidative enzyme boosting the enzymatic conversion of recalcitrant polysaccharides. Science 330:219-222.

13. Bissaro B, Røhr ÅK, Müller G, Chylenski P, Skaugen M, Forsberg Z, Horn SJ, Vaaje-Kolstad G, Eijsink VGH. 2017. Oxidative cleavage of polysaccharides by monocopper enzymes depends on H_2O_2. Nat Chem Biol 13:1123-1128.
14. Gregory RC, Hemsworth GR, Turkenburg JP, Hart SJ, Walton PH, Davies GJ. 2016. Activity, stability and 3-D structure of the Cu(ii) form of a chitin-active lytic polysaccharide monooxygenase from *Bacillus amyloliquefaciens*. Dalton Trans 45:16904-16912.
15. Forsberg Z, Mackenzie AK, Sørlie M, Røhr AK, Helland R, Arvai AS, Vaaje-Kolstad G, Eijsink VGH. 2014. Structural and functional characterization of a conserved pair of bacterial cellulose-oxidizing lytic polysaccharide monooxygenases. Proc Natl Acad Sci U S A 111:8446-8451.
16. Nakagawa YS, Kudo M, Loose JS, Ishikawa T, Totani K, Eijsink VGH, Vaaje-Kolstad G. 2015. A small lytic polysaccharide monooxygenase from *Streptomyces griseus* targeting α-and β-chitin. FEBS J 282:1065-1079.
17. Sabbadin F, Hemsworth GR, Ciano L, Henrissat B, Dupree P, Tryfona T, Marques RDS, Sweeney ST, Besser K, Elias L, Pesante G, Li Y, Dowle AA, Bates R, Gomez LD, Simister R, Davies GJ, Walton PH, Bruce NC, McQueen-Mason SJ. 2018. An ancient family of lytic polysaccharide monooxygenases with roles in arthropod development and biomass digestion. Nat Commun 9:756.
18. Hunt DE, Gevers D, Vahora NM, Polz MF. 2008. Conservation of the chitin utilization pathway in the Vibrionaceae. Appl Environ Microbiol 74:44-51.
19. Lin H, Yu M, Wang X, Zhang XH. 2018. Comparative genomic analysis reveals the evolution and environmental adaptation strategies of vibrios. BMC Genomics 19:135.
20. Uchiyama T, Kaneko R, Yamaguchi J, Inoue A, Yanagida T, Nikaidou N, Regue M, Watanabe T. 2003. Uptake of *N,N'*-diacetylchitobiose [$(GlcNAc)_2$] via the phosphotransferase system is essential for chitinase production by *Serratia marcescens* 2170. J Bacteriol 185:1776-82.
21. Eisenbeis S, Lohmiller S, Valdebenito M, Leicht S, Braun V. 2008. NagA-dependent uptake of *N*-acetyl-glucosamine and *N*-acetyl-chitin oligosaccharides across the outer membrane of *Caulobacter crescentus*. J Bacteriol 190:5230-8.
22. Keyhani NO, Li XB, Roseman S. 2000. Chitin catabolism in the marine bacterium *Vibrio furnissii* - Identification and molecular cloning of a chitoporin. J Biol Chem 275:33068-33076.
23. Suginta W, Chumjan W, Mahendran KR, Schulte A, Winterhalter M. 2013. Chitoporin from *Vibrio harveyi,* a channel with exceptional sugar specificity. J Biol Chem 288:11038-11046.
24. Park JK, Keyhani NO, Roseman S. 2000. Chitin catabolism in the marine bacterium *Vibrio furnissii* - Identification, molecular cloning, and characterization of a *N-N* '-diacetylchitobiose phosphorylase. J Biol Chem 275:33077-33083.
25. Erken M, Lutz C, McDougald D. 2015. Interactions of Vibrio spp. with zooplankton. Microbiol Spectr 3.
26. Lutz C, Erken M, Noorian P, Sun S, McDougald D. 2013. Environmental reservoirs and mechanisms of persistence of *Vibrio cholerae*. Front Microbiol 4:375.
27. Pruzzo C, Vezzulli L, Colwell RR. 2008. Global impact of *Vibrio cholerae* interactions with chitin. Environ Microbiol 10:1400-10.
28. Egidius E, Wiik R, Andersen K, Hoff K, Hjeltnes B. 1986. *Vibrio salmonicida* sp. nov., a new fish pathogen. Int J Syst Evol Microbiol 36:518-520.
29. Hjerde E, Lorentzen MS, Holden MT, Seeger K, Paulsen S, Bason N, Churcher C, Harris D, Norbertczak H, Quail MA, Sanders S, Thurston S, Parkhill J, Willassen NP, Thomson NR. 2008. The genome sequence of the fish pathogen *Aliivibrio salmonicida* strain LFI1238 shows extensive evidence of gene decay. BMC Genomics 9:616.

30. Kashulin A, Sørum H, Hjerde E, Willassen NP. 2015. IS elements in *Aliivibrio salmonicida* LFI1238: Occurrence, variability and impact on adaptability. Gene 554:40-49.
31. Klancher CA, Yamamoto S, Dalia TN, Dalia AB. 2020. ChiS is a noncanonical DNA-binding hybrid sensor kinase that directly regulates the chitin utilization program in *Vibrio cholerae*. Proc Natl Acad Sci U S A 117:20180-20189.
32. Li X, Roseman S. 2004. The chitinolytic cascade in Vibrios is regulated by chitin oligosaccharides and a two-component chitin catabolic sensor/kinase. Proc Natl Acad Sci U S A 101:627-31.
33. Debnath A, Mizuno T, Miyoshi SI. 2020. Regulation of chitin-dependent growth and natural competence in *Vibrio parahaemolyticus*. Microorganisms 8.
34. Metzger LC, Matthey N, Stoudmann C, Collas EJ, Blokesch M. 2019. Ecological implications of gene regulation by TfoX and TfoY among diverse Vibrio species. Environ Microbiol 21:2231-2247.
35. Yin Y, Mao X, Yang J, Chen X, Mao F, Xu Y. 2012. dbCAN: a web resource for automated carbohydrate-active enzyme annotation. Nucleic Acids Res 40:W445-W451.
36. Biasini M, Bienert S, Waterhouse A, Arnold K, Studer G, Schmidt T, Kiefer F, Cassarino TG, Bertoni M, Bordoli L. 2014. SWISS-MODEL: modelling protein tertiary and quaternary structure using evolutionary information. Nucleic Acids Res 42:W252-W258.
37. Hsieh YC, Wu YJ, Chiang TY, Kuo CY, Shrestha KL, Chao CF, Huang YC, Chuankhayan P, Wu WG, Li YK, Chen CJ. 2010. Crystal structures of *Bacillus cereus* NCTU2 chitinase complexes with chitooligomers reveal novel substrate binding for catalysis: a chitinase without chitin binding and insertion domains. J Biol Chem 285:31603-15.
38. Suzuki K, Suzuki M, Taiyoji M, Nikaidou N, Watanabe T. 1998. Chitin binding protein (CBP21) in the culture supernatant of *Serratia marcescens* 2170. Biosci Biotechnol Biochem 62:128-135.
39. Vaaje-Kolstad G, Horn SJ, van Aalten DMF, Synstad B, Eijsink VGH. 2005. The non-catalytic chitin-binding protein CBP21 from *Serratia marcescens* is essential for chitin degradation. J Biol Chem 280:28492-28497.
40. Wong E, Vaaje-Kolstad G, Ghosh A, Hurtado-Guerrero R, Konarev PV, Ibrahim AFM, Svergun DI, Eijsink VGH, Chatterjee NS, van Aalten DMF. 2012. The *Vibrio cholerae* colonization factor GbpA possesses a modular structure that governs binding to different host surfaces. PLoS Path 8.
41. Chiu E, Hijnen M, Bunker RD, Boudes M, Rajendran C, Aizel K, Olieric V, Schulze-Briese C, Mitsuhashi W, Young V, Ward VK, Bergoin M, Metcalf P, Coulibaly F. 2015. Structural basis for the enhancement of virulence by viral spindles and their in vivo crystallization. Proc Natl Acad Sci USA 112:3973-3978.
42. Aachmann FL, Sørlie M, Skjåk-Bræk G, Eijsink VGH, Vaaje-Kolstad G. 2012. NMR structure of a lytic polysaccharide monooxygenase provides insight into copper binding, protein dynamics, and substrate interactions. Proc Natl Acad Sci U S A 109:18779-84.
43. Loose JSM, Arntzen MO, Bissaro B, Ludwig R, Eijsink VGH, Vaaje-Kolstad G. 2018. Multipoint precision binding of substrate protects lytic polysaccharide monooxygenases from self-destructive off-pathway processes. Biochemistry 57:4114-4124.
44. Khider M, Hansen H, Hjerde E, Johansen JA, Willassen NP. 2019. Exploring the transcriptome of luxI− and ΔainS mutants and the impact of N-3-oxo-hexanoyl-L- and N-3-hydroxy-decanoyl-L-homoserine lactones on biofilm formation in *Aliivibrio salmonicida*. PeerJ 7:e6845.
45. Khider M, Hjerde E, Hansen H, Willassen NP. 2019. Differential expression profiling of DeltalitR and DeltarpoQ mutants reveals insight into QS regulation of

motility, adhesion and biofilm formation in *Aliivibrio salmonicida*. BMC Genomics 20:220.
46. Pedersen HL, Hjerde E, Paulsen SM, Hansen H, Olsen L, Thode SK, Santos MT, Paulssen RH, Willassen NP, Haugen P. 2010. Global responses of *Aliivibrio salmonicida* to hydrogen peroxide as revealed by microarray analysis. Mar Genomics 3:193-200.
47. Brurberg MB, Nes IF, Eijsink VGH. 1996. Comparative studies of chitinases A and B from *Serratia marcescens*. Microbiology 142:1581-1589.
48. Suzuki K, Sugawara N, Suzuki M, Uchiyama T, Katouno F, Nikaidou N, Watanabe T. 2002. Chitinases A, B, and C1 of *Serratia marcescens* 2170 produced by recombinant *Escherichia coli*: enzymatic properties and synergism on chitin degradation. Biosci Biotechnol Biochem 66:1075-1083.
49. Tuveng TR, Hagen LH, Mekasha S, Frank J, Arntzen MØ, Vaaje-Kolstad G, Eijsink VGH. 2017. Genomic, proteomic and biochemical analysis of the chitinolytic machinery of *Serratia marcescens* BJL200. BBA - Proteins Proteom 1865:414-421.
50. Monge EC, Tuveng TR, Vaaje-Kolstad G, Eijsink VGH, Gardner JG. 2018. Systems analysis of the glycoside hydrolase family 18 enzymes from *Cellvibrio japonicus* characterizes essential chitin degradation functions. J Biol Chem 293:3849-3859.
51. Synstad B, Gåseidnes S, Van Aalten DM, Vriend G, Nielsen JE, Eijsink VGH. 2004. Mutational and computational analysis of the role of conserved residues in the active site of a family 18 chitinase. FEBS J 271:253-262.
52. Synstad B, Vaaje-Kolstad G, Cederkvist FH, Saua SF, Horn SJ, Eijsink VGH, Sørlie M. 2008. Expression and characterization of endochitinase C from *Serratia marcescens* BJL200 and its purification by a one-step general chitinase purification method. Biosci Biotechnol Biochem 72:715-723.
53. Loose JSM, Forsberg Z, Fraaije MW, Eijsink VGH, Vaaje-Kolstad G. 2014. A rapid quantitative activity assay shows that the *Vibrio cholerae* colonization factor GbpA is an active lytic polysaccharide monooxygenase. FEBS Lett 588:3435-3440.
54. Suginta W, Chuenark D, Mizuhara M, Fukamizo T. 2010. Novel beta-*N*-acetylglucosaminidases from *Vibrio harveyi* 650: cloning, expression, enzymatic properties, and subsite identification. BMC Biochem 11:40.
55. Chitlaru E, Roseman S. 1996. Molecular cloning and characterization of a novel β-*N*-Acetyl-D-glucosaminidase from *Vibrio furnissii*. J Biol Chem 271:33433-33439.
56. Choi KH, Seo JY, Park KM, Park CS, Cha J. 2009. Characterization of glycosyl hydrolase family 3 beta-*N*-acetylglucosaminidases from *Thermotoga maritima* and *Thermotoga neapolitana*. J Biosci Bioeng 108:455-9.
57. Tsujibo H, Fujimoto K, Tanno H, Miyamoto K, Imada C, Okami Y, Inamori Y. 1994. Gene sequence, purification and characterization of *N*-acetyl-beta-glucosaminidase from a marine bacterium, *Alteromonas sp.* strain O-7. Gene 146:111-5.
58. Cheng Q, Li H, Merdek K, Park JT. 2000. Molecular characterization of the beta-*N*-acetylglucosaminidase of *Escherichia coli* and its role in cell wall recycling. J Bacteriol 182:4836-40.
59. Yadava U, Vetting MW, Al Obaidi N, Carter MS, Gerlt JA, Almo SC. 2016. Structure of an ABC transporter solute-binding protein specific for the amino sugars glucosamine and galactosamine. Acta Crystallogr F Struct Biol Commun 72:467-72.
60. Oiki S, Mikami B, Maruyama Y, Murata K, Hashimoto W. 2017. A bacterial ABC transporter enables import of mammalian host glycosaminoglycans. Sci Rep 7:1069.
61. Wei X, Guo Y, Shao C, Sun Z, Zhurina D, Liu D, Liu W, Zou D, Jiang Z, Wang X, Zhao J, Shang W, Li X, Liao X, Huang L, Riedel CU, Yuan J. 2012. Fructose uptake

in *Bifidobacterium longum* NCC2705 is mediated by an ATP-binding cassette transporter. J Biol Chem 287:357-67.
62. Hayes CA, Dalia TN, Dalia AB. 2017. Systematic genetic dissection of chitin degradation and uptake in *Vibrio cholerae*. Environ Microbiol 19:4154-4163.
63. Bennati-Granier C, Garajova S, Champion C, Grisel S, Haon M, Zhou S, Fanuel M, Ropartz D, Rogniaux H, Gimbert I, Record E, Berrin JG. 2015. Substrate specificity and regioselectivity of fungal AA9 lytic polysaccharide monooxygenases secreted by *Podospora anserina*. Biotechnol Biofuels 8:90.
64. Isaksen T, Westereng B, Aachmann FL, Agger JW, Kracher D, Kittl R, Ludwig R, Haltrich D, Eijsink VGH, Horn SJ. 2014. A C4-oxidizing lytic polysaccharide monooxygenase cleaving both cellulose and cello-oligosaccharides. J Biol Chem 289:2632-2642.
65. Kittl R, Kracher D, Burgstaller D, Haltrich D, Ludwig R. 2012. Production of four *Neurospora crassa* lytic polysaccharide monooxygenases in *Pichia pastoris* monitored by a fluorimetric assay. Biotechnol Biofuels 5:79.
66. Hangasky JA, Iavarone AT, Marletta MA. 2018. Reactivity of O_2 versus H_2O_2 with polysaccharide monooxygenases. Proc Natl Acad Sci U S A 115:4915-4920.
67. Kuusk S, Bissaro B, Kuusk P, Forsberg Z, Eijsink VGH, Sørlie M, Väljamäe P. 2018. Kinetics of H_2O_2-driven degradation of chitin by a bacterial lytic polysaccharide monooxygenase. J Biol Chem 293:523-531.
68. Vaaje-Kolstad G, Bøhle LA, Gåseidnes S, Dalhus B, Bjørås M, Mathiesen G, Eijsink VGH. 2012. Characterization of the chitinolytic machinery of *Enterococcus faecalis* V583 and high-resolution structure of its oxidative CBM33 enzyme. J Mol Biol 416:239-254.
69. Hamre AG, Eide KB, Wold HH, Sørlie M. 2015. Activation of enzymatic chitin degradation by a lytic polysaccharide monooxygenase. Carbohyd Res 407:166-169.
70. Yang Y, Li J, Liu X, Pan X, Hou J, Ran C, Zhou Z. 2017. Improving extracellular production of *Serratia marcescens* lytic polysaccharide monooxygenase CBP21 and *Aeromonas veronii* B565 chitinase Chi92 in *Escherichia coli* and their synergism. AMB Express 7:170.
71. Paspaliari DK, Loose JS, Larsen MH, Vaaje-Kolstad G. 2015. *Listeria monocytogenes* has a functional chitinolytic system and an active lytic polysaccharide monooxygenase. FEBS J 282:921-936.
72. Filandr F, Kavan D, Kracher D, Laurent C, Ludwig R, Man P, Halada P. 2020. Structural dynamics of lytic polysaccharide monooxygenase during catalysis. Biomolecules 10.
73. Feng Y, Chien KY, Chen HL, Chiu CH. 2012. Pseudogene recoding revealed from proteomic analysis of salmonella serovars. J Proteome Res 11:1715-9.
74. Kuo CH, Ochman H. 2010. The extinction dynamics of bacterial pseudogenes. PLoS Genet 6.
75. Pink RC, Wicks K, Caley DP, Punch EK, Jacobs L, Carter DRF. 2011. Pseudogenes: pseudo-functional or key regulators in health and disease? RNA 17:792-798.
76. Milligan MJ, Lipovich L. 2015. Pseudogene-derived lncRNAs: emerging regulators of gene expression. Front Genet 5.
77. Mondal M, Nag D, Koley H, Saha DR, Chatterjee NS. 2014. The *Vibrio cholerae* extracellular chitinase ChiA2 is important for survival and pathogenesis in the host intestine. PloS one 9:e103119.
78. Frederiksen RF, Yoshimura Y, Storgaard BG, Paspaliari DK, Petersen BO, Chen K, Larsen T, Duus JØ, Ingmer H, Bovin NV. 2015. A diverse range of bacterial and eukaryotic chitinases hydrolyzes the LacNAc (Galβ1–4GlcNAc) and LacdiNAc (GalNAcβ1–4GlcNAc) motifs found on vertebrate and insect cells. J Biol Chem 290:5354-5366.

79. Songsiriritthigul C, Pantoom S, Aguda AH, Robinson RC, Suginta W. 2008. Crystal structures of *Vibrio harveyi* chitinase A complexed with chitooligosaccharides: implications for the catalytic mechanism. J Struct Biol 162:491-499.
80. Nagashima T, Tange T, Anazawa H. 1999. Dephosphorylation of phytate by using the *Aspergillus niger* phytase with a high affinity for phytate. Appl Environ Microbiol 65:4682-4684.
81. Choonia HS, Lele S. 2013. Three phase partitioning of β-galactosidase produced by an indigenous *Lactobacillus acidophilus* isolate. Sep Purif Technol 110:44-50.
82. Kirn TJ, Jude BA, Taylor RK. 2005. A colonization factor links *Vibrio cholerae* environmental survival and human infection. Nature 438:863-866.
83. Bhowmick R, Ghosal A, Das B, Koley H, Saha DR, Ganguly S, Nandy RK, Bhadra RK, Chatterjee NS. 2008. Intestinal adherence of *Vibrio cholerae* involves a coordinated interaction between colonization factor GbpA and mucin. Infect Immun 76:4968-4977.
84. Leisner JJ, Larsen MH, Jørgensen RL, Brøndsted L, Thomsen LE, Ingmer H. 2008. Chitin hydrolysis by *Listeria* spp., including *L. monocytogenes*. Appl Environ Microbiol 74:3823-3830.
85. Askarian F, Uchiyama S, Masson H, Sørensen HV, Golten O, Bunaes AC, Mekasha S, Røhr AK, Kommedal E, Ludviksen JA, Arntzen MO, Schmidt B, Zurich RH, van Sorge NM, Eijsink VGH, Krengel U, Mollnes TE, Lewis NE, Nizet V, Vaaje-Kolstad G. 2021. The lytic polysaccharide monooxygenase CbpD promotes *Pseudomonas aeruginosa* virulence in systemic infection. Nat Commun 12:1230.
86. Mitsuhashi W, Kawakita H, Murakami R, Takemoto Y, Saiki T, Miyamoto K, Wada S. 2007. Spindles of an entomopoxvirus facilitate its infection of the host insect by disrupting the peritrophic membrane. J Virol 81:4235-4243.
87. Nørstebo SF, Paulshus E, Bjelland AM, Sørum H. 2017. A unique role of flagellar function in *Aliivibrio salmonicida* pathogenicity not related to bacterial motility in aquatic environments. Microb Pathog 109:263-273.
88. Bjelland AM, Sørum H, Tegegne DA, Winther-Larsen HC, Willassen NP, Hansen H. 2012. LitR of *Vibrio salmonicida* is a salinity-sensitive quorum-sensing regulator of phenotypes involved in host interactions and virulence. Infect Immun 80:1681-1689.
89. Nørstebo SF, Lotherington L, Landsverk M, Bjelland AM, Sørum H. 2018. *Aliivibrio salmonicida* requires O-antigen for virulence in Atlantic salmon (*Salmo salar* L.). Microb Pathog 124:322-331.
90. Milton DL, O'Toole R, Horstedt P, Wolf-Watz H. 1996. Flagellin A is essential for the virulence of *Vibrio anguillarum*. J Bacteriol 178:1310-9.
91. Aslanidis C, de Jong PJ. 1990. Ligation-independent cloning of PCR products (LIC-PCR). Nucleic Acids Res 18:6069-74.
92. Manoil C, Beckwith J. 1986. A genetic approach to analyzing membrane protein topology. Science 233:1403-8.
93. Forsberg Z, Nelson CE, Dalhus B, Mekasha S, Loose JSM, Crouch LI, Røhr ÅK, Gardner JG, Eijsink VGH, Vaaje-Kolstad G. 2016. Structural and functional analysis of a lytic polysaccharide monooxygenase important for efficient utilization of chitin in *Cellvibrio japonicus*. J Biol Chem 291:7300-7312.
94. Wagner TM, Janice J, Paganelli FL, Willems RJ, Askarian F, Pedersen T, Top J, de Haas C, van Strijp JA, Johannessen M, Hegstad K. 2018. *Enterococcus faecium* TIR-domain genes are part of a gene cluster which promotes bacterial survival in blood. Int J Microbiol 2018:1435820.
95. Tiukova IA, Brandenburg J, Blomqvist J, Sampels S, Mikkelsen N, Skaugen M, Arntzen MO, Nielsen J, Sandgren M, Kerkhoven EJ. 2019. Proteome analysis of xylose metabolism in *Rhodotorula toruloides* during lipid production. Biotechnol Biofuels 12:137.

96. Cox J, Hein MY, Luber CA, Paron I, Nagaraj N, Mann M. 2014. Accurate proteome-wide label-free quantification by delayed normalization and maximal peptide ratio extraction, termed MaxLFQ. Mol Cell Proteomics 13:2513-26.
97. Tyanova S, Temu T, Cox J. 2016. The MaxQuant computational platform for mass spectrometry-based shotgun proteomics. Nat Protoc 11:2301-2319.
98. Huang L, Zhang H, Wu P, Entwistle S, Li X, Yohe T, Yi H, Yang Z, Yin Y. 2018. dbCAN-seq: a database of carbohydrate-active enzyme (CAZyme) sequence and annotation. Nucleic Acids Res 46:D516-D521.
99. Almagro Armenteros JJ, Tsirigos KD, Sonderby CK, Petersen TN, Winther O, Brunak S, von Heijne G, Nielsen H. 2019. SignalP 5.0 improves signal peptide predictions using deep neural networks. Nat Biotechnol 37:420-423.
100. Gasteiger E, Gattiker A, Hoogland C, Ivanyi I, Appel RD, Bairoch A. 2003. ExPASy: The proteomics server for in-depth protein knowledge and analysis. Nucleic Acids Res 31:3784-8.
101. Perez-Riverol Y, Csordas A, Bai J, Bernal-Llinares M, Hewapathirana S, Kundu DJ, Inuganti A, Griss J, Mayer G, Eisenacher M, Perez E, Uszkoreit J, Pfeuffer J, Sachsenberg T, Yilmaz S, Tiwary S, Cox J, Audain E, Walzer M, Jarnuczak AF, Ternent T, Brazma A, Vizcaino JA. 2019. The PRIDE database and related tools and resources in 2019: improving support for quantification data. Nucleic Acids Res 47:D442-D450.
102. Simon R, Priefer U, Puhler A. 1983. A broad host range mobilization system for in vivo genetic-engineering - transposon mutagenesis in Gram-negative bacteria. Bio-Technology 1:784-791.
103. Vaaje-Kolstad G, Houston DR, Riemen AHK, Eijsink VGH, van Aalten DMF. 2005. Crystal structure and binding properties of the *Serratia marcescens* chitin-binding protein CBP21. J Biol Chem 280:11313-11319.

TABLES

Table 1. Growth rate and max cell density of *Al. salmonicida* and derivative mutant strains

Strain	Rate constant μ ($hours^{-1}$)	Generation time (hours)	Max cell density (OD_{600})
Wild type	0.43 ± 0.01	17.5 ± 0.4	1.60 ± 0.08
Δ*As*Chi18A	na	na	0.82 ± 0.03
Δ*As*LPMO10A	0.27 ± 0.07	29.1 ± 8.2	1.25 ± 0.08
Δ*As*LPMO10B	0.28 ± 0.01	26.8 ± 1.1	1.15 ± 0.04
ΔAΔB	0.28 ± 0.02	26.8 ± 1.7	1.24 ± 0.04
ΔAΔBΔChi	na	na	0.58 ± 0.02
Wild type control media	na	na	0.37 ± 0.05

Table 2. Gene expression of *AsChi18A, AsLPMO10A, AsLPMO10B* and *AsChi18B$_p$*. Exp = Exponential phase, Stat.= Stationary phase. Data shown as positive ("+" on green background) or negative ("-" on blue background) detection of expression, based on three biological replicates. *AsChi18A (VSAL_I0757), AsLPMO10A (VSAL_II0134), AsLPMO10B (VSAL_II0217)* and *AsChi18B$_p$ (VSAL_I0902*).

	GlcNAc		$(GlcNAc)_2$		Glucose		β-Chitin	
	Exp.	Stat.	Exp.	Stat.	Exp.	Stat.	Exp.	Stat.
AsChi18A	+	+	+	-	+	+	+	+
AsLPMO10A	+	+	+	+	+	-	+	-
AsLPMO10B	+	-	-	-	-	-	-	-
AsChi18B$_p$	+	-	+	-	+	-	+	-

Table 3. **Description of target genes**

Gene name	Protein name	CAZy family	CAZyme name
VSAL_I0757 chiA	Endochitinase chiA	GH18	*As*Chi18A
VSAL_II0134 gbpA	GlcNAc-binding protein A	AA10	*As*LPMO10A
VSAL_II0217	Chitinase B	AA10	*As*LPMO10B

Table 4. Primers used for construction of in frame deletion mutants.

Primer	Sequence 5'-3'
*AsGH18*_YF	GAAGGGCCCCACTAGTCGCACACTGATTTATCACACT
*AsGH18*_IR	GTTCATTAATGTCAGACTGTTAATGAAAATCCGTTTCAT
*AsGH18*_IF	CATTAACAGTCTGACATTAATGAACGCTCAATAA
*AsGH18*_YR	ACCGTCGACCCTCGAGGTGTTCTAATAGCGGGCATT
*AsLPMO10A*_YF	GAAGGGCCCCACTAGTGGGTACAAGATTGTTGCTTTT
AsLPMO10A _IR	ATCCCAAGCCATCGTTGAGCATTTATTCATCATTTATTC
AsLPMO10A _IF	AAATGCTCAACGATGGCTTGGGATAAAATCTAACCA
AsLPMO10A _YR	ACCGTCGACCCTCGAGGTGTACGGATGTTCTAACATC
*AsLPMO10B*_YF	GAAGGGCCCCACTAGTCCGTCAATCATCAACTAGAGA
AsLPMO10B _IR	TCCCCATTCTATTGTATTTGTCATATTTCATCCTTGTCT
AsLPMO10B _IF	AATACAATA GAATGGGGAGTATGGCGA
AsLPMO10B _YR	ACCGTCGACCCTCGAGTTTCTTGTCACCCATGATCAC

Table 5. Complete list of strains and vectors.

Strain or plasmid	Comment	Ref.
LFI1238	*Aliivibrio salmonicida* strain LFI1238	§
S17-1 λpir	*Escherichia coli* conjugation donor strain S17-1 λpir	(102)
AsΔChi18A	LFI1238 containing gene deletion ΔChi18A	*
AsΔLPMO10A	LFI1238 containing gene deletion ΔLPMO10A	*
AsΔLPMO10B	LFI1238 containing gene deletion ΔLPMO10B	*
AsΔLPMO10A-Δ10B	LFI1238 containing gene deletions ΔLPMO10A and ΔLPMO10B	*
AsΔLPMO10A-Δ10B-ΔChi	LFI1238 containing gene deletions ΔLPMO10A, ΔLPMO10B and ΔChi18A	*
pDM4	pDM4 SacB suicide plasmid/ cloning vector	(90)
pDM4-AsΔChi18A	pDM4-construct designed for allelic exchange and deletion of AsChi18A	*
pDM4-AsΔLPMO10A	pDM4-construct designed for allelic exchange and deletion of AsLPMO10A	*
pDM4-AsΔLPMO10B	pDM4-construct designed for allelic exchange and deletion of AsLPMO10B	*

§Originally isolated by the Norwegian Institute of Fisheries and Aquaculture Research, N-9291 Tromsø, Norway, but provided by Simen Foyn Nørstebø for this study. *This study.

Table 6. Cloning primers for *As*LPMO10A and -B and *As*Chi18A

Cloning primers	**Sequence (5'-3')**
pNIC-CH/*As*LPMOA (forward)	**TTAAGAAGGAGATATACTATG**ATGAATAAATGCAGTACCAA
pNIC-CH/*As*LPMOA (reverse)	AATGGCTTGGGACAAAATCTAA**GCGCACCATCATCACCACCATT**
pNIC-CH/*As*LPMOB (forward)	**TTAAGAAGGAGATATACTATG**ACCAACACGATTAAAATCAATTC
pNIC-CH/*As*LPMOB (reverse)	AATGGGGTGTGTGGCGCTAA**GCGCACCATCATCACCACCATT**
pNIC-CH/*As*GH18A (forward)	**TTAAGAAGGAGATATACTATG**AAACGTATCTTTATTAACAGT
pNIC-CH/*As*GH18A (reverse)	TGATGAATGCGCAA**GCGCACCATCATCACCACCATT**

Table 8. Pseudogenes analyzed. Gene locus, product name and CAZyme based name.

Gene locus	Product	CAZyme based name
VSAL_I0763	Chitinase A (fragment)	na
VSAL_I0902	Chitinase A (fragment)	*As*Chi18Bp
VSAL_I1414	Putative chitinase (pseudogene)	*As*Chi19p
VSAL_I1942	Chitinase (pseudogene)	*As*Chi18Cp
VSAL_I2352	Chitoporin (pseudogene)	na
VSAL_I1108	Chitodextrinase (fragment)	na

FIGURES

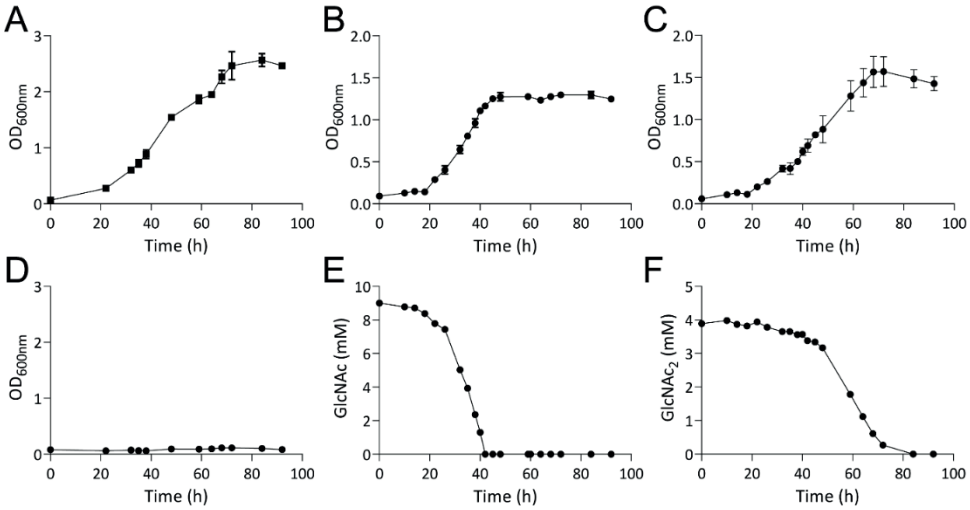

Figure 1. Utilization of Glucose, GlcNAc and $(GlcNAc)_2$. Panels A to C show the growth of *Al. salmonicida* LFI1238 in minimal media supplemented with 0.2 % glucose, 0.2% GlcNAc (9.0 mM) or 0.2 % $(GlcNAc)_2$ (4.7 mM), respectively. Growth in defined media without supplementation of carbon source (negative control) is shown in panel D. Growth results are shown as mean value of three biological replicates and the standard deviation is indicated. Panels E & F show the depletion of soluble substrates by *Al. salmonicida*, determined by sampling of the culture supernatant of one replicate different time points through the growth time-period and quantification of GlcNAc (panel E) or $(GlcNAc)_2$ (panel F) by ion exclusion chromatography. Results are shown as the mean value of three technical replicates.

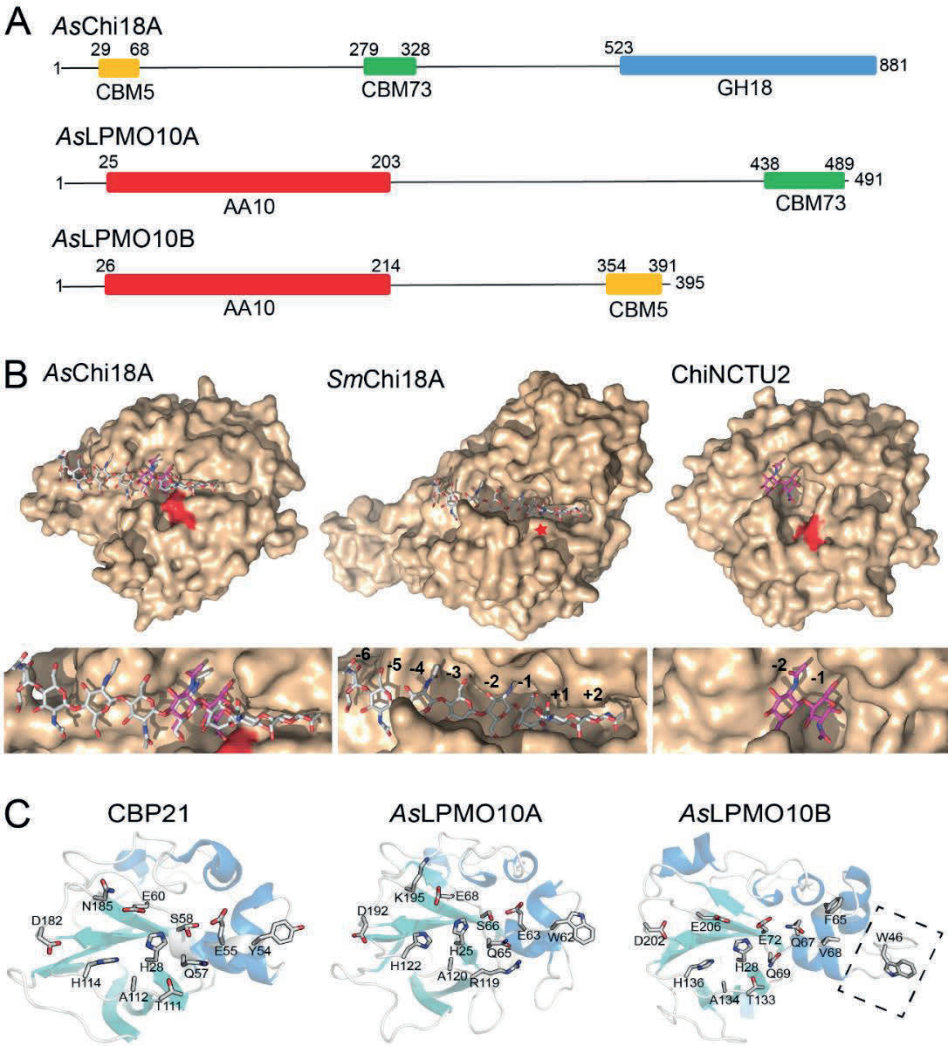

Figure 2. Predicted domains and three dimentional structures of the *A. salmonicida* chitinase and LPMOs. **(A)** Prediction of CAZy domains of the chitinolytic enzymes was performed using the dbCAN server. Numbers indicate the position in the sequence. The theoretical molecular weight of the proteins calculated by the ProtParam tool (in the absence of the predicted signal peptide) is 87.4, 52.5 and 41.2 kDa for *As*Chi18A, *As*LPMO10A and *As*LPMO10B, respectively. Signal peptides were determined by the SignalP 4.0 server (http://www.cbs.dtu.dk/services/SignalP/) and represent residues 1-29, 1-25 and 1-26 for *As*Chi18A, *As*LPMO10A and *As*LPMO10B, respectively. The GenBank protein identifiers for the enzymes are CAQ78442.1 (*As*Chi18A, also called "endochitinase A"), CAQ80888.1 (*As*LPMO10A, also called "chitin binding protein") and CAQ80971.1 (*As*LPMO10B, also called "chitinase B"). **(B)** The homology model of *As*Chi18A (left structure) and the structures of *Sm*Chi18A deep clefted *exo*-chitinase from *S. marcescens* (middle structure) and the *Bacillus*

cereus GH18 ChiNCTU2 shallow clefted chitinase (37) are shown in light brown surface representation with the catalytic acids colored red (or indicated by a red star for *Sm*ChiA, as it is concealed by other amino acids). Ligands are shown in stick representation with gray (chitooctaose; *Sm*Chi18A) and purple (chitobiose; ChiNCTU2) colored carbon atoms. Subsites are indicated by numbering. Ligands shown in the *As*Chi18A substrate binding cleft are derived from structural superimpositions of the *As*Chi18A model with *Sm*Chi18A or ChiNCTU2 and are provided for illustrational purposes only. The template used for modelling the *As*Chi18A catalytic GH18 domain was PDB ID 3N1A (apo-enzyme structure of ChiNCTU2 from *B. cereus*) and gave a Qmean value of -1.99, which represents a good quality model. **(C)** The crystal structure of CBP21 (PDB ID 2BEM) and the homology models for *As*LPMO10A and *As*LPMO10B are shown in cartoon representation. For CBP21, the side chains of the amino acids that have been shown to be invovled in substrate binding by experimental evidence (42, 43, 103) are shown in stick representation. The corresponding amino acids in *As*LPMO10A and *As*LPMO10B are also shown in stick representation. One exception is W46 of *As*LPMO10B, which is not present in the two other enzymes. The latter residue is positioned on an insertion that potentially extends the putative binding surface (indicated by rectangle with dashed lines). In CBP21, Ser58 is shown with two alternative side chain conformations. Swiss Model was used with default paramters to generate the homology models of *As*LPMO10A and -B, using PDB structures 2XWX (66.5% sequence identity to *As*LPMO10A) and 4YN2 (43.6% sequence identity to *As*LPMO10B) as templates, respectively. The Q-mean scores obtained were -1.65 for *As*LPMO10A model and -3.34 for *As*LPMO10B

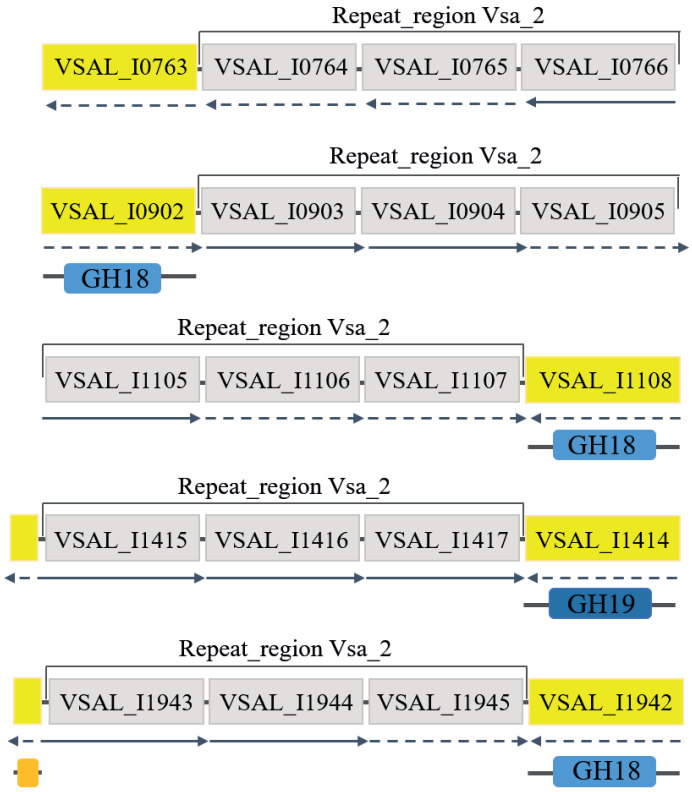

Figure 3. Sequence analysis of putative chitinase pseudogenes. The gene locus and insertion sequence elements are shown in yellow and gray, respectively, with the locus name indicated. Solid lined arrow direction indicates reading frame direction, while dashed lined arrows indicate pseudogenes. CAZyme annotation of the pseudogenes genes was done using dbCAN2 and the resulting enzyme activity prediction is displayed below each gene. Annotation of VSAL_I0763, VSAL_I0902, VSAL_I1108 was performed with the truncated chitinase/chitodextrinase sequence. VSAL_I1414 and VSAL_I1942 were analyzed using the full-length sequences including repeat region. The illustrations representing the ORFs are not to scale.

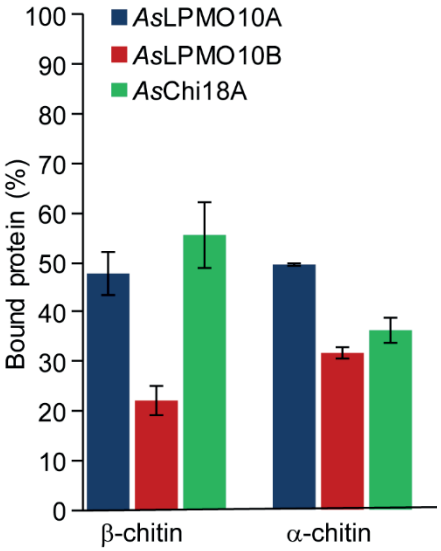

Figure 4. Substrate binding of *As*Chi18A, *As*LPMO10A and -B. Each bar shows the percentage of bound proteins after 2 h of incubation at 30 °C. Reactions contained 10 mg/mL of substrate, 0.75 µM (LPMOs) or 0.50 µM (*As*Chi18A) of enzymes and 10 mM of Tris-HCl buffer at pH 7.5. All reactions were run in triplicates and the standard deviations are indicated by error bars.

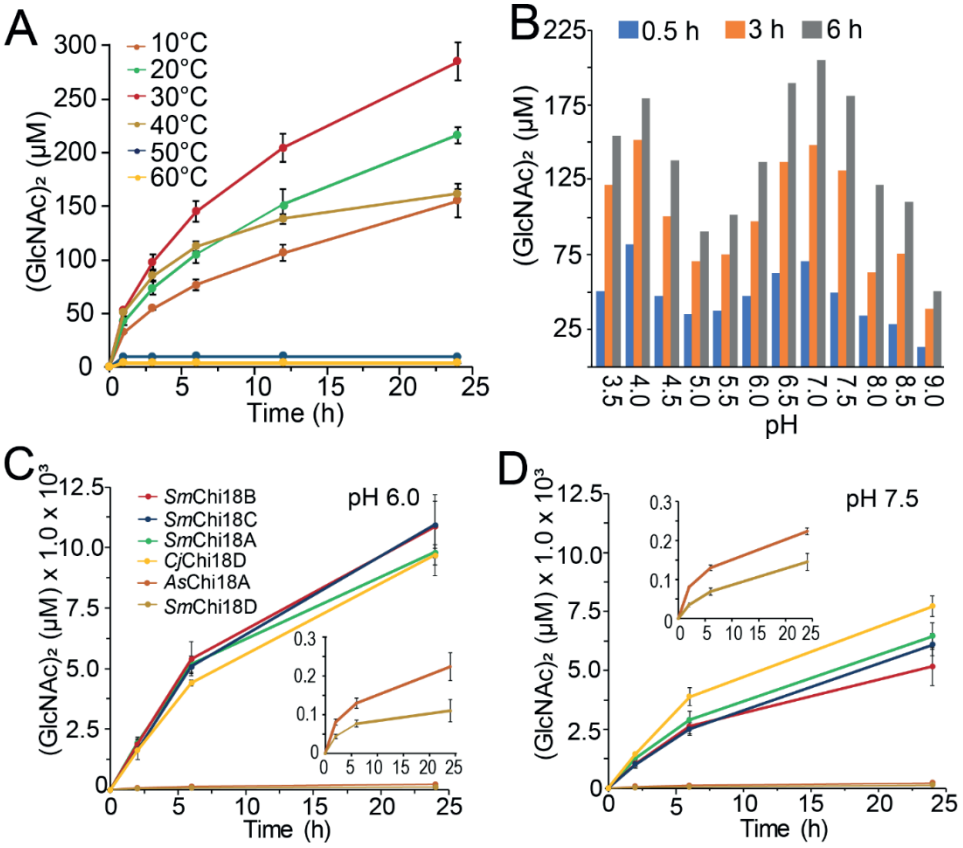

Figure 5. Enzymatic properties of *As*Chi18A. Production of $(GlcNAc)_2$ by *As*Chi18A analysed at various temperatures (A) and pH values (B). The activity of *As*Chi18A was also compared to the chitinases from *Serratia marcescens* (*Sm*Chi18A, -B, -C and -D) and *C. japonicus* (*Cj*Chi18D) at pH 6.0 (C) and 7.5 (D). All reactions conditions included 10 mg/mL β-chitin and 0.5 μM enzyme. For data displayed in panel A, reactions were carried out at pH 7.5. For the data displayed in panel B, all reactions were incubated at 30 ºC. Buffers used were formic acid pH 3.5, acetic acid pH 4.0 and 4.5, ammonium acetate pH 4.5 and 5.0, MES pH 5.5, 6.0 and 6.5, BisTris-HCl pH 7.0, Tris-HCl pH 7.5 and 8.0 and Bicine pH 8.5 and 9.0. The amounts of $(GlcNAc)_2$ presented are based on the average of three independent reactions containing 10 mg/mL β-chitin, 0.5 μM enzyme and 10 mM buffer. The insets in panel C and D show magnified views of reactions catalysed by *As*Chi18A and *Sm*Chi18D. Standard deviations are indicated by error bars (n=3).

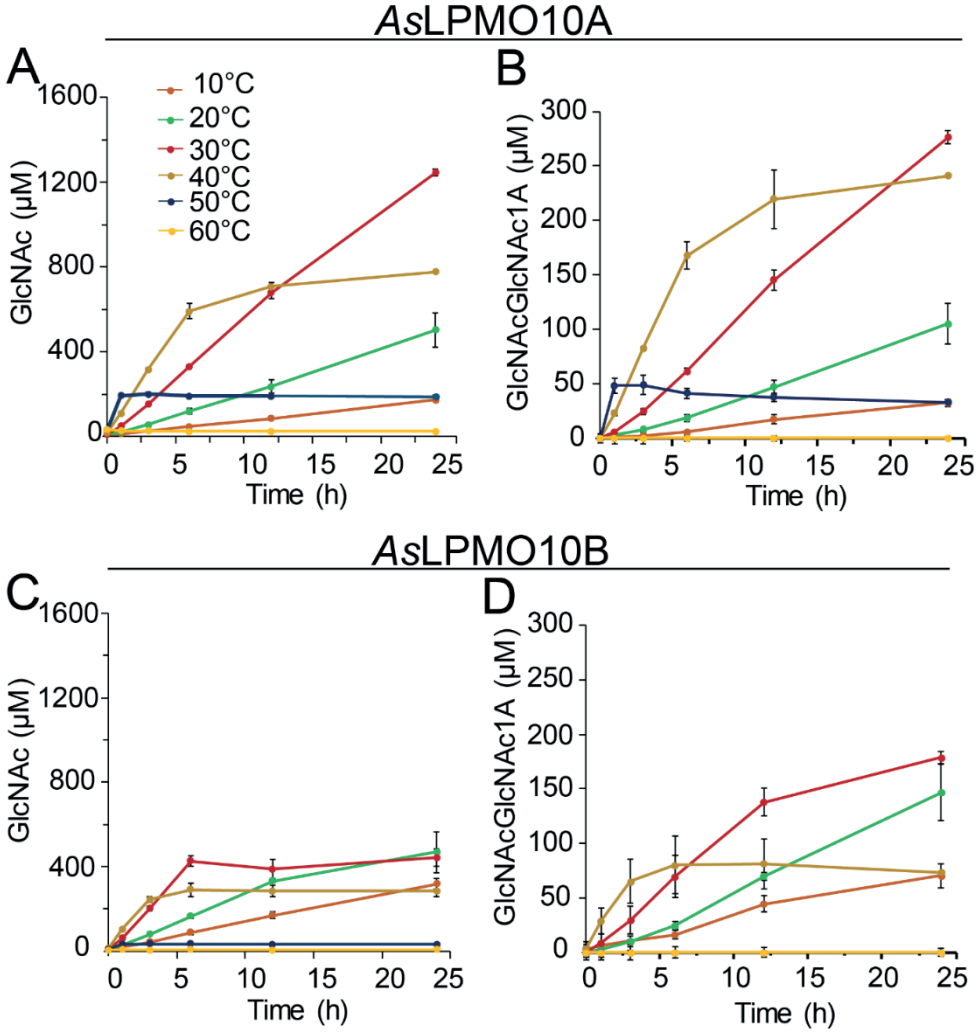

Figure 6. Operational temperature stability of *A. salmonicida* LPMOs. The activity of *As*LPMO10A and *As*LPMO10B is indicated by the production of GlcNAc is shown in panel A and C, respectively. Since the end-product of chitin degradation by the LPMOs are oxidized chitooligosaccharides (Fig. S4) that are inconvenient to quantify, the reaction products obtained from the reactions were depolymerized by Chitobiase that completely converts the oligosaccharide mixture to GlcNAc and oxidized $(GlcNAc)_2$ (i.e. GlcNAcGlcNAc1A). The quantities of the latter products formed by the LPMOs, are shown in panel B and D. The amounts presented are based on the average of three independent reactions, which contained 10 mg/mL of β-chitin, 1 μM of enzyme, 1 mM of ascorbic acid and 10 mM of Tris-HCl buffer at pH 7.5, incubated at different temperatures between 10 and 60 °C (colour code provided in panel A). Standard deviations are indicated by error bars.

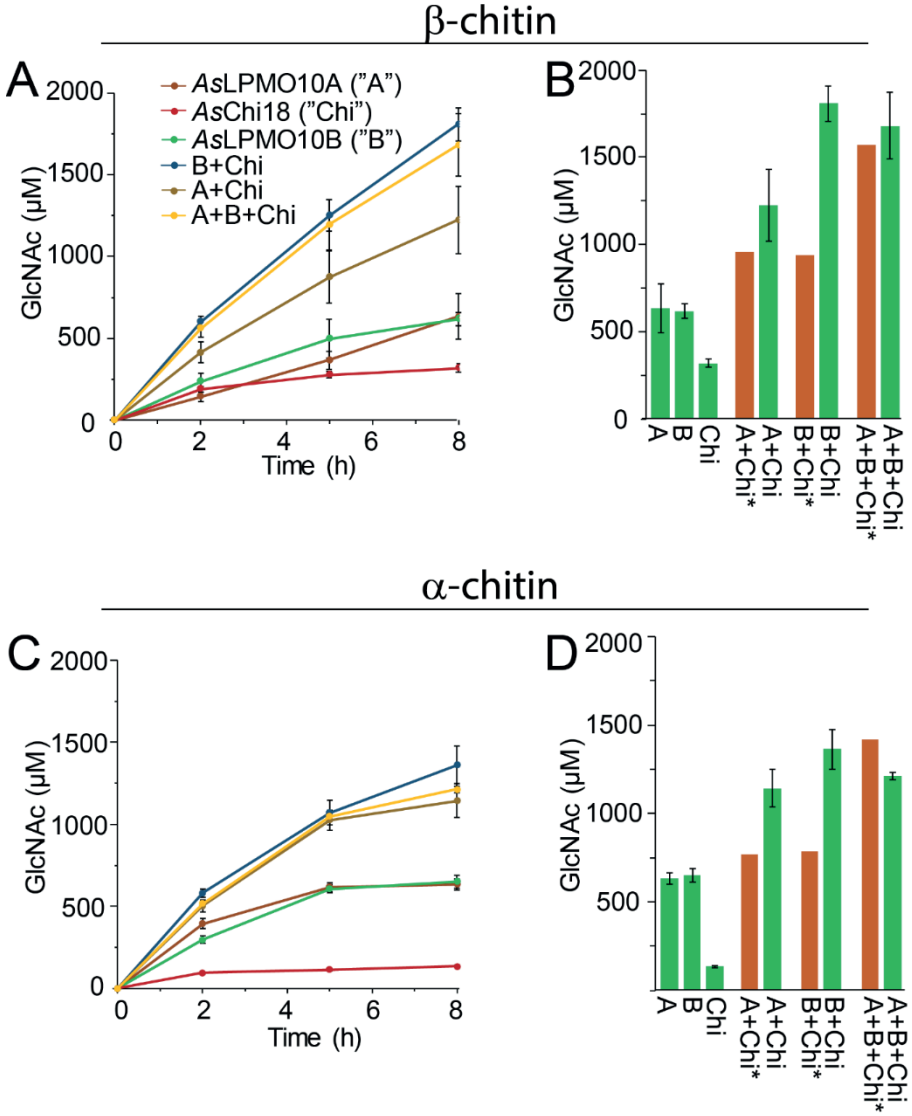

Figure 7. Synergistic activity of *As*LPMO10s and *As*Chi18A on chitin. Panels A and C show the production of GlcNAc by the individual and combined enzymes on β- and α-chitin, respectively. Panels B and D show the theoretically calculated amounts of GlcNAc based on the sum of its production by the individual enzymes (*, brown bars) and the detected amounts of GlcNAc by combining the enzymes after 8 h (green bars). The amounts presented are based on the average of three independent reactions containing 10 mg/mL of chitin substrate, 1 μM of LPMOs and/or 0.5 μM of GH18, 1 mM of ascorbic acid and 10 mM of Tris-HCl buffer at pH 7.5, incubated at 30 °C for 8 h. Standard deviations are indicated by error bars (n=3).

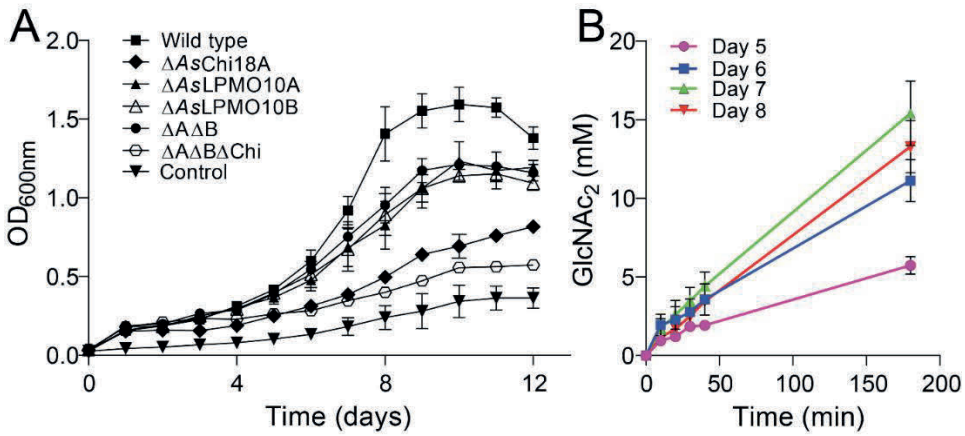

Figure 8. Growth of *Al. salmonicida* LFI1238 and derivate gene-deletion strains on β-chitin. (A) The growth of *Al. salmonicida* LFI1238 at 12 °C in minimal media supplemented with 1 % β-chitin. (B) Chitinase activity in the culture supernatant of *Al. salmonicida* growing on β-chitin. The chitinase activity was assayed by mixing a sample of the culture supernatant sampled at various time points with 15 mM chitopentaose and quantifying the $(GlcNAc)_2$ resulting from hydrolysis over a period of 180 minutes. Error bars indicate standard deviation (n =3).

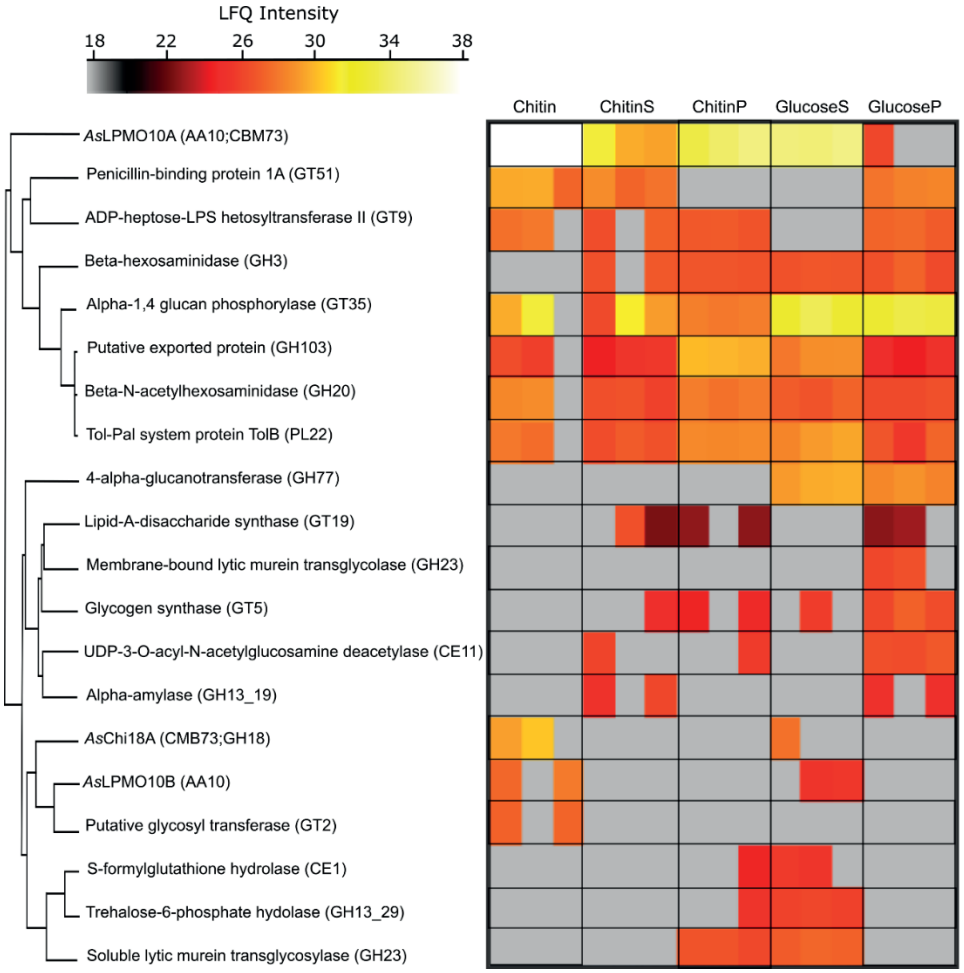

Figure 9. CAZymes expressed by *Al. salmonicida* LFI1238. Heatmap presentation of identified CAZymes and label free quantification intensities ranging from low intensity (grey), medium intensity (red) to high intensity (white). The data is presented as three biological replicates. Conditions are as following: proteins eluted from chitin obtained from the culturing experiment (Chitin), culture supernatant proteins from the chitin cultivation experiment (ChitinS), proteins extracted from the bacterial cells obtained from the chitin cultivation experiment (ChitinP), culture supernatant proteins obtained from culturing the bacterium on glucose (GlucoseS) and proteins extracted bacterial cell pellet from the glucose cultivation experiment (GlucoseP).

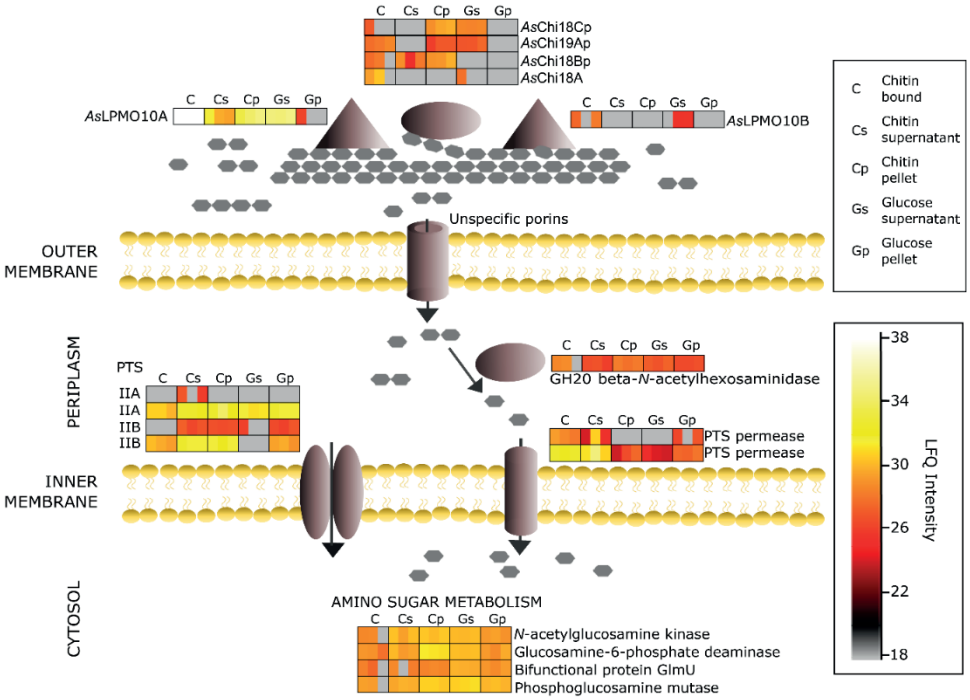

Figure 10. Putative chitin utilization pathway by *Al. salmonicida LFI238*. Illustration of detected proteins by label-free proteomics, aligned with their putative roles in the utilization pathway and the MaxLFQ Intensities**.** Enzymes acting on chitin: *As*Chi18A (B6EH15), *As*LPMO10A (B6EQB6), *As*LPMO10B (B6EQJ6), putative pseudogene chitinases (VSAL_I1414, VSAL_I1942, VSAL_I0902). Transport across membranes: Phosphotransferase system (PTS) component IIA (B6EGW5), PTS permease for *N*-acetylglucosamine and glucose (B6EHL6), PTS system, Lactose/Cellobiose specific IIB subunit (B6EMG0), PTS system permease for *N*-acetylglucosamine and glucose (B6ERZ1). Hydrolysis of $(GlcNAc)_2$ into GlcNAc: beta-*N*-acetylhexosaminidase GH20 (B6EGV7), Amino sugar metabolism: Glucosamine-6-phosphate deaminase (B6EN78), UDP-*N*-acetylglucosamine pyrophosphorylase (B6EHG2), Phosphoglucosamine mutase (B6END8), *N*-acetyl-D-glucosamine kinase (B6EKQ4). A bar chart comparing the log2 LFQ values of the putative chitinolytic enzymes is shown in Fig. S9.

The fish pathogen *Aliivibrio salmonicida* LFI1238 can degrade and metabolize chitin despite major gene loss in the chitinolytic pathway

Anna Skåne[1], Giusi Minniti[1], Jennifer S.M. Loose, Sophanit Mekasha, Bastien Bissaro, Geir Mathiesen, Magnus Ø. Arntzen and Gustav Vaaje-Kolstad*

Faculty of Chemistry, Biotechnology and Food Science, Norwegian University of Life Sciences (NMBU), Ås, Norway

[1]These authors contributed equally to the work

*Corresponding author. Email; gustav.vaaje-kolstad@nmbu.no

Supplementary material

Supplemtary figures

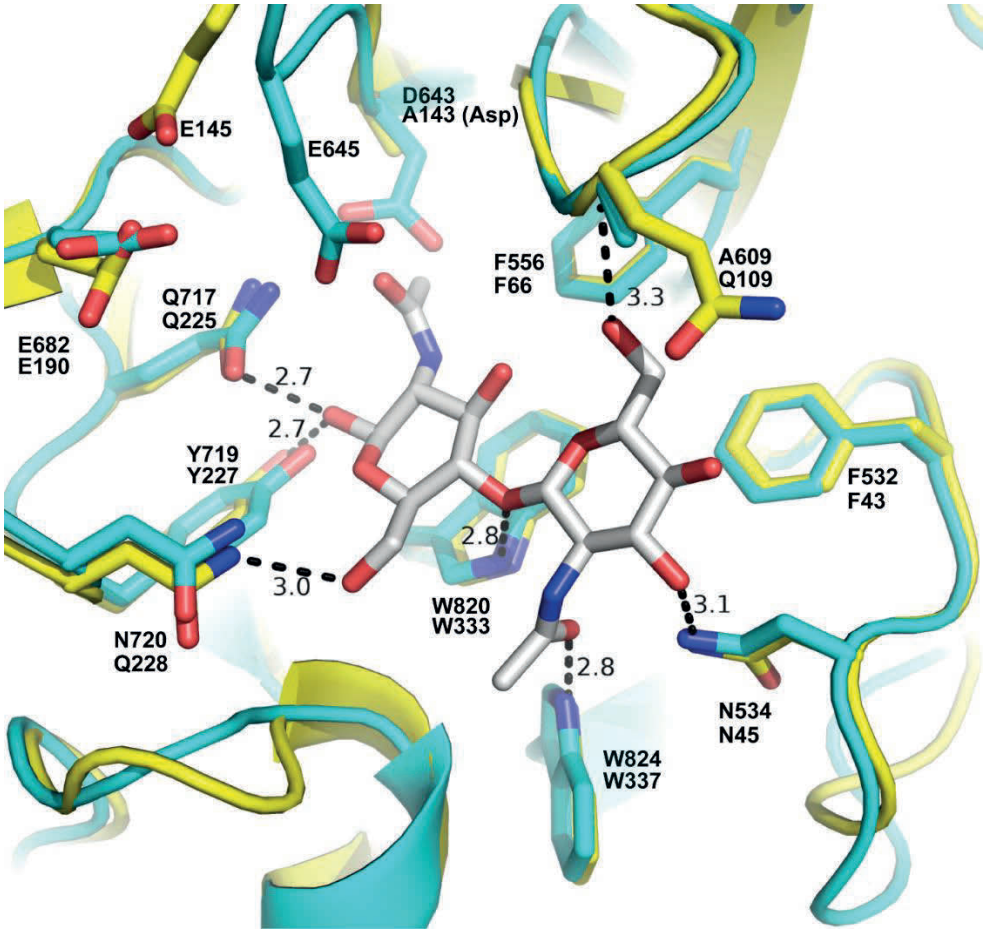

Figure S1. Active site of the *As*Chi18A homology model superimposed on ChiNCTU2 (D143A variant). Proteins are shown as cartoon representation with side chains shown in stick representation (*As*Chi18A colored cyan, ChiNCTU2 D143A [PDB id: 3N13] colored yellow). Side chains are labeled showing *As*Chi18A amino acid numbers above the ChiNCTU2 numbers. The chitobiose ligand bounbd in the -1 and -2 subsite of the ChiNCTU2 active is shown in stick representation with gray colored carbon atoms. Hydrogen bonds are illustrated by dashed lines and distances (Å) are indicated. It should be noted that the positioning of the ChiNCTU2 catalytic acid, E145, deviates from the position observed in the ChiNCTU2 wild type structure (which is more similar to the positioning of AsChi18A E645) due to the absence of an Asp at position 143.

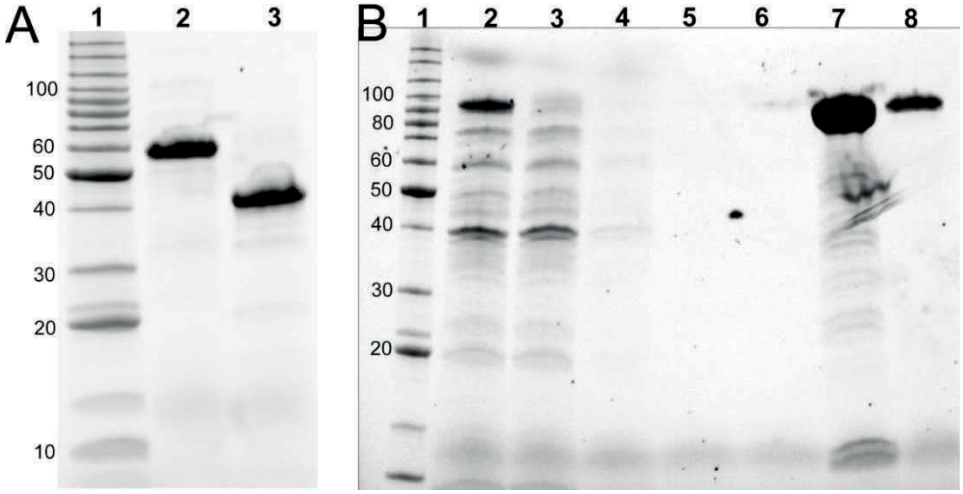

Figure S2. Analysis of protein purity. SDS-PAGE was used to determine protein purity. Panel A shows an SDS-PAGE gel with lanes displaying protein benchmark ladder (Invitrogen) in lane 1, *As*LPMO10A in lane 2 and *As*LPMO10B in lane 3. The SDS-PAGE gel in panel B displays the stages of protein purification for *As*Chi18A, showing the protein benchmark ladder in lane 1, cell free extract from an induced culture in lane 2, flow through in lane 3, wash fraction in lane 4-6 and the eluted protein in lanes 7 and 8. Only fractions containing highly pure protein were used in biochemical assays. All proteins used in biochemical assays were estimated to be >95% pure.

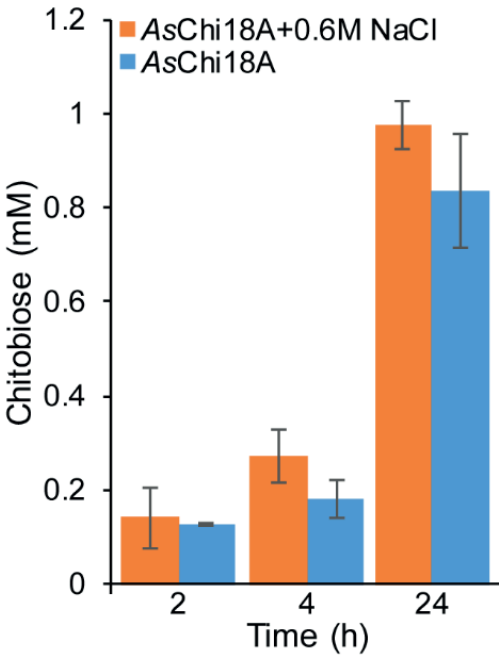

Figure S3. Influence of NaCl on *As*Chi18A activity. The amount of $(GlcNAc)_2$ (chitobiose) released from 10 mg/mL β-chitin in Tris-HCl pH 7.5 by 1.0 mM *As*Chi18A in the presence and absence of 0.6 M NaCl was evaluated at three time points (n=3). Reactions were incubated at 30°C.

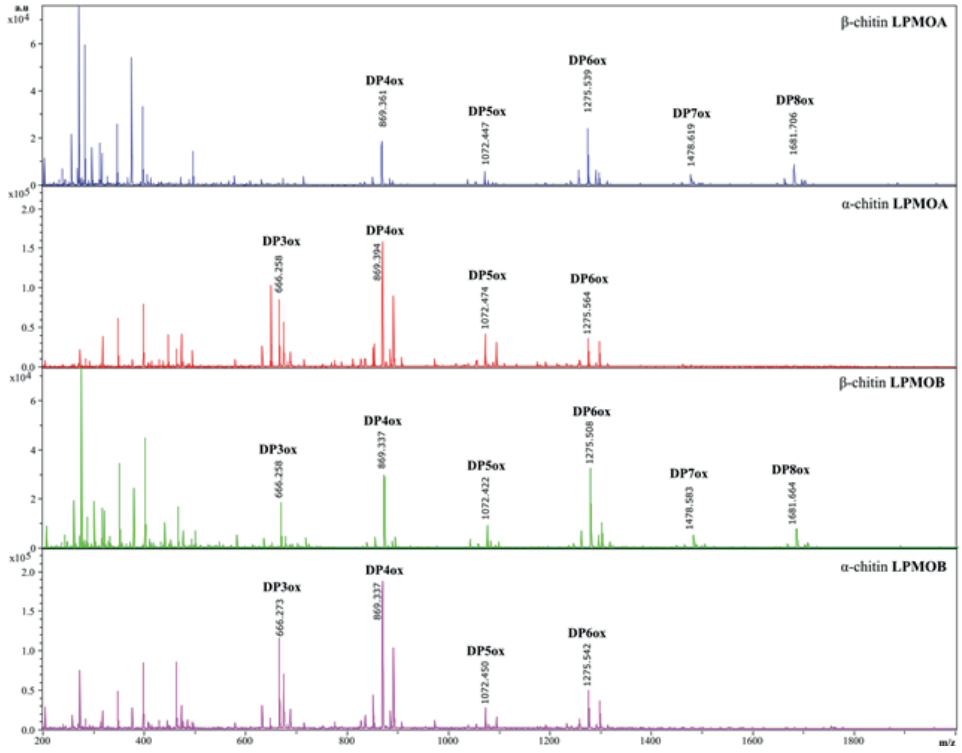

Figure S4. MALDI-TOF MS analysis of oxidized products generated by *As*LPMO10A and -B from *A. salmonicida* on chitin (α and β). The MS spectra show soluble C1 oxidized chito-oligosaccarides, i.e. aldonic acids. The degree of polymerization of each product is indicated by "DPn ox", where n equals the number of monosaccharides in the chain. The main peaks are labelled with the respective masses.

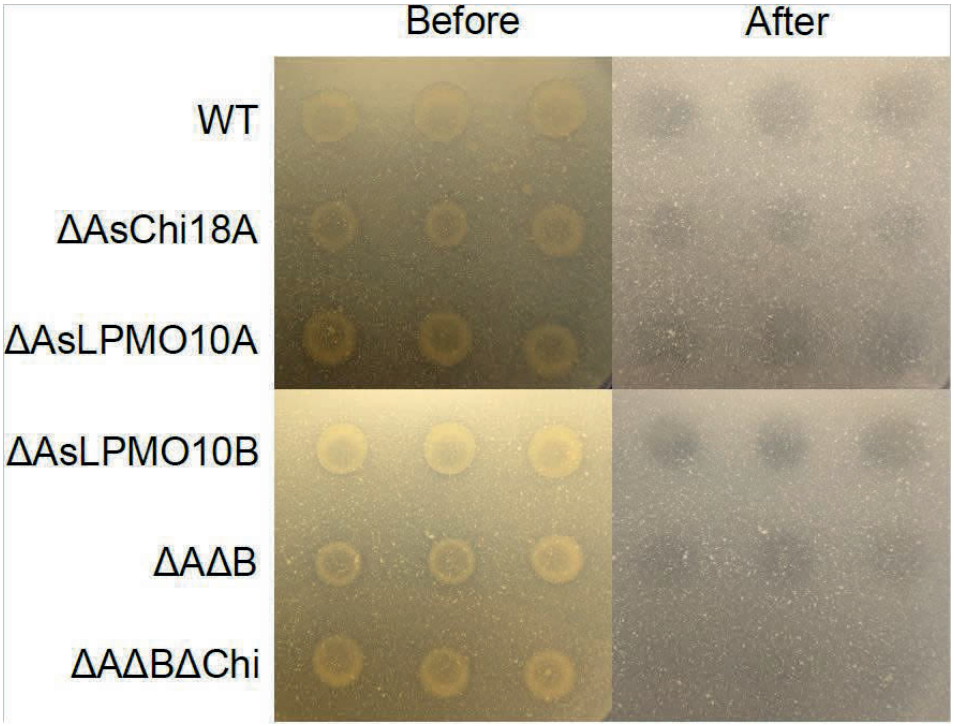

Figure S5. Chitin degradation assay. Images show photographs of agar plates containing LB25 supplemented with 2% colloidal chitin with *Al. salmonicida* variants (indicated on the left side of the image) spotted in triplicate and allowed to grow at 12 °C for 20 days. The photographs show the agar plates before (left) and after (right) the colonies had been removed by gentle washing. Halos indicate chitin degradation.

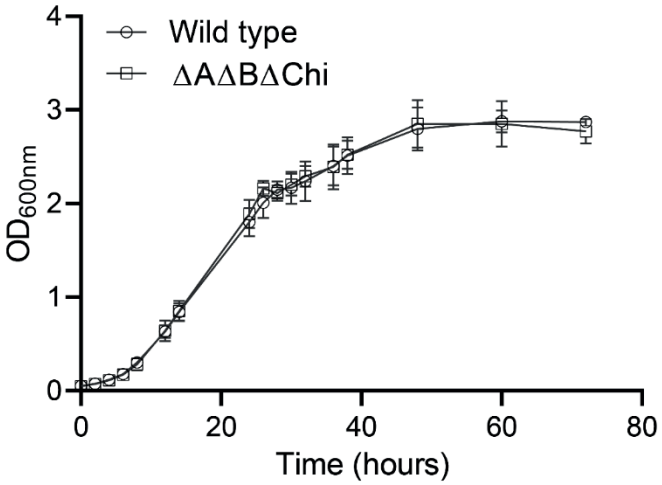

Figure S6. Growth of *Al. salmonicida* LFI1238 variants. Growth of the wild type *Al. salmonicida* LFI1238 strain compared to the triple knock-out strain (ΔAΔBΔChi) in LB25 broth. Standard deviation is indicated by error bars (n=3).

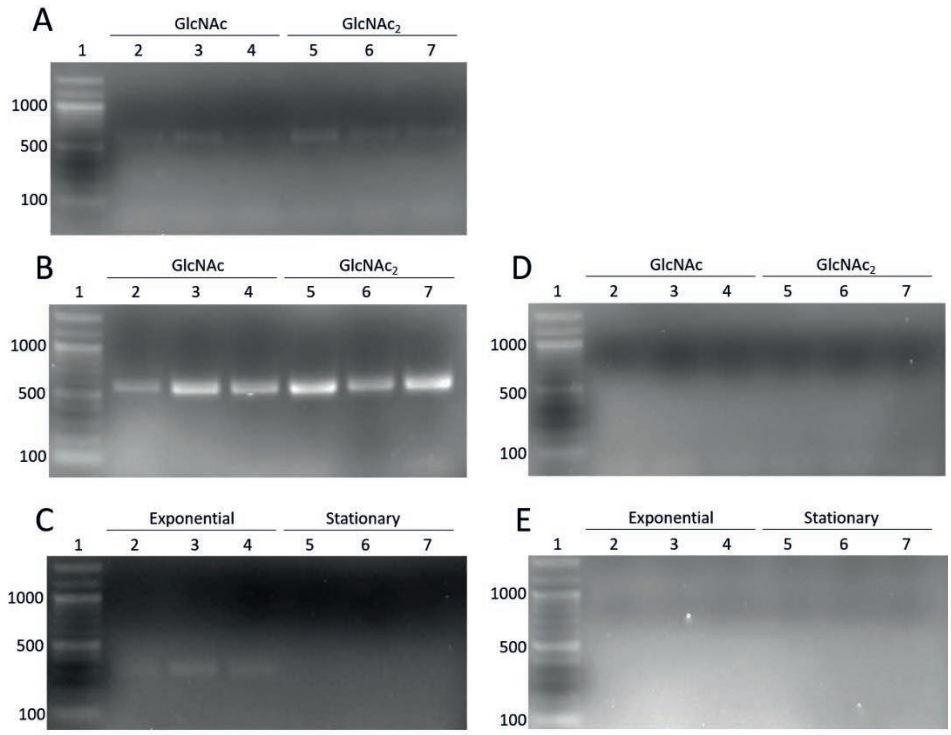

Figure S7. Gene expression analysis by PCR amplification of cDNA. Panel A and B shows the products formed in PCR experiments using cDNA from samples obtained during exponential growth in GlcNAc and $GlcNAc_2$ combined with primer pairs *GH18Expression* and *10AExpression*, respectively. Panel D shows the PCR experiments using -RT controls as template combined with primer pair *10AExpression.* The -RT templates used in Panel D corresponds to the cDNA applied to Panel A and B. Panel C shows the products formed in PCR experiments using cDNA from samples obtained during exponential and stationary growth in glucose combined with primer pair *I0902Expression*. In this case gene expression was evaluated as positive (+) during exponential growth (lane 2-4) and negative (-) during stationary growth (lane 5-7). Panel E shows the products formed in PCR experiments using the -RT samples corresponding to the cDNA template used in Panel C combined with primer pair *I0902Expression*. Lane 1; 100 bp DNA ladder, lanes 2-4 or 5-7; biological replicates within the same condition.

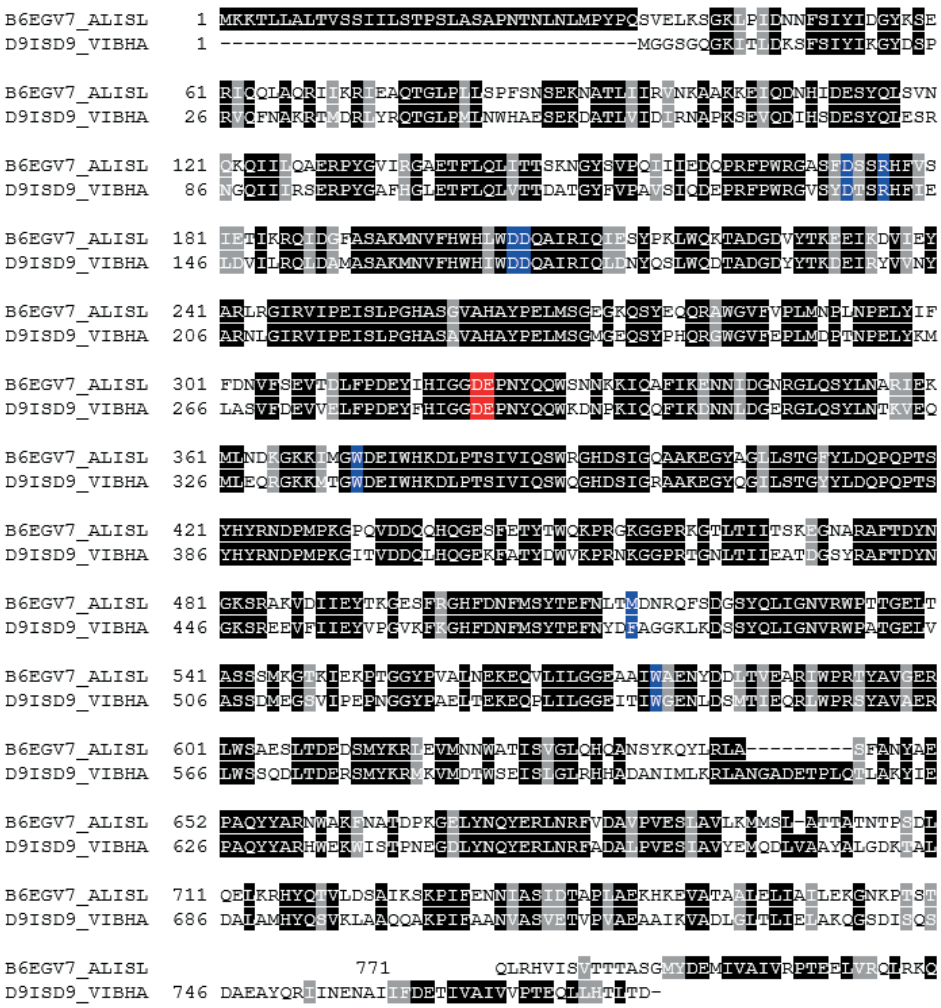

Figure S8. Pairwise sequence alignment of the *Al. salmonicida* GH20 (UniProt ID B6EGV7) and *Vibrio harvey* GH20 *Vh*NAG1 (UniProt ID D9ISD9). The alignment was made using the EMBOSS pairwise sequence alignment tool using default parameters. The Alignment was formatted using BoxShade. Based on data from W. Suginta et al. (1), catalytic amino acids are shown in red shading and amino acids involved in substrate binding are shown in blue shading.

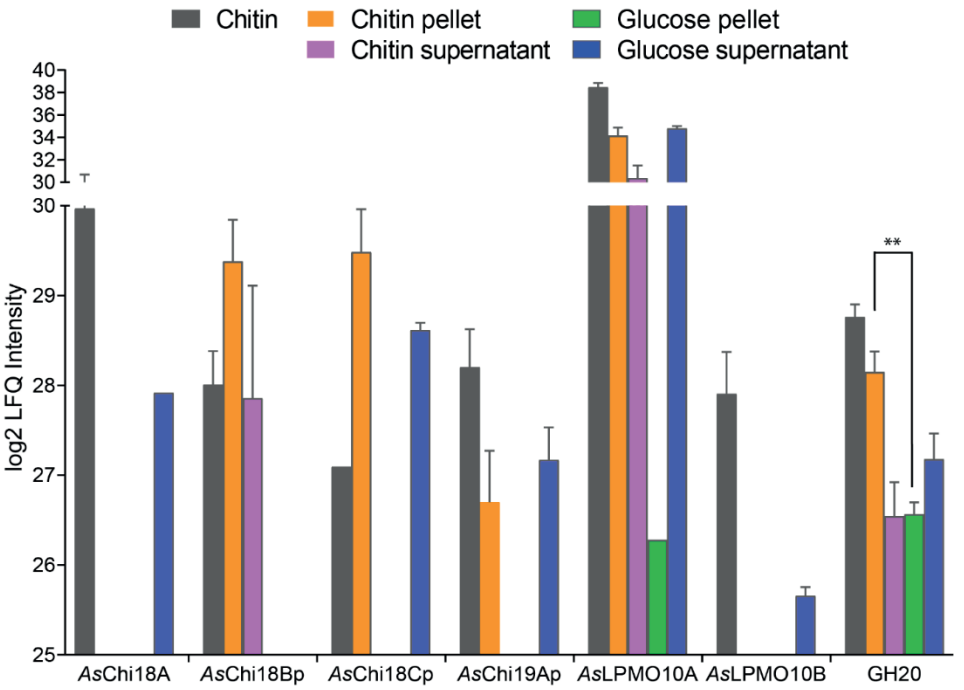

Figure S9. ***Al. salmonicida* protein abundances.** The abundance of selected *Al. salmonicida* proteins related to chitin catabolism displayed in bar chart format as a supplement to Figure 9. Log2 LFQ values shown represent the average values obtained from the label free proteomics data (Supplementary Dataset 1). Error bars are shown for proteins that were detected in two or three biological replicates. The GH20 β-*N*-acetylhexosaminidase was calculated to have a statistically significant 1.58 log2 fold higher abundance during growth on chitin compared to glucose (p=0.0082; paired two-tailed t test).

Supplementary tables

Table S1. Growth rate measurements and max cell density of *Al. salmonicida* cultivated in glucose, GlcNAc and $GlcNAc_2$

Carbon source	Rate constant μ ($hours^{-1}$)	Generation time (hours)	Max cell density (OD_{600})
Glucose	0.065 ± 0.025	5.36 ± 2.17	2.63 ± 0.094
GlcNAc	0.069 ± 0.029	5.16 ± 2.00	1.31 ± 0.022
$GlcNAc_2$	0.055 ± 0.021	4.95 ± 0.89	1.58 ± 0.145

Mean ± SD of three biological replicates.

Table S2. Identified CAZymes sorted by their putative biological processes, according to gene ontology (GO) annotations.

CAZy	Uniprot	Biological process
		Carbohydrate metabolic process [GO:0005975]
AA10	B6EQJ6	*As*LPMO10B
CBM73;GH18	B6EH15	*As*Chi18A
GH13_19	B6EGT4	Alpha-amylase
GH20	B6EGV7	Putative beta-N-acetylhexosaminidase
GT35	B6EQ29	Alpha-1,4 glucan phosphorylase
GH77	B6EQ30	4-alpha-glucanotransferase
GH3	B6ERJ6	Beta-hexosaminidase*
		Chitin binding [GO:0008061]
AA10;CBM73	B6EQB6	*As*LPMO10A
		Cell cycle, cell division, protein import [GO:0007049/ 0051301/ 0017038]
PL22	B6EGK3	Tol-Pal system protein TolB
		Formaldehyde catabolic process [GO:0046294]
CE1	B6EH03	S-formylglutathione hydrolase
		Glycogen biosynthetic process [GO:0005978]
GT5	B6EQL7	Glycogen synthase
		Lipid A biosynthetic process [GO:0009245]
CE11	B6ELH0	UDP-3-O-acyl-N-acetylglucosamine deacetylase
GT19	B6EJW7	Lipid-A-disaccharide synthase
		Lipopolysaccharide biosynthetic process [GO:0009103]
GT9	B6EPB8	ADP-heptose-LPS heptosyltransferase II
		Peptidoglycan metabolic process [GO:0000270]
GH23	B6EJV5	Membrane-bound lytic murein transglycosylase D
GH23	B6EGC8	Soluble lytic murein transglycosylase
		Trehalose catabolic process [GO:0005993]
GH13_29	B6ERJ9	Trehalose-6-phosphate hydrolase
		Not assigned
GH103	B6EIW0	Putative exported protein
GT2	B6EKR9	Putative glycosyl transferase
GT51	B6EM36	Penicillin-binding protein 1A

*Also, Cell cycle [GO:0007049];cell division [GO:0051301];cell wall organization [GO:0071555];peptidoglycan biosynthetic process [GO:0009252];peptidoglycan turnover [GO:0009254];regulation of cell shape [GO:0008360]

Table S3. Primers designed for construction of flanking regions and fusion product, sequencing and selection/verification of transconjugates and mutants.

Primer	Sequence 5'-3'
*AsGH18*_For	GCTGATGGCGTGATCAAC
*AsGH18*_Rev	GGCGCGTGCTAATTTCAA
*AsLPMO10A*_For	GGCTGCTATTGTCACAGAATA
*AsLPMO10A*_Rev	AAGCCTAATAAAGCACACCCA
*AsLPMO10B*_For	GATGAGGTGTACCATCTTGAA
AsLPMO10B _Rev	TGTAATAGAATGTCACCAGCA
pDM4_Seq_F	CGGGAGAGCTCAGGTTAC
pDM4_Seq_R	GGCTTCTGTTTCTATCAGCT

Table S4. Primers applied for amplification of target genes using cDNA.

Primer	*Sequence (5'- 3')*	*Product size (bp)*
GH18Expression_F	AGTCAAGCATCAGCCAAGAAAG	566
GH18Expression_R	TAAGGCAAGGCTCGATCCAG	
10AExpression_F	ATTCGGTCCTGCTGATGG	565
10AExpression_R	ATTTGCTTGACCTTGTGTTGC	
10BExpression_F	TCAAGCGTGTCAGTCTGC	441
10BExpression_R	TGCCAACGAGTGTAGAGC	
I0902Expression_F	ATGCACAAGGTCGATCTG	297
I0902Expression_R	ATGGGATGTACTTGTCGC	

Supplementary references

1. Suginta W, Chuenark D, Mizuhara M, Fukamizo T. 2010. Novel beta-N-acetylglucosaminidases from Vibrio harveyi 650: cloning, expression, enzymatic properties, and subsite identification. BMC Biochem 11:40.

Paper II

Chitinolytic enzymes confer pathogenicity of *Aliivibrio salmonicida* LFI1238 in the invasive phase of cold-water vibriosis (CWV)

Anna Skåne[1], Per Kristian Edvardsen[1], Gabriele Cordara[3], Jennifer S.M. Loose[1], Kira D. Leitl[3], Ute Krengel[3], Henning Sørum[2], Fatemeh Askarian[1 ‡*]and Gustav Vaaje-Kolstad[1‡*]

[1]Faculty of Chemistry, Biotechnology and Food Science, Norwegian University of Life Sciences (NMBU), Ås, Norway.
[2] Department of Paraclinical Sciences, Faculty of Veterinary Medicine, Norwegian University of Life Sciences (NMBU), Oslo, Norway.
[3]Department of Chemistry, University of Oslo, P.O. Box 1033 Blindern, NO-0315 Oslo, Norway.

Chitinolytic enzymes confer pathogenicity of *Aliivibrio salmonicida* LFI1238 in the invasive phase of cold-water vibriosis (CWV)

Anna Skåne[1], Per Kristian Edvardsen[1], Gabriele Cordara[3], Jennifer S.M. Loose[1], Kira D. Leitl[3], Ute Krengel[3], Henning Sørum[2], Fatemeh Askarian[1] ‡*and Gustav Vaaje-Kolstad[1‡*]

[1]Faculty of Chemistry, Biotechnology and Food Science, Norwegian University of Life Sciences (NMBU), Ås, Norway.
[2] Department of Paraclinical Sciences, Faculty of Veterinary Medicine, Norwegian University of Life Sciences (NMBU), Oslo, Norway.
[3]Department of Chemistry, University of Oslo, P.O. Box 1033 Blindern, NO-0315 Oslo, Norway.

‡These authors contributed equally to this work.
*Correspondence: gustav.vaaje-kolstad@nmbu.no , fatemeh.askarian@nmbu.no,

Abstract
Aliivibrio (Vibrio) salmonicida is the causative agent of cold-water vibriosis in salmonids (*Oncorhynchus mykiss* and *Salmo salar* L.) and gadidae (*Gadus morhua* L.). Virulence-associated factors that are essential for the full spectrum of *Al. salmonicida* pathogenicity are largely unknown. Chitin-active lytic polysaccharide monooxygenases (LPMOs) have been indicated to play roles in both chitin degradation and virulence in a variety of pathogenic bacteria. In the present study we investigated the role of LPMOs in the pathogenicity of *Al. salmonicida* LFI238 in Atlantic salmon (*Salmo salar* L.). In vivo challenge experiments using isogenic deletion mutants of the two LPMOs encoding genes *AsLPMO10A* and *AsLPMO10B*, showed that both LPMOs, and in particular *As*LPMO10B, were important in the invasive phase of cold-water vibriosis. Crystallographic analysis of the *As*LPMO10B AA10 LPMO domain (to 1.4 Å resolution) revealed high structural similarity to viral fusolin, an LPMO known to enhance the virulence of insecticidal agents. Finally, exposure to Atlantic salmon serum resulted in substantial proteome re-organization of the *Al. salmonicida* LPMO deletion variants compared to the wild type strain, indicating the struggle of the bacterium to adapt to the host immune components.

Datasets are available for download through the following links:

http://arken.nmbu.no/~gustko/Paper_II/Dataset%201.xlsx
http://arken.nmbu.no/~gustko/Paper_II/Dataset%202.xlsx
http://arken.nmbu.no/~gustko/Paper_II/Dataset%203.xlsx

Introduction

Aliivibrio salmonicida (*Vibrio salmonicida* before transfer to genus *Aliivibrio*) is the causative agent of cold-water vibriosis (CWV) in salmonids (*Oncorhynchus mykiss* and *Salmo salar* L.) and gadidae (*Gadus morhua* L.), an acute infectious disease consistent with severe hemorrhagic septicemia (1-4). Once the pathogen enters the bloodstream (5), *Al. salmonicida* can disseminate in many sites, *e.g.* sinusoids of the head kidney/lymphoid organ, leukocytes, and endothelial cells (6), and even actively proliferate in blood upon passing a latent stage (5, 7, 8). Notably, histopathological changes caused by the bacterium are found to be associated with the bacterial burden (6). Although CWV is under control by vaccination, virulence-associated factors that are essential for the full spectrum of *Al. salmonicida* pathogenicity are largely unknown. So far, in vitro and in vivo studies have demonstrated that the salinity-sensitive quorum-sensing regulator LitR (9), LPS O-antigen (10), motility/flagellation (11), and the *lux* operon (12) are required for full virulence of *Al. salmonicida*.

Chitinolytic enzymes include chitinases (glycoside hydrolases 18 and 19 (GH18 and -19) and lytic polysaccharide monooxygenases (LPMOs), with the latter classified in the auxiliary activities 10 family (AA10) according to the classification by the Carbohydrate Active Enzymes database (CAZy (13)). Such enzymes are associated with the modification, binding, depolymerization, and catabolism of chitin (14-18). LPMOs were discovered in 2010 (18), and thus represented a recent addition to the chitin degradation machinery. These copper-dependent, redox enzymes cleave chitin chains by an oxidative reaction and synergize with chitinases in chitin degradation reactions (18-21). Intriguingly, genes encoding LPMOs are found in an array of pathogenic bacteria (22), and there is an extensive amount of literature implicating their role in numerous biological processes including bacterial pathogenicity (22-29). Direct evidence for a role of LPMOs in virulence was recently published by Askarian et al. (2021), who showed that the LPMO of the opportunistic human pathogen *Pseudomonas aeruginosa*, called CbpD, was important for establishing systemic- and lung infections, where the role of the enzyme was attributed to attenuation of the terminal cascade of the complement system (30). A somewhat different role has been proposed for the *Vibrio cholerae* LPMO, GbpA, which binds chitin and mucins, mediating bacterial colonization of epithelial cell surfaces (31). Similar to LPMOs, chitinases have also been indicated as virulence factors. For example, *Listeria monocytogenes* ChiA was found to promote bacterial viability within the liver and spleen of mice (25), and the chitinase (ChiA) of *Legionella pneumophila*, has been shown to enhance bacterial persistence within the lungs of mice in vivo (32). Recently, is has been shown that *L. pneumophila* ChiA is involved in hydrolysis of the peptide bonds of mucin-like proteins (33), suggesting novel mechanisms of mucin degradation.

The *Al. salmonicida* LFI1238 genome harbors genes encoding two family AA10 LPMOs (*AsLPMO10A, AsLPMO10B*) and one chitinase GH18 (*AsChi18A*). All three enzymes can depolymerize chitin and are important for the ability of the bacterium to utilize chitin as a nutrient source (34). However, the authors noticed several features that could indicate additional roles of the enzymes, for instance a remarkably low chitinolytic activity of the chitinase, and constitutive expression of *As*LPMO10A (this protein is one of the most abundant proteins produced by the bacterium). In addition, the whole genome sequencing analysis of *Al. salmonicida*

LFI1238 had previously shown several points of mutation or insertion of mobile genetic elements within crucial genes associated with the chitinolytic machinery (*e.g.* several chitinases, a chitoporin and a protein important for regulating expression of the chitin degradative loci (35)). Cumulatively, these results suggest the contribution of the chitinolytic enzymes to other or additional functions beyond chitin degradation and utilization by *Al. salmonicida*. Thus, the current work set out to elucidate the putative immune evasive properties of *As*LPMO10A (A) and *As*LPMO10B (B) in *Al. salmonicida* pathogenesis during CWV in Atlantic salmon. Using a series of isogenic mutants (△A, △B and △AB), we found that the LPMOs contributed to the pathogenicity of *Al. salmonicida* in the invasive phase of CWV.

Results

Phylogenetic analysis

The sequence and biochemical properties of *As*LMO10A and *As*LPMO10B have previously been biochemically characterized (34), but their putative orthologs in other fish pathogens are not known. To determine the latter and to simultaneously obtain an overview of LPMOs in bacteria associated with fish disease, the genomes of fish pathogens (36) were scanned for LPMO-encoding genes that subsequently were subjected to phylogenetic analysis (Fig. 1). The analysis showed that LPMOs are present in the majority of aerobic Gram-negative bacteria investigated, but to a lesser extent in Gram-positives. *As*LPMO10A clusters with LPMOs from a variety of bacterial families, whereas *As*LPMO10B clusters with representatives mostly restricted to the Vibrionaceae.

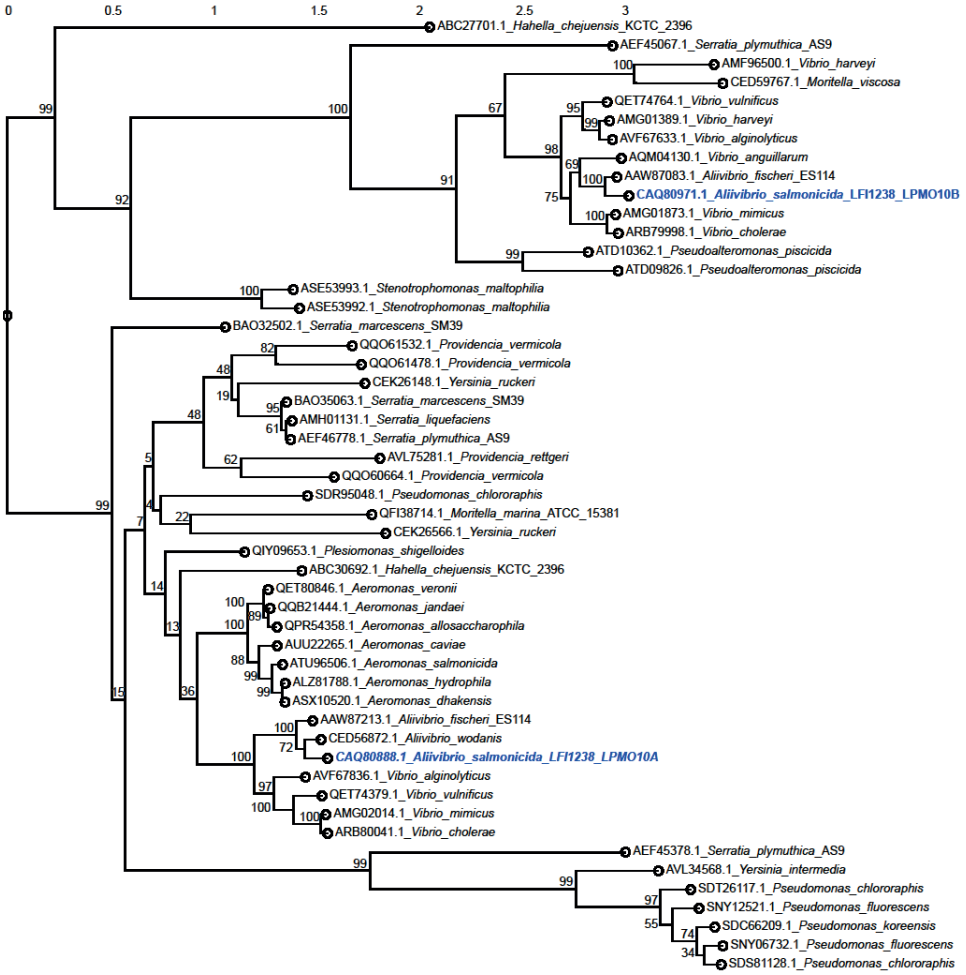

Figure 1. Phylogenetic tree of family AA10 LPMOs from fish pathogens. Alignment and phylogenetic reconstructions were performed using the "build" function of ETE3 v3.1.1 21 (37) that utilizes PhyML v20160115 (38). Branch support values were computed from 100 bootstrapped trees. Refseq identifiers for the proteins are indicated next to the name of the bacterial species. The *Al. salmonicida* LPMOs are indicated in blue colored bold formatting.

Proteomic profiling

Gene deletions may induce alterations in protein regulation by the bacterium to adapt to this impairment. Such re-organization can be readily visualized by comparing the proteomic response of wild type (WT) and gene-deletion variants confronted with host factors. Thus, comparative label free quantitative proteomics was used to determine the putative proteomic response of wild type, ΔA, ΔB and ΔAB strains when exposed to Atlantic salmon serum (SS). The bacteria were grown to early exponential phase and incubated for 1 hour in the absence or presence of SS, prior to being harvested. In total, 1725 proteins were identified, corresponding to almost half the predicted proteome of *Al. salmonicida* (Dataset

1). The whole cell proteomes of the deletion mutants were compared to that of the wild type in the absence and presence of SS. The comparison showed significant regulation of 61 (ΔA), 27 (ΔB) and 32 (ΔAB) and 46 (ΔA) and 70 (ΔB) and 94 (ΔAB) in the absence or presence of SS, respectively (Fig. 2A). In the absence of SS, the most significantly upregulated protein was RpoC for ΔB and ΔAB and Rne for ΔA (Dataset 2). Beside RpoC, RpoB and Rne was found to be among the top three hits of the upregulated proteins in most of the deletion mutants (Dataset 2). The protein Rne was found to be common for all (Dataset 3, Fig. 2B).

In the presence of SS, proteins related to motility, chemotaxis, quorum sensing and stress response were identified as significantly regulated (Fig. 2C, Dataset 2). The ΔA deletion strain resulted in up-regulation of CheW (Chemotaxis protein CheW), CheA (Phosphorelay protein LuxU) and FlgL (Flagellar P-ring protein). The latter protein was identified as up-regulated in all deletion variants after exposure to SS (Fig. 2B), whereas in absence of SS it was downregulated in the ΔB strain (Fig. 2C). Moreover, exposure to SS, resulted in up-regulation of FlhF (Flagellar biosynthesis protein), LuxI (Autoinducer synthesis protein) and chaperone protein HtpG in the ΔB and ΔAB strains. Proteins related to stress response were down-regulated in ΔA (*e.g.* CatA (Catalase), TrxB (Thioredoxin reductase), CspV (Cold shock protein)) and ΔB (*e.g.* Bcp (Putative peroxiredoxin), TrxB and VSAL_I1529 (Putative glutaredoxin)) in presence of SS (Fig. 2C, Dataset 2). Notably, proteins with peptidase and protease related activity were identified as differentially regulated both in absence and presence of serum. Specifically, in absence of SS, deletion of *As*LPMO10A resulted in up-regulation of Prc (Tail-specific protease) and SohB (Probable protease SohB), and down-regulation of HslU (ATP-dependent protease ATPase subunit HslU) compared to wild type (Fig. 2C, Dataset 2). It should be noted that HslU is not directly a protease, but rather a subunit of the heat-shock locus HslV-HslU complex associated with the proteasome of many bacteria (39, 40). After incubation with SS, Lon protease and PepB (peptidase B) were up-regulated in ΔA and ΔAB respectively. The protein called BsmA, involved in cell aggregation for biofilm development, was found to be down-regulated in the ΔB deletion mutant (Fig. 2C, Dataset 2). Host integration factor subunit B (IhfB) was down-regulated in ΔA and ΔAB in presence of SS compared to wild type, while subunit A (IhfA) was up-regulated in the B deletion mutant compared to wild type (Fig. 2C, Dataset 2). Notably, the host integration factor is implicated in regulation of virulence related factors in *V. cholerae* (41), *Vibrio vulnificus* (42) *Vibrio harveyi* (43) and *Vibrio fluvialis* (44). Interestingly, the transposon VSAL_I0029 was up-regulated in both ΔB and ΔAB. The function of this transposon is not known; however, it is located closely to a reported T6SS effector VSAL_I0031 (45). This gene encodes a so-called MIX (Marker for type sIX) effector, and these effectors have C-terminal domains predicted to contain different antibacterial or anti-eukaryotic properties (45). Finally, *As*LPMO10B was not detected in any samples, whereas *As*LPMO10A was observed in both wild type and ΔB (but not significantly regulated in any condition).

Together, these data indicate that deletion of the LPMO encoding genes in *Al. salmonicida* results in a significantly altered proteome compared to wild type. Moreover, the number of differentially regulated proteins in the ΔB and ΔAB strains were remarkably increased in presence of SS.

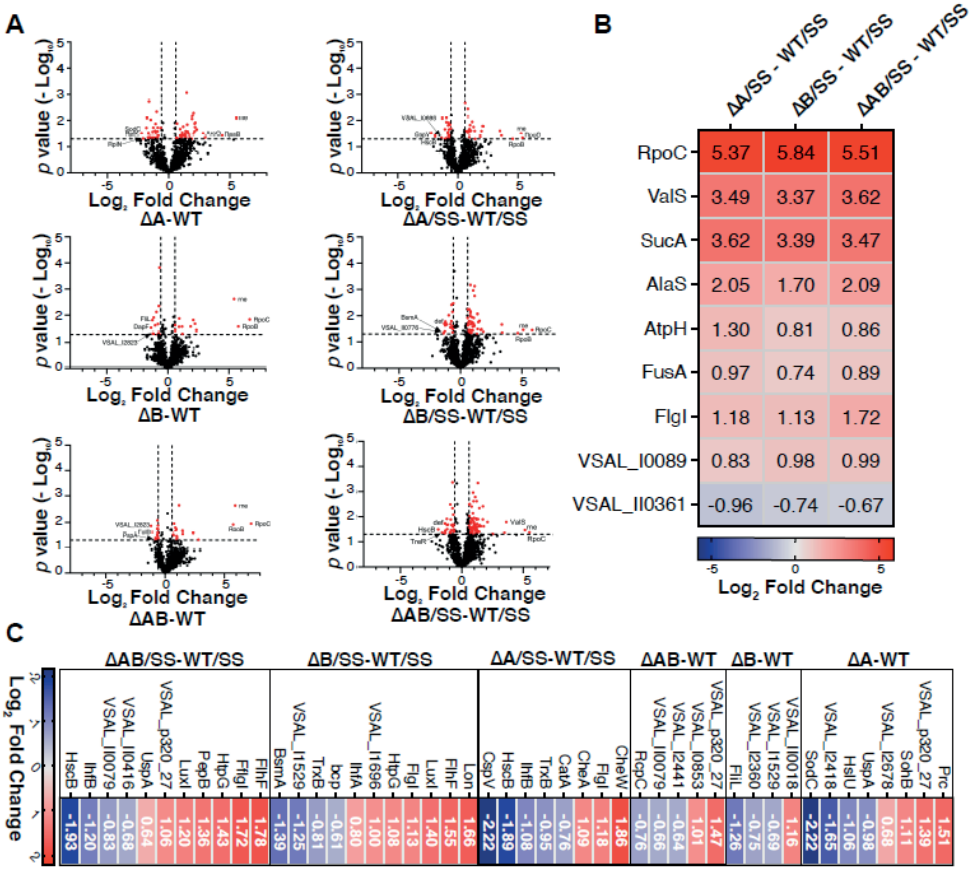

Figure 2. Significantly regulated proteins of *Al. salmonicida* deletion variants exposed to Atlantic salmon serum. (A) Volcano plots showing the *p*-values of significance and Log_2 fold change values comparing ΔA, ΔB or ΔAB against WT in the absence (left panel) and presence (right panel) of salmon serum (SS). Dotted line(s) traversing the y- and x-axis indicate the significance cutoff at p = 0.05 (log_{10} = 1.3) and (±) 1.5-fold change (log_2 = 0.58) in protein abundance. Significance was determined by a paired two-tailed t-test. (B) Heatmaps showing the fold change values (log_2) of significantly regulated proteins common for all deletion mutants. (C) Heatmap showing fold change values (Log_2) of significantly regulated proteins related to motility, chemotaxis, quorum sensing, protease activity and general stress response.

In vivo immersion challenge experiments to establish chronic septicemia

To provide insight into the contribution of LPMOs in the virulence properties of *Al. salmonicida,* an immersion challenge was carried out using the wild type and the deletion variants (Δ*A*, Δ*B,* ΔAB). In an experiment using a total of 1340 Atlantic salmon smolts, fish were immersed in a high concentration of *Al. salmonicida* variants for 30 min, followed by water exchange (Fig. 3A). Immersion in approximately 1.2-2.7×10^7 CFU/mL wild type and gene deletion strains resulted in

a persistent bacteremia (Figs. 3 and 4) without exhaustive killing (Fig. 3B). The examined conditions resulted in a low number of accumulated mortalities (below 10%) in the wild type and deletion strains over the course of the challenge (Fig. 3B). Furthermore, the employed concentrations resulted in successful establishment of septicemia as all sampled fish were positive for presence of *Al. salmonicida* in blood 10 min post-infection (Fig. 3C). The presence of fin rot was observed evenly within all treatments but did not contribute to an extensive rate of mortality as reflected in the mock treatment (Fig. 3B).

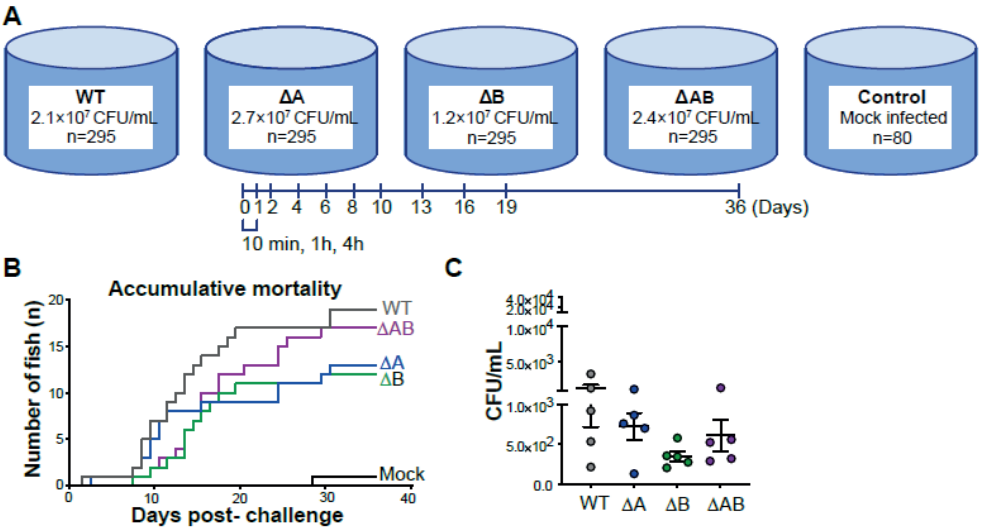

Figure 3. Immersion challenge to establish persistent septicemia. (A) Challenge groups and infection doses represented by colony forming units (CFU) pr mL *Al. salmonicida* containing seawater. (B) Accumulative mortality. (C) Presence of *Al. salmonicida* WT and deletion variants in blood after 10 minutes of exposure. Bacteria (WT, ΔA, ΔB or ΔAB) were isolated from the drawn blood of Atlantic salmon following immersion challenge. Data are shown as individual values (n=5) with mean ± SEM representing colony forming units (CFU) pr mL blood.

Bacterial burden in blood

Fish challenged with wild type, ΔA, ΔB and ΔAB, and sampled at multiple time points post-challenge showed the presence of *Al. salmonicida* in a various degree throughout the complete sampling period, indicating the successful establishment of CWV in our experimental condition (Figs. 4 and 5). A decrease of the bacterial number in whole salmon blood was observed between days 1-6 compared to 1h post-challenge in wild type, ΔA, ΔB and ΔAB infected fish (Fig. 4). At 8 days post infection, the group challenged with the wild type strain showed large individual variation and a significant increase in bacterial burden compared to the ΔB mutants but not ΔA and ΔAB infected fish (Fig. 4). The ΔB strain generally showed lower individual variation and lower CFU/ml blood compared to the other strains at days

10-13 post infection, indicating some loss of resistance towards host blood immune components.

Taken together these data indicate that in general *As*LPMO10A and -B were not critical for the viability and survival of *Al. salmonicida* in salmon blood in the early- or late- stage of infection in vivo, albeit *As*LPMO10B was found to be important in the invasive phase of CWV.

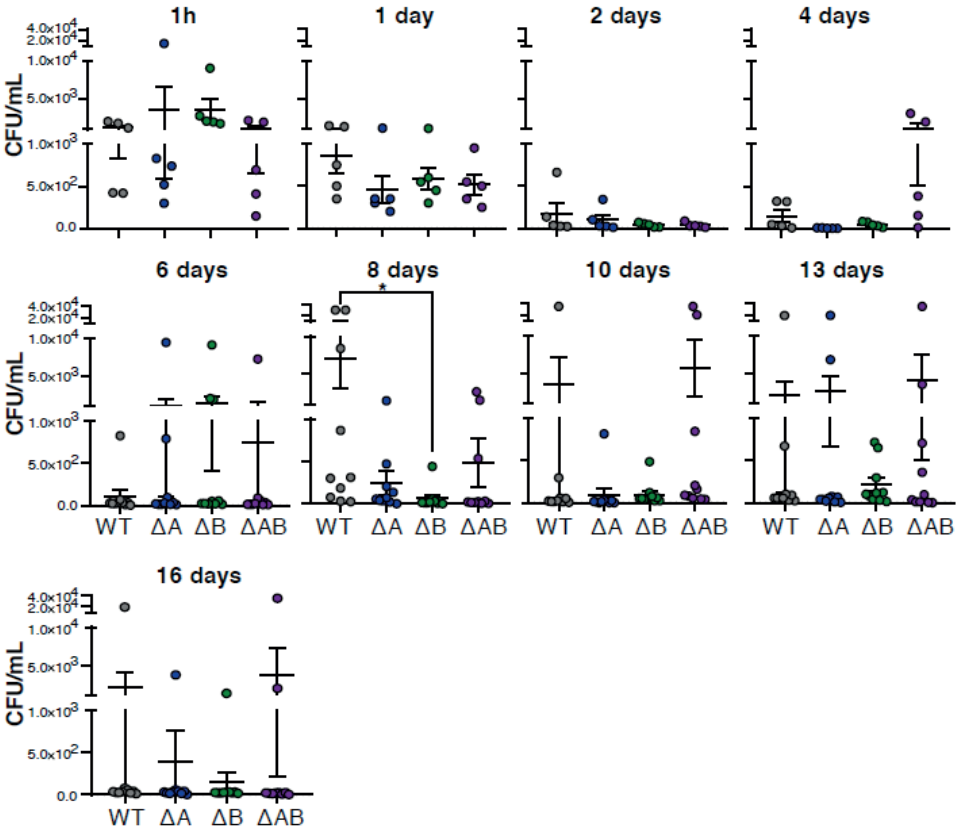

Figure 4. Presence of *Al. salmonicida* variants in blood from 1 hour to 16 days post-challenge. Bacteria (WT, ΔA, ΔB or ΔAB) were isolated from drawn whole blood of Atlantic salmon following immersion challenge. Data are shown as individual values (n=5-10) with mean ± SEM representing colony forming units (CFU) pr mL blood.

Bacterial burden in tissues and organs

Next, samples were taken from the various tissues and organs to evaluate whether LPMOs were critical in viability of *Al. salmonicida* in organs over the course of chronic CWV infection. Assessing the bacterial burden revealed that despite *Al. salmonicida* being absent in skin and gills of the sampled fish at day 1-6 post-infection, wild type and ΔA were recovered from all sampled fish at 8 days post

challenge (Fig. 5A, panels 1-2). In the ΔB and ΔAB infected groups, the recovery was estimated 60-80% and 20-30%, respectively (Fig. 5A, panels 1-2). A quantitative analysis of bacterial burden in the spleen and liver revealed significant increase in the recovered wild type compared to the ΔB and ΔAB mutant strains 8 days post-challenge (Fig. 5B, right and left panels). Interestingly, the number of recovered ΔA strain was attenuated in the spleen (Fig. 5B, right panel), but not liver (Fig. 5B, left panel) at day 8 post-infection. All infected groups showed reduced recovery of *Al. salmonicida* from skin, gills, head kidneys, liver and spleen at the later time-points as the CWV entered into the decline phase. Of note, the ΔB strain was not detected in sampled organs after 8 days post challenge, whereas the ΔAB strain was detected at levels similar to fish challenged with the wild type (Fig. 5A).

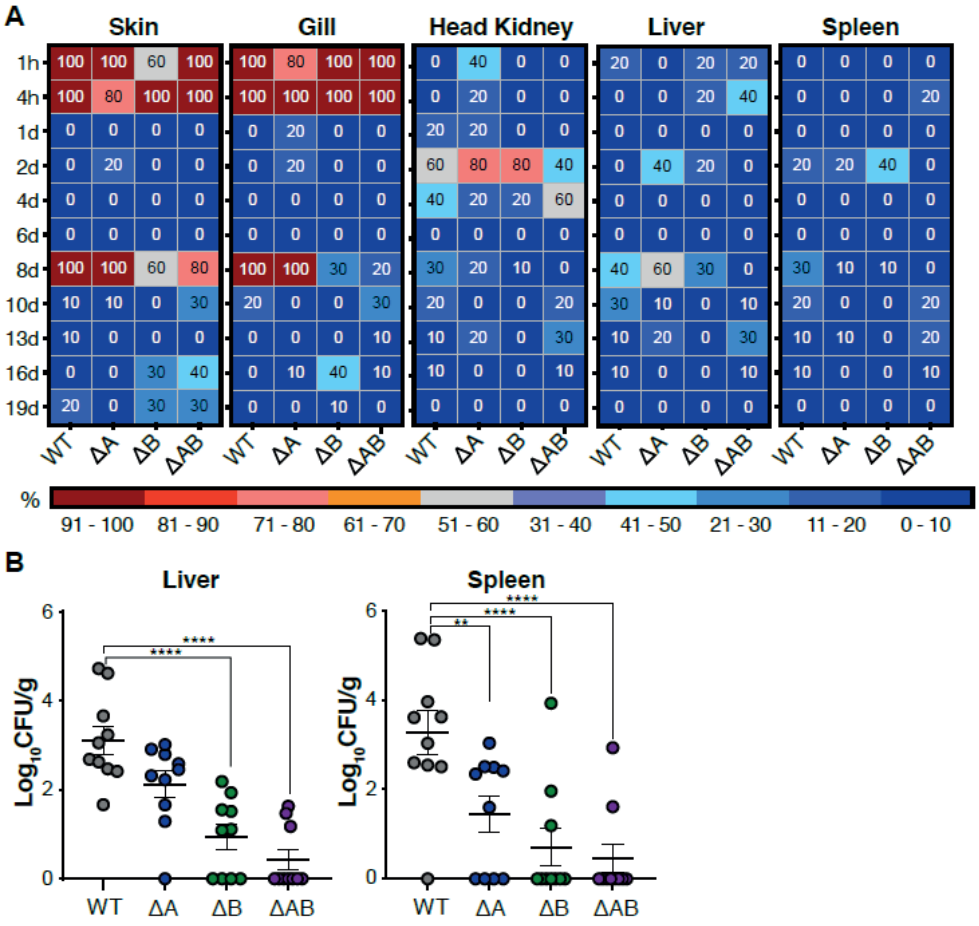

Figure 5. Presence of *Al. salmonicida* variants from tissue and organs over the course of CWV infection. (A) Percentage of sampled fish that were positive for presence of *Al. salmonicda* from 1 hour to 19 days post immersion challenge with WT, ΔA, ΔB and ΔAB. (B) Bacteria (WT, ΔA, ΔB or ΔAB) were isolated from the homogenized spleen or liver of Atlantic salmon following 8 days post-

immersion challenge. Data are shown as individual values (n=10) with mean ± SEM representing colony forming units (CFU) per gram organ.

As the difference in the bacterial burden was well reflected in the spleen, the expression of selected proinflammatory markers (Interleukin-1β (IL-1β and TNFα) and complement factors C3 and C5 were further evaluated via RT-qPCR in the wild type and ΔAB infected fish in this organ (Fig. 6). The induction of proinflammatory markers were comparable in wild type and ΔAB infected salmon. The expression of the complement components, C3 and C5, showed a higher induction of C5 in wild type, albeit no statistically significant difference was obtained.

In summary, these data demonstrate the importance of *As*LPMO10A and -B in the invasive phase of CWV caused by *Al. salmonicida* although the transcriptional induction of inflammatory and complement markers were comparable in all infected fish at 10 days post immersion challenge.

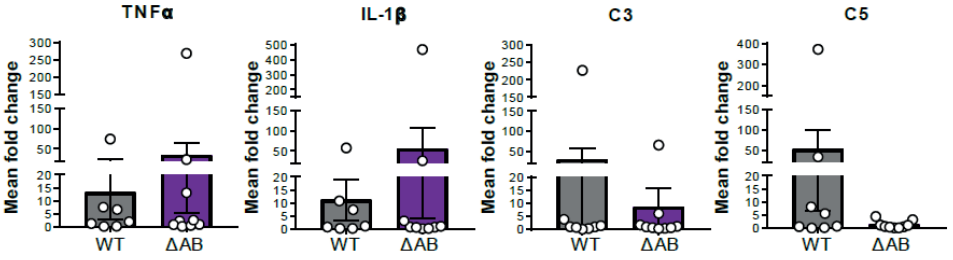

Figure 6. Mean fold change of host immune parameters in Atlantic salmon spleen 10 days after challenge with wild type (WT) and the ΔAB deletion strain. The data is shown as mean fold change ± SEM compared to the mock infected group (n=5). The fold changes represent 2^(-ΔΔCq) were ΔΔCq = ΔCq (Cq of target gene – average Cq of house-keeping genes EF1A and β-actin) of the individual samples from WT and ΔAB infected groups- mean ΔCq (Cq of target gene – Cq of house-keeping genes) of the mock infected group. Target genes; TNFα (Tumor necrosis factor α), IL-1β (Interleukin 1-β), C3 (Complement component 3) and C5 (Complement component 5-2).

Structure of *As*LPMO10B

A structural investigation of *As*LPMO10B was initiated to find a rationale for its preeminent role as a facilitator during host invasion. The X-ray crystal structure of the family AA10 LPMO domain of the protein (amino acid residues 26-214; Fig. 8A) was solved to a resolution of 1.35 Å and deposited in the Protein Data Bank (PDB; PDB ID: 7OKR). *As*LPMO10B carries the canonical (46) fibronectin-like/immunoglobulin-like β-sandwich core structure (Fig. 8B), consisting of seven β-strands arranged as two juxtaposing β-sheets. The β-sandwich supports the histidine brace catalytic motif (His26, His136) and the putative co-substrate coordinating amino acid (Glu206), which shows conformational flexibility and was modeled in two alternative conformations (Fig. 8C). The histidine brace is loaded with a copper ion, an expected consequence of the sample preparation process,

and confirmed by anomalous scattering. Copper shows an incomplete square planar coordination, hinting at the presence of Cu (I) at the metal-binding site. The latter is likely a consequence of the well-documented photoreduction of Cu (II) during X-ray data collection (47). The model also contains 109 water molecules from the first and second coordination sphere and three polyethylene glycol fragments (PEG) from the crystallization conditions. We also observe electron density "above" the copper site (Fig. S1), where the putative ligand would bind, which may represent a citrate molecule from the buffer. A search for structural homologues was run on the DALI server (48) (ekhidna2.biocenter.helsinki.fi/dali), using the coordinates of the new LPMO domain. The list of results contains matches from various members of the LPMO AA10 subfamily, confirming its correct genomic assignment. A visual inspection of the structural alignment with the top ten hits helped to further refine the assignment to the *subcluster 2* described by Vaaje-Kolstad *et al*. (46), which includes members that display substrate promiscuity for either chitin or cellulose. The match with the highest score (Z score: 27.2, r.m.s.d.: 1.8 Å) was Tma12, a putative AA10 LPMO from the fern *Tectaria macrodonta* (PDB ID: 6IF7; sequence identity: 33.3%). Tma12 has been proven to shield its host from predators by exerting an entomotoxic activity (49). Their structural superposition reveals a possible site for *As*LMPO10B *O*-linked glycosylation at Thr166, matching the *N*-linked glycosylation of Tma12 at Asn158. A PEG molecule modeled in close proximity of Thr166 partially superposes with the polar groups of the *N*-linked glycan decorating Tma12, further supports the hypothesis of *O*-glycosylation.

While carrying the distinctive loop 2 (L2) structural element of cluster 2, the AA10 module of *As*LPMO10B shows several matches to elements from cluster 4, which groups together LPMOs of viral origin. Among them is fusolin from insect poxviruses (PDB ID: 4YN2 (50)) which has 35.5% sequence identity to *As*LPMO10B and therefore was used as a model for solving the structure (see *Materials and methods*). Their structural alignment (r.m.s.d.: 1.5 Å) shows the conservation of a tryptophan residue on the far edge of L2 (Trp46, Fig. 8D). The tryptophan is oriented parallel to the substrate binding surface and is positioned similar to the tyrosine residue essential for catalysis in the cellulolytic *Lentinus similis* LPMO9A (Tyr203). In *Ls*LPMO9A, Tyr203 is carried by the long C-terminal loop (LC), absent in both *As*LPMO10B and fusolin, and it provides a stacking interaction with the cellulose substrate (Fig. 8D; (PDB ID: 5ACI)(51)). Quite interestingly, LPMOs which possess both the C-terminal loop and L2, as the *Thermoascus aurantiacus* GH61 isozyme A (PDB ID: 2YET)(52), carry aromatic amino acids on both, at the position occupied by Trp46 in *As*LPMO10B and Tyr203 in fusolin (Fig. 8D).

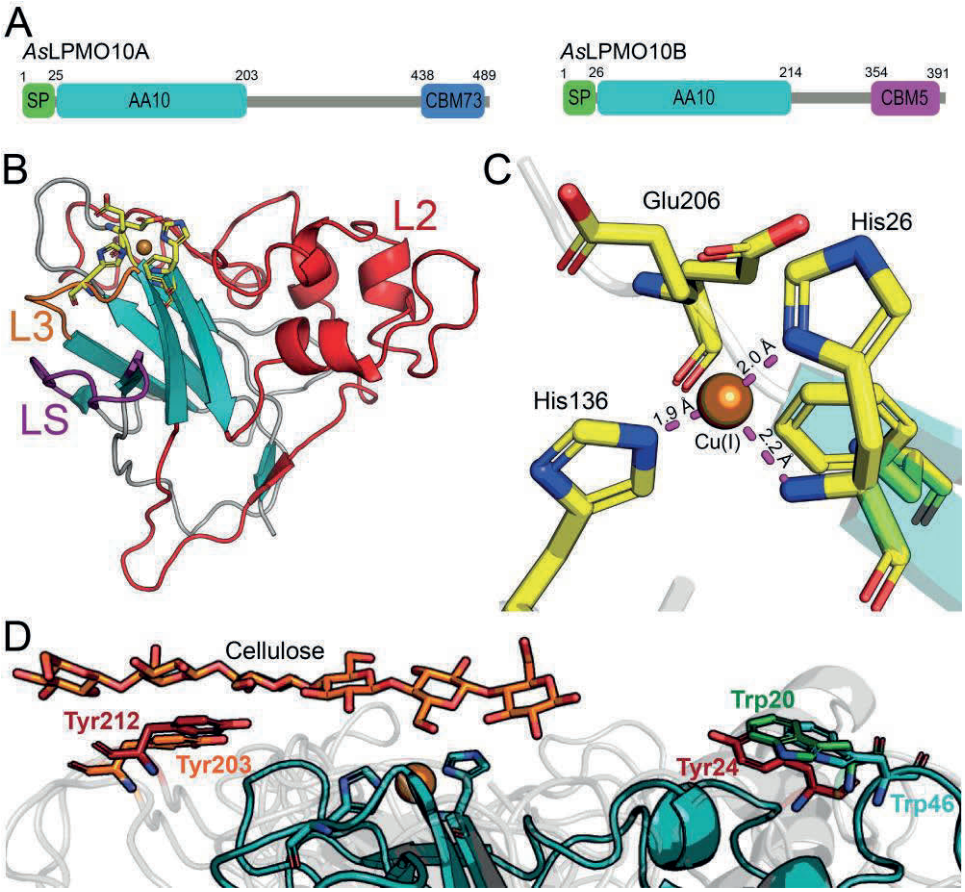

Figure 8. X-ray crystal structure of the *As*LPMO10B AA10 LPMO domain. (A) Domain architecture of *As*LPMO10A and -B. Domain boundaries are indicated by amino acid sequence numbers. SP indicates signal peptide. CBM indicates carbohydrate binding domain family. (B) Cartoon representation of the crystal structure, with the topology assigned as described by Vaaje-Kolstad *et al*. (46). The loop short (LS, purple), loop 2 (L2, red), loop 3 (L3, orange) and active site residues (yellow) are indicated by different colors and labeled. (C) Active site of *As*LPMO10B, domain 1. The copper ion (bronze) is coordinated by the N-terminus, the side chain Nδ1 of His26 and the side chain Nε1 of His136, forming the so-called histidine brace motif (distance to copper indicated). In the AA10 family, a phenylalanine residue (Phe208) replaces the tyrosine residue found in many other LPMOs, which provides a loose axial coordination for the copper ion. Glu206 was refined in two alternative conformations. In other LPMOs, this residue is often replaced by a glutamine residue. (D) Conservation of substrate-docking aromatic amino acids among LPMOs. Loop-2 Trp46 from *As*LPMO10B (teal) is conserved in the viral LPMO fusolin (Trp20; green), a close structural homolog (PDB ID: 4YN2). Their placement mimics Tyr203 (orange), a substrate-binding residue found on the long C-terminal loop (LC) in *Lentinus similis* LPMO 9A (PDB ID: 5ACI). LPMOs that carry both LC and L2 loops bear aromatic amino acids matching the position of both Trp46 and Tyr203 (*e.g.* Tyr24 and Tyr212 on

Thermoascus aurantiacus GH61 isozyme A, PDB ID: 2YET). The structures of the three proteins were aligned by secondary structure matching (SSM).

Discussion

To gain insight into the potential roles of chitinolytic enzymes in virulence, the current study set out to elucidate the putative immune evasive properties of *As*LPMO10A and *As*LPMO10B in the pathogenesis of *Al. salmonicida* in Atlantic salmon. Given the putative role of LPMOs in mucin binding and attachment of bacteria to mucosal surfaces (31, 53), we hypothesized that *As*LPMO10A and -B could be harnessed in the initial phase of binding to, and penetration of, the host outer barrier. The fact that the *A. salmonicida* LPMOs are chitin degrading enzymes (34), combined with the proposed presence of chitin in Atlantic salmon scales (54, 55) gave additional points of relevance to the hypothesis. A challenge model able to probe all phases of pathogenesis was therefore chosen, namely an immersion challenge where the Atlantic salmon smolts were exposed to *Al. salmonicida* in the aqueous environment. Considering that rapid disease development and high mortality may mask potential differences between groups, the infection dose selected was aimed to establish chronic septicemia without exhaustive killing. Our results indicated that neither of the LPMOs are critical for *Al. salmonicida* in passing the outer barrier since all fish were positive for the presence of *Al. salmonicida* wild type and deletion variants after 10 minutes in the challenge bath, and no significant difference between the groups was observed (Fig. 3C). On the other hand, the LPMOs were found to be important for the invasive phase of CWV. Particularly *As*LPMO10B showed a significantly lower bacterial burden in blood, spleen and liver compared to the wild type strain 8 days post challenge (Figs. 4 and 5). Similar observations have been made for the opportunistic pathogen *Listeria monocytogenes,* where a LPMO deletion strain was attenuated in the spleen and liver three days post systemic infection in mice (25). The *P. aeruginosa* LPMO (so called CbpD) was found to be important for pathogenesis of *P. aeruginosa* over the course of systemic infection via attenuation of the terminal complement pathway (30). Neither *As*LPMO10A or -B are especially similar to CbpD (25.6 and 28.4 % sequence identity, respectively), but *As*LPMO10A contains an N-terminal family AA10 LPMO domain and a C-terminal family CBM73 chitin binding domain similar to CbpD (Fig. 8A). Moreover, we note the structural similarity of the *As*LPMO10B AA10 domain with the chitin-active AA10-domain of viral fusolin, which strongly enhances the infectivity of entomopoxviruses (50, 56, 57) and that represents an LPMO domain serving to enhance the virulence of a pathogen.

An interesting trait of *Al. salmonicida* is its possession of two distinctly different LPMOs. Several other pathogens also share this trait, but many also only carry a single LPMO in their genome (Fig. 1), including *P. aeruginosa* for which the LPMO clearly is a virulence factor (30). Can it be that the two LPMOs have different functions? Both *Al. salmonicida* LPMOs cleave chitin chains by oxidation and contribute to chitin catabolism (34), but *As*LPMO10A is expressed at high abundance and independent on growth medium, and have shown a slightly higher rate of chitin oxidation compared to *As*LPMO10B (34). In the context of the slightly different phenotypes observed for the *As*LPMO10A and-B deletion variants in this

study, it is not unlikely that these LPMOs play different roles in *Al. salmonicida* pathogenesis.

Deletion of LPMOs resulted in an altered proteome response compared to the wild type, in the presence and absence of Atlantic salmon serum (Fig. 2). Intriguingly, the ΔB and ΔAB strains showed a remarkably higher number of significantly regulated proteins in the presence of the serum compared to the absence of the latter (Fig. 2, panel A). Moreover, general regulation of stress response related proteins, chemotaxis related proteins (ΔA strain), and up-regulation of LuxI in the ΔA and ΔAB strains are intriguing observations (Fig. 2, panel C). The latter protein, LuxI, is important for the regulation of motility and biofilm formation (58). It should be noted that a substantial proteome alteration was also observed for the *P. aeruginosa* LPMO deletion strain when exposed to human serum (compared to the wild type; (30)), indicating the struggle of the pathogens to interfere with host immune responses when lacking the LPMO(s).

In conclusion, we have shown that the LPMOs of *Al. salmonicida* are moonlighting enzymes that not only contribute in chitin catabolism (34), but also play a role in the pathogenicity of the bacterium in the invasive phase of CWV in Atlantic salmon. Many LPMOs and chitinases of opportunistic pathogens have been shown to depolymerize chitin and also to contribute to chitin catabolism of the bacterium (59, 60). Therefore, it is likely that chitinolytic enzymes not merely have functions for acquisition of nutrients, but also for protection of the bacteria towards host defense mechanisms.

Materials and methods

Bacterial strains

Al. salmonicida strain LFI1238 originally isolated from the head kidney of an Atlantic cod that died from CWV, and derivative mutant strains (Table 1) were routinely cultivated at 12 °C in liquid Luria Broth (LB) supplemented with 2.5% sodium chloride (LB25; 10 g/L tryptone, 5 g/L yeast extract, 12.5 g/L NaCl) or solid LB25 supplemented with 15 g/L agar powder (LA25). In-Frame deletion of *AsLPMO10A*, *AsLPMO10B* and *AsLPMO10A△10B* and genes in strain LFI1238 were described in our previous study (34).

Table 1. List of bacterial strains.

Strain	Description	Ref.
LFI1238	*Aliivibrio salmonicida* strain LFI1238	§
*As*ΔLPMO10A	LFI1238 containing gene deletion *ΔLPMO10A*	*
*As*ΔLPMO10B	LFI1238 containing gene deletion *ΔLPMO10B*	*
*As*ΔLPMO10A/Δ10B	LFI1238 containing gene deletions *ΔLPMO10A* and *ΔLPMO10B*	*

§Originally isolated by the Norwegian Institute of Fisheries and Aquaculture Research, N-9291 Tromsø, Norway, but provided by Simen Foyn Nørstebø for this study.
*(34)

Atlantic salmon challenge

Housing and ethical statement. Atlantic salmon (*Salmo salar* L.) challenge experiments were designed according to the «Norwegian Regulation on Animal Experimentation» (regulation as of June 2015, nr 781), which was approved by The Norwegian Research Animal Authorities (FOTS ID: 16416). All experiments were carried out at the Norwegian Institute for Water Research (NIVA, Solbergstrand, Norway). Fish were monitored daily and upon showing clinical signs of disease during the experimental period were collected and euthanized by an overdose of Benzoak® (ACD Pharmacuticals As, Leknes, Norway).

Challenge procedures. The challenge involved 1340 unvaccinated Atlantic salmon parr (average weight 60 g), which were obtained from Center for Fish Research, Department of Animal and Aquacultural Sciences, NMBU. Fish were transported according to the Norwegian Regulations on transport of Aquatic Animals and allocated in their designed experimental groups. Ahead of the immersion challenges, parr-smolt transformation was induced by gradually increasing the salinity of the tank water from 12 to 33 ppm over a period of 11 days, followed by one-week acclimation at 33 ppm. Fish were kept in separate tanks (1400 L) with flow-through of sea water from the Oslofjord (45-50 meters depth). The average temperature and salinity of intake water was 9.9 °C and 33.5 ppm respectively. The fish were fed a rate corresponding 1 % of the biomass.

The challenge was carried out using 1260 animals randomly divided into 4 experimental groups of 295 fish and one control group (80 fish). The control group was mock challenged with Luria Broth supplemented with 3 % NaCl (LB3). The water level was first lowered to 350-400 L. Water intake was temporarily stopped, and ~4 L cultures of wild type *Al. salmonicida* LFI1238 or LPMO gene deletion strains ΔAsLPMO10A, ΔLPMO10B and ΔAsLPMO10AΔLPMO10B were added directly to the fish tanks. After 30 min the water intake was re-opened and increased to 700 L/h. Water samples were collected before re-opening the water intake. Five to ten live fish from each experimental group were sampled from 10 min into the challenge bath and up to 19 days post challenge. The smolts were monitored for 36 days.

Obtaining blood samples from infected fish. For collection of blood samples, fish were anesthetized in a water bath containing Benzoak Vet (ACD Pharmaceuticals AS). Blood was sampled from the caudal vein using the VACUETTE® system and VACUETTE® 4 mL NH Sodium Heparin tubes (Greiner bio-one), 100 and 10 µl of sampled blood was immediately spread onto LA25 in duplicates and incubated at 12 °C 3-5 days**.**

Evaluation of bacterial burden in tissues and organs. The bacterial burden was monitored by collection of bacteriological samples up to 19 days post challenge. Samples were collected from skin, gills, spleen, liver and head kidney by using 1 µl sterile disposable inoculation loops (Sarstedt) and patching on LA25 in the following order; midline of skin, outermost lamella of gills, dissection and puncture of spleen, liver and head kidney. Plates were incubated 4-5 days at 12 °C.

Tissue samples. Tissue intended for RNA isolation was dissected using sterile scalpels and disposable forceps (VWR International), washed twice in Dulbecco's Phosphate Buffered Saline (PBS, Sigma-Aldritch) and transferred to 15 mL Falcon tubes containing 1-2 mL of protect® Bacteria Reagent (Qiagen). For determination of CFU/mg, the samples were transferred to 2 mL FastPrep® tubes (MP Biomedicals) pre-prepared with 100 µl sterile 1.4 mm ceramic beads (OMNI International) and 200 µl PBS. The tubes were weighed before and after sampling, homogenized by using FastPrep (MP Biomedicals), 4 ms, 3 x 5 seconds. Volumes of 100 and 10 µl were spread onto LA25 in duplicates and incubated at 12 ˚C for 3-5 days before calculation of colony forming units/ (mg organ) (CFU/mg).
Necroscopy. Euthanized and deceased fish were autopsied to determine the cause of death. External and internal signs were examined, and bacterial samples taken from the head kidney, liver and spleen unless otherwise stated. The bacteriological samples were taken by puncturing the organs with 1 µl sterile disposable inoculation loops (Sarstedt) and streaking onto LA25. *Al. salmonicida* was recovered from the head kidney, spleen and liver, in bacteriological samples taken during necroscopy. Culture results were evaluated together with pathological changes such as external and internal hemorrhages, fluid in cavity, discolored liver and swollen spleen.

RNA isolation, reverse transcription and real-time PCR. Spleen samples obtained from infected/mock infected Atlantic salmon were supplemented with RNAprotect and kept at -80 C. To isolate RNA, the samples were thawed on ice, was decanted, and the tissue transferred to 2 mL FastPrep® tubes (MP Biomedicals) containing 200 µl sterile 1.4 mm ceramic beeds and 1 mL ice cold TRIzol® Reagent (Ambion life technologies). The tissues were homogenized using FastPrep (MP Biomedicals) at 4 m/s 3x10 seconds, followed by 5 min incubation at RT and addition of 200 µl chloroform (EMSURE® EMD Millipore). The samples were shaken by hand for 15 seconds and incubated 2-3 min at room temperature before centrifugation at 12000xg for 15 min at 4 °C. Next, 400 µl of the aqueous phase was transferred to 1.5 mL RNase-free microfuge tubes (Ambion) and mixed with equal amounts of 70 % ethanol. The solution was transferred to an RNAeasy spin column (Qiagen) and the RNA extracted according to the manufacturer's protocol. The genomic DNA (gDNA) was removed by the Heat&Run gDNA removal kit (ArcticZymes®) according to the manufacturer's instruction. Copy DNA (cDNA) synthesis was performed using iScript™ Reverse Transcription Super mix (Bio-Rad). A no reverse transcriptase control was included in the analysis. The RT-qPCR was run in 96 well plates (BIO-RAD) in a CFX96 Touch™ Real-Time PCR Detection System (BIO-RAD) using iTaq Universal SYBR Green super mix according to the manufacturer's protocol (BIO-RAD) using relevant primers (Table 3). Polymerase activation and DNA denaturation for 30 seconds at 95 °C was followed by 40 cycles of 5 sec denaturation at 95 °C, annealing/extension and plate read at 60 °C for 30 seconds. Melt curve analysis was performed from 65 °C-95 °C, with 0.5 °C increases.

Real time data analysis / gene expression analysis. Host gene expression of selected immune parameters/immune genes was assessed by ΔΔCq analysis of RT-qPCR data (61). Normalization factors for each sample was determined by calculating the geometric mean of house-keeping/reference genes β-actin and

$EF1A_A$ (62). For each gene assessed, all individual Cq values were transformed to quantities and normalized against the normalization factor of the sample. Gene expression data are shown as fold change (± standard error of the mean, SEM) relative to the control group (5 fish sampled 10 dpc).

Table 2. primers applied for gene expression analysis by RT-qPCR

Description	Primers	Sequence 5'- 3'	Ref.
β-actin (BG933897.1)	β-actin-F β-actin-R	CCAAAGCCAACAGGGAGAAG AGGGACAACACTGCCTGGAT	(62)
Elongation factor 1Aa (AF321836.1)	EF1A-F EF1A-R	CCCCTCCAGGACGTTTACAAA CACACGGCCCACAGGTACA	(62)
Complement component 5-2 (CA364804)	C5-F C5-R	AGAACTCTTCCGAGTTGGCATGGT AGTGATGCTGGGATCCATCTCTGA	(63)
Complement component 3 (XM_014186867.1)	C3-F C3-R	TCCCTGGTGGTCACCAGTACAC ATGATGGTGGACTGTGTGGATC	(64)
Tumor necrosis factor α (NM_001123589.1)	TNFα-F TNFα-R	AGGTTGGCTATGGAGGCTGT TCTGCTTCAATGTATGGTGGG	(65)
Interleukin 1-β (AY617117.1)	IL-1β-F IL-1β-R	GCTGGAGAGTGCTGTGGAAGA TGCTTCCCTCCTGCTCGTAG	(65)

Proteomics. Starter cultures of wild type, ΔA, ΔB and ΔAB were grown in LB25, in triplicate, for 48 hours at 10 °C with shaking. Next, the cultures were diluted in LB25 to an OD600 of 0.1 and grown until they reached early logarithmic phase (OD_{600nm} = 0.4-0.5). After reaching early logarithmic phase, the cultures were split in two and incubated for 1 hour in the absence or presence of 1% Atlantic salmon serum (SS). Thereafter, 1 mM beta-glycerophosphate (Sigma), 1 mM sodium orthovanadate (Sigma), 20 mM sodium pyrophosphate (Sigma), 1mM phenylmethylsulfonyl fluoride (PMSF, Sigma), and 1× Complete Mini EDTA-free protease inhibitors (Roche) were added to the samples. The bacterial pellets and supernatants were separated by centrifugation (4500 × *g*, 15 min, 4 °C). The pellets were washed once with PBS and centrifuged, before being resuspended in lysis buffer containing 20 mM Tris-HCl (pH 7.5), 0.1 M NaCl, 1 mM EDTA, 1× Complete Mini EDTA-free protease inhibitors, and lysozyme (0.5 $mg \cdot ml^{-1}$). Cells were disrupted by sonication (20×, 5 s off-5 s on, 26% amp), and the cellular debris was cleared by centrifugation (4500 × g, 30 min, 4 °C).

The protein samples were boiled in NuPAGE LDS sample buffer and 30 mM dithiothreitol (DTT) for 5 min before being loaded onto Mini-PROTEAN® TGX Stain- Free™ Gels (Bio-Rad laboratories, Hercules, CA, USA). The gels were run at 200 V for 5-10 min using the BIO-RAD Mini-PROTEAN® Tetra System. The gels were stained with Coomassie brilliant blue R250 and cut into small gel pieces, which were transferred to 2 mL LoBind tubes. The gel pieces were washed in 200 µL of water for 15 min and decoloured by 200 µL 50 % acetonitrile (ACN), 25 mM ammonium bicarbonate (AmBic) at room temperature (RT) for 15 min. Decolouring

was performed twice. After washing and decolouring, the gel bits were left to shrink and dehydrate for 5 min in 100 µL 100 % ACN. In order to reduce and alkylate the proteins, the gel pieces were first incubated for 30 min at 56 °C in a solution containing 10 mM DTT and 100 mM AmBic, and then with 55 mM iodo-acetamide and 100mM AmBic for 30 min at RT. Thereafter, the gel pieces were dehydrated using 100 % ACN and digested overnight at 37 °C in a solution containing 0.3 µg of trypsin. The next day, the digestion was stopped by adding 70 µL 0.5 % trifluoroacetic acid (TFA). For peptide extraction, the gel pieces were sonicated for 10 min and afterwards centrifuged (16 000 × *g*, 5 min). The supernatants were then transferred to the StageTips for desalting. This procedure was repeated once more, however for the second round the gel pieces were added 70 µL 0.1 % TFA before sonication.

For desalting and cleaning up the extracted peptides, StageTips were used. These were made accordingly: Using an 18 g blunt-ended needle, two pieces of Empore C18 membrane (6683-U, Sigma) were cut out. By a length of 1/32" peeksil capillary or equivalent, the membrane pieces were pushed firmly into a 200 µl pipette tip. The StageTips were mounted onto LoBind tubes, by a hole in the lids, which were cut out beforehand (66). The tips were activated by transferring 50 µL of methanol to the tips. Afterwards, the tubes were centrifuged (2500 × *g*, 5 min), and the flowthrough was discarded. For equilibration, 100 µL of 0.1 % TFA were added and centrifuged as before. The flowthrough was discarded, and the peptide solution was loaded into the tips after sonication, as described in the previous section. 100 µL of 0.1 % TFA were added, centrifuged as earlier, and the flowthrough removed. For eluting the peptides, 50 µL of a solution containing 80 % ACN and 0.1 % TFA were added and centrifuged as above. The peptides were evaporated using a SpeedVac system until dryness. Afterwards, the peptides were redissolved in 12 µL of a solution containing 0.05 % TFA and 2 % ACN.

The peptides were separated by a nano UPLC (nanoElute, Bruker) operating a C18 reverse-phase column, using a pre-installed program with a 120 min gradient, and analyzed by a trapped ion mobility spectrometry and a quadrupole time of flight mass spectrometer (timsTOF Pro, Bruker). 200 ng of each sample was loaded into the UPLC MS/MS system. The raw files were processed with MaxQuant (version 1.6.17.0) for label-free quantification (LFQ) and searched against the UniProt *Al. salmonicida* proteome: UP000001730. The digestion mode was set to specific with Trypsin/P as the digestive enzyme, and a maximum of two missed cleavages were allowed. "Match between runs" was applied using default parameters and the peptides were filtered with a 1 % level false discovery rate (FDRs) using a revert decoy database. Carbamidomethylation of cysteines were included in the search as a fixed modification, while protein N-terminal acetylation, oxidation of methionines and deamidation of glutamines were included as variable modifications. For data analysis Perseus version 1.6.15.0 was used, and the quantitate values were $\log_2$ transformed. Valid values were filtered with minimum 2 values in each group for each of the comparisons, and missing values were imputed. Significantly up- or downregulated proteins were determined by performing Student's *t*-test (p = 0.05). For the volcano plots, differentially expressed proteins were defined by having p-values of ≤ 0.05 ($\log_{10}$ = 1.3) and log2 fold change >1.5 ($\log_2$ = 0.58).

Protein production and purification

The AA10 domain of *As*LPMO10B was subcloned in the pNIC expression vector by adding a stop codon directly after the codon representing amino acid 217 (D217) in the original *As*LPMO10B expression construct described in (34). Expression and periplasmic extraction of the protein was performed identically to the protocol described in (34). The protein was purified using a three-step method with chilled buffers and columns or at 4°C. First, the periplasmic extract was adjusted to the IEX running buffer (20 mM MES pH 5.5, 0.1 mM EDTA) and loaded onto an equilibrated 5 mL HiTrap Q FF column (Cytiva) with a flow rate of 6 mL/min. After unbound protein had passed the column, the bound protein was eluted by applying a linear gradient to 500 mM NaCl in 250 mL. Fractions containing *As*LPMO10B were collected, adjusted to the HIC running buffer (1 M $(NH_4)_2SO_4$, 20 mM Tris-HCl pH 8.0, 0.1 mM EDTA) and further purified using an equilibrated 5 mL HiTrap Phenyl FF (HS) column. The protein was loaded at 3 mL/min. After unbound protein had passed, the bound protein was eluted by applying a 200 mL linear gradient to 0 M $(NH_4)_2SO_4$. The fractions containing *As*LPMO10B were collected and concentrated using an Amicon Ultra-15 Centrifugal Filter Unit with a 10 kDa cutoff (Milipore). Finally, 1.5 mL of the concentrated eluate was run through a Superdex 75 120 mL SEC column (Cytiva) using 20 mM Tris-HCl pH 8.0, 150 mM NaCl, 0.1mM EDTA as running buffer. Pure AsLPMO10B was collected, concentrated and stored at 4°C until further use.

Protein crystallization, X-ray structure determination and refinement

The *As*LPMO10B AA10 domain was crystallized by the vapor diffusion hanging-drop method. Before setting up crystallization trials, the protein was saturated with Cu(II) by adding a 3-fold molar excess of $CuSO_4$ after adding 1 mM CaCl2 (to saturate EDTA in the buffer). Excess copper was removed with a HiTrap desalting 5 mL column (GE Life Sciences). The buffer was exchanged to 5 mM Tris-HCl pH 8.0 and subsequently concentrated to 30 mg/mL using Vivaspin 20 (10-kDa molecular weight cutoff) centrifugal concentrators (Sartorius Stedim Biotech GmbH). The concentrated protein was stored at 4 °C until use. Crystallization cocktails were prepared in a pre-greased 48-well VDX plate (Hampton Research) and mixed on silanized coverslips with the protein solution in a 1:1 volume ratio. Diffraction-quality crystals grew after 30-60 min incubation at 20°C, from a reservoir solution containing 0.1 M Na-phosphate/citrate pH 4.2 and 40 % PEG 300. Crystals were cryoprotected by complementing the crystallization solution with 25% glucose, flash-cooled in liquid nitrogen and stored in a CX-100 Taylor-Wharton dry shipper for synchrotron data collection.

Diffraction data were collected at the MAX-IV synchrotron (Lund, Sweden), on the BioMAX beamline (67) (Dectris EIGER16M Hybrid-pixel detector) (68). Data collection was carried out at 100K, at a wavelength of 0.9763 Å, covering a total oscillation range of 360° with 0.1° oscillations. Diffraction data were integrated, merged and truncated using the EDNA (69) software pipeline, and the integration and scaling output was reindexed using REINDEX, a component of the CCP4 crystallography software suite (70). Crystals belong to space group $P6_5$, with unit cell parameters a = 71.1 Å, b = 71.1 Å, c = 100.3 Å and one molecule in the asymmetric unit. Data collection and scaling statistics are reported in Table S1. The structure was solved by molecular replacement using the program PHASER

(71), from the CCP4 suite. The structure of *Wiseana spp. entomopoxivirus* fusolin (PDB ID: 4YN2 (50)) served as search model (35.5% sequence identity). The search model was edited, removing alternative conformations for all residues using the CCP4 tool PDBCUR, and truncating mismatching portions with SCULPTOR. Refinement was carried out using data to 1.35 Å, alternating between cycles of real-space refinement using Coot (72) and maximum likelihood refinement against anomalous data with REFMAC5 (73). The molecular replacement output was examined and improved by first removing ill-defined side chains and loops, then adding missing structural elements in a step-wise fashion as the quality of the electron density map improved. After improving the protein main chain, water molecules were added based on compatible electron density and hydrogen-bonding interactions. A peak in the phased anomalous difference map confirmed the presence of copper bound in the center of the histidine brace motif. Toward the end of the refinement process, missing side chains or alternative conformations were built, and their relative occupancies refined with PHENIX.refine (74). As the last step, the very high data-to-parameter ratio (~32) allowed to perform full anisotropic B-factor refinement, including ligands and water molecules. The coordinates and structure factors were deposited in the PDB (75) with PDB ID: 7OKR.

Acknowledgements
This work was supported by grants from the Research Council of Norway (grants no 249865 to GV-K, 272201 to UK). We would like to thank Bjørn-Reidar Hansen at the Center for Fish Research, Department of Animal and Aquacultural Sciences, NMBU, for assistance with obtaining and transporting the Atlantic salmon parr and for providing Atlantic salmon serum. We would also like to than the NIVA Research Facility at Solbergstrand for facilitating the challenge experiment, Camilla Skagen-Sandvik, Thea Os Andersen and Amanda Kristine Votvik for assistance in fish sampling and Morten Skaugen for assistance given in the proteomics experiment. Finally, we acknowledge services provided by the UiO Structural Biology Core Facilities. X-ray data were collected at the BioMAX beamline at the MAX IV, Lund, Sweden. We are grateful to local contact Ana Gonzales for providing assistance in using the BioMAX beamline.

Author contributions
A.S. Planned and conducted the challenge experiment, RT-qPCR analysis and analyzed all data. J.S.M.L produced, purified and crystallized *As*LPMO10B. P.K.T.E. performed proteomics experiments and analysis. H.S. planned and supervised the challenge experiment and analyzed data. F.A. planned and supervised experiments and analyzed data. G.V-K. Conceptualized, planned and supervised the study and analyzed data. K.D.L., G.C. and U.K. performed structural analysis. All authors and wrote and revised the manuscript.

References

1. Egidius E, Wiik R, Andersen K, Hoff KA, Hjeltnes B. 1986. *Vibrio salmonicida Sp*-Nov, a New Fish Pathogen. Int J Syst Bacteriol 36:518-520.
2. Schrøder MB, Espelid S, Jørgensen TØ. 1992. Two serotype of *Vibrio salmonicida* isolated from diseased cod (*Gadus morhua* L.); virulence, immunological studies and advanced experiments. Fish Shellfish Immunol 2.
3. Egidius E, Andersen K, Clausen E, Raa J. 1981. Cold-water vibriosis or 'Hitra disease' in Norwegian salmonid farming. J Fish Dis 4:353-354.
4. Poppe TT, Håstein T, Salte R. 1985. "Hitra Disease" (Haemorrhagic Syndrome) in Norwegian Salmon Farming: Present Status, Fish Shellfish Pathol.
5. Kashulin A, Sørum H. 2014. A novel in vivo model for rapid evaluation of *Aliivibrio salmonicida* infectivity in Atlantic salmon. Aquaculture 420–421:112-118.
6. Totland GK, Nylund A, Holm KO. 1988. An ultrastructural study of morphological changes in Atlantic salmon, *Salmo salar* L., during the development of cold water vibriosis. J Fish Dis 11:1-13.
7. Bjelland AM, Johansen R, Brudal E, Hansen H, Winther-Larsen HC, Sørum H. 2012. Vibrio salmonicida pathogenesis analyzed by experimental challenge of Atlantic salmon (Salmo salar). Microbial Pathogenesis 52:77-84.
8. Bjelland A, Fauske AK, Nguyen A, Orlien I, Østgaard I, Sørum H. 2013. Expression of *Vibrio salmonicida* virulence genes and immune response parameters in experimentally challenged Atlantic salmon (*Salmo salar* L.). Front Microbiol 4.
9. Bjelland AM, Sørum H, Tegegne DA, Winther-Larsen HC, Willassen NP, Hansen H. 2012. LitR of *Vibrio salmonicida* Is a Salinity-Sensitive Quorum-Sensing Regulator of Phenotypes Involved in Host Interactions and Virulence. Infect Immun 80:1681-1689.
10. Norstebo SF, Lotherington L, Landsverk M, Bjelland AM, Sorum H. 2018. *Aliivibrio salmonicida* requires O-antigen for virulence in Atlantic salmon (*Salmo salar L.*). Microb Pathog 124:322-331.
11. Nørstebo SF, Paulshus E, Bjelland AM, Sørum H. 2017. A unique role of flagellar function in *Aliivibrio salmonicida* pathogenicity not related to bacterial motility in aquatic environments. Microb Pathog 109:263-273.
12. Nelson EJ, Tunsjø HS, Fidopiastis PM, Sørum H, Ruby EG. 2007. A Novel *lux* Operon in the Cryptically Bioluminescent Fish Pathogen *Vibrio salmonicida* Is Associated with Virulence. Appl Environ Microbiol 73:1825-1833.
13. Lombard V, Golaconda Ramulu H, Drula E, Coutinho PM, Henrissat B. 2014. The carbohydrate-active enzymes database (CAZy) in 2013. Nucleic Acids Res 42:D490-5.
14. Zhou X, Zhu H. 2020. Current understanding of substrate specificity and regioselectivity of LPMOs. Bioresour 7:11.
15. Eijsink VGH, Petrovic D, Forsberg Z, Mekasha S, Røhr ÅK, Várnai A, Bissaro B, Vaaje-Kolstad G. 2019. On the functional characterization of lytic polysaccharide monooxygenases (LPMOs). Biotechnol Biofuels 12:58.
16. Oyeleye A, Normi YM. 2018. Chitinase: diversity, limitations, and trends in engineering for suitable applications. Biosci Rep 38:BSR2018032300.
17. Nakagawa YS, Kudo M, Loose JS, Ishikawa T, Totani K, Eijsink VG, Vaaje-Kolstad G. 2015. A small lytic polysaccharide monooxygenase from *Streptomyces griseus* targeting alpha- and beta-chitin. Febs j 282:1065-79.
18. Vaaje-Kolstad G, Westereng B, Horn SJ, Liu Z, Zhai H, Sørlie M, Eijsink VGH. 2010. An oxidative enzyme boosting the enzymatic conversion of recalcitrant polysaccharides. Science 330:219-222.
19. Bissaro B, Røhr ÅK, Müller G, Chylenski P, Skaugen M, Forsberg Z, Horn SJ, Vaaje-Kolstad G, Eijsink VGH. 2017. Oxidative cleavage of polysaccharides by monocopper enzymes depends on H2O2. Nat Chem Biol 13:1123-1128.

20. Forsberg Z, Nelson CE, Dalhus B, Mekasha S, Loose JSM, Crouch LI, Røhr ÅK, Gardner JG, Eijsink VGH, Vaaje-Kolstad G. 2016. Structural and Functional Analysis of a Lytic Polysaccharide Monooxygenase Important for Efficient Utilization of Chitin in *Cellvibrio japonicus*. J Biol Chem 291:7300-7312.
21. Vaaje-Kolstad G, Horn SJ, van Aalten DM, Synstad B, Eijsink VG. 2005. The non-catalytic chitin-binding protein CBP21 from *Serratia marcescens i*s essential for chitin degradation. J Biol Chem 280:28492-7.
22. Frederiksen RF, Paspaliari DK, Larsen T, Storgaard BG, Larsen MH, Ingmer H, Palcic MM, Leisner JJ. 2013. Bacterial chitinases and chitin-binding proteins as virulence factors. Microbiology 159:833-47.
23. Wong E, Vaaje-Kolstad G, Ghosh A, Hurtado-Guerrero R, Konarev PV, Ibrahim AFM, Svergun DI, Eijsink VGH, Chatterjee NS, van Aalten DMF. 2012. The *Vibrio cholerae* colonization factor GbpA possesses a modular structure that governs binding to different host surfaces. PLoS Path 8:e1002373-e1002373.
24. Kirn TJ, Jude BA, Taylor RK. 2005. A colonization factor links *Vibrio cholerae* environmental survival and human infection. Nature 438:863-6.
25. Chaudhuri S, Bruno JC, Alonzo F, 3rd, Xayarath B, Cianciotto NP, Freitag NE. 2010. Contribution of chitinases to *Listeria monocytogenes* pathogenesis. Appl Environ Microbiol 76:7302-7305.
26. Dishaw LJ, Giacomelli S, Melillo D, Zucchetti I, Haire RN, Natale L, Russo NA, De Santis R, Litman GW, Pinto MR. 2011. A role for variable region-containing chitin-binding proteins (VCBPs) in host gut–bacteria interactions. PNAS 108:16747-16752.
27. Mondal M, Nag D, Koley H, Saha DR, Chatterjee NS. 2014. The *Vibrio cholerae* extracellular chitinase ChiA2 is important for survival and pathogenesis in the host intestine. PLoS One 9:e103119.
28. Agostoni M, Hangasky JA, Marletta MA. 2017. Physiological and Molecular Understanding of Bacterial Polysaccharide Monooxygenases. Microbiol Mol Biol Rev 81:e00015-17.
29. Lee CG, Silva CAD, Cruz CSD, Ahangari F, Ma B, Kang M-J, He C-H, Takyar S, Elias JA. 2011. Role of Chitin and Chitinase/Chitinase-Like Proteins in Inflammation, Tissue Remodeling, and Injury. Annu Rev Physiol 73:479-501.
30. Askarian F, Uchiyama S, Masson H, Sørensen HV, Golten O, Bunæs AC, Mekasha S, Røhr ÅK, Kommedal E, Ludviksen JA, Arntzen MØ, Schmidt B, Zurich RH, van Sorge NM, Eijsink VGH, Krengel U, Mollnes TE, Lewis NE, Nizet V, Vaaje-Kolstad G. 2021. The lytic polysaccharide monooxygenase CbpD promotes *Pseudomonas aeruginosa* virulence in systemic infection. Nat Commun 12:1230.
31. Bhowmick R, Ghosal A, Das B, Koley H, Saha DR, Ganguly S, Nandy RK, Bhadra RK, Chatterjee NS. 2008. Intestinal adherence of *Vibrio cholerae* involves a coordinated interaction between colonization factor GbpA and mucin. Infect Immun 76:4968-4977.
32. DebRoy S, Dao J, Söderberg M, Rossier O, Cianciotto NP. 2006. *Legionella pneumophila* type II secretome reveals unique exoproteins and a chitinase that promotes bacterial persistence in the lung. PNAS 103:19146-19151.
33. Rehman S, Grigoryeva LS, Richardson KH, Corsini P, White RC, Shaw R, Portlock TJ, Dorgan B, Zanjani ZS, Fornili A, Cianciotto NP, Garnett JA. 2020. Structure and functional analysis of the *Legionella pneumophila* chitinase ChiA reveals a novel mechanism of metal-dependent mucin degradation. PLoS Path 16:e1008342.
34. Skåne A, Minniti G, Loose JSM, Mekasha S, Bissaro B, Mathiesen G, Arntzen MØ, Vaaje-Kolstad G. 2021. The fish pathogen *Aliivibrio salmonicida* LFI1238 can degrade and metabolize chitin despite major gene loss in the chitinolytic pathway. bioRxiv doi:10.1101/2021.03.24.436902:2021.03.24.436902.

35. Hjerde E, Lorentzen MS, Holden MT, Seeger K, Paulsen S, Bason N, Churcher C, Harris D, Norbertczak H, Quail MA, Sanders S, Thurston S, Parkhill J, Willassen NP, Thomson NR. 2008. The genome sequence of the fish pathogen *Aliivibrio salmonicida* strain LFI1238 shows extensive evidence of gene decay. BMC Genomics 9:616.
36. Austin B, Austin D. 2007. Bacterial Fish Pathogens: Diseases of Farmed and Wild Fish doi:10.1007/978-1-4020-6069-4.
37. Huerta-Cepas J, Serra F, Bork P. 2016. ETE 3: Reconstruction, Analysis, and Visualization of Phylogenomic Data. Mol Biol Evol 33:1635-1638.
38. Guindon S, Dufayard J-F, Lefort V, Anisimova M, Hordijk W, Gascuel O. 2010. New Algorithms and Methods to Estimate Maximum-Likelihood Phylogenies: Assessing the Performance of PhyML 3.0. Syst Biol 59:307-321.
39. Seong IS, Kang MS, Choi MK, Lee JW, Koh OJ, Wang J, Eom SH, Chung CH. 2002. The C-terminal Tails of HslU ATPase Act as a Molecular Switch for Activation of HslV Peptidase J Biol Chem 277:25976-25982.
40. Rashid Y, Kamran Azim M, Saify ZS, Khan KM, Khan R. 2012. Small molecule activators of proteasome-related HslV peptidase. Bioorg Med Chem Lett 22:6089-6094.
41. Stonehouse E, Kovacikova G, Taylor RK, Skorupski K. 2008. Integration host factor positively regulates virulence gene expression in *Vibrio cholerae*. J Bacteriol 190:4736-48.
42. Jeong HS, Kim SM, Lim MS, Kim KS, Choi SH. 2010. Direct Interaction between Quorum-sensing Regulator SmcR and RNA Polymerase Is Mediated by Integration Host Factor to Activate vvpE Encoding Elastase in *Vibrio vulnificus*. J Biol Chem 285:9357-9366.
43. Chaparian RR, Olney SG, Hustmyer CM, Rowe-Magnus DA, van Kessel JC. 2016. Integration host factor and LuxR synergistically bind DNA to coactivate quorum-sensing genes in *Vibrio harveyi*. Mol Microbiol 101:823-840.
44. Pan J, Zhao M, Huang Y, Li J, Liu X, Ren Z, Kan B, Liang W. 2018. Integration Host Factor Modulates the Expression and Function of T6SS2 in *Vibrio fluvialis*. Front Microbiol 9.
45. Salomon D, Klimko JA, Trudgian DC, Kinch LN, Grishin NV, Mirzaei H, Orth K. 2015. Type VI Secretion System Toxins Horizontally Shared between Marine Bacteria. PLOS Pathogens 11:e1005128.
46. Vaaje-Kolstad G, Forsberg Z, Loose JSM, Bissaro B, Eijsink VGH. 2017. Structural diversity of lytic polysaccharide monooxygenases. Curr Opin Struct Biol 44:67-76.
47. Gudmundsson M, Kim S, Wu M, Ishida T, Momeni MH, Vaaje-Kolstad G, Lundberg D, Royant A, Ståhlberg J, Eijsink VGH, Beckham GT, Sandgren M. 2014. Structural and Electronic Snapshots during the Transition from a Cu(II) to Cu(I) Metal Center of a Lytic Polysaccharide Monooxygenase by X-ray Photoreduction. J Biol Chem 289:18782-18792.
48. Holm L. 2020. DALI and the persistence of protein shape. Protein Sci 29:128-140.
49. Yadav SK, Archana, Singh R, Singh PK, Vasudev PG. 2019. Insecticidal fern protein Tma12 is possibly a lytic polysaccharide monooxygenase. Planta 249:1987-1996.
50. Chiu E, Hijnen M, Bunker RD, Boudes M, Rajendran C, Aizel K, Oliéric V, Schulze-Briese C, Mitsuhashi W, Young V. 2015. Structural basis for the enhancement of virulence by viral spindles and their in vivo crystallization. PNAS 112:3973-3978.
51. Frandsen KEH, Simmons TJ, Dupree P, Poulsen J-CN, Hemsworth GR, Ciano L, Johnston EM, Tovborg M, Johansen KS, von Freiesleben P, Marmuse L, Fort S, Cottaz S, Driguez H, Henrissat B, Lenfant N, Tuna F, Baldansuren A, Davies GJ, Lo Leggio L, Walton PH. 2016. The molecular basis of polysaccharide cleavage by lytic polysaccharide monooxygenases. Nat Chem Biol 12:298-303.

52. Quinlan RJ, Sweeney MD, Lo Leggio L, Otten H, Poulsen J-CN, Johansen KS, Krogh KBRM, Jørgensen CI, Tovborg M, Anthonsen A, Tryfona T, Walter CP, Dupree P, Xu F, Davies GJ, Walton PH. 2011. Insights into the oxidative degradation of cellulose by a copper metalloenzyme that exploits biomass components. PNAS 108:15079-15084.
53. Jang KK, Gil SY, Lim JG, Choi SH. 2016. Regulatory Characteristics of *Vibrio vulnificus* gbpA Gene Encoding a Mucin-binding Protein Essential for Pathogenesis. J Biol Chem 291:5774-5787.
54. Tang WJ, Fernandez J, Sohn JJ, Amemiya CT. 2015. Chitin is endogenously produced in vertebrates. Curr Biol 25:897-900.
55. Wagner G, Lo J, Laine R, Almeder M. 1993. Chitin in the epidermal cuticle of a vertebrate (*Paralipophrys trigloides*, Blenniidae, Teleostei). Cell Mol Life Sci 49:317-319.
56. Mitsuhashi W, Miyamoto K. 2003. Disintegration of the peritrophic membrane of silkworm larvae due to spindles of an entomopoxvirus. J Invertebr Pathol 82:34-40.
57. Mitsuhashi W, Kawakita H, Murakami R, Takemoto Y, Saiki T, Miyamoto K, Wada S. 2007. Spindles of an entomopoxvirus facilitate its infection of the host insect by disrupting the peritrophic membrane. J Virol 81:4235-4243.
58. Khider M, Hansen H, Hjerde E, Johansen JA, Willassen NP. 2019. Exploring the transcriptome of luxI− and ΔainS mutants and the impact of N-3-oxo-hexanoyl-L- and N-3-hydroxy-decanoyl-L-homoserine lactones on biofilm formation in *Aliivibrio salmonicida*. PeerJ 7:e6845.
59. Meibom KL, Li XB, Nielsen AT, Wu CY, Roseman S, Schoolnik GK. 2004. The *Vibrio cholerae* chitin utilization program. Proc Natl Acad Sci USA 101.
60. Paspaliari DK, Loose JS, Larsen MH, Vaaje-Kolstad G. 2015. *Listeria monocytogenes* has a functional chitinolytic system and an active lytic polysaccharide monooxygenase. Febs j 282:921-936.
61. Vandesompele J, De Preter K, Pattyn F, Poppe B, Van Roy N, De Paepe A, Speleman F. 2002. Accurate normalization of real-time quantitative RT-PCR data by geometric averaging of multiple internal control genes. Genome Biol 3:research0034.1.
62. Olsvik PA, Lie KK, Jordal A-EO, Nilsen TO, Hordvik I. 2005. Evaluation of potential reference genes in real-time RT-PCR studies of Atlantic salmon. BMC Mol Biol 6:21-21.
63. Škugor S, Jørgensen SM, Gjerde B, Krasnov A. 2009. Hepatic gene expression profiling reveals protective responses in Atlantic salmon vaccinated against furunculosis. BMC Genomics 10:503.
64. Løvoll M, Johnsen H, Boshra H, Bøgwald J, Sunyer JO, Dalmo RA. 2007. The ontogeny and extrahepatic expression of complement factor C3 in Atlantic salmon (*Salmo salar*). Fish Shellfish Immunol 23:542-552.
65. Hynes NA, Furnes C, Fredriksen BN, Winther T, Bøgwald J, Larsen AN, Dalmo RA. 2011. Immune response of Atlantic salmon to recombinant flagellin. Vaccine 29:7678-87.
66. Yu Y, Smith M, Pieper R. 2014. A spinnable and automatable StageTip for high throughput peptide desalting and proteomics. Protoc Exch doi:10.1038/protex.2014.033.
67. Ursby T, Ahnberg K, Appio R, Aurelius O, Barczyk A, Bartalesi A, Bjelcic M, Bolmsten F, Cerenius Y, Doak RB, Eguiraun M, Eriksson T, Friel RJ, Gorgisyan I, Gross A, Haghighat V, Hennies F, Jagudin E, Norsk Jensen B, Jeppsson T, Kloos M, Lidon-Simon J, de Lima GMA, Lizatovic R, Lundin M, Milan-Otero A, Milas M, Nan J, Nardella A, Rosborg A, Shilova A, Shoeman RL, Siewert F, Sondhauss P, Talibov VO, Tarawneh H, Thanell J, Thunnissen M, Unge J, Ward C, Gonzalez A,

Mueller U. 2020. BioMAX - the first macromolecular crystallography beamline at MAX IV Laboratory. J Synchrotron Radiat 27:1415-1429.
68. Casanas A, Warshamanage R, Finke AD, Panepucci E, Olieric V, Noll A, Tampe R, Brandstetter S, Forster A, Mueller M, Schulze-Briese C, Bunk O, Wang M. 2016. EIGER detector: application in macromolecular crystallography. Acta Crystallogr Sect D 72:1036-1048.
69. Incardona M-F, Bourenkov GP, Levik K, Pieritz RA, Popov AN, Svensson O. 2009. EDNA: a framework for plugin-based applications applied to X-ray experiment online data analysis. J Synchrotron Radiat 16:872-879.
70. Winn MD, Ballard CC, Cowtan KD, Dodson EJ, Emsley P, Evans PR, Keegan RM, Krissinel EB, Leslie AGW, McCoy A, McNicholas SJ, Murshudov GN, Pannu NS, Potterton EA, Powell HR, Read RJ, Vagin A, Wilson KS. 2011. Overview of the CCP4 suite and current developments. Acta Crystallogr Sect D 67:235-242.
71. McCoy AJ, Grosse-Kunstleve RW, Adams PD, Winn MD, Storoni LC, Read RJ. 2007. Phaser crystallographic software. J Appl Crystallogr 40:658-674.
72. Emsley P, Lohkamp B, Scott WG, Cowtan K. 2010. Features and development of Coot. Acta Crystallogr Sect D 66:486-501.
73. Murshudov GN, Skubak P, Lebedev AA, Pannu NS, Steiner RA, Nicholls RA, Winn MD, Long F, Vagin AA. 2011. REFMAC5 for the refinement of macromolecular crystal structures. Acta Crystallogr Sect D 67:355-367.
74. Liebschner D, Afonine PV, Baker ML, Bunkoczi G, Chen VB, Croll TI, Hintze B, Hung L-W, Jain S, McCoy AJ, Moriarty NW, Oeffner RD, Poon BK, Prisant MG, Read RJ, Richardson JS, Richardson DC, Sammito MD, Sobolev OV, Stockwell DH, Terwilliger TC, Urzhumtsev AG, Videau LL, Williams CJ, Adams PD. 2019. Macromolecular structure determination using X-rays, neutrons and electrons: recent developments in Phenix. Acta Crystallogr Sect D 75:861-877.
75. Berman HM, Westbrook J, Feng Z, Gilliland G, Bhat TN, Weissig H, Shindyalov IN, Bourne PE. 2000. The Protein Data Bank. Nucleic Acids Res 28:235-242.

Chitinolytic enzymes confer pathogenicity of *Aliivibrio salmonicida* LFI1238 in the invasive phase of cold-water vibriosis (CWV)

Anna Skåne[1], Per Kristian Edvardsen[1], Gabriele Cordara[3], Jennifer S.M. Loose[1], Kira D. Leitl[3], Ute Krengel[3], Henning Sørum[2], Fatemeh Askarian[1] ‡*and Gustav Vaaje-Kolstad[1‡*]

[1]Faculty of Chemistry, Biotechnology and Food Science, Norwegian University of Life Sciences (NMBU), Ås, Norway.
[2] Department of Paraclinical Sciences, Faculty of Veterinary Medicine, Norwegian University of Life Sciences (NMBU), Oslo, Norway.
[3]Department of Chemistry, University of Oslo, P.O. Box 1033 Blindern, NO-0315 Oslo, Norway.

‡These authors contributed equally to this work.
*Correspondence: gustav.vaaje-kolstad@nmbu.no , fatemeh.askarian@nmbu.no,

Supplementary material

Table S1. Data collection and refinement statistics.

	AsLPMO10B-D1[a]
A. Data collection	
Beamline	MAX-IV BioMAX
Wavelength (Å)	0.9763
Space group	$P6_5$
Cell parameters – *a*, *b*, *c* (Å)	71.1, 71.1, 100.3
Resolution (Å)[b]	33.5-1.35 (1.40-1.35)
R_{merge} (all I^+ and I^-) (%)[bc]	9.7 (>100)
R_{merge} (within I^+/I^-) (%)[bc]	9.3 (>100)
R_{meas} (all I^+ and I^-) (%)[bd]	9.9 (>100)
R_{meas} (within I^+/I^-) (%)[bd]	9.8 (>100)
$R_{p.i.m.}$ (all I^+ and I^-) (%)[be]	2.2 (54.5)
$R_{p.i.m.}$ (within I^+/I^-) (%)[be]	3.1 (83.0)
$CC_{1/2}$[bf]	99.9 (54.5)
Mean I / σ(I)[b]	15.3 (0.9)
Completeness (%)[b]	99.9 (99.7)
Multiplicity[b]	18.2 (9.7)
No. reflections (unique)	62730 (6133)
Wilson B-factor	20.2
B. Refinement	
Resolution (Å)	33.5-1.35
R_{work}/R_{free} (%)[g]	13.9 / 16.2
Macromolecules / a.s.u.	1
No. atoms	
Protein	1715
Water	109
Ligands	22
B-factor (Å²)	
Protein	28.5
Water	37.3
Ligands	66.3
r.m.s.d. from ideal values	
Bond lengths (Å)	0.02
Bond angles (deg.)	1.86
Ramachandran plot	
Core region (%)	97.9
Outliers (%)	0
PDB ID	7OKR

[a]Friedel pairs were treated as different reflections.
[b]Values in parentheses refer to highest resolution shell
[c]$R_{merge} = \Sigma_{\mathbf{h}}\Sigma_j |I_{\mathbf{h}j} - \langle I_{\mathbf{h}}\rangle| / \Sigma_{\mathbf{h}}\Sigma_j I_{\mathbf{h}j}$, where $\langle I_{\mathbf{h}}\rangle$ is the mean intensity of symmetry-related reflections $I_{\mathbf{h}}$
[d]$R_{meas} = \Sigma_{\mathbf{h}} [N_{\mathbf{h}}/(N_{\mathbf{h}}-1)]^{1/2} \Sigma_i |I_{\mathbf{h}j} - \langle I_{\mathbf{h}}\rangle| / \Sigma_{\mathbf{h}}\Sigma_i I_{\mathbf{h}j}$, where N is the redundancy of reflection **h**
[e]$R_{p.i.m.} = \Sigma_{\mathbf{h}} [1/(N_{\mathbf{h}}-1)]^{1/2} \Sigma_j |I_{\mathbf{h}j} - \langle I_{\mathbf{h}}\rangle| / \Sigma_{\mathbf{h}}\Sigma_j I_{\mathbf{h}j}$
[f]The high resolution cut-off was chosen despite the low $CC_{1/2}$ ensuring the presence of a low signal-to-noise ratio by visual inspection of the electron density map
[g]R_{free} was calculated from 5% of randomly selected reflections for each data set

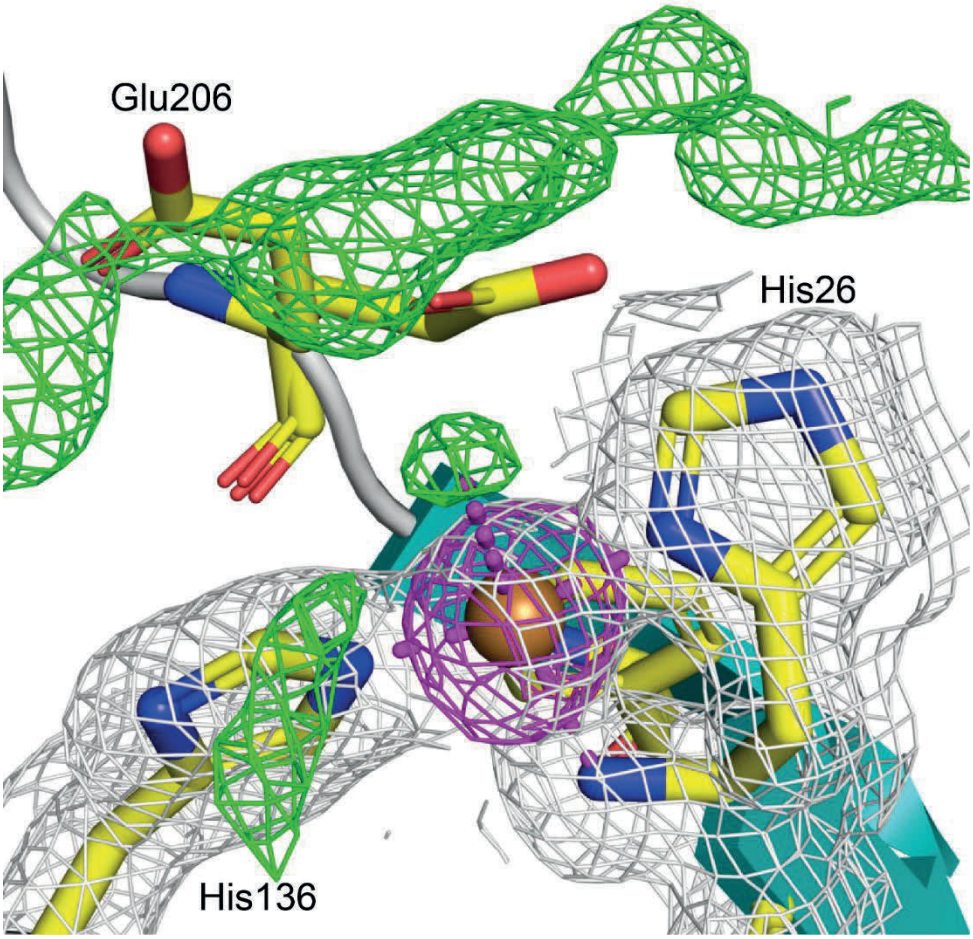

Figure S1. **Electron density at the *As*LPMO10B LPMO domain catalytic center.** The figure shows the σA-weighted 2m*F*o-*F*c electron density map contoured at 1.0 σ around the histidine brace motif (light grey) and the phased anomalous difference map peak validating the presence of copper at its center (magenta, contoured at 4.5 σ). The weighted *F*o-*F*c difference density map (green) reveals the presence of a large ligand left unmodelled. The ligand completes the coordination of the catalytic copper from the solvent side, mirroring the substrate.

Paper III

Comparative proteomic profiling reveals specific adaptation of *Vibrio anguillarum* to oxidative stress, iron deprivation and components of innate immunity

Anna Skåne[1], Jennifer S.M. Loose[1], Gustav Vaaje-Kolstad*[1] and Fatemeh Askarian*[1]

[1]Faculty of Chemistry, Biotechnology and Food Science, Norwegian University of Life Sciences (NMBU), Ås, Norway.

Comparative proteomic profiling reveals specific adaption of *Vibrio anguillarum* to oxidative stress, iron deprivation and humoral components of innate immunity

Anna Skåne, Jennifer S.M. Loose, Gustav Vaaje-Kolstad‡* and Fatemeh Askarian‡*

Faculty of Chemistry, Biotechnology and Food Science, Norwegian University of Life Sciences (NMBU), Ås, Norway.

‡These authors contributed equally to this work.
*correspondence: fatemeh.askarian@nmbu.no, gustav.vaaje-kolstad@nmbu.no

ABSTRACT
The gram-negative bacterium *Vibrio (Listonella) anguillarum* (VA) is the causative agent of vibriosis, a terminal hemorrhagic septicemia affecting the aquacultural industry across the globe. The success of VA as a pathogen comes through its ability to explicitly disarm the immune system of the host by evasive strategies achieved through expression of virulence factors involved in resistance to immunologic clearance. In the current study we used comparative label free quantitative proteomics to map how VA adapts its proteome in vitro to conditions that mimics vibriosis-related stress such as exposure to oxidative stress (H_2O_2), opsonization with complement factors via incubation with Atlantic salmon serum, and iron deprivation upon supplementation of 2,2'-dipyridyl (DIP) to the growth medium. We also studied how regulation of virulence factors may be governed by the bacterial growth phase and nutrient availability. All conditions investigated revealed stress-specific proteomic adaption and only nine proteins were found to be commonly regulated in all conditions. Notably, iron deprivation and exposure to Atlantic salmon serum both evoked upregulation of iron acquisition mechanisms and key virulence factors. The modulation of multiple metabolic pathways that was observed upon exposure to all examined conditions reflects the struggle of the pathogen to obtain physiological adaptation. A general observation made for all stress-related conditions was regulation of multiple metabolic pathways, which highlights the importance of controlling metabolite levels in the context of vibriosis associated stress. The findings made in the present study represent a source of potential virulence determinants that can be of use in the search for means to avoid/control future vibriosis outbreaks.

Datasets are available for download through the following links:

http://arken.nmbu.no/~gustko/Paper_III/Dataset%201.xlsx
http://arken.nmbu.no/~gustko/Paper_III/Dataset%202.xlsx
http://arken.nmbu.no/~gustko/Paper_III/Dataset%203.xlsx
http://arken.nmbu.no/~gustko/Paper_III/Dataset%204.xlsx
http://arken.nmbu.no/~gustko/Paper_III/Dataset%205%20.xlsx
http://arken.nmbu.no/~gustko/Paper_III/Dataset%206.xlsx

1. INTRODUCTION

Today, aquaculture is a growing part of the economy and is responsible for 50% of the fish consumed globally. The growth in this sector is accompanied with incidents of disease outbreaks that are of concern to both animal welfare and economical aspects. The gram-negative bacterium *Vibrio (Listonella) anguillarum* (VA) is the causative agent of vibriosis, a disease associated with severe hemorrhagic septicemia in various marine and brackish water cultured and wild fish, as well as in marine invertebrates (*e.g.,* bivalves and crustaceans) (1). So far, a total of 23 serotypes of VA have been described (O1 to O23), of which mainly serotypes O1 and O2 are associated with vibriosis in aquaculture (2, 3). In fish, the disease commonly arises by colonization and subsequent breaching of the skin barrier, or through the gut, especially in larvae (1, 4). Once VA passes the outer barrier, the infectious agent uses several strategies to cope with stress, evade host immunity, and establish a severe systemic infection (Reviewed in (5)).

The full mechanism of VA pathogenesis is not completely understood, but many virulence determinants have been characterized, including lipopolysaccharides (LPS; *e.g*. O-antigen polysaccharide) (6, 7), multiple iron-acquisition systems (8, 9), motility (*e.g.,* FlaA, MotA, CheR) (10-13), production of exopolysaccharide (14), quorum-sensing (*e.g.* VanT) (15), hemolytic (*e.g.* Vah1-5 and Rtx) (16, 17) and proteolytic (*e.g*., EmpA and PrtV) (18, 19) activities. Some of the virulence factors such as the LPS O-antigen are attributed to multiple functions in VA including evasion of phagocytosis by epithelial cells (6) and attenuation of serum-mediated killing in rainbow trout (7). A recent study has demonstrated that a VA O2 serotype adjusts its expression of virulence factors genes in response to both iron levels and temperature fluctuation (20). In this regard, the Type VI secretion system (T6SS) (VtsA-H) plays a crucial role in the regulation of RpoS, a stress response regulator in VA (21). The T6SS is associated with the hemolysin co-regulated protein (Hcp) that is known to be important for secretion of bacterial effectors such as hemolysins (22).

The viability of VA in the blood is governed by a complex interplay between VA*,* immune cells and humoral innate immune components, such as complement proteins, proteases, esterases, antimicrobial peptides and lysozyme (1). Phagocytosis of the opsonized VA by immune cells initiates a cascade of downstream events, including induction of oxidative burst and release of reactive oxygen species (ROS). These ROS are generated by NADPH oxidases and include superoxide anion, hydrogen peroxide (H_2O_2), hydroxyl radicals, hypochlorous acid and chloramines (23). Many bacteria have developed strategies for handling oxidative stress, for example by producing detoxifying enzymes, such as catalase and superoxide dismutase, (reviewed in (24, 25)) and enzymatic pathways dedicated to the repair of oxidized proteins (26). The importance of phagocytosis in combating VA- associated vibriosis has been studied in a variety of species, including gilthead seabream (*Sparus aurata* L.) (27, 28), sea bass (*Dicentrarchus labrax* L.) (29), rainbow trout (*Oncorhynchus mykiss*) (30, 31), and ayu (*Plecoglossus altivelis*) (32-34). The inhibition of leukocyte respiratory burst and apoptosis has been reported as a major evasion mechanism of VA in sea bass (29).

An important property of the host environment is the limited availability of free iron. Iron is an essential micronutrient for all living organisms and iron acquisition systems therefore represent a vital strategy in bacterial pathogenesis

(35, 36). VA has a well-developed iron acquisition apparatus consisting of three siderophore systems (vanchrobactin, anguibactin and piscibactin) and a gene cluster encoding nine heme uptake-related proteins (*e.g.,* HuvABCD, TonB1) (37). Iron transport systems known to be important in other Vibrio species such as *Vibrio parahaemolyticus* and *Vibrio cholerae*, are also present in the genomes of many VA strains, including genes encoding transport systems for unchelated ferrous iron (*feoABC*), ferric iron (*fbpABC*$_1$ and *fbpABC*$_2$) and siderophore ferrichrome transport (*fhuABCD*) (8, 38, 39). Most importantly, the plasmid pJM1 is present in the majority of serotype O1 strains and encodes the anguibactin synthesis machinery, a major virulence determinant for VA (8, 40-43).

Expression of the virulence repertoire of a bacterium is a determinant of its pathogenesis and resistance to antimicrobial immune responses. Thus, the current study aimed to obtain molecular insights into the proteome profile of VA serotype O1 strain NB10 upon exposure to different types of stresses mimicking vibriosis in vitro. This NB10 strain was originally isolated at the Umeå Marine Research Centre, Norrbyn, Sweden during a natural outbreak of vibriosis (44, 45). Our data shed light on the adaptation of VA to oxidative stress, iron limitations and humoral components of innate immunity, and offer new insights into virulence determinants associated with the response of VA over the course of vibriosis.

2. MATERIALS AND METHODS

2.1 Bacterial strain and growth media

The *V. anguillarum* NB10 (VA) strain used in this study was obtained as a gift from Prof. Hans Wolf-Watz (University of Umeå, Sweden). The bacterium was routinely cultured in bacteriologic Luria Broth (LB) supplemented with 2 % NaCl (Sigma, w/v) (abbreviated "LB$_S$") at 25 °C in ambient air with agitation (220 rpm) or on agar plates that containing LB$_S$ solidified with agar (7 g/L). When indicated, VA was grown in M9 minimal medium (Gibco) supplemented with 1 % NaCl (Sigma, w/v), 0.2 % Casamino Acids (Difco, w/v), and 0.5 % glucose (Sigma, w/v) (abbreviated as "M9$_{VA}$") pre-heated to room temperature.

2.2. Collection of pooled salmon serum

Pooled Atlantic salmon serum (S) was obtained from 5 Atlantic salmon (*Salmo salar* L.; approximately 1-1.5 kg in size) sourced from the Norwegian University of Life Sciences fish laboratory. The fish were killed by a sharp blow to the head prior to blood drawing, and blood was collected in non-heparinized tubes by puncture of the caudal vein plexus and allowed to clot for 10-20 minutes on ice. After centrifugation (10 min, 2000 × *g*), serum was immediately collected, pooled, and stored at −80 °C.

2.3. Harvesting of samples for proteomics analysis

Cultures of VA were obtained by inoculating 5 mL LB$_S$ with fresh colonies followed by overnight incubation at 25 °C with agitation at 220 rpm. To identify the VA proteome at different stages of the bacterial growth phase, the overnight culture was diluted 1:100 (total volume of 5 ml) in LB$_S$ and incubated at 25 °C with agitation, closely monitoring optical density at 600 nm (OD$_{600}$). Samples were harvested at OD$_{600}$ 0.3-0.4, 0.6-0.7, and >1.0 and pelleted by centrifugation (4000 × *g* for 10 min at 4 °C).

To evaluate the VA proteome response to opsonization with S, iron limitation or oxidative stress, the overnight culture of VA was diluted 1:100 in $M9_{VA}$ and incubated at 25 °C with agitation (220 rpm). Upon reaching to OD_{600} 0.5-0.6, VA cultures were left untreated (control) or supplemented with either pooled Atlantic salmon serum (S, 10 % v/v), 2,2'-dipyridyl (DIP, Sigma) at the final concentration of 200 µM, or H_2O_2 (Sigma) at the final concentration of 1 µM, 1 mM and 10 mM. Next, following 30 minutes (S and H_2O_2) or 1 h (DIP) incubation, samples (1 mL) were collected and centrifuged at 4000 × *g* for 10 min at 4 °C.

The sample supernatants were transferred to a 2 mL low protein binding tube (Eppendorf), and immediately stored at -80 °C. The bacterial pellets were washed twice by resuspension in ice-cold phosphate-buffered saline (PBS, Sigma) and finally stored at -80 °C. The bacterial pellet was further processed as described in section 2. 4. The experiments were performed in biological triplicates.

2. 4. Protein extraction and nano HPLC-MS/MS analysis

Frozen bacterial pellets were thawed on ice, resuspended in 200 µL lysis buffer that contained PBS, 1 mM EDTA, 1 mM DTT and homogenized by bead beating (Fastprep, MP Biomedicals) in three one-minute intervals at 6 m/s. Following lysis, the lysis suspension was centrifuged at 14000 rpm and 4 °C for 10 min. The supernatant was sterile filtered (0.22 µm) and transferred to a LoBind tube (Eppendorf). To precipitate the proteins, TCA (10 % v/v) were added to the samples. The samples were vortexed and frozen overnight at -18 °C. The next day, the samples were thawed and centrifuged (14000 rpm, 4 °C, 15 min). The supernatant was discarded, and the pellet was washed in 300 µL 90 % acetone-HCl (0.01 M). The sample was centrifuged (14000 rpm, 4 °C, 15 min), the supernatant was discarded, and the pellet was air-dried for approximately 5 min. The protein pellet was dissolved in 55 µL 7 M urea, 20 mM TrisHCl pH 8.0. Prior to reduction and alkylation, the pH was measured (≥ pH 7.8) and the protein concentration was estimated using Bradford reagent (BioRad). To reduce the proteins, 10 mM DTT was added to the samples followed by incubation in a thermomixer (Eppendorf) (400 rpm, RT, 30 min). Subsequently, the proteins were alkylated by adding 15 mM IAA followed by 30 min static incubation at RT in the dark. The samples were diluted in 20 mM Tris-HCl pH 8.0 to reduce the amount of Urea to 1 M prior to trypsinization (1/40 of the protein concentration). The trypsinization was carried out overnight at 37 °C in a thermomixer (Eppendorf) at 400 rpm. The next day, the reaction was quenched by adding 1 % TFA (v/v). The sample volume was reduced to approximately 150 µL in a SpeedVac (Eppendorf) at 40 °C. The resulting peptides were cleaned by using ZipTips (C18 solid-phase extraction). For this purpose, the ZipTips were equilibrated by pipetting up and down in 100 % MeOH (3X), 70 % (v/v) ACN-0.1 % (v/v) TFA (1X) and 0.1 % (v/v) TFA (2X). The peptides were bound to the C18 material by pipetting up and down (4X). The tip was wiped with a tissue and the samples were washed with 0.1 % TFA. The peptides were eluted in 10 µL 70 % (v/v) ACN-0.1 % (v/v) TFA. The samples were dried in a SpeedVac and eluted in 10 µL 2 % (v/v) ACN-0.1 % (v/v) TFA.

Peptides were analyzed as previously described (46). In brief, peptides were loaded onto a nanoHPLC-MS/MS system (Dionex Ultimate 3000 UHPLC; Thermo Scientific) coupled to a Q-Exactive hybrid quadrupole orbitrap mass spectrometer (Thermo Scientific). Thereafter, peptides were separated using an

analytical column (Acclaim PepMap RSLC C18, 2 µm, 100 Å, 75 µm i.d., 50 cm, nanoViper) with a 90-minutes gradient from 3.2 to 44 % (v/v) acetonitrile in 0.1 % (v/v) formic acid at a flow rate 300 nL/min. The Q-Exactive mass spectrometer was operated in data-dependent mode acquiring one full scan (400-1500 m/z) at R=70000 followed by (up to) 10 dependent MS/MS scans at R=35000.
The raw data were analyzed using MaxQuant version 1.6.17.0, and proteins were identified and quantified using the MaxLFQ algorithm (47). The data were searched (October, 2020) against the UniProt VA (strain ATCC 68554 / 775) proteome (UP000006800; 3722 sequences), which is essentially identical to the proteome of NB10. In addition, reversed sequences of all protein entries were concatenated to the database to estimate the false discovery rates. The tolerance levels used for matching to the database were 4.5 ppm for MS and 20 ppm for MS/MS. Trypsin/P was used as a digestion enzyme and 2 missed cleavages were allowed. Carbamidomethylation of cysteines was set as a fixed modification and protein N-terminal acetylation, whereas oxidation of methionine and deamidation of asparagine and glutamine were allowed as variable modifications. All identifications were filtered to achieve a protein false discovery rate (FDR) of 1 %. Perseus version 1.6.2.3 (48) was used for data analysis, and the quantitative values were log_2-transformed. The proteins were considered as detected when they were present in at least two out of three replicates of one examined condition. All identified proteins were additionally annotated with putative carbohydrate-active functions as predicted by dbCAN2 (49).

2. 5. Evaluation of LPMO expression using droplet digital PCR™

The expression of *LPMO* was assessed using droplet digital PCR™ (ddPCR™, Bio-Rad). The expression was assessed during bacterial growth in LB_S. Upon reaching OD_{600} of 0.3 and >1, 1 mL of bacterial culture was transferred to an RNase/DNase-free tube and supplemented with 1 mL of RNA protect (Qiagen). The samples were immediately vortexed for 5 seconds, incubated at least 5 min at RT, and centrifuged (10 min, 4000-5000 × *g*, 4 °C). The pellet was stored at -80 °C until cell lysis and RNA isolation. RNA isolation was performed using Qiagen RNeasy Mini Kit (Qiagen) using the Quick-Start protocol. To disrupt the bacterial cell wall, the pellet was lysed using 200 µL Tris-EDTA pH 8.0 supplemented with 1 mg/mL lysozyme (Sigma), vortexed for 10 seconds, and subsequently incubated at room temperature for 45 min. Next, 700 µL buffer RLT (kit buffer, Qiagen) supplemented with 10 µL/mL β-mercaptoethanol were added to the sample and mixed vigorously before proceeding with the protocol. The RNA integrity and quantity were determined by Nanodrop. Residual genomic DNA (gDNA) was removed using the HL-dsDNase digestion (ArcticZymes®) according to the manufacturer's instructions. The cDNA synthesis was performed using iScript™ Reverse Transcription Supermix (Bio-Rad), and the synthesized cDNA was stored at -20 °C until analysis. Droplet digital PCR analysis was performed using EvaGreen ddPCR™(Bio-Rad) according to the manufacturer's recommendations. The analysis was conducted using *lpmO*$_{VA}$ detection primers *lpmO*$_{VA}$-ddPCR-FW: CGCGGCAAAATACCTGTTAC and *lpmO*$_{VA}$-ddPCR-RV: CAACAGCTTGAACATGAGCC. No template/no reverse transcriptase controls were included as negative controls.

2. 6. Data deposition:
The mass spectrometry proteomics data have been deposited to the ProteomeXchange Consortium (50) via the PRIDE (50) partner repository with the dataset identifier PXD025367.

2. 7. Data analysis
Data were analyzed and plotted either using GraphPad Prism 8.0 or Perseus (Maxquant). When indicated, data are presented as the means ± standard error of the mean (SEM), unless otherwise indicated. Two-way ANOVA and Student's t-test (paired) in the GraphPad Prism software package or Perseus were used to identify statistical significance ($p < 0.05$), respectively. Proteins were considered significantly differentiated in abundance with a *p*-value <0.05 and up-regulated or down-regulated with a 1.5-fold change cut-off. The detail associated with statistical analysis of the proteomic data is described in detail under relevant sub-sections. Venn-diagrams were generated via the web-based tool developed by Heberle et al., (51). Networking and KEGG pathway enrichment analysis were performed using the STRING database (52).

3. RESULTS
The effect of the growth phase and nutritional stress on the VA proteome. To assess the influence of the growth phase and growth medium on the VA proteome profile, the bacterium was grown in bacteriologic medium (LB_S) and sampled for proteomic analysis in early-logarithmic ($OD_{600\ nm}$ = 0.3), mid-logarithmic ($OD_{600\ nm}$ = 0.6), and stationary growth phase ($OD_{600\ nm}$ >1). Proteomic analysis of these conditions identified 1261 proteins of which 1070 were shared under the above-examined conditions (Fig. 1A and Fig. S1, Dataset 1). Two-dimensional principal component analysis (PCA) revealed strong coherence between biological replicates and showed the formation of two distinct clusters (PC1 = 38.8 % and PC2 = 16.0 %), where the VA translational response from the exponential phase was clearly distinguished from the stationary phase (Fig. 1B). To further verify our proteomics analysis, a random gene (locus tag VAA_01311, which encodes a lytic polysaccharide monooxygenase, gene henceforth called "*lpmO$_{VA}$*" was selected to assess the transcription (at the mRNA level) and the translational response of VA at different growth phases. The *lpmO$_{VA}$* mRNA abundance was estimated ~1600 and ~4300 copies/100 ng RNA at exponential and stationary growth phases, respectively (Fig. 1C, left panel). This result was in accordance with the translational response of this protein (LPMO) in our label-free quantitative proteomics analysis (LFQ intensity; Fig. 1C, right panel). Comparing the proteome response of VA at mid-logarithmic ($OD_{600\ nm}$ = 0.6) and stationary growth phase ($OD_{600\ nm}$ >1) against early-logarithmic ($OD_{600\ nm}$ = 0.3) revealed significant up-regulation of 49 and 92, and down-regulation of 25 and 97 proteins, respectively (Fig. 1D left and right panels, Dataset 2). Venn analysis revealed that most of the significantly regulated proteins were unique to the growth phase of the bacterium (Fig. 1E). The up-regulated (Fig. 1F) and down-regulated (Fig. S1B) proteins were highly interconnected. Importantly, the functions of these significantly regulated proteins were majorly attributed to metabolic pathways, with particular enrichment of secondary metabolite biosynthesis and antibiotic biosynthesis in the up-regulated proteins (Fig. 1F). The expression of several virulence factors associated with VA pathogenesis (Fig. 1G), including motility (*e.g.*, FliA, FliK, FlgD, FlgN),

chemotaxis (*e.g.*, CheY), iron acquisition (*e.g.*, HuvB, AngH, AngM), export of polysaccharide (Wza), were significantly altered at the stationary phase compared to the early exponential growth phase (Fig. 1G), indicating that the pathogenicity of VA can be regulated via stationary- or exponential-phase specific virulence determinants.

Next, to evaluate the versatility and adaptability of VA to environmental changes, we further determined the proteome response of VA in NaCl-containing Luria broth (LB_S) and minimal medium ($M9_{VA}$) at mid-logarithmic phase ($OD_{600\ nm}$ = 0.6; Dataset 3). PCA analysis (PC1 = 19.3 % and PC2 = 13.0 %) revealed a distinct proteome profile of VA when comparing bacteriologic medium (LB_S) and nutrient-limited condition represented by $M9_{VA}$ (Fig. S2A). Volcano plot analyses showed that exposure of VA to a nutrient-limited condition ($M9_{VA}$) resulted in differential regulation of 343 proteins in $M9_{VA}$ vs. LB_S of which 160 and 180 proteins were up- and down-regulated, respectively (Fig. 1H, Dataset 3). KEGG pathway analysis using the STRING database (52) further revealed depletion of proteins involved in the biosynthesis of secondary metabolites, antibiotics and in particular amino acids, and enrichment of proteins involved in the metabolism of carbon, pyruvate, fructose and mannose and citrate cycle when comparing VA grown in LB_S compared to $M9_{VA}$ (Fig. 1I). Alternation of VA metabolism was also reflected in the altered abundance of several carbohydrate-active enzymes (CAZymes; Fig. 1J), of which seven were found to be up-regulated (β-glycosidases represented by glycoside hydrolase families GH1, GH2 and GH3, α-galactosidases represented by GH36, carbohydrate phosphorylases represented by GH94, glycosyl transferases represented by GT28 and carbohydrate esterases of the CE1 family) and three were found to be down-regulated (a representative of the diverse glycosyl transferase GT2 family, an α-glycosidase of GH13 and a carbohydrate oxidase of the AA3 family) in LB_S versus $M9_{VA}$. Importantly, five out of seven of the up-regulated enzymes are glycosyl hydrolases (GH), a widespread group of enzymes that hydrolyze glycosidic bonds between two or more carbohydrates or between a carbohydrate and a non-carbohydrate moiety (53), and that often are related to carbohydrate catabolism.

Since bacterial stress responses are determinants of their resistance to antimicrobial immune responses, we further evaluated the VA translational response to oxidative stress, iron limitation, and opsonization with complement components via supplementation of H_2O_2, 2,2′-Dipyridyl (DIP) and serum to in vitro growth condition ($M9_{VA}$). In total, 1034 proteins were shared across all examined conditions (Fig. S2A left panel, Dataset 1). PCA analysis (PC1 = 19.3 % and PC2 = 13.0 %) resulted in three main clusters that reflect the distinct in vitro stress response of VA compared to typical bacteriologic media conditions (Fig. S2B). Qualitative (protein identity) and quantitative (i.e. up-regulation or down-regulation) analysis revealed that some of the detected proteins were unique to the examined conditions (Fig. S2A left and right panels) and provide the basis for further description and discussion below.

Proteomic response of VA to oxidative stress. To assess the translational responses of oxidative stress on VA, we compared VA proteomes in the absence and presence of increasing concentrations of H_2O_2 (1 µM, 1 mM, or 10 mM). PCA analysis revealed distinct clustering of the VA proteome response to 10 mM H_2O_2 compared to 1 µM and 1 mM, respectively (Fig. S2A). Volcano plot analysis

showed that the number of significantly regulated proteins increased in response to increasing concentrations of H_2O_2 in the $M9_{VA}$ medium (Fig. 2A). Upon exposure to 1 µM, 1 mM and 10 mM H_2O_2, 23, 48 and 111 proteins were significantly regulated, respectively (Fig. 2A, Dataset 4). Notably, 24 significantly regulated proteins were shared at least under two examined H_2O_2 conditions (Fig. 2B, Dataset 4). Of note, pseudouridine synthases (RsuA and RluC), exopolysaccharide synthesis related protein (WbfD), UDP-sugar diphosphatase (NutA), long-chain fatty acid transport protein (FadL-2), neutrophil-activating protein A (VAA_01966), tetratricopeptide repeat family protein (MshN) and magnesium transporter MgtE (VAA_01744) were among the top list of significantly up-regulated proteins. Among these proteins, exopolysaccharide biosynthesis-related protein (WbfD) and the neutrophil-activating protein A are of special interest. WbfD is involved in the anchoring of VA to fish scales (14), whereas the *Helicobacter pylori* ortholog of VAA_01966 is a major ROS stimulator in human leukocytes (54). The following proteins including, 3-oxoacyl-[acyl-carrier protein] reductase (AlsO), acetolactate synthase (AlsS), ion-translocating oxidoreductase complex subunit C (RnfC) and several proteins associated with sulfur metabolism (CysC, CysK, CysM) were commonly down-regulated under all examined H_2O_2 concentrations.

Since the proteomic response of VA to H_2O_2 was concentration-dependent, we further focused on the regulated proteins that were unique to each condition. Two proteins associated with oxidative stress including dihydrolipoamide dehydrogenase (VAA_02624) (55) and peroxiredoxin (VAA_02625) (56) were identified as up-regulated proteins that were unique to the supplementation of 1 µM H_2O_2 (Fig. 2C left panel, Dataset 4). The mitochondrial enzyme dihydrolipoamide dehydrogenase is known to be sensitive to H_2O_2 (55) whereas peroxiredoxins express peroxidase activity towards H_2O_2 and are thought to protect cells from oxidative stress (56). Exposure to 1 mM H_2O_2 resulted in significant up-regulation of 26 proteins unique to the examined in vitro condition including, the transmembrane regulatory protein (ToxS), chain length regulator (Wzc), and O-antigen export system ATP-binding protein (VAA_02481) (Fig. 2C middle panel, Dataset 4). The two latter proteins are involved in transport and biosynthesis of exopolysaccharide and LPS (14). The two lowest H_2O_2 concentrations resulted in significant down-regulation of 22 proteins associated with metabolism such as thymidine phosphorylase (DeoA), carbamoyl-phosphate synthase small chain (CarA), phosphatidylserine decarboxylase pro-enzyme (Psd), ion-translocating oxidoreductase complex subunit C (RnfC) and 3-oxoacyl-[acyl-carrier protein] reductase (AlsO) and motility regulator, *e.g.* RNA polymerase sigma factor FliA (Figs. 2B-C, Dataset 4).

Addition of 10 mM H_2O_2 to VA growth medium, a potentially lethal condition, altered expression of several proteins unique to the condition (Fig. 2C, Dataset 4). Several of these proteins were associated with the integrity of the VA outer membrane, including BamA, OmpK, BamC, LptD, VAA_03672, VAA_03060 (Fig. 2C). The top three unique up-regulated proteins were cytochrome c domain-containing protein (VAA_03558; FC=4.2), an uncharacterized protein (VAA_02533; FC=3.0) and arginine/ornithine antiporter (VAA_02565; FC=2.8). The VA cytochrome C domain-containing protein amino acid sequence is 77% identical to cytochrome c554 of *Vibrio parahaemolyticus* with an unknown function (57). The arginine/ornithine antiporter amino acids sequence is 43% identical to

ArcD in *Streptococcus suis* that contributes to the biological fitness of the bacterium (58). The STRING-based pathway enrichment analysis further revealed that increased concentrations of H_2O_2 influenced the central metabolism of VA (Fig. 2D). More specifically, the highest concentration of H_2O_2 resulted in down-regulation of several central metabolic pathways associated with amino acid synthesis (*e.g.*, IlvD, DapF, MetH, CysM, CysK, HisB and AlsS), antibiotics (*e.g.*, IlvD, DapF, VAA_01746, CysM, VAA_0118, CysK, PurF and AlsS), secondary metabolites (*e.g.*, Psd, MetH, PanC, VAA_01187 and HisB) and sulfur metabolism (*e.g.*, CysM, CysA, CysK and CysC). Importantly, alteration of metabolism is known as an adaptive strategy in bacteria to mitigate oxidative stress (Reviewed in (59)).

Proteome profile of VA upon opsonization with Atlantic salmon serum. Upon exposure of VA to Atlantic salmon serum (S), 121 proteins including several virulence factors were significantly regulated (Fig. 3A, Dataset 5). Siderophore-interacting protein (SIP or VAA_01637, $\log_2$ FC=4.5) and the ribosomal subunit S50 protein L32 (RpmF, $\log_2$ FC=3.8) (Fig. 3B) were the top two up-regulated proteins. Orthologs of SIP/ VAA_01637 have been shown to be involved in iron acquisition or virulence in other bacteria (60, 61). In *V. cholerae* the SIP protein, called ViuB, utilizes ferric vibriobactin and is controlled by the Fur regulator (61). In correlation with the latter observation, the VA Fur transcriptional regulator was also up-regulated upon exposure to serum (Figs. 3B-C). Furthermore, several other proteins of various functions were up-regulated, including transcriptional regulators (*e.g.* CsrA and VanT), proteins associated with chemotaxis and motility (*e.g.*, CheZ, FlaA, FliS) and stress responses including, small heat shock protein (LbpA), thioredoxin (YbbN), chaperone (co-chaperone protein HscB homolog), ATP-dependent protease subunit (HslV), Lon protease (Lon) (Fig. 3B). STRING analysis of the significantly up-regulated proteins (Fig. 3C) revealed clustering of the proteins associated with the iron acquisition/homeostasis including virulence associated plasmid pJM1, anguibactin biosynthesis (AngM, AngB/G, AngH,), ferric-anguibactin receptor (FatA), ferric anguibactin binding protein (FatB and FatA) and putative ABC transporter (Uniprot ID Q6W4S5). FatA- FatD are essential for the iron transport process (62), whereas FatA is an outer membrane receptor for ferric anguibactin (63, 64) and FatB is a membrane associated periplasmic binding protein (65). Fur and a plasmid pJM1-derived antisense RNA (RNAα) are the negative regulators of FatA and FatB (66). The main network cluster additionally contained the chromosome encoded hemin receptor HuvA, which is associated with heme transport and virulence (Fig. 3C) (67). Interestingly, the virulence related hemolysin CorC/Vah2, capable of lysing erythrocytes (17), was also found up-regulated upon exposure to serum (Fig. 3B,C). Also noteworthy is the up- regulation of the small cluster containing stress response/ chaperones/ proteases (LbpA, HslV, Lon and a thioredoxin, or- co chaperone protein named YbbN). LbpA belongs to the small heat shock protein (HsP20) family that contributes to protection of proteins from unfolding/aggregating during stress (68, 69). The Lon protease is known to be important for survival and virulence of other bacterial strains such as *V. cholera* (70). HslV is a protease subunit of a proteasome-like degradation complex believed to be a general protein degrading machinery, important for removing and recirculating of unfolded and/ or aggregated proteins. YbbN is a thioredoxin, or co-chaperone protein. The up-

regulation of this protein cluster highlights the stress response of VA upon exposure to complement components.

Analysis of the significantly down-regulated proteins revealed several proteins related to a variety of functions, but also several proteins that were assigned to unknown functions. Pathway enrichment analysis of significantly down-regulated proteins in VA identified enrichment of several pathways related to biosynthesis of secondary metabolites, antibiotics and glycolysis/glucogenesis (Fig. 3D).

Stress response of VA to iron deprivation. To assess the response of VA to iron-limiting conditions, bacteria were exposed to 200 μM 2,2′-Dipyridyl (DIP) for 60 min. Volcano plot analysis showed altered expression of 60 proteins, of which 20 and 40 were up- or down-regulated, respectively (Fig. 4A and Supplementary Dataset 5). Most of the up-regulated proteins were also found to be among the list of differentially regulated proteins under other examined stress-inducing conditions. As expected, several of the significantly up-regulated proteins were associated with biosynthesis/homeostasis of siderophores including members of the FecCD transport family, ferrichrome-iron receptor (FhuA), vanchrobactin-specific isochorismatase (VabB), iron-sulfur cluster insertion protein (ErpA), hemin receptors HuvA and co-chaperone HscB. The two latter proteins represent a putative outer membrane transporter that are capable of binding to heme (HuvA was also up-regulated by serum exposure), and a chaperone specifically involved in the maturation of iron-sulfur cluster-containing proteins, respectively. In addition, five of the identified regulated proteins were unique to the iron deprivation conditions (Fig. 4B), namely 50S ribosomal protein L31 type B (RpmE2), isochorismatase (VabB), two-component response regulator protein (VAA_01443), Fe-S carrier protein (ErpA) and a L-ascorbate 6-phosphate lactonase (UlaG). Of these, two were related to the iron acquisition or iron-related functions: isochorismatase is a hydrolase involved in synthesis of siderophores (reviewed in (8)) and ErpA that shares 70% amino acid sequence identity with an ortholog in *Escherichia coli* that has been shown to take part in inserting Fe-S cofactors in iron-sulphur cluster proteins (71). Several other regulators associated with motility (FlaA Flagellin), carbon storage (CsrA) or the two-component response (VAA_01443) were also up-regulated under iron starvation. In addition, several proteins known to be associated with stress response including FAD assembly factor (SdhE, FC=3.331), 50S ribosomal protein L31 type B (RpmE2, FC=3.240), cytochrome d ubiquinol oxidase subunit (VAA_03161;, FC=3.183), small heat shock protein (VAA_00852; FC=2.886) and thioredoxin (VAA_02116; FC=1.202) were also among the list of significantly up-regulated proteins under iron deprivation (Dataset 5).

Analysis of the down-regulated proteins revealed the association of the stress response with a variety of processes, including cell division (ZipA and MinD), key regulators of virulence or stress mediators including poC, Dxs, AphB (transcriptional regulator, LysR family), and FliA (Fig. 4B and Dataset 5). Similar to the other investigated conditions, STRING-based pathway analysis revealed that the majority of the significantly down-regulated proteins were assigned to a variety of metabolic processes (Fig. 4D). Interestingly, the PCA analysis of the datasets showed co-clustering of proteomes obtained from exposure to 10 mM H_2O_2 and 2,2′-Dipyridyl (DIP) (Fig. S2A) and several of the significantly regulated

proteins (*e.g.*, ferrichrome receptor FhuA and cell division inhibitor (VAA_02327; MinD) were shared under both examined conditions (Fig. 4D).

Regulated proteins common to all vibriosis-mimicking stress conditions. To obtain a better overview of the proteins that were commonly up- or down-regulated under all examined stress-inducing conditions in vitro (H_2O_2, serum and DIP), a Venn diagram was generated (Fig. 5A). For simplification, all differentially regulated proteins under H_2O_2 treatments were assembled as one unified list. The analysis revealed that 9 regulated proteins were common under all treatments (Fig. 5A). Several of these up-regulated proteins were involved in different biological functions including, virulence (e.g., motility [FlaA] and heme uptake [HuvA]), iron-sulphur cluster protein maturation (co-chaperone protein [HscB]) and mitochondrial function (e.g., CydA-1b [VAA_03161], YgfY and a protein involved in purine metabolism (QueD)) (Fig. 5B). HscB is known to be important for maturation of iron-sulphur cluster proteins (72) and CydA-1b (cytochrome bd-I ubiquinol oxidase) has been shown to be responsible for oxidation of ubiquinol during metabolism (73). An uncharacterized protein VAA_00242 belonging to the HBL/NHE enterotoxin family was down-regulated in all examined conditions. Amino acid sequence analysis revealed this protein shares 99% sequence identity with the cytotoxin MakA from *V. cholerae.* MakA is a part of the motility-associated killing factor operon (*makDCBA)*, which is secreted via the flagellum channel and involved in cytotoxin export of *V. cholerae* (74).

In conclusion, our data show that VA adjusts its proteome response differentially according to the environmental stresses and that only few proteins are commonly regulated across all conditions.

Differentially regulated hypothetical proteins. Several regulated proteins were annotated as hypothetical or uncharacterized proteins in the VA genome. To obtain a better understanding of their putative functions, their amino acid sequences were further analyzed using the InterPro database search tool (75) (Table S1) for domain and orthologs prediction. Interestingly, proteins VAA_01403 (FC=2.5 in serum *vs* no serum) and VAA_02532 (FC=1.6 in serum *vs* no serum) showed high sequence similarity to transcriptional regulator MarR (multiple antibiotic resistance regulator) and DNA-binding protein HU-alpha in the Vibrionaceae, respectively (Table S1). Members of the MarR/SlyA family of transcriptional regulators have been shown to play important roles in the regulation of several genes, including virulence determinants (76).

4. DISCUSSION

Establishment of infection requires adaptation of the bacterium to multiple host defense strategies and involves the orchestration of multiple virulence factors. Of these, some are common to all types of stress, whereas others are highly adapted and regulated in response to defined properties of the stress conditions. A trait that was common to all conditions investigated in the current study was down-regulation of metabolic pathways, demonstrating that VA reorganized its metabolically related proteome to adapt to the environmental challenge or milieu encountered. This is a trait that can been related to virulence as some bacteria are known to manage oxidative stress by altering the metabolic redox homeostasis of the cells (59). Metabolic modulation is also a mechanism bacteria use for immune

evasion since the host immune system is tuned to detect and respond to certain bacterial secondary metabolites that can be mitigated by down-regulating specific pathways (77).

The dominant stress-response observed across all stress-conditions was related to iron acquisition, a pivotal function for VA virulence (reviewed by (8); Fig. 6). Since iron is an essential element of nutritional immunity in bacteria, host systems are essentially depleted for free iron (and other micronutrients) to prevent bacterial sustenance and proliferation. Thus, the success of pathogens in host colonization relies on iron acquisition systems that can sequester iron from iron-containing host proteins (35, 36). Importantly, the iron acquisition-related response evoked by iron depletion using DIP was different compared to the response obtained by serum exposure. Specifically, anguibactin related proteins and other proteins related to iron acquisition, were only up-regulated in serum and not in DIP. This indicates that the bacterium has different mechanisms for acquiring iron that might depend on the environmental stimuli. The serum conditions are more host-specific than DIP, which could indicate that the anguibactin siderophore system is adapted to specifically sequestering iron from the host environment. This is in line with the plasmid (pJM1) encoding synthesis of the anguibactin siderophore, which is known to be a major virulence factor of VA (8, 40-43). One of the dominant iron-containing proteins in Atlantic salmon serum is hemoglobin. Upon exposure to serum, profound expression of erythrocyte-disrupting hemolysins, hemoglobin degrading proteases and proteins representing the hemin uptake system would be expected. Interestingly, the hemin uptake protein HuvA was up-regulated in all stress-inducing conditions, indicating that its expression is a general stress response. In the context of HuvA, the hemolysin Vah2, which is known to contribute to virulence of VA in rainbow trout and to lyse erythrocytes (17), is expectedly uniquely up-regulated in the serum-condition. Like for anguibactin, this indicates that the expression of some virulence factors is regulated by specific factors, whereas others, like HuvA and more (Fig. 5 & 6), are regulated by a general stress response regulator, or by separate regulators that respond to a variety of conditions.

Since many of the proteomic changes observed were related to mechanisms and pathways requiring several interacting proteins, it was of interest to scrutinize the significantly regulated response regulators that may play the role of orchestrating protein expression. Of special interest was CsrA, the carbon storage regulator (also known as Rsm “repressor of stationary phase metabolites”), that was found up-regulated by both DIP and serum. CsrA is an extensively studied RNA binding protein that is responsible for posttranscriptional regulation of gene expression. The regulator has been linked to a large variety of functions, including carbon metabolism, stress response and virulence (78). In enteropathogenic *E. coli*, CsrA is involved in regulating the expression of several key virulence and metabolic genes (79), which aligns with the observations made for VA exposed to DIP and serum. This may indicate that CsrA is involved in adaptation of VA to host environment. A second notable up-regulated transcription factor is VAA_001403/MarR (multiple antibiotic resistance regulator), a non-annotated VA protein that was observed enriched in response to serum. Other members of the MarR family of transcriptional regulators in pathogens such as *Salmonella typhimurium* (SlyA), *Yersinia enterocolitica* (RovA) and in *V. cholerae* (AphA), have been shown to play key roles in virulence properties (76). It is likely

that MarR plays a role in transcription of virulence factor genes required for adaptation to bloodstream infection.

A common mechanism for host killing of invading pathogens is the infliction of oxidative stress, especially during phagocytosis (23). Thus, many pathogens have developed mechanisms for resisting such stress by producing ROS detoxification enzymes. Of the proteins up-regulated upon oxidative stress, a highly relevant candidate that may participate in H_2O_2 detoxification is VAA_01966 (also called neutrophil-activating protein, NapA). This protein is a member of the DNA-binding protein from starved cells (Dps) family, contains a ferritin-domain, and was found significantly up-regulated in all three H_2O_2 conditions. In *Salmonella enterica*, Dps is involved in resisting iron-dependent killing by H_2O_2, and promotes virulence and survival in macrophages (80). The neutrophil-activating protein (NapA) of *H. pylori* is a major virulence factor, and it has been shown to protect *H. pylori* from oxidative stress (54). Importantly, deletion of Dps in *V. cholerae* impaired the bacterium resistance to hydroperoxides and multiple environmental stressors and colonization of mice intestine in vivo (81). The VA NapA amino acid sequence shares, 78.0 % identity to *V. cholerae* Dps and 31.7 % with *H. pylori* NapA, suggesting similar functions, thus possibly a role in H_2O_2 detoxification. Several bacteria can mitigate oxidative stress by modulating their metabolism, e.g. resulting in pooling of ketoacids that can act as antioxidants (59). It is not unlikely that the metabolic modulation observed for VA can partly function according to the latter mechanism. Interestingly, several proteins in sulphur metabolism were down-regulated upon exposure to H_2O_2. The sulphur containing amino acids cysteine and methionine are very sensitive to oxidation and it is possible that the bacterium adapts a lifestyle less reliant on sulphur containing proteins during oxidative stress. Indeed, sulphur containing proteins were reported highly oxidized in a proteomic study of phagocytized *E. coli* (82). The latter study also reported almost complete oxidation of many outer membrane proteins. The highest H_2O_2 concentration used in the present study showed up-regulation of multiple outer membrane proteins and permeases, which may be a compensatory mechanism to restore membrane function.

In conclusion, our data show that VA adjusts its proteome response uniquely to the to the type of environmental stresses, which highlights the multi-faceted arsenal of proteins employed by VA to interfere with host immune responses, including hemolysis, invasion, degrading of extracellular matrix and resistance to immunologic clearance. The modulation of metabolic pathways that was observed upon exposure to all examined conditions reflects the struggle of the pathogen to obtain physiological adaptation to the stress associated with the host environment.

ACKNOWLEDGEMENTS

This work was supported by grant no. 249865 from the Research Council of Norway. We would like to thank Prof. Henning Sørum for critical reading of the manuscript, Prof. Hans Wolf-Watz for providing the *V. anguillarum* NB10 strain and Dr. Magnus Ø. Arntzen for processing the proteomic data.

REFERENCES

1. Frans I, Michiels CW, Bossier P, Willems KA, Lievens B, Rediers H. 2011. *Vibrio anguillarum* as a fish pathogen: virulence factors, diagnosis and prevention. J Fish Dis 34:643-661.
2. Sørensen UB, Larsen JL. 1986. Serotyping of *Vibrio anguillarum*. Appl Environ Microbiol 51:593-597.
3. Larsen JL, Pedersen K, Dalsgaard I. 1994. *Vibrio anguillarum* serovars associated with vibriosis in fish. J Fish Dis 17:259-267.
4. Weber B, Chen C, Milton DL. 2010. Colonization of fish skin is vital for *Vibrio anguillarum* to cause disease. Environ Microbiol Rep 2:133-139.
5. Ji Q, Wang S, Ma J, Liu Q. 2020. A review: Progress in the development of fish *Vibrio spp*. vaccines. Immunol Lett 226:46-54.
6. Lindell K, Fahlgren A, Hjerde E, Willassen N-P, Fällman M, Milton DL. 2012. Lipopolysaccharide O-Antigen Prevents Phagocytosis of *Vibrio anguillarum* by Rainbow Trout (*Oncorhynchus mykiss*) Skin Epithelial Cells. PLoS One 7:e37678.
7. Boesen HT, Pedersen K, Larsen JL, Koch C, Ellis AE. 1999. *Vibrio anguillarum* resistance to rainbow trout (*Oncorhynchus mykiss*) serum: role of O-antigen structure of lipopolysaccharide. Infect Immun 67:294-301.
8. Li Y, Ma Q. 2017. Iron Acquisition Strategies of *Vibrio anguillarum*. Front Cell Infect Microbiol 7 342.
9. Balado M, Lages MA, Fuentes-Monteverde JC, Martínez-Matamoros D, Rodríguez J, Jiménez C, Lemos ML. 2018. The Siderophore Piscibactin Is a Relevant Virulence Factor for *Vibrio anguillarum* Favored at Low Temperatures. Front Microbiol 9:1766.
10. Milton DL, O'Toole R, Horstedt P, Wolf-Watz H. 1996. Flagellin A is essential for the virulence of *Vibrio anguillarum*. J Bacteriol 178:1310-1319.
11. O'Toole R, Milton DL, Wolf-Watz H. 1996. Chemotactic motility is required for invasion of the host by the fish pathogen *Vibrio anguillarum*. Mol Microbiol 19:625-37.
12. O'Toole R, Lundberg S, Fredriksson SA, Jansson A, Nilsson B, Wolf-Watz H. 1999. The chemotactic response of *Vibrio anguillarum* to fish intestinal mucus is mediated by a combination of multiple mucus components. J Bacteriol 181:4308-17.
13. Ormonde P, Hörstedt P, O'Toole R, Milton DL. 2000. Role of motility in adherence to and invasion of a fish cell line by *Vibrio anguillarum*. J Bacteriol 182:2326-2328.
14. Croxatto A, Lauritz J, Chen C, Milton DL. 2007. *Vibrio anguillarum* colonization of rainbow trout integument requires a DNA locus involved in exopolysaccharide transport and biosynthesis. Environ Microbiol 9:370-82.
15. Croxatto A, Chalker VJ, Lauritz J, Jass J, Hardman A, Williams P, Cámara M, Milton DL. 2002. VanT, a Homologue of *Vibrio harveyi* LuxR, Regulates Serine, Metalloprotease, Pigment, and Biofilm Production in *Vibrio anguillarum*. J Bacteriol 184:1617-1629.
16. Li L, Rock JL, Nelson DR. 2008. Identification and Characterization of a Repeat-in-Toxin Gene Cluster in *Vibrio anguillarum*. Infect Immun 76:2620-2632.
17. Rodkhum C, Hirono I, Crosa JH, Aoki T. 2005. Four novel hemolysin genes of *Vibrio anguillarum* and their virulence to rainbow trout. Microb Pathog 39.
18. Norqvist A, Norrman B, Wolf-Watz H. 1990. Identification and characterization of a zinc metalloprotease associated with invasion by the fish pathogen *Vibrio anguillarum*. Infect Immun 58:3731-6.
19. Denkin SM, Nelson DR. 2004. Regulation of *Vibrio anguillarum* empA Metalloprotease Expression and Its Role in Virulence. Appl Environ Microbiol 70:4193-4204.

20. Lages MA, Balado M, Lemos ML. 2019. The Expression of Virulence Factors in *Vibrio anguillarum* Is Dually Regulated by Iron Levels and Temperature. Front Microbiol 10:2335-2335.
21. Weber B, Hasic M, Chen C, Wai SN, Milton DL. 2009. Type VI secretion modulates quorum sensing and stress response in *Vibrio anguillarum*. Environ Microbiol 11:3018-28.
22. Ishikawa T, Rompikuntal PK, Lindmark B, Milton DL, Wai SN. 2009. Quorum Sensing Regulation of the Two hcp Alleles in *Vibrio cholerae* O1 Strains. PLoS One 4:e6734.
23. Hodgkinson JW, Grayfer L, Belosevic M. 2015. Biology of Bony Fish Macrophages. Biology 4:881-906.
24. Howell ML, Alsabbagh E, Ma JF, Ochsner UA, Klotz MG, Beveridge TJ, Blumenthal KM, Niederhoffer EC, Morris RE, Needham D, Dean GE, Wani MA, Hassett DJ. 2000. AnkB, a periplasmic ankyrin-like protein in *Pseudomonas aeruginosa*, is required for optimal catalase B (KatB) activity and resistance to hydrogen peroxide. J Bacteriol 182:4545-4556.
25. Barnes AC, Bowden TJ, Horne MT, Ellis AE. 1999. Peroxide-inducible catalase in *Aeromonas salmonicida* subsp. *salmonicida* protects against exogenous hydrogen peroxide and killing by activated rainbow trout, *Oncorhynchus mykiss* L., macrophages. Microb Pathog 26:149-58.
26. Ezraty B, Gennaris A, Barras F, Collet J-F. 2017. Oxidative stress, protein damage and repair in bacteria. Nat Rev Microbiol 15:385-396.
27. Chaves-Pozo E, Muñoz P, López-Muñoz A, Pelegrín P, García Ayala A, Mulero V, Meseguer J. 2005. Early innate immune response and redistribution of inflammatory cells in the bony fish gilthead seabream experimentally infected with *Vibrio anguillarum*. Cell Tissue Res 320:61-68.
28. Sepulcre M, Pelegrín P, Mulero V, Meseguer J. 2002. Characterisation of gilthead seabream acidophilic granulocytes by a monoclonal antibody unequivocally points to their involvement in fish phagocytic response. Cell Tissue Res 308:97-102.
29. Sepulcre MP, Sarropoulou E, Kotoulas G, Meseguer J, Mulero V. 2007. *Vibrio anguillarum* evades the immune response of the bony fish sea bass (*Dicentrarchus labrax* L.) through the inhibition of leukocyte respiratory burst and down-regulation of apoptotic caspases. Mol Immunol 44:3751-3757.
30. Honda A, Kodama H, Moustafa M, Yamada F, Mikami T, Izawa H. 1986. Phagocytic activity of macrophages of rainbow trout against *Vibrio anguillarum* and the opsonising effect of antibody and complement. Vet Sci Res J 40:328-332.
31. Boesen HT, Larsen MH, Larsen JL, Ellis AE. 2001. In vitro interactions between rainbow trout (*Oncorhynchus mykiss*) macrophages and *Vibrio anguillarum* serogroup O2a. Fish Shellfish Immunol 11:415-431.
32. Jiang R, Lu X-J, Lu J-F, Chen J. 2021. Characterization of ayu (*Plecoglossus altivelis*) urocortin: The function of an endocrine factor in monocyte/macrophage regulation. Dev Comp Immunol 117:103978.
33. Nie L, Cai S-Y, Sun J, Chen J. 2019. MicroRNA-155 promotes pro-inflammatory functions and augments apoptosis of monocytes/macrophages during *Vibrio anguillarum* infection in ayu, Plecoglossus altivelis. Fish Shellfish Immunol 86:70-81.
34. Chen J, Chen Q, Lu X-J, Li C-H. 2014. LECT2 improves the outcomes in ayu with *Vibrio anguillarum* infection via monocytes/macrophages. Fish Shellfish Immunol 41:586-592.
35. Skaar EP. 2010. The Battle for Iron between Bacterial Pathogens and Their Vertebrate Hosts. PLoS Path 6:e1000949.
36. Sheldon JR, Laakso HA, Heinrichs DE. 2016. Iron Acquisition Strategies of Bacterial Pathogens. Microbiol Spectr 4.

37. Mourino S, Osorio CR, Lemos ML. 2004. Characterization of heme uptake cluster genes in the fish pathogen *Vibrio anguillarum*. J Bacteriol 186.
38. Payne SM, Mey AR, Wyckoff EE. 2015. Vibrio Iron Transport: Evolutionary Adaptation to Life in Multiple Environments. Microbiol Mol Biol Rev 80:69-90.
39. Castillo D, Alvise PD, Xu R, Zhang F, Middelboe M, Gram L. 2017. Comparative Genome Analyses of *Vibrio anguillarum* Strains Reveal a Link with Pathogenicity Traits. mSystems 2:e00001-17.
40. Actis LA, Fish W, Crosa JH, Kellerman K, Ellenberger SR, Hauser FM, Sanders-Loehr J. 1986. Characterization of anguibactin, a novel siderophore from *Vibrio anguillarum* 775(pJM1). J Bacteriol 167:57-65.
41. Crosa JH. 1980. A plasmid associated with virulence in the marine fish pathogen *Vibrio anguillarum* specifies an iron-sequestering system. Nature 284:566-568.
42. Crosa JH, Schiewe MH, Falkow S. 1977. Evidence for plasmid contribution to the virulence of fish pathogen *Vibrio anguillarum*. Infect Immun 18:509-513.
43. Naka H, Crosa JH. 2012. Identification and characterization of a novel outer membrane protein receptor FetA for ferric enterobactin transport in *Vibrio anguillarum* 775 (pJM1). BioMetals 25:125-133.
44. Holm KO, Nilsson K, Hjerde E, Willassen NP, Milton DL. 2015. Complete genome sequence of *Vibrio anguillarum* strain NB10, a virulent isolate from the Gulf of Bothnia. Stand Genomic Sci 10:60.
45. Norqvist A, Hagström A, Wolf-Watz H. 1989. Protection of rainbow trout against vibriosis and furunculosis by the use of attenuated strains of *Vibrio anguillarum*. Appl Environ Microbiol 55:1400-1405.
46. Tiukova IA, Brandenburg J, Blomqvist J, Sampels S, Mikkelsen N, Skaugen M, Arntzen MØ, Nielsen J, Sandgren M, Kerkhoven EJ. 2019. Proteome analysis of xylose metabolism in *Rhodotorula toruloides* during lipid production. Biotechnol Biofuels. 12(137. doi:10.1186/s13068-019-1478-8.
47. Cox J, Hein MY, Luber CA, Paron I, Nagaraj N, Mann M. 2014. Accurate proteome-wide label-free quantification by delayed normalization and maximal peptide ratio extraction, termed MaxLFQ. Mol Cell Proteomics 13:2513-26.
48. Tyanova S, Temu T, Cox J. 2016. The MaxQuant computational platform for mass spectrometry-based shotgun proteomics. Nat Protoc 11:2301-2319.
49. Huang L, Zhang H, Wu P, Entwistle S, Li X, Yohe T, Yi H, Yang Z, Yin Y. 2018. dbCAN-seq: a database of carbohydrate-active enzyme (CAZyme) sequence and annotation. Nucleic Acids Res 46:D516-D521.
50. Perez-Riverol Y, Csordas A, Bai J, Bernal-Llinares M, Hewapathirana S, Kundu DJ, Inuganti A, Griss J, Mayer G, Eisenacher M, Perez E, Uszkoreit J, Pfeuffer J, Sachsenberg T, Yilmaz S, Tiwary S, Cox J, Audain E, Walzer M, Jarnuczak AF, Ternent T, Brazma A, Vizcaino JA. 2019. The PRIDE database and related tools and resources in 2019: improving support for quantification data. Nucleic Acids Res 47:D442-D450.
51. Heberle H, Meirelles GV, da Silva FR, Telles GP, Minghim R. 2015. InteractiVenn: a web-based tool for the analysis of sets through Venn diagrams. BMC Bioinformatics 16:169.
52. Szklarczyk D, Gable AL, Lyon D, Junge A, Wyder S, Huerta-Cepas J, Simonovic M, Doncheva NT, Morris JH, Bork P, Jensen LJ, Mering CV. 2019. STRING v11: protein-protein association networks with increased coverage, supporting functional discovery in genome-wide experimental datasets. Nucleic Acids Res 47:D607-d613.
53. Lombard V, Golaconda Ramulu H, Drula E, Coutinho PM, Henrissat B. 2014. The carbohydrate-active enzymes database (CAZy) in 2013. Nucleic Acids Res 42:D490-5.
54. Satin B, Del Giudice G, Della Bianca V, Dusi S, Laudanna C, Tonello F, Kelleher D, Rappuoli R, Montecucco C, Rossi F. 2000. The Neutrophil-Activating Protein

(Hp-Nap) of *Helicobacter pylori* Is a Protective Antigen and a Major Virulence Factor. J Exp Med 191:1467-1476.
55. Yan LJ, Sumien N, Thangthaeng N, Forster MJ. 2013. Reversible inactivation of dihydrolipoamide dehydrogenase by mitochondrial hydrogen peroxide. Free Radic Res 47:123-33.
56. Heo S, Kim S, Kang D. 2020. The Role of Hydrogen Peroxide and Peroxiredoxins throughout the Cell Cycle. Antioxidants (Basel) 9.
57. Akazaki H, Kawai F, Chida H, Hirano T, Hakamata W, Park SY, Nishio T, Oku T. 2010. Expression, purification, physicochemical characterization and structural analysis of cytochrome c554 from *Vibrio parahaemolyticus* strain RIMD2210633. Biosci Biotechnol Biochem 74:1113-5.
58. Fulde M, Willenborg J, Huber C, Hitzmann A, Willms D, Seitz M, Eisenreich W, Valentin-Weigand P, Goethe R. 2014. The arginine-ornithine antiporter ArcD contributes to biological fitness of *Streptococcus suis*. Front Cell Infect Microbiol 4:107-107.
59. Lemire J, Alhasawi A, Appanna VP, Tharmalingam S, Appanna VD. 2017. Metabolic defence against oxidative stress: the road less travelled so far. J Appl Microbiol 123:798-809.
60. Tu J, Lu F, Miao S, Ni X, Jiang P, Yu H, Xing L, Yu S, Ding C, Hu Q. 2014. The siderophore-interacting protein is involved in iron acquisition and virulence of R*iemerella anatipestifer* strain CH3. Vet Microbiol 168:395-402.
61. Butterton JR, Calderwood SB. 1994. Identification, cloning, and sequencing of a gene required for ferric vibriobactin utilization by *Vibrio cholerae*. J Bacteriol 176:5631-8.
62. Köster WL, Actis LA, Waldbeser LS, Tolmasky ME, Crosa JH. 1991. Molecular characterization of the iron transport system mediated by the pJM1 plasmid in Vibrio anguillarum 775. J Biol Chem 266:23829-23833.
63. Waldbeser LS, Tolmasky ME, Actis LA, Crosa JH. 1993. Mechanisms for negative regulation by iron of the fatA outer membrane protein gene expression in *Vibrio anguillarum* 775. J Biol Chem 268:10433-10439.
64. Actis LA, Potter SA, Crosa JH. 1985. Iron-regulated outer membrane protein OM2 of *Vibrio anguillarum* is encoded by virulence plasmid pJM1. J Bacteriol 161(2), 736–742:736-742.
65. Actis LA, Tolmasky ME, Crosa LM, Crosa JH. 1995. Characterization and regulation of the expression of FatB, an iron transport protein encoded by the pJM1 virulence plasmid. Mol Immunol 17:197-204.
66. Chen Q, Crosa JH. 1996. Antisense RNA, Fur, Iron, and the Regulation of Iron Transport Genes in *Vibrio anguillarum*. J Biol Chem 271:18885-18891.
67. Mazoy R, Osorio CR, Toranzo AE, Lemos ML. 2003. Isolation of mutants of *Vibrio anguillarum* defective in haeme utilisation and cloning of huvA, a gene coding for an outer membrane protein involved in the use of haeme as iron source. Arch Microbiol 179:329-38.
68. Kitagawa M, Matsumura Y, Tsuchido T. 2000. Small heat shock proteins, IbpA and IbpB, are involved in resistances to heat and superoxide stresses in *Escherichia coli*. FEMS Microbiol Lett 184:165-171.
69. Matuszewska M, Kuczyńska-Wiśnik D, Laskowska E, Liberek K. 2005. The Small Heat Shock Protein IbpA of *Escherichia coli* Cooperates with IbpB in Stabilization of Thermally Aggregated Proteins in a Disaggregation Competent State*. J Biol Chem 280:12292-12298.
70. Rogers A, Townsley L, Gallego-Hernandez AL, Beyhan S, Kwuan L, Yildiz FH. 2016. The LonA Protease Regulates Biofilm Formation, Motility, Virulence, and the Type VI Secretion System in *Vibrio cholerae*. J Bacteriol 198:973-85.
71. Hasnat AM, Zupok A, Olas JJ, Mueller-Roeber B, Leimkühler S. 2021. A-type carrier proteins are involved in [4Fe-4S] cluster insertion into the radical SAM

protein MoaA for the synthesis of active molybdoenzymes. J Bacteriol doi:10.1128/jb.00086-21.
72. Vickery LE, Cupp-Vickery JR. 2007. Molecular chaperones HscA/Ssq1 and HscB/Jac1 and their roles in iron-sulfur protein maturation. Crit Rev Biochem Mol Biol 42:95-111.
73. Borisov VB, Gennis RB, Hemp J, Verkhovsky MI. 2011. The cytochrome bd respiratory oxygen reductases. Biochim Biophys Acta 1807:1398-413.
74. Dongre M, Singh B, Aung KM, Larsson P, Miftakhova R, Persson K, Askarian F, Johannessen M, von Hofsten J, Persson JL, Erhardt M, Tuck S, Uhlin BE, Wai SN. 2018. Flagella-mediated secretion of a novel *Vibrio cholerae* cytotoxin affecting both vertebrate and invertebrate hosts. Commun Biol 1:59.
75. Blum M, Chang HY, Chuguransky S, Grego T, Kandasaamy S, Mitchell A, Nuka G, Paysan-Lafosse T, Qureshi M, Raj S, Richardson L, Salazar GA, Williams L, Bork P, Bridge A, Gough J, Haft DH, Letunic I, Marchler-Bauer A, Mi H, Natale DA, Necci M, Orengo CA, Pandurangan AP, Rivoire C, Sigrist CJA, Sillitoe I, Thanki N, Thomas PD, Tosatto SCE, Wu CH, Bateman A, Finn RD. 2021. The InterPro protein families and domains database: 20 years on. Nucleic Acids Res 49:D344-d354.
76. Ellison DW, Miller VL. 2006. Regulation of virulence by members of the MarR/SlyA family. Curr Opin Microbiol 9:153-159.
77. Olive AJ, Sassetti CM. 2016. Metabolic crosstalk between host and pathogen: sensing, adapting and competing. Nat Rev Microbiol 14:221-34.
78. Romeo T, Babitzke P. 2018. Global Regulation by CsrA and Its RNA Antagonists. Microbiol Spectr 6:10.1128/microbiolspec.RWR-0009-2017.
79. Katsowich N, Elbaz N, Pal RR, Mills E, Kobi S, Kahan T, Rosenshine I. 2017. Host cell attachment elicits posttranscriptional regulation in infecting enteropathogenic bacteria. Science 355:735-739.
80. Pacello F, Ceci P, Ammendola S, Pasquali P, Chiancone E, Battistoni A. 2008. Periplasmic Cu,Zn superoxide dismutase and cytoplasmic Dps concur in protecting *Salmonella enterica* serovar Typhimurium from extracellular reactive oxygen species. Biochim Biophys Acta 1780:226-32.
81. Xia X, Larios-Valencia J, Liu Z, Xiang F, Kan B, Wang H, Zhu J. 2017. OxyR-activated expression of Dps is important for *Vibrio cholerae* oxidative stress resistance and pathogenesis. PLoS One 12:e0171201.
82. Xie K, Bunse C, Marcus K, Leichert LI. 2019. Quantifying changes in the bacterial thiol redox proteome during host-pathogen interaction. Redox Biol 21:101087-101087.

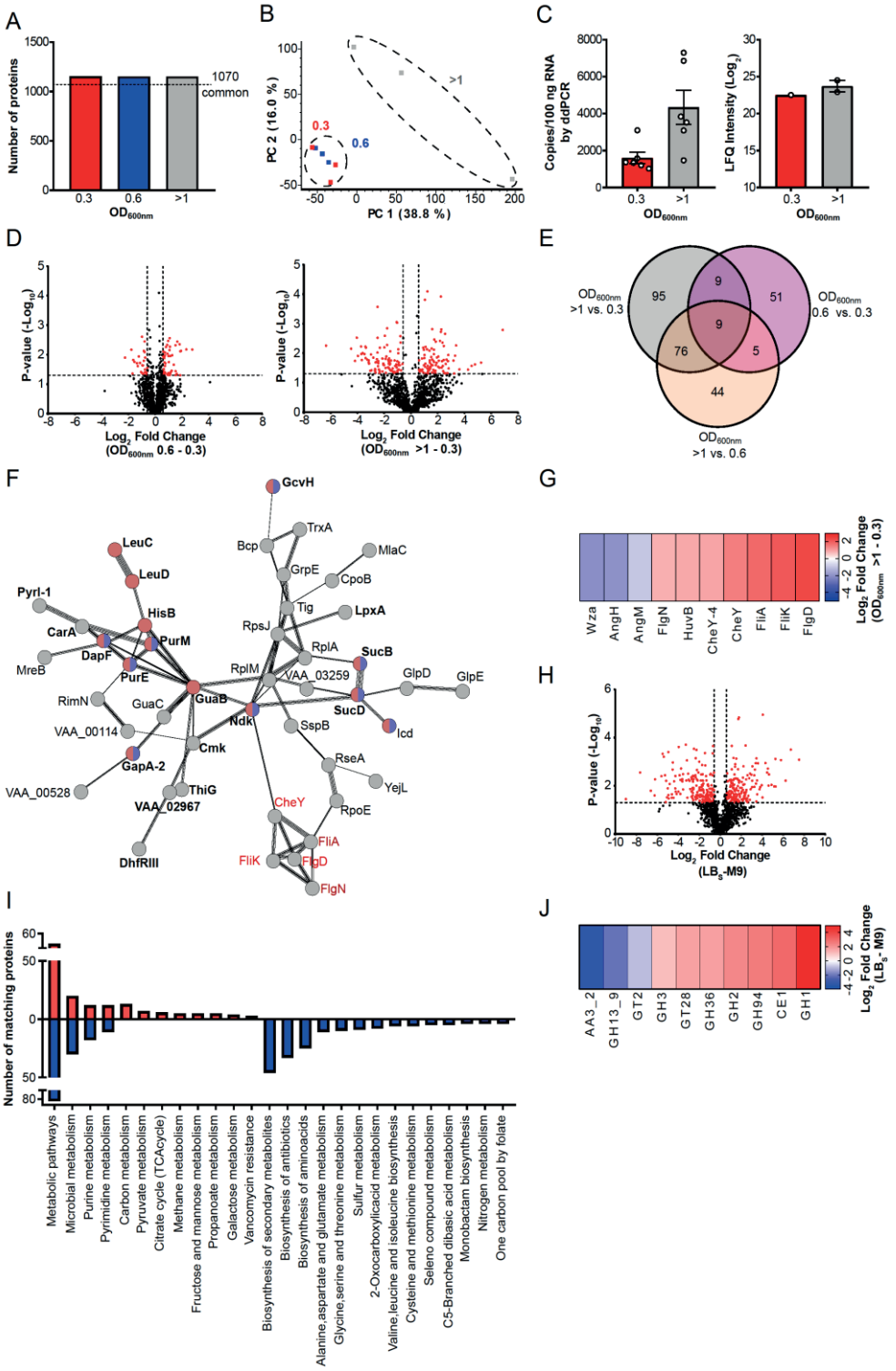
A
Number of proteins
1070 common
0.3
0.6
>1
OD600nm
B
PC 2 (16.0 %)
PC 1 (38.8 %)
0.3
0.6
>1
C
Copies/100 ng RNA by ddPCR
LFQ Intensity (Log2)
OD600nm
D
P-value (-Log10)
Log2 Fold Change (OD600nm 0.6 - 0.3)
Log2 Fold Change (OD600nm >1 - 0.3)
E
OD600nm >1 vs. 0.3
OD600nm 0.6 vs. 0.3
OD600nm >1 vs. 0.6
95
9
51
9
76
5
44
F
GcvH
LeuC
LeuD
Pyrl-1
HisB
CarA
PurM
DapF
MreB
PurE
RimN
GuaC
GuaB
VAA_00114
Cmk
GapA-2
VAA_00528
ThiG
VAA_02967
DhfRIII
TrxA
Bcp
MlaC
GrpE
CpoB
Tig
LpxA
RpsJ
RplA
SucB
RplM
VAA_03259
GlpD
GlpE
SucD
Ndk
SspB
Icd
RseA
YejL
RpoE
CheY
FliA
FliK
FlgD
FlgN
G
Wza
AngH
AngM
FlgN
HuvB
CheY-4
CheY
FliA
FliK
FlgD
Log2 Fold Change (OD600nm >1 - 0.3)
H
P-value (-Log10)
Log2 Fold Change (LBs-M9)
I
Number of matching proteins
Metabolic pathways
Microbial metabolism
Purine metabolism
Pyrimidine metabolism
Carbon metabolism
Pyruvate metabolism
Citrate cycle (TCAcycle)
Methane metabolism
Fructose and mannose metabolism
Propanoate metabolism
Galactose metabolism
Vancomycin resistance
Biosynthesis of secondary metabolites
Biosynthesis of antibiotics
Biosynthesis of aminoacids
Alanine,aspartate and glutamate metabolism
Glycine,serine and threonine metabolism
Sulfur metabolism
2-Oxocarboxylicacid metabolism
Valine,leucine and isoleucine biosynthesis
Cysteine and methionine metabolism
Seleno compound metabolism
C5-Branched dibasic acid metabolism
Monobactam biosynthesis
Nitrogen metabolism
One carbon pool by folate
J
AA3_2
GH13_9
GT2
GH3
GT28
GH36
GH2
GH94
CE1
GH1
Log2 Fold Change (LBs - M9)

Figure 1. The effect of growth phase and nutritional stress on the VA proteome. (A) Bar charts showing the total number of quantified proteins in VA upon growing in LB_S ($OD_{600\ nm}$ = 0.3, 0.6 and >1.0). The number of shared proteins across examined conditions are indicated. **(B)** Principal component analysis (PCA) performed on VA proteome upon growing in LB_S ($OD_{600\ nm}$ = 0.3, 0.6 and >1.0). The quantified proteins were plotted in two-dimensional principal component space by PC1 (38.8 %) and PC2 (16.0 %) for the individual replicates. **(C)** The transcriptional (left panel, *lpmO*$_{VA}$) and translational (right panel, $LPMO_{VA}$) response of lytic polysaccharide mono-oxygenase upon growing of VA in LB_S at early exponential ($OD_{600\ nm}$ = 0.3) and stationary growth phase (>1.0) using ddPCR (left panel) and label free quantitative proteomic analysis (right panel). **(D)** Volcano plots of identified proteins upon growing of VA at different phases of growth in LB_S. Red dotted line(s) through y-axis and x-axis, indicate cut off values for significance that were set to fold change (FC) $\geq$ 1.5 (log_2=0.58) and $p \leq 0.05$ ($-log_{10}$=1.3). **(E)** Venn diagrams illustrating significantly regulated proteins upon growing of VA at different phases of growth in LB_S. **(F)** STRING analysis of significantly up-regulated proteins of VA in LBs at stationary ($OD_{600\ nm}$ >1) versus early exponential ($OD_{600\ nm}$ =0.3) growth phases. Singletons and nodes that were disconnected from the main network were omitted from visualization. Proteins that are marked in bold or red are associated with the metabolic pathways or virulence, respectively. Red and blue nodes indicate proteins associated with the biosynthesis of secondary metabolites and antibiotics, respectively. **(G)** Heatmap of selected regulated virulence factors of VA (*e.g.*, motility, chemotaxis, iron acquisition) upon growth of the bacterium in LBs at stationary- ($OD_{600\ nm}$ >1) versus early exponential -($OD_{600\ nm}$ =0.3) growth phases. Blue and red color represents down- or up-regulated proteins, respectively. **(H)** Volcano plot of the VA proteome upon growing the bacterium ($OD_{600\ nm}$ = 0.6) in LB_S compared to $M9_{VA}$. Red dotted line(s) through y-axis and x-axis, indicate cut off values for significance that were set to fold change (FC) $\geq$ 1.5 (log_2=0.58) and $p \leq 0.05$ ($-log_{10}$=1.3). **(I)** KEGG pathway enrichment analysis performed using the list of significantly up (red)- or down (blue)-regulated proteins in LB_S compared to $M9_{VA}$. The y- and x-axis indicate the number of matching proteins and the enriched pathway, respectively. **(J)** Heatmap of significantly up (red) and down (blue)-regulated CAZymes identified upon growing VA in LB_S compared to $M9_{VA}$.

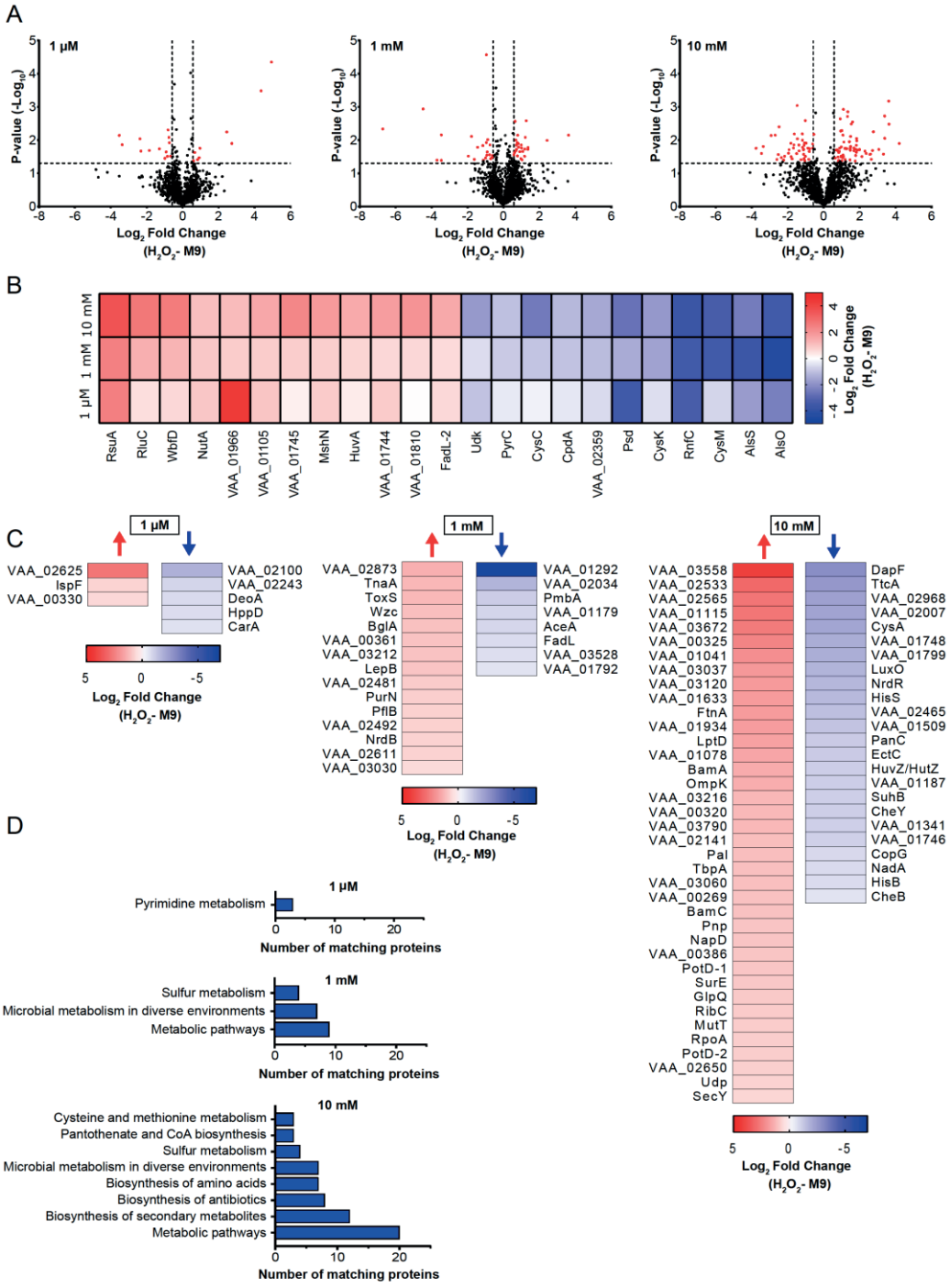
A
1 µM
1 mM
10 mM
P-value (-Log10)
Log2 Fold Change
(H2O2- M9)
B
1 µM 1 mM 10 mM
RsuA RluC WbfD NutA VAA_01966 VAA_01105 VAA_01745 MshN HuvA VAA_01744 VAA_01810 FadL-2 Udk PyrC CysC CpdA VAA_02359 Psd CysK RnfC CysM AlsS AlsO
Log2 Fold Change (H2O2- M9)
C
1 µM
VAA_02625 IspF VAA_00330
VAA_02100 VAA_02243 DeoA HppD CarA
1 mM
VAA_02873 TnaA ToxS Wzc BglA VAA_00361 VAA_03212 LepB VAA_02481 PurN PflB VAA_02492 NrdB VAA_02611 VAA_03030
VAA_01292 VAA_02034 PmbA VAA_01179 AceA FadL VAA_03528 VAA_01792
10 mM
VAA_03558 VAA_02533 VAA_02565 VAA_01115 VAA_03672 VAA_00325 VAA_01041 VAA_03037 VAA_03120 VAA_01633 FtnA VAA_01934 LptD VAA_01078 BamA OmpK VAA_03216 VAA_00320 VAA_03790 VAA_02141 Pal TbpA VAA_03060 VAA_00269 BamC Pnp NapD VAA_00386 PotD-1 SurE GlpQ RibC MutT RpoA PotD-2 VAA_02650 Udp SecY
DapF TtcA VAA_02968 VAA_02007 CysA VAA_01748 VAA_01799 LuxO NrdR HisS VAA_02465 VAA_01509 PanC EctC HuvZ/HutZ VAA_01187 SuhB CheY VAA_01341 VAA_01746 CopG NadA HisB CheB
D
1 µM
Pyrimidine metabolism
Number of matching proteins
1 mM
Sulfur metabolism
Microbial metabolism in diverse environments
Metabolic pathways
10 mM
Cysteine and methionine metabolism
Pantothenate and CoA biosynthesis
Sulfur metabolism
Microbial metabolism in diverse environments
Biosynthesis of amino acids
Biosynthesis of antibiotics
Biosynthesis of secondary metabolites
Metabolic pathways

Figure 2. The effect of H_2O_2 as an oxidative stressor on the VA proteome. (A) Volcano plots of identified proteins upon growing VA at increasing concentrations of H_2O_2 (0, 1 µM, 1 mM, 10 mM). Red dotted line(s) through y-axis and x-axis, indicate cut off values for significance that were set to fold change (FC) $\geq$ 1.5 (log_2=0.58) and $p \leq 0.05$ ($-log_{10}$=1.3). **(B)** Heatmap of significantly up (red)- and down (blue)-regulated proteins that were shared in at least two out of the three examined concentrations of H_2O_2. **(C)** Heatmaps of significantly up (red)- and down (blue)-regulated proteins that were unique to each examined H_2O_2 concentration. **(D)** KEGG pathway enrichment analysis performed using the list of significantly up (red)- or down (blue)-regulated proteins upon exposure of VA to increasing concentrations of H_2O_2 versus absence. The x- and y-axis represent the number of matching proteins and the enriched pathway, respectively.

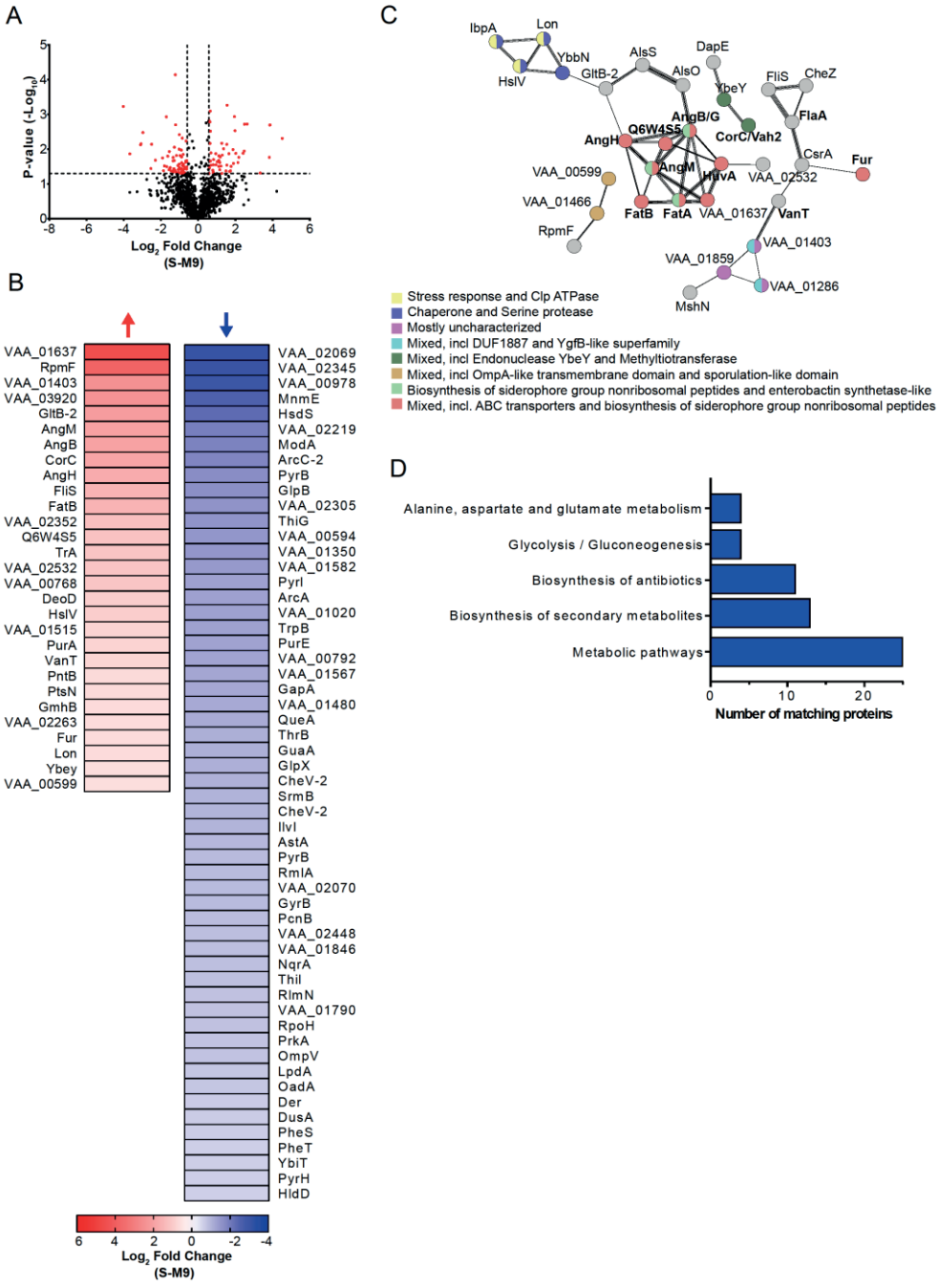
A
P-value (-Log10)
Log2 Fold Change
(S-M9)
B
VAA_01637
RpmF
VAA_01403
VAA_03920
GltB-2
AngM
AngB
CorC
AngH
FliS
FatB
VAA_02352
Q6W4S5
TrA
VAA_02532
VAA_00768
DeoD
HslV
VAA_01515
PurA
VanT
PntB
PtsN
GmhB
VAA_02263
Fur
Lon
Ybey
VAA_00599
VAA_02069
VAA_02345
VAA_00978
MnmE
HsdS
VAA_02219
ModA
ArcC-2
PyrB
GlpB
VAA_02305
ThiG
VAA_00594
VAA_01350
VAA_01582
PyrI
ArcA
VAA_01020
TrpB
PurE
VAA_00792
VAA_01567
GapA
VAA_01480
QueA
ThrB
GuaA
GlpX
CheV-2
SrmB
CheV-2
IlvI
AstA
PyrB
RmlA
VAA_02070
GyrB
PcnB
VAA_02448
VAA_01846
NqrA
ThiI
RlmN
VAA_01790
RpoH
PrkA
OmpV
LpdA
OadA
Der
DusA
PheS
PheT
YbiT
PyrH
HldD
Log2 Fold Change
(S-M9)
C
IbpA
Lon
YbbN
HslV
GltB-2
AlsS
AlsO
DapE
YbeY
FliS
CheZ
FlaA
AngB/G
Q6W4S5
AngH
CorC/Vah2
CsrA
Fur
VAA_00599
AngM
HlyA
VAA_02532
VAA_01466
FatB
FatA
VAA_01637
VanT
RpmF
VAA_01403
VAA_01859
VAA_01286
MshN
Stress response and Clp ATPase
Chaperone and Serine protease
Mostly uncharacterized
Mixed, incl DUF1887 and YgfB-like superfamily
Mixed, incl Endonuclease YbeY and Methyltiotransferase
Mixed, incl OmpA-like transmembrane domain and sporulation-like domain
Biosynthesis of siderophore group nonribosomal peptides and enterobactin synthetase-like
Mixed, incl. ABC transporters and biosynthesis of siderophore group nonribosomal peptides
D
Alanine, aspartate and glutamate metabolism
Glycolysis / Gluconeogenesis
Biosynthesis of antibiotics
Biosynthesis of secondary metabolites
Metabolic pathways
Number of matching proteins

Figure 3. Proteome profile of VA upon exposure to Atlantic salmon serum. **(A)** Volcano plots of identified proteins upon incubation of VA with normal Atlantic salmon serum (S) versus absence ($M9_{VA}$ marked as M9 in the figure). Red dotted line(s) through y-axis and x-axis, indicate cut off values for significance that were set to fold change (FC) $\geq$ 1.5 (log_2=0.58) and $p \leq 0.05$ ($-log_{10}$=1.3). **(B)** Heatmap of significantly up (red)- and down (blue)-regulated proteins that were unique to supplementation of salmon serum (S. **(C)** STRING analysis of significantly up-regulated proteins in VA that were associated with supplementation of salmon serum versus absence. Singletons and nodes that were disconnected from the main network were omitted from visualization. Proteins that are marked in bold are associated virulence/VA pathogenesis. Red/light green, blue and purple nodes represent proteins associated with iron acquisition, chaperones/protease activity and uncharacterized function, respectively. A detail description is indicated in the figure. **(D)** KEGG pathway enrichment analysis of significantly down-regulated proteins upon supplementation of serum to $M9_{VA}$ versus $M9_{VA}$. The x- and y-axis represent the number of matching proteins and the enriched pathway, respectively.

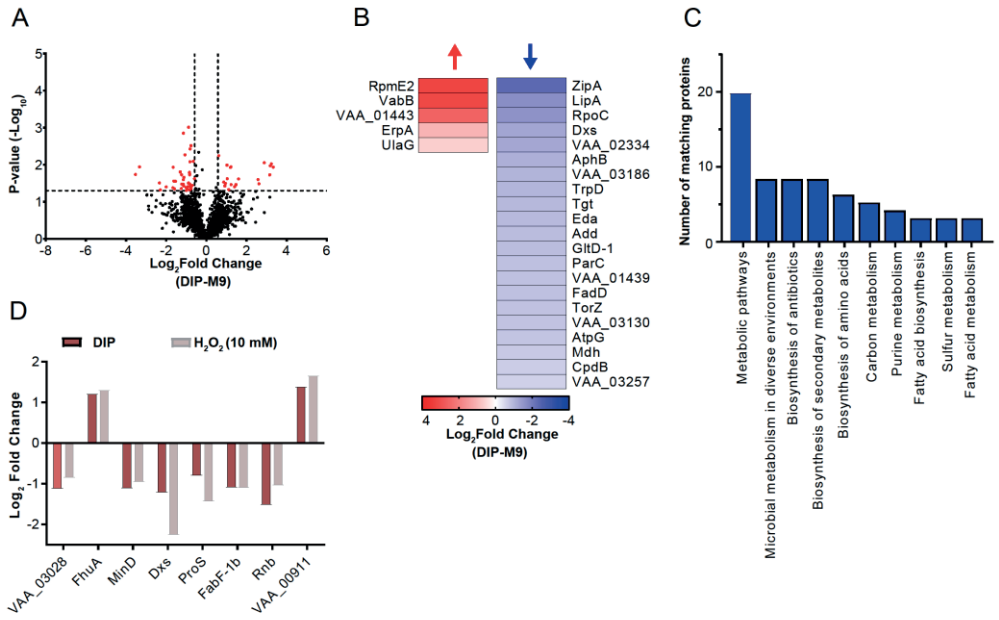

Figure 4. Proteomic response of VA to iron deprivation. (A) Bar graph comparing significantly regulated proteins shared upon treatment with DIP and 10 mM H_2O_2. The y-axis indicates the value of Log_2 Fold change. **(B)** Volcano plots of identified proteins upon exposure of VA to DIP versus absence. Red dotted line(s) through y-axis and x-axis, indicate cut off values for significance that were set to fold change (FC) $\geq$ 1.5 (log_2=0.58) and $p \leq 0.05$ ($-log_{10}$=1.3). **(C)** Heatmap of significantly up (red)- and down (blue)-regulated proteins that were unique to DIP. **(D)** KEGG pathway enrichment analysis on significantly down-regulated proteins upon DIP to $M9_{VA}$ versus $M9_{VA}$. The y- and x-axis indicate the number of matching proteins and the enriched pathway, respectively.

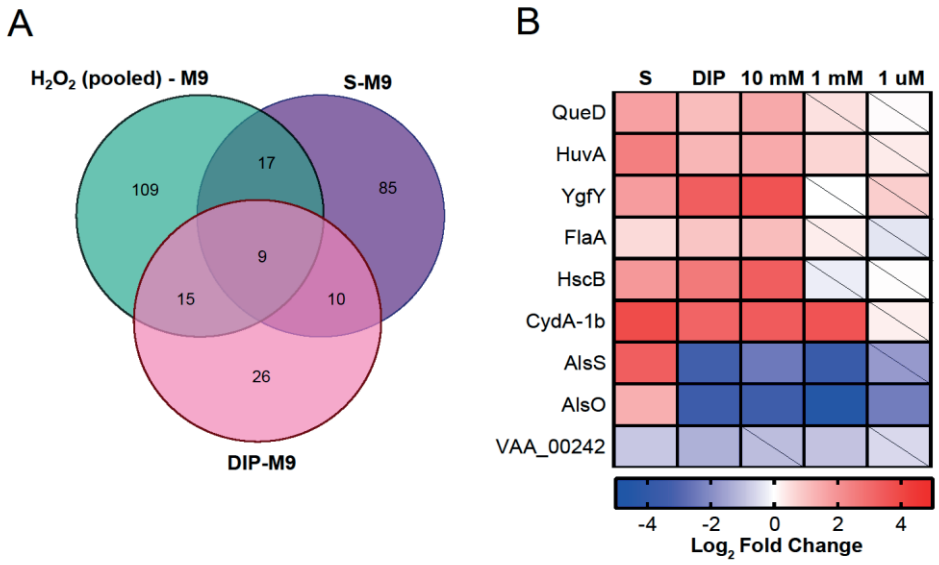

Figure 5. Regulated proteins common to all vibriosis-mimicking stress conditions. (A) Venn diagram comparing all examined conditions including iron deprivation (DIP versus $M9_{VA}$), exposure to serum (S versus $M9_{VA}$) and oxidative stresses (H_2O_2, all tested concentrations, versus $M9_{VA}$). **(B)** Heatmap of significantly up (red)- and down (blue)-regulated proteins that were shared under all examined conditions (described in A). Rectangles with diagonal lines represent proteins that were not significantly regulated under a particular condition.

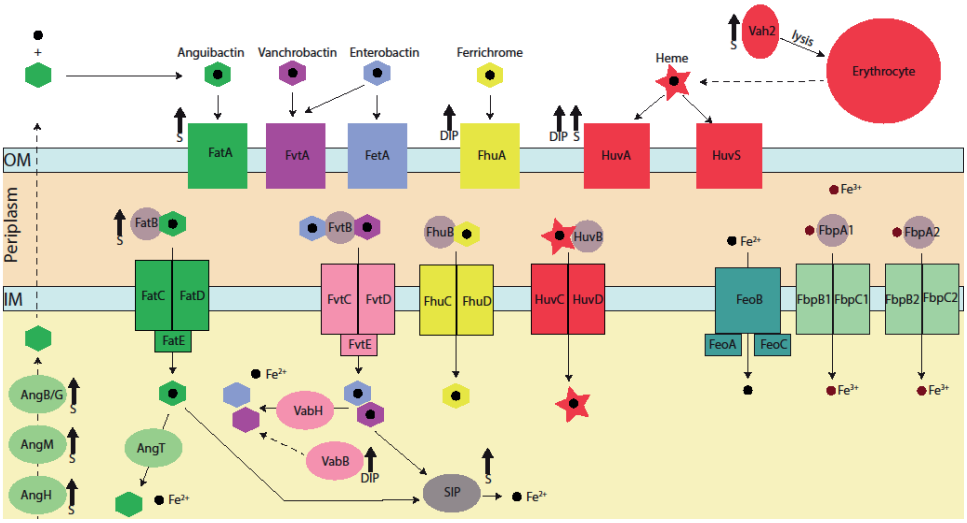

Figure 6. Iron acquisition systems in *V. anguillarum*. Schematic illustration of the various iron acquisition systems used by VA (reviewed by (8). To reduce complexity, some proteins that are not relevant to the findings in the current study are not shown. It should be noted that the ferrichrome system has not been experimentally confirmed. Thick, upward pointing arrows with either S (serum) or DIP (iron deprivation) indicate proteins that were up-regulated in our experimental conditions. Dashed lines indicated pathways that are not complete.

Comparative proteomic profiling reveals specific adaption of *Vibrio anguillarum* to oxidative stress, iron deprivation and humoral components of innate immunity

Anna Skåne, Jennifer S.M. Loose, Gustav Vaaje-Kolstad‡* and Fatemeh Askarian‡*

Faculty of Chemistry, Biotechnology and Food Science, Norwegian University of Life Sciences (NMBU), Ås, Norway.

‡These authors contributed equally to this work.
*correspondence: fatemeh.askarian@nmbu.no, gustav.vaaje-kolstad@nmbu.no

Supplementary material

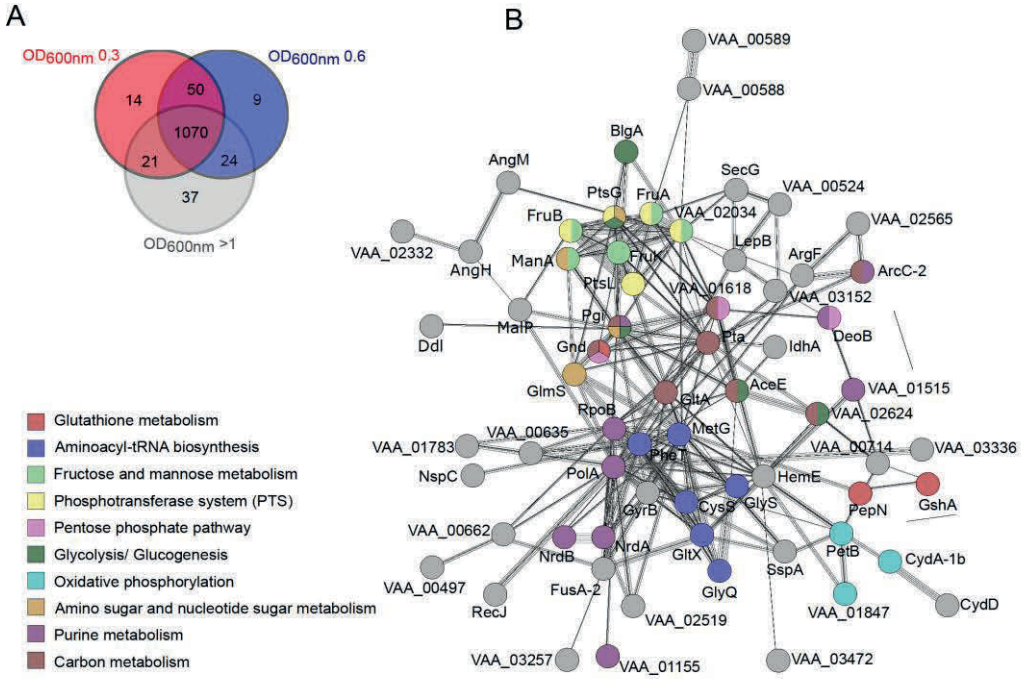
A
OD600nm 0.3
OD600nm 0.6
OD600nm >1
14
50
9
1070
21
24
37
B
VAA_00589
VAA_00588
BlgA
AngM
SecG
VAA_00524
PtsG
FruA
FruB
VAA_02034
VAA_02565
VAA_02332
AngH
ManA
FruK
LepB
ArgF
ArcC-2
PtsI
VAA_01618
VAA_03152
Pgi
MalP
Ddl
Pfa
DeoB
Gnd
IdhA
GlmS
AceE
VAA_01515
GltA
RpoB
VAA_02624
VAA_00635
MetG
VAA_01783
PheT
VAA_00714
VAA_03336
NspC
PolA
HemE
GshA
PepN
GyrB
CysS
GlyS
VAA_00662
NrdB
NrdA
GltX
PetB
CydA-1b
SspA
VAA_00497
FusA-2
GlyQ
RecJ
VAA_01847
CydD
VAA_02519
VAA_03257
VAA_01155
VAA_03472
Glutathione metabolism
Aminoacyl-tRNA biosynthesis
Fructose and mannose metabolism
Phosphotransferase system (PTS)
Pentose phosphate pathway
Glycolysis/ Glucogenesis
Oxidative phosphorylation
Amino sugar and nucleotide sugar metabolism
Purine metabolism
Carbon metabolism
C
Number of matching proteins
40
20
0
-20
-40
Metabolic pathways
Carbon metabolism
Biosynthesis of secondary metabolites
Biosynthesis of antibiotics
C5-Branched dibasic acid metabolism
Microbial metabolism in diverse environments
Purine metabolism
Aminoacyl-tRNA biosynthesis
Fructose and mannose metabolism
Phosphotransferase system (PTS)
Glycolysis / Gluconeogenesis
Amino sugar and nucleotide sugar metabolism
Oxidative phosphorylation
Pentose phosphate pathway
Glutathione metabolism

Figure S1. The effect of growth phase and nutritional stress on the VA proteome. (A) Venn diagram comparing the proteome response of VA upon growing in LB_S $OD_{600\ nm}$= 0.3, LB_S $OD_{600\ nm}$= 0.6 and LB_S $OD_{600\ nm}$= >1. **(B)** STRING analysis of significantly down-regulated proteins in the VA proteome upon growing in LB_S at stationary ($OD_{600\ nm}$ >1) versus early exponential growth phase ($OD_{600\ nm}$ = 0.3). Singletons and nodes disconnected from the network have been removed. **(C)** KEGG pathways significantly enriched among the up-regulated and down-regulated proteins in LB_S $OD_{600\ nm}$ >1 compared to LB_S $OD_{600\ nm}$ = 0.3. The x-axis represents the number of matching proteins in each of the KEGG pathways indicated on the y-axis. Red color represents positive regulation, while blue represent negative regulation.

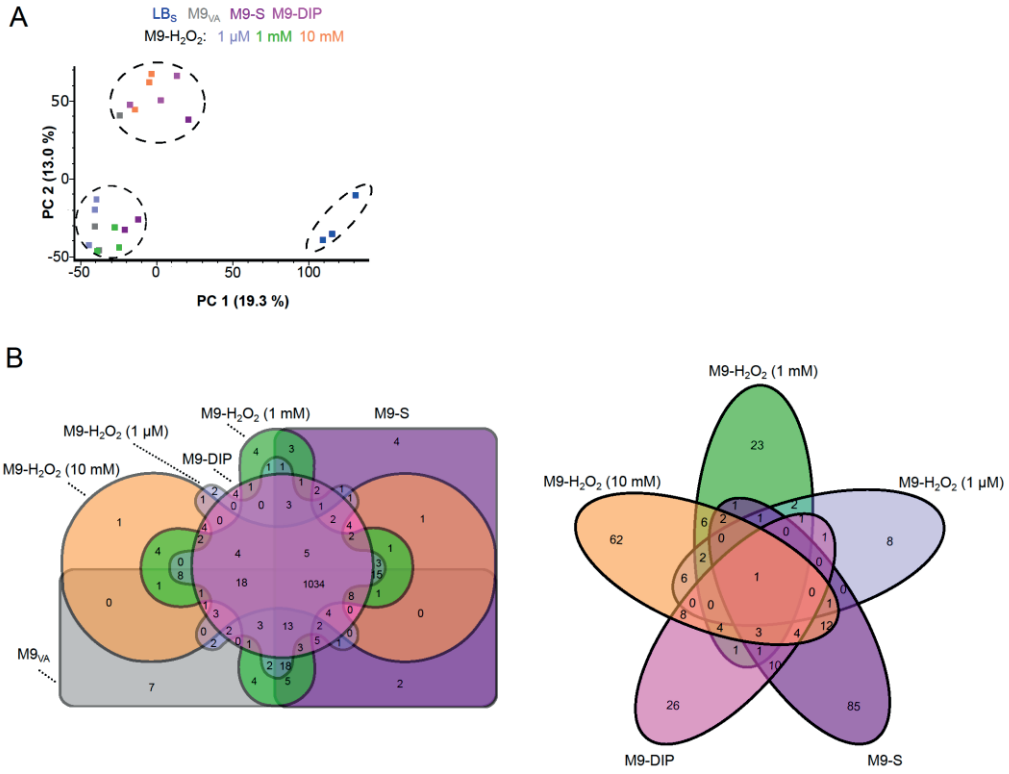

Figure S2. Proteomic response of VA to vibriosis-mimicking stressors. (A) Principal component analysis (PCA) performed on identified proteins by growing of VA in $M9_{VA}$ ($OD_{600\ nm}$ = 0.6) with and without supplementation of S, DIP or H_2O_2. The proteome response of VA upon growing in bacteriologic media (LB_S, $OD_{600\ nm}$ = 0.6) was also included in the analysis. The quantified proteins were plotted in two-dimensional principal component space by PC1 (19.3 %) and PC2 (13.0 %) for the individual replicates. **(B)** Venn diagram illustrating the proteome response of VA upon growing in $M9_{VA}$ with or supplementation of S, DIP or H_2O_2 (left panel). A Venn diagram comparing the significantly regulated proteins was also generated under the same examined condition as described above (right panel)

ISBN: 978-82-575-1830-1
ISSN: 1894-6402

Norwegian University
of Life Sciences

Postboks 5003
NO-1432 Ås, Norway
+47 67 23 00 00
www.nmbu.no